Preliminary Report

of

The Hakuho Maru Cruise KH-87-3

July 1 - August 13, 1988

Izu-Ogasawara (Bonin), East Mariana Basin
and Yap Trench

(WESTPAC, ODP Site Survey)

Ocean Research Institute
University of Tokyo
1989

Preliminary Report

of

The Hakuho Maru Cruise KH-87-3

July 1 - August 13, 1988

Izu-Ogasawara (Bonin), East Mariana Basin
and Yap Trench

(WESTPAC, ODP Site Survey)

by

The Scientific Members of the Cruise

Edited by

Kazuo KOBAYASHI

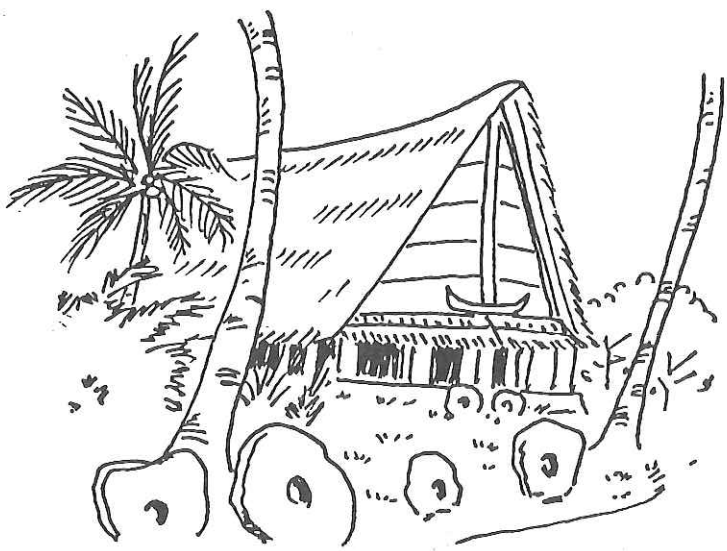

Illustrated by H. Katao

PREFACE

The cruise KH 87-3 of the Research Vessel Hakuho Maru began at Tokyo Harumi Pier July 1, 1987 and ended there August 13, 1987. The entire cruise was devoted to geological and geophysical investigation of the northwestern Pacific Basin and its margin including trench, arc and backarc regions. It was divided into three legs (Leg 1: July 1 to 16, Leg 2: July 21 to 31, Leg 3: August 3 to 13) by two ports of call; Guam from July 16 to July 21 and Yap from July 31 to August 3 considering variety of regional interests and major methods of investigation in each region. As I was asked to stay at Tokyo late July to August for my official responsibility of planning and construction of a new research vessel, duty of chief scientist of the cruise was transferred to Prof. J. Segawa after July 17 at Guam. Cooperation of members of the cruise was greatly appreciated.

In Leg 1 a fore-arc region (lower landward slope) of the Izu-Ogasawara (Bonin) Trench was one of the principal targets of study. A huge amount of rocks were collected by several dredge hauls at the upper slopes of forearc seamounts. From one located at 30°55'N near Tori-Shima ultramafic and mafic rocks were recovered and examined on board as well as in the shore-based laboratory to search for their origin. Relatively fresh pillow lavas were collected from a deep "Uyeda" Ridge which appears to be subducted to the Izu-Ogasawara (Bonin) Trench. Very elongated (nearly EW perpendicular to the trench axis) shape and extraordinary great depth (its crest is as deep as or deeper than 6,000m, faulted down toward the trench axis) of this ridge together with geochemistry of basalts will provide an interesting problem for dabate of its origin and history. Deep-sea camera observation of the bottom surface indicated in-situ exposure of some rocks. Ogasawara Plateau was also dredged and some additions to the previous works (KT 86-9, KH 84-1 and KH 82-4) were obtained.

Along the latitude of 30°51'N to 31°N an electromagnetic study of deeper part beneath the arc was undertaken using 5 OBM (Ocean Bottom Magnetometers)and one OBP (Ocean Bottom Proton Magnetometer). These instruments were successfully retrieved several months later by another ship and their records have been analyzed. A trial use of an improved long-baseline transponder navigation system yielded very good results of position fixing. Sound propagation experiment was tested using IES (Inverted Echo Sounder). Piston corings hit bottom at the northernmost Mariana Ridge at which water depths do not exceed CCD (the carbonate compensation depth) to investigate species of calcareous microfossils in this region. Heat flow measurement was also attemped.

Geomagnetic field was continuously measured during the entire periods of this cruise while sailing by both a towed proton magnetometer and a three-component fluxgate magnetometer installed on the upper deck of the ship. In the last few days of Leg 1 and most of Leg 2 survey tracks of the vessel were planned to identify magnetic lineations in the oldest parts of

the Pacific Ocean in the East Mariana Basin, which revised previously proposed identification and provided new knowledge on distribution of the M-sequence. Single-channel digital seismic reflection survey was conducted in the Ogasawara Plateau region as well as in the East Mariana Basin.

Three different models of seagoing gravimeters were operated during the cruise to mutually calibrate their performance. Results of gravity anomalies obtained by these instruments are very useful to geophysical interpretation of topography and magnetic anomalies. Participation of three gravity scientists in the present cruise was realized by a kind arrangement between the JSPS (Japan Society for Promotion of Sciences) and the Academia Sinica. We are all gratefull to their thoughtful support for this attempt.

Leg 3 of the present cruise was mostly focused to survey of the Yap Trench. The research was linked to onland geology which was studied during the port of call and at their previous visits (KH 86-1). Morphology of the Sumisu Rift was surveyed during return trip from Yap to Tokyo.

Dredge hauls at several sites were made really successful by use of unpublished Seabeam data offered by the Hydrographic Department, Maritime Safety Agency of Japan. Base maps for the Uyeda Ridge and Ogasawara Plateau were reproduced by us using their Seabeam map. Bathymetric contours in the MAGBAT charts were drawn using the GEBCO Digital Bathymetric Data offered by JODC (Japan Ocean Data Center). We wish to express our sincere thanks to them for allowing us to use these data.

Parts of the present cruise were undertaken as site survey of the ODP (Ocean Drilling Program) for drillings in the surveyed regions planned to take place in 1989 and afterward. Members of this expedition are grateful to officials of Monbusho (Ministry of Education, Science and Culture) for their general and financial support of the program. We are indebted to Dr. B. Taylor for his kind advice on the dredge sites in Tori-Shima fore-arc. This cruise was declared to be conducted in the framework of the WESTPAC program, although no visitors under this program participated in the present cruise. We acknowledge effort of the officials of the WESTPAC-IOC and Monbusho for this program.

Preliminary reports of the cruise KT 86-9 of the R. V. Tansei Maru is included in this volume. Results of the cruise are closely related to this cruise. Both were actually planned to mutually supplement each other. Great help of officers and crew of two research vessels is acknowledged.

One chapter on heat flow measurement in the Japan Basin erroneously printed in the previous report (KH 86-2) is attached at the end and attention for correction is asked to readers possibly common to both reports.

January 1989

Kazuo KOBAYASHI

CONTENTS

Annex:

1. SCIENTISTS ABOARD THE R.V. HAKUHO MARU FOR THE CRUISE KH 87-3

KOBAYASHI, Kazuo*	[Chief Scientist]	Ocean Research Institute, University of Tokyo
ABE, Shintaro**		Department of Earth Sciences, Chiba University
ADACHI, Yasuhisa		Department of Earth Sciences, Kobe University
ASANUMA, Toshio*		Department of Earth Sciences, Chiba University
ASHI, Juichiro		Ocean Research Institute, University of Tokyo
FUJIMOTO, Hiromi		Ocean Research Institute, University of Tokyo
FUJIOKA, Kantaro***++		Ocean Research Institute, University of Tokyo
FURUTA, Toshio		Ocean Research Institute, University of Tokyo
ISHII, Teruaki**		Ocean Research Institute, University of Tokyo
KASUMI, Yoshinobu		Department of Earth Sciences, Chiba University
KIMURA, Gaku***		Faculty of Education, Kagawa University
KINOSHITA, Masataka***		Earthquake Research Institute, University of Tokyo
KOIZUMI, Kin-ichiro		Ocean Research Institute, University of Tokyo
KONISHI, Kenji*		Department of Geology, Kanazawa University
KURAMOTO, Shin'ichi***		Ocean Research Institute, University of Tokyo
MAEKAWA, Hirokazu**		Department of Earth Sciences, Kobe University
MATSUOKA, Hiromi		Department of Geology, Kanazawa University
MIKI, Masako		Department of Earth Sciences, Kobe University
MURAKAMI, Hideyuki		Ocean Electronics, Co. (Kaiyo Denshi K.K.)
NAKANISHI, Masao		Ocean Research Institute, University of Tokyo
OZAWA, Hiroaki**		Department of Geology, University of Tokyo
SAYANAGI, Keizo		Ocean Research Institute, University of Tokyo
SEGAWA, Jiro+		Ocean Research Institute, University of Tokyo
TAKEUCHI, Akira***		College of General Education, Toyama University
TAKEUCHI, Tomoyoshi*		University of Electro-Communications
TAMAKI, Kensaku**		Ocean Research Institute, University of Tokyo
TOH, Hiroaki		Ocean Research Institute, University of Tokyo
WATANABE, Masaharu		Ocean Research Institute, University of Tokyo
YANG, Chul Soo		Ocean Research Institute, University of Tokyo
LIANG, Chu Jian		Institute of Geodesy and Geophysics, Academia Sinica, Wuhan, China
PAN, Xian Zhang		Institute of Geodesy and Geophysics, Academia Sinica, Wuhan, China
ZHANG, Xian Lin		Institute of Geodesy and Geophysics, Academia Sinica, Wuhan, China

* from July 1 (Tokyo) to July 17 (Guam) only
** from July 1 (Tokyo) to August 1 (Yap) only
*** from August 2 (Yap) to August 13 (Tokyo) only

\+ acting Chief Scientist: from July 17 to August 1
++ acting Chief Scientist: from August 2 to August 13

2. INDEX MAPS OF KH 87-3

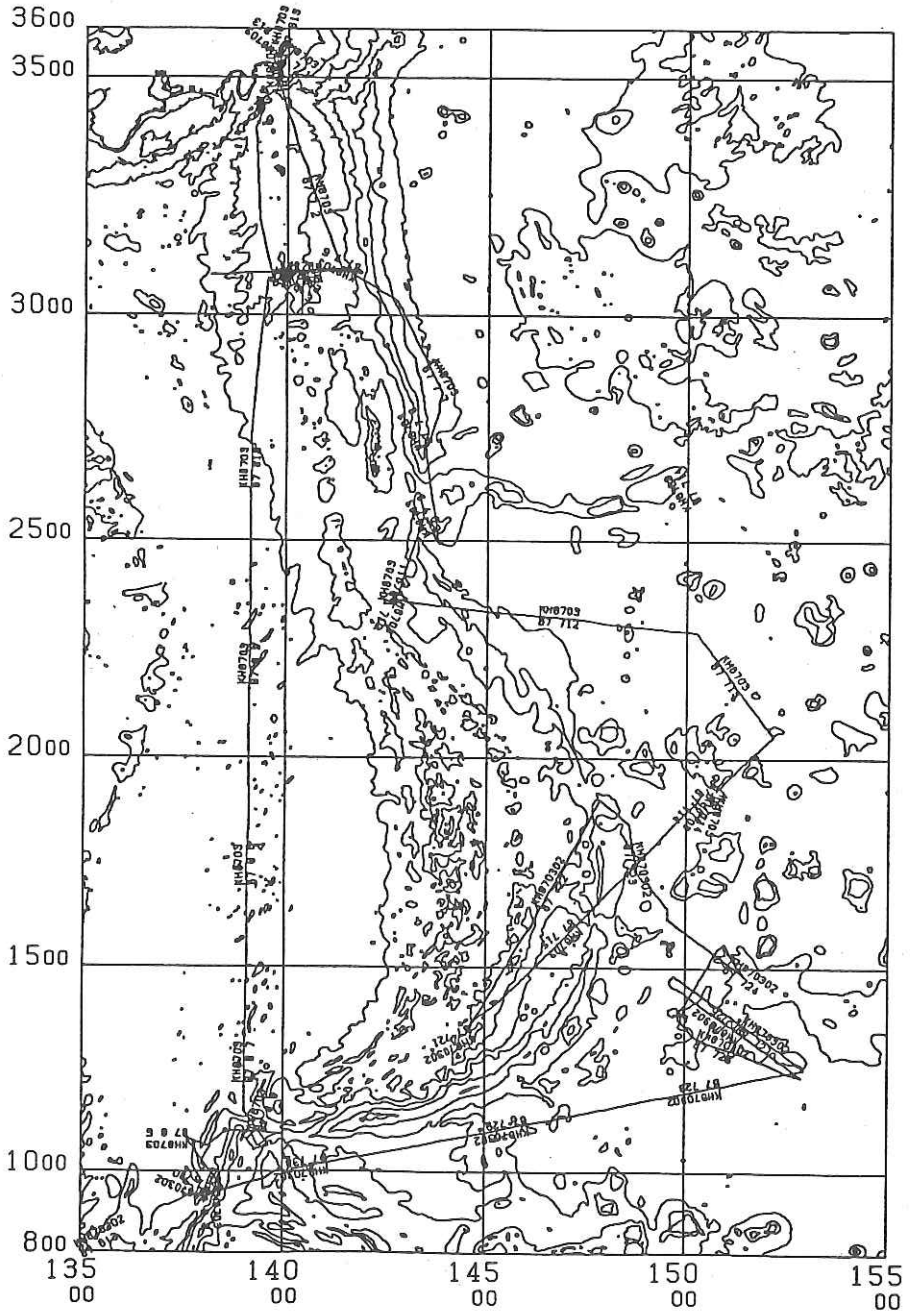

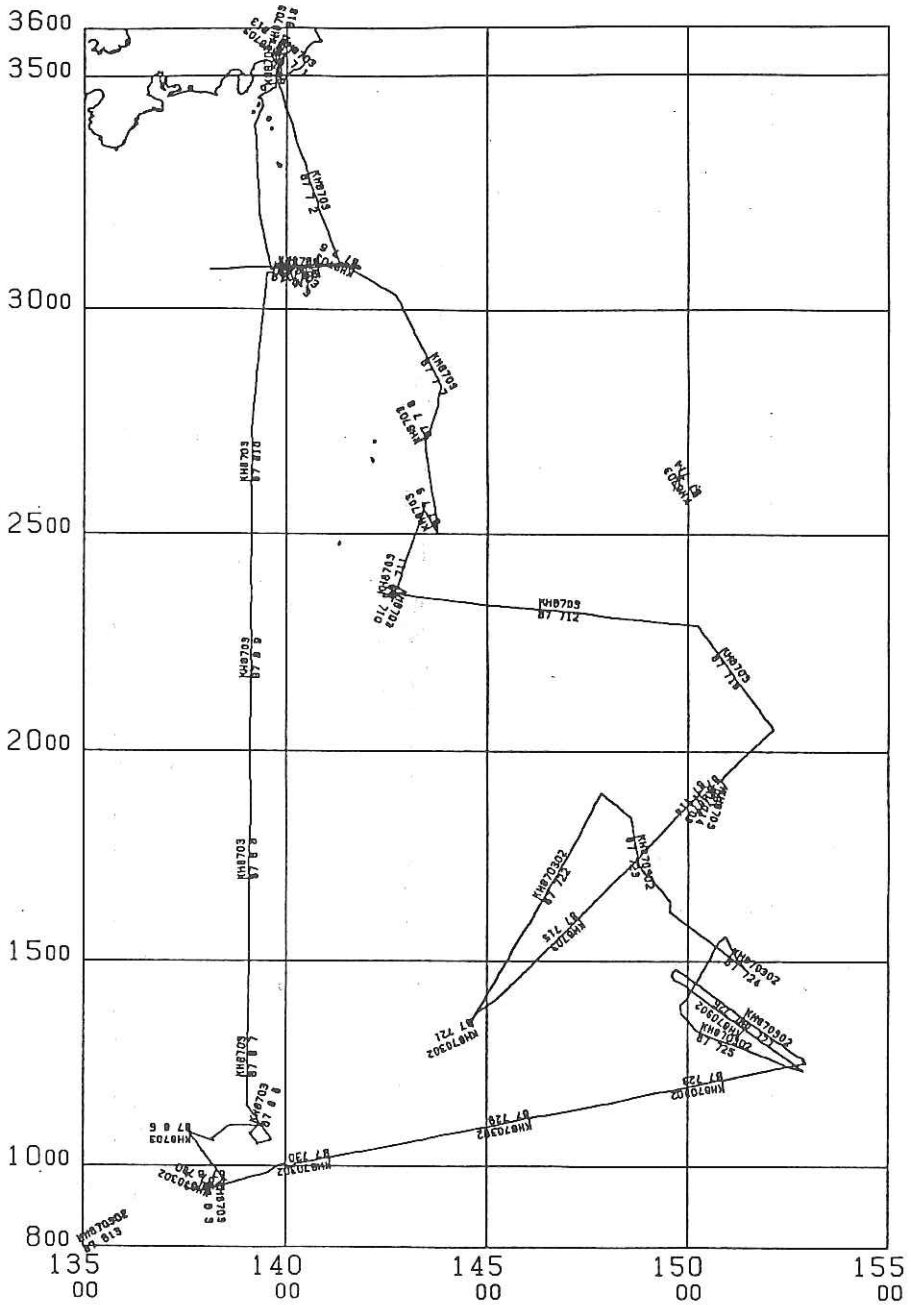
3600
3500
3000
2500
2000
1500
1000
800
135 00
140 00
145 00
150 00
155 00

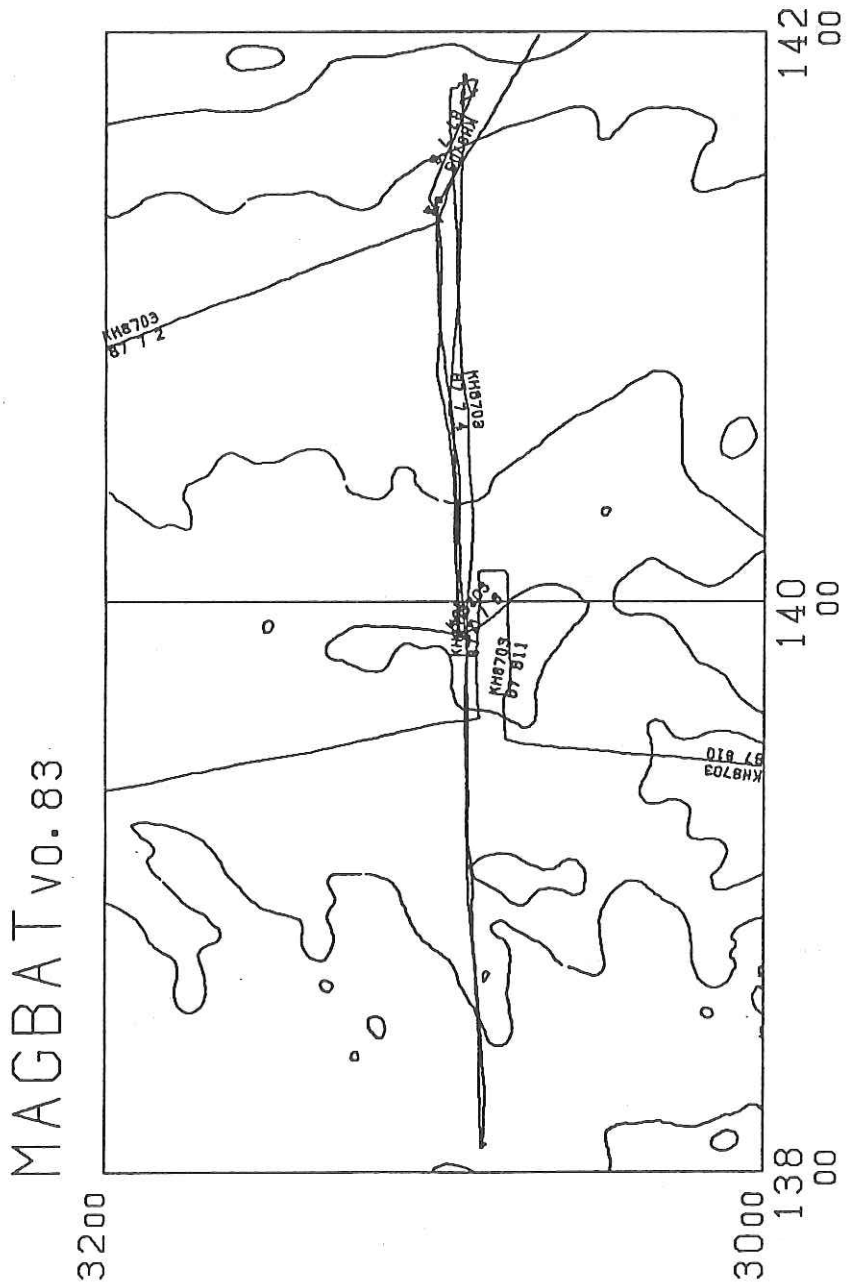
MAGBAT v0.83
3200
3000
138 00
140 00
142 00
KH8703 87 712
KH8703 87 714
KH8703 87 811
KH8703 87 810

3. LIST OF RESEARCH STATIONS IN THE CRUISE KH 87-3

Site No.	Position Lat.(N)	Long.(E)	Investigation	Water Depth(M)	Date & Time		Remarks
					July		
JK12	30°56.0'	139°52.7'	set OBM-S1	2280	3	08:27	Lv surface
JK14	30°59.7'	141°20.6'	set OBM-SMZ	3100	3	16:54	Lv surface
1	30°55.5'	141°45.3'	Dredge Haul	4670	3	22:09	on Bottom
	30°55.7'	141°49.3'	[D-1]	4080	4	02:50	final on Bottom
JK11	30°53.0'	139°01.3'	set OBM-S3	2000	4	18:05	Lv surface
JK10	30°51.1'	138°05.4'	set OBM-S5-ORI	4020	5	00:17	Lv surface
JK13-1	30°57.1'	140°39.1'	set OBP	2380	5	12:52	Lv surface
JK13-2	30°57.3'	140°39.3'	set OBM-C3	2370	5	13:45	Lv surface
2	30°54.9'	141°48.8'	Dredge Haul	3970	5	22:41	on Bottom
	30°55.5'	141°46.8'	[D-2]	4250	6	00:22	final on Bottom
3	30°53.4'	141°46.7'	Dredge Haul	4170	6	03:58	on Bottom
	30°54.4'	141°49.6'	[D-3]	4100	6	06:47	final on Bottom
4	27°11.1'	143°31.6'	Camera	5450	7	20:58	Start of Shots
	27°11.5'	143°31.3'	[C-1]	5740	7	22:19	End of Shots
5	27°08.3'	143°26.7'	Dredge Haul	6070	8	10:39	on Bottom
	27°09.5'	143°26.3'	[D-4]	5820	8	13:49	final on Bottom
6	25°25.4'	143°30.0'	Camera	2360	9	11:18	Start of Shots
	25°25.6'	143°29.6'	[C-2]	2360	9	12:38	End of Shots
7	25°26.4'	143°30.2'	Dredge Haul	1930	9	14:05	on Bottom
	25°27.3'	143°31.0'	[D-5]	2090	9	15:37	final on Bottom
8	25°31.6'	143°24.7'	Dredge Haul	2660	9	17:53	on Bottom
	25°32.7'	143°24.8'	[D-6]	2670	9	18:54	final on Bottom
9	23°34.8'	142°41.8'	Piston Coring [P-1]	3180	10	13:59	Hit on Bottom
10	23°37.3'	142°43.1'	Heat Flow	3210	10	17:15	Hit HF-1
	23°37.5'	142°43.3'				17:41	Hit HF-2
11	23°39.1'	142°43.9'	Transponder	3270	10	19:39	Start
	23°40.7'	142°44.3'		3300	10	21:59	End

Site No.	Position Lat.(N)	Long.(E)	Investigation	Water Depth(M)	Date & Time	Remarks
12	23°37.6'	142°34.2'	Piston Coring [P-2]	3170	11 Aug. 09:49	Hit on Bottom
13	9°19.0'	137°59.4'	Dredge Haul	1950	3 17:50	on Bottom
	9°18.9'	137°58.7'	[D-7]	1880	3 18:17	final on Bottom
14	9°20.9'	137°57.5'	Camera	-	3	Start of Shots
	9°20.8'	137°56.9'	[C-3]	1350	3	End of Shots
15	9°20.6'	137°57.4'	Dredge Haul	1400	3 22:07	on Bottom
	9°20.5'	137°56.6'	[D-8]	1210	3 22:52	final on Bottom
16	9°21.5'	137°56.3'	Dredge Haul	1250	4 00:43	on Bottom
	9°21.3'	137°55.8'	[D-9]	940	4 01:38	final on Bottom
17	9°21.7'	137°56.4'	Camera	-	4 02:51	Start of Shots
	9°21.5'	137°56.1'	[C-4]	1050	4 03:52	End of Shots
18	9°36.9'	138°26.0'	Dredge Haul	6200	4 10:28	on Bottom
	9°37.9'	138°25.5'	[D-10]	6190	4 11:29	final on Bottom
19	9°40.3'	138°22.3'	Dredge Haul	5270	4 15:39	on Bottom
	9°41.6'	138°20.9'	[D-11]	4680	4 17:26	final on Bottom
20	10°46.9'	137°35.7'	Heat Flow-A	4800	5 04:33	Hit A
	10°46.9'	137°35.4'	[HF-3] -B	4800	5 04:55	Hit B
	10°47.2'	137°35.5'	-C	4800	5 05:16	Hit C
21	10°46.6'	137°35.9'	Piston Coring [P-3]	4807	5 08:37	Hit on Bottom
22	10°35.6'	138°06.2'	Piston Coring [P-4]	4320	5 16:00	Hit on Bottom
23	10°35.5'	138°06.0'	Heat Flow [HF-4]	4350	5 17:53	Hit
24	10°57.6'	138°36.5'	Camera	-	6 00:36	Start of Shots
	10°57.8'	138°36.0'	[C-5]	2100	6 01:56	End of Shots
25	10°58.4'	139°19.6'	Piston Coring [P-5]	7330	6 09:42	Hit on Bottom
26	10°45.3'	139°05.2'	Heat Flow-A	4100	6 15:50	Hit A
	10°45.2'	139°05.3'	[HF-5] -B	4100	6 16:22	Hit B
	10°45.1'	139°05.3'	-C	4100	6 16:49	Hit C
27	10°29.0'	139°15.7'	Heat Flow [HF-6]	5140	6 21:53	Hit

4. CONFIGURATION OF THE PROTON MAGNETOMETER SYSTEM FOR KH 87-3 CRUISE

M. Nakanishi, T. Furuta, K. Sayanagi and K. Tamaki

Geomagnetic total force was measured in the whole legs of this cruise by a proton precession magnetometer except while the ship was drifting for station work. The system for measurement consists of a magnetometer unit, a data processing unit and a navigation-controlled unit. The magnetometer unit is composed of a console and a sensor with a toroidal coil towed after the ship by a nonmagnetic cable with a length of 250 m. The data processing unit consists of two sets of microcomputers. One microcomputer is used to control the entire system as well as to record data. The other is to calculate magnetic anomalies from measured data and to display their profiles. The ship's position is provided by a Loran-C receiver. The framework of this system is illustrated in Fig. 4-1.

The method of measurement and data logging are as follows;

1. The console of the proton magnetometer provides an exciting signal to the sensor at an interval of 30 seconds.
2. The period of protons' precessional motion around the direction of the geomagnetic field is transmitted through the cable to the magnetometer console and counted.
3. The period is converted from an analog signal to digital and fed through a parallel cable to a microcomputer controlling the system.
4. The microcomputer receives the period data every 30 seconds and navigation data such as day, hour, minute, second, latitude, longitude, ship's speed against seafloor and its heading from the navigation unit with 4 seconds interval. This magnetometer system is controlled by this date.
5. The microcomputer calculates the geomagnetic total force from the data of precessional period.
6. All the data are logged in a 8-inch floppy disk, printed out with one minute interval and transmitted through a serial cable (RS-232C) to the processing microcomputer. They are also fed to a microcomputer of the Kobe Univ.
7. The processing microcomputer receiving the data calculates a reference geomagnetic field at the site and magnetic anomaly by subtracting it from a measured geomagnetic total force.
8. Profiles of magnetic anomalies are displayed on a rolled paper with a time axis and data of anomalies are logged in a 5-inch floppy disk.

All the programs for this system are written in N88-BASIC (MS-DOS), which run on MS-DOS by compilation.

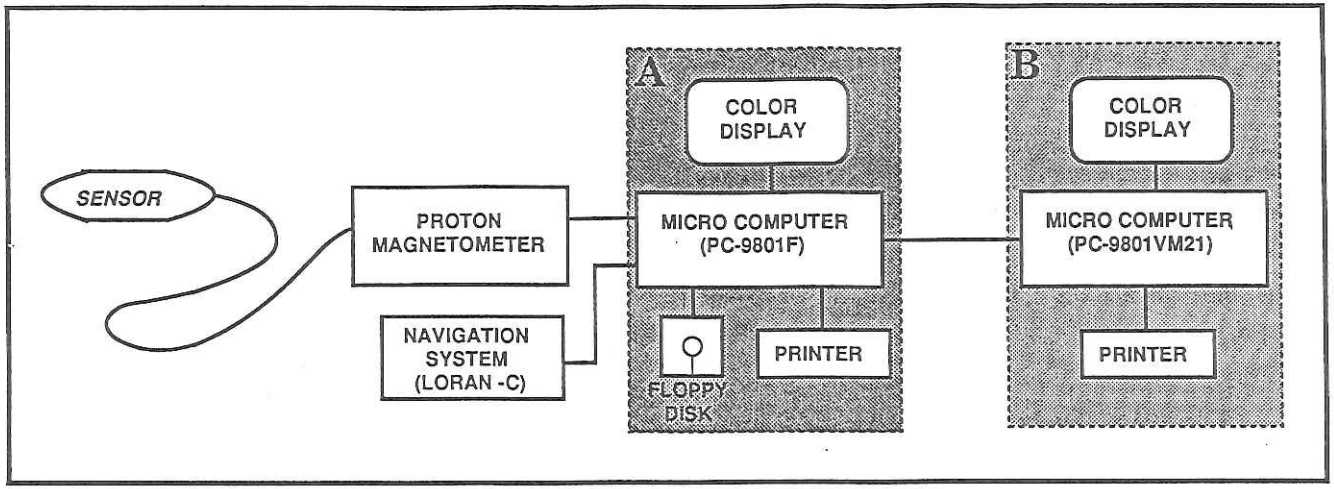

Fig. 4-1 General view of the proton magnetometer system. Arrows indicate flows of data. A is a microcomputer unit that controlls this system and records data. B is for real-time display of magnetic anomalyprofiles.

5. GEOMAGNETIC SURVEY AROUND IZU-OGASAWARA TRENCH AND OGASAWARA PLATEAU (KH 87-3 AND KT 86-9)

(KH87-3) M. Nakanishi, K. Sayanagi, T. Furuta, and K. Tamaki
(KT86-9) M. Nakanishi

Tracks on which geomagnetic total force was measured in both KH87-3 and KT 86-9 cruises near the Izu-Ogasawara trench are shown in Fig. 5-1. Magnetic anomaly pattern near this area previously reported was obscured. Based on a rough sketch of available data, we planed tracks of the two cruises so as to be nearly perpendicular to the trend of the Japanese lineation set which exists in the vicinity of the surveyed area.

Fig. 5-2 shows magnetic anomaly profiles along three tracks in Fig. 5-1. Profile 1 and 2 are situated in an area east of the trench. Profile 3 is situated near the trench axis. Dotted line in Fig. 5-2 indicates the trench axis and dashed lines indicate magnetic lineations. Amplitudes of anomalies are about 600 nT in thier maximum and gradually decrease as approaching the trench. In spite of their smaller amplitudes the magnetic lineations can be identified west of the trench axis. Correlation of magnetic anomalies in the profiles 1 and 2 is shown in Fig. 5-3. The model profile is calculated on the basis of the geomagnetic reversal time scale of Kent and Gradstein (1985). Lineations from M13 (137 Ma) to M18 (144 Ma) are identified.

Profiles of magnetic anomalies on the Ogasawara plateau are shown in Fig. 5-2 (shaded portion) and Fig. 5-4. Direction of profiles from 2 to 5 is roughly north-south. That of profiles 6 and 7 is about east-west. Negative anomalies surpass positive anomalies on the plateau. The largest negative anomaly is about -800nT. Wavelengths of anomalies of thenorth-east anomalies are several ten kilometers. Those of the east-west anomalies are a few hundred kilometers. This seems to indicate the strike of magnetic source layers of the basement body in the plateau is roughly about east-west.

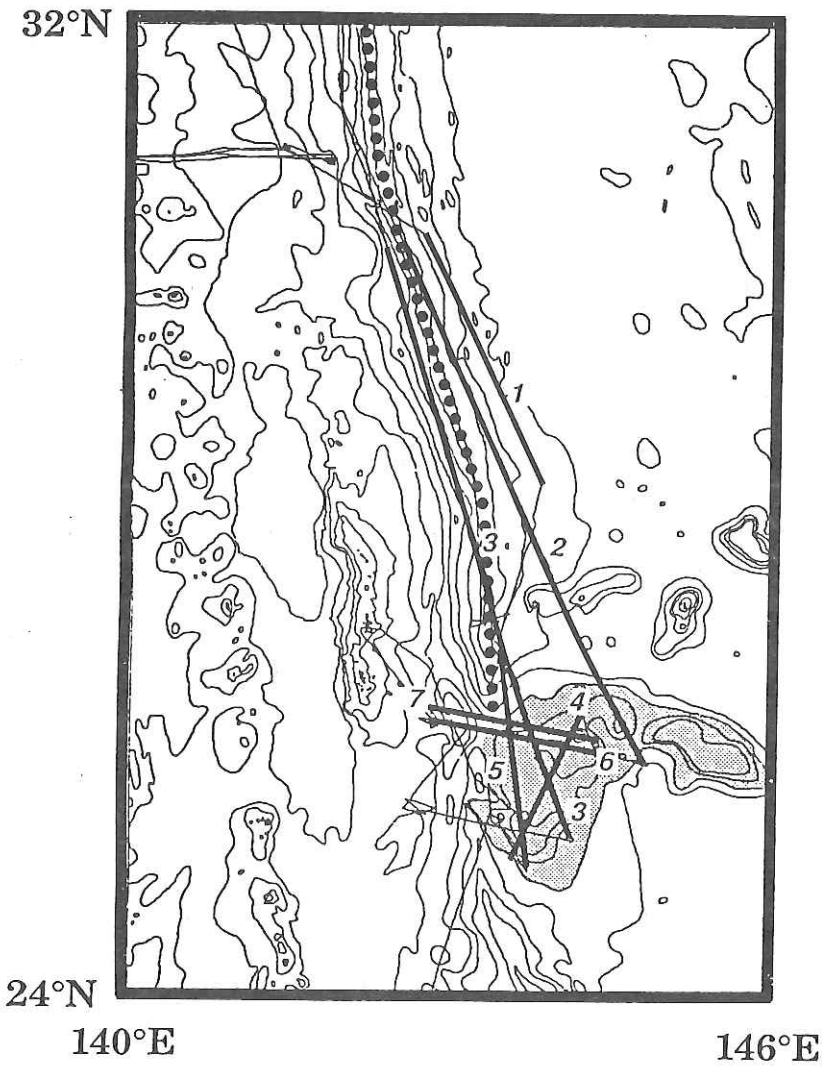

Fig. 5-1 Tracks of geomagnetic total force measurement during both KH87-3 and KT86-9 cruises. Numerical figures on the tracks are cited in Figs. 5-2, 5-3 and 5-4. Dotted line is the axis of the Izu-Ogasawara Trench. The hatched zone is the Ogasawara Plateau. The bathymetric contours are prepared on the basis of GEBCO (General Bathymetric Chart of the Oceans) digital bathymetric file compiled by JODC (Japan Ocean Data Center). The contour interval is 1,000 m.

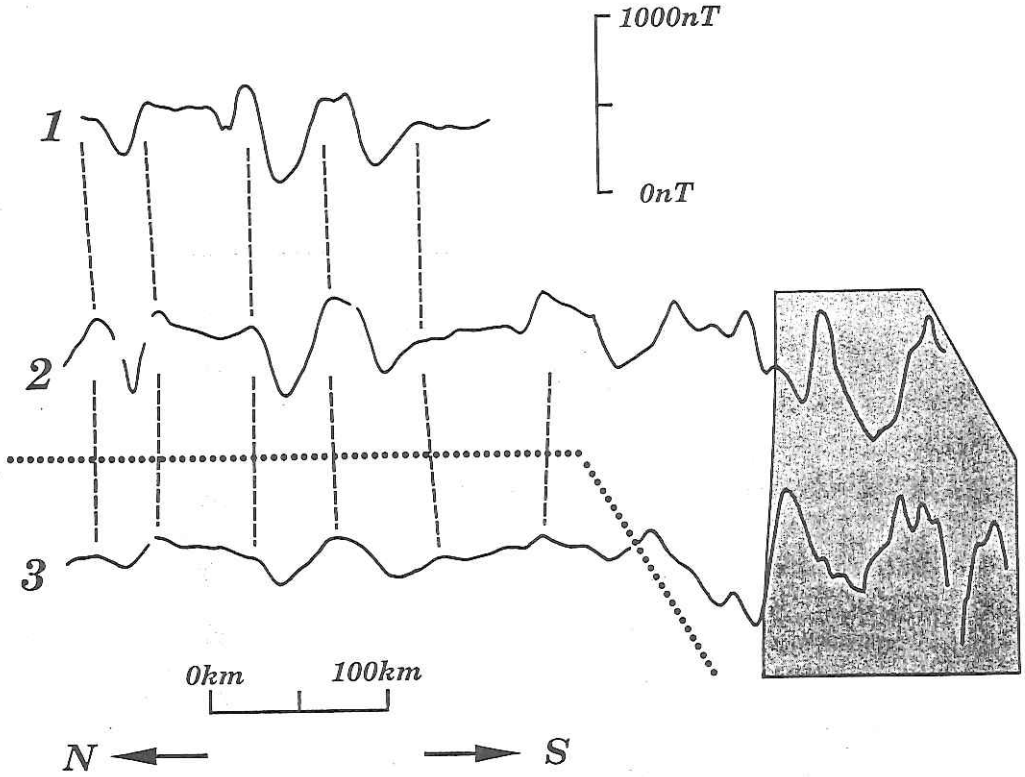

Fig. 5-2 Profiles of geomagnetic anomalies in the vicinity of the Izu-OgasawaraTrench. Dotted line is the axis of the Izu-Ogasawara trench. Dashed lines are magnetic anomaly lineations. The hatched zone is the Ogasawara Plateau. Magnetic anomalies are calculated referring to IGRF (Internal Geomagnetic Reference Field; IAGA, Division I Working Group 1, 1985). Profile labels refer to Fig. 5-1.

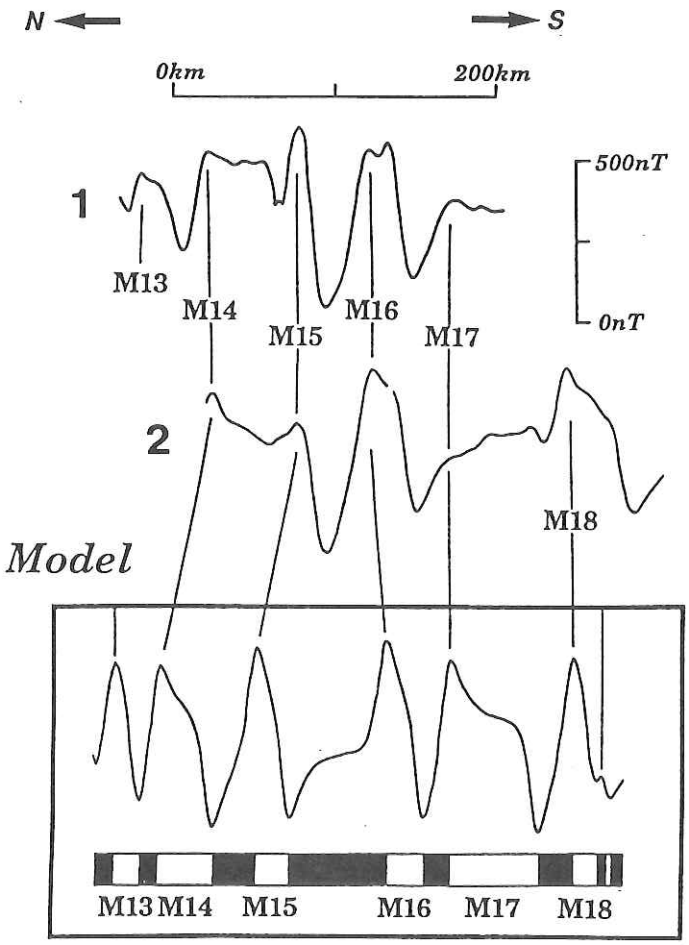

Fig. 5-3 Correlations of magnetic anomaly lineations. The bottom profile is synthesized on the basis of the geomagnetic reversal time scale of Kent and Gradstein (1985). Profile labels refer to Fig. 5-1.

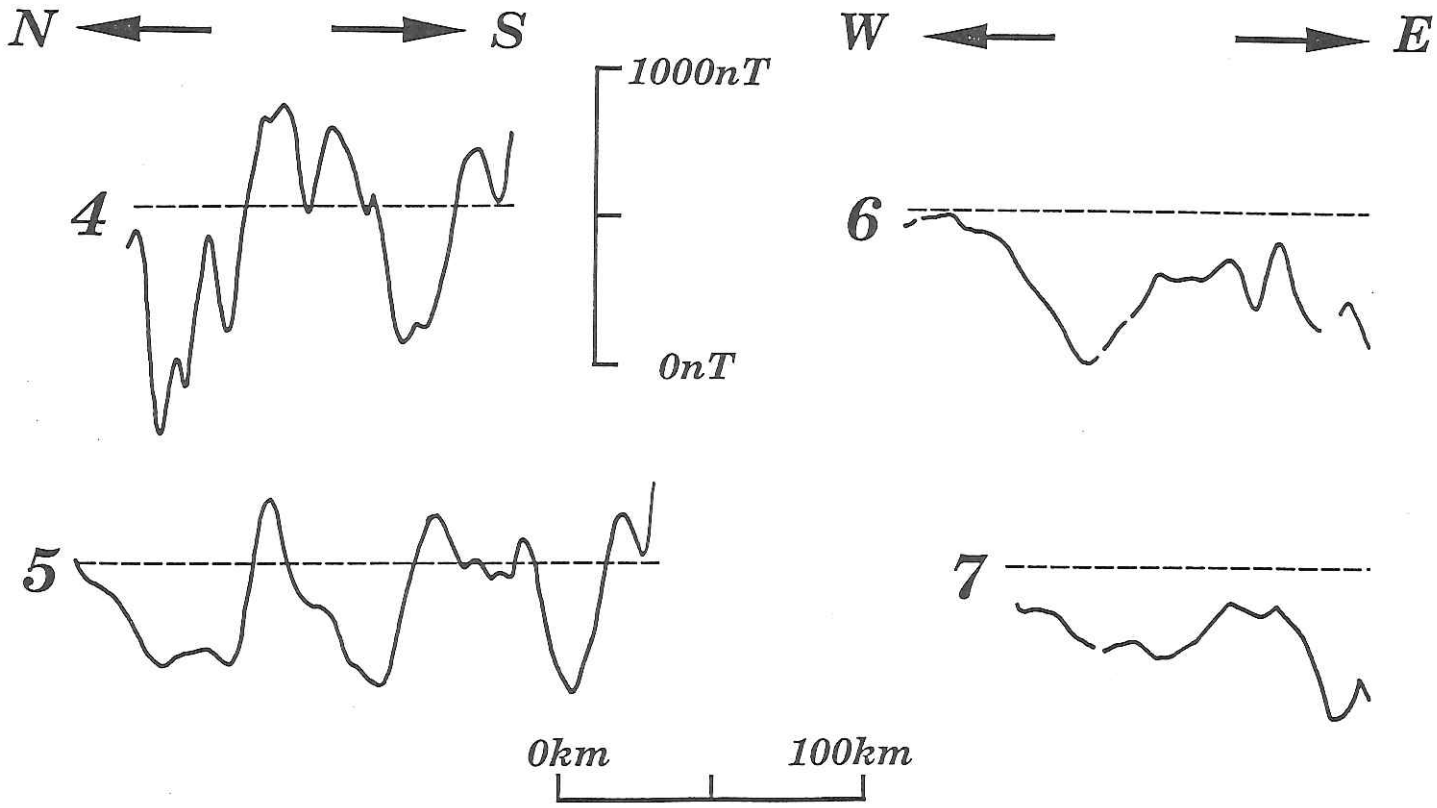

Fig. 5-4 Magnetic anomaly profiles on the Ogasawara Plateau. Dashed lines are zero level. Other conventions as in Fig. 5-2.

6. GEOMAGNETIC SURVEY OF THE EAST MARIANA BASIN

K. Tamaki, M. Nakanishi, K. Sayanagi and K. Kobayashi

6-1. INTRODUCTION

Aerial distribution of the geomagnetic total force in the East Mariana Basin was surveyed during Legs 1 and 2 of the KH 87-3 cruise (Fig. 6-1,2, and 3). The last few days of the Leg 1 and full 10 days of the Leg 2 were devoted to this geomagnetic survey. The surveyed area is divided into two parts, separated by the Magellan Seamounts trending nearly east-west. The area surveyed in Leg 1 is the northern part of the East Mariana Basin, north of it, while that in Leg 2 is situated in the southwestern part of the East Mariana Basin, south of the Magellan Seamounts.

6-2. OBJECTIVES OF THE SURVEY

The previous mapping of the magnetic anomaly lineations in the northwestern Pacific suggests that the East Mariana Basin is the oldest part of the Pacific Plate (Cande et al.,1979). The Japanese, Hawaiian and Phoenic Mesozoic magnetic anomaly lineations all get older as they approach the East Mariana Basin. Magnetic anomaly lineations of the East Mariana Basin, however, have been unmapped until mid '80s, since the geomagnetic anomalies are weak with amplitudes less than 100 nT and the survey tracks are scarce in the basin.

Recently, Handshumacher et al. (in press) revealed magnetic anomaly lineations at the northern part of the East Mariana Basin. They identified magnetic anomalies from M26 to M38 on the basis of newly obtained aeromagnetic data. The anomalies M30 to M38 were newly discoverved in Mesozoic oceanic basins in the world. They presented improved Mesozoic magnetic reversal sequences.

Target of our survey in the northern part of the East Mariana Basin is to confirm the sequence of anomalies; M30 to M38. Although Handschumacher et al's data densely cover the basin, their tracks have not been extended to the northern area, a precisely-mapped Japanese lineations zone. So, we aimed at connecting their results with the well-mapped area of the Japanese lineations and attempted to confirm comformity between the newly proposed M30 - M38 sequence and previously mapped anomalies younger than M29.

Target for Leg 2 is to identify magnetic anomaly lineations in the southeastern part of the East Mariana Basin previously revealed by research

cruises conducted by the Hawaiian Institute of Geophysics in 1980 and the Lamont-Doherty Geological Observatory in 1979. The data were released through NOAA Geophysical Data Center. We designed the survey tracks to connect the data of both institutes with ours.

6-3. RESULTS OF OBSERVATION

Results of the survey in the northern part of the East Mariana Basin are that magnetic anomalies, M30 - M38, newly proposed by Handschumacher et al. (in press) are misordered. Our profile, which was carefully designed to reveal the best record of M27 - M30 connection, suggests that M29 was misidentified by them to be M30. So, the magnetic anomalies M30 - M38 should be renamed as M29 - M37.

Unidentified magnetic anomaly lineations in the southern part of the East Mariana Basin were identified as M22 to M37. M22 was newly mapped at the northernmost extension of our survey track. The mapping of M22 with a characteristic anomaly pattern was a key of our successful identification. Another key of our success is correlation of the profiles of Legs 1 and 2. The correlation suggests that magnetic reversal sequence of M22 to M37 is probably improved with addition of several new events.

REFERENCES

Cande, S. C., R. L. Larson, and J. L. LaBreque: Magnetic lineations in the Pacific Jurassic quiet zone. Earth Planet. Sci. Lett., **41**, 434-440, 1978.

Handschmacher, D. W., W. W. Sager, T. W. C. Hilde, and D. R. Bracey: Pre-Cretaceous tectonic evolution of the Pacific Plate and extension of the geomagnetic porality reversal time scale with implications for the origin of the Jurassic 'Quiet Zone'. Tectonophys., in press.

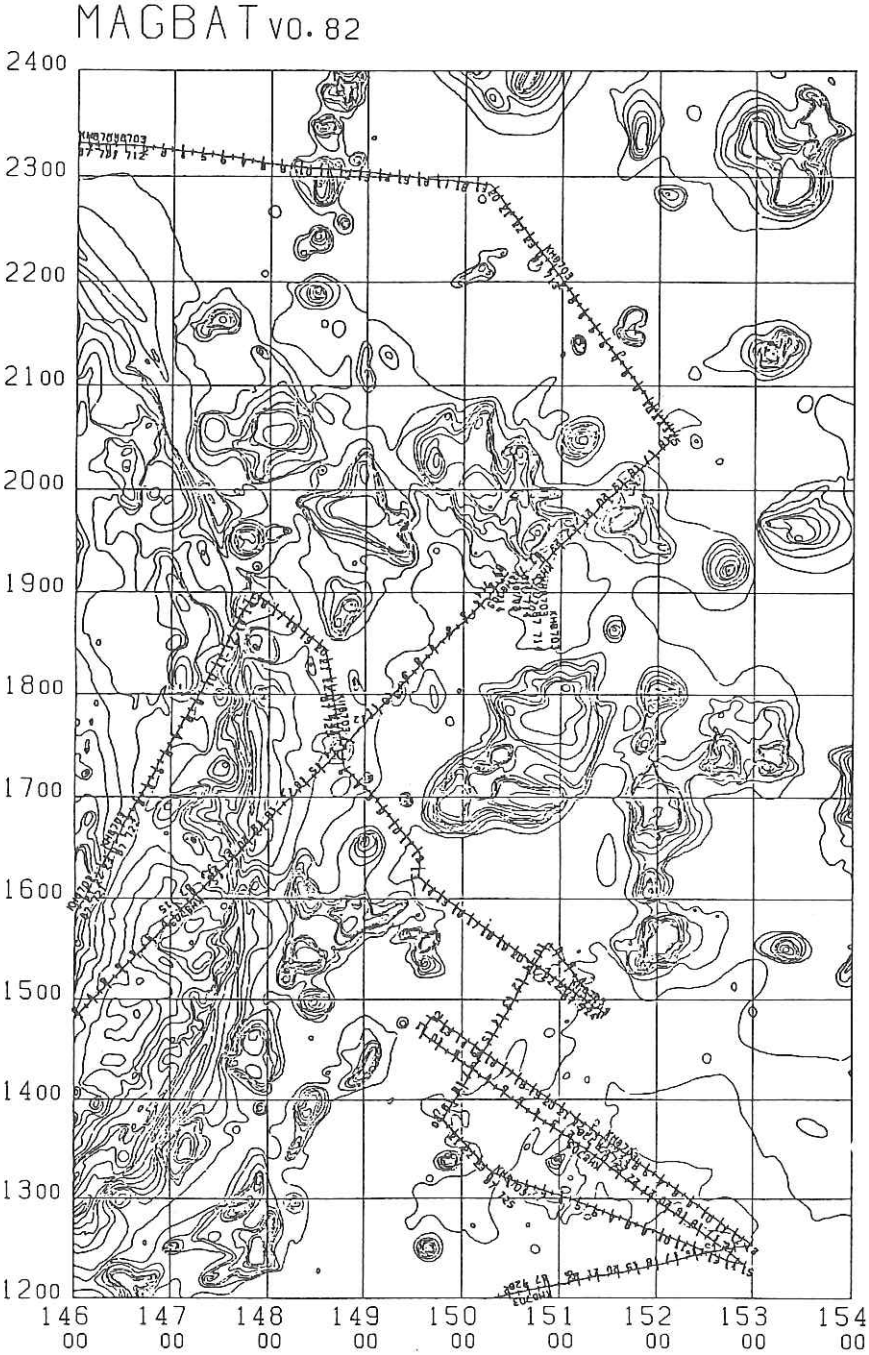

Fig. 6-1 Survey tracks of the East Mariana Basin during KH 87-3 cruise.

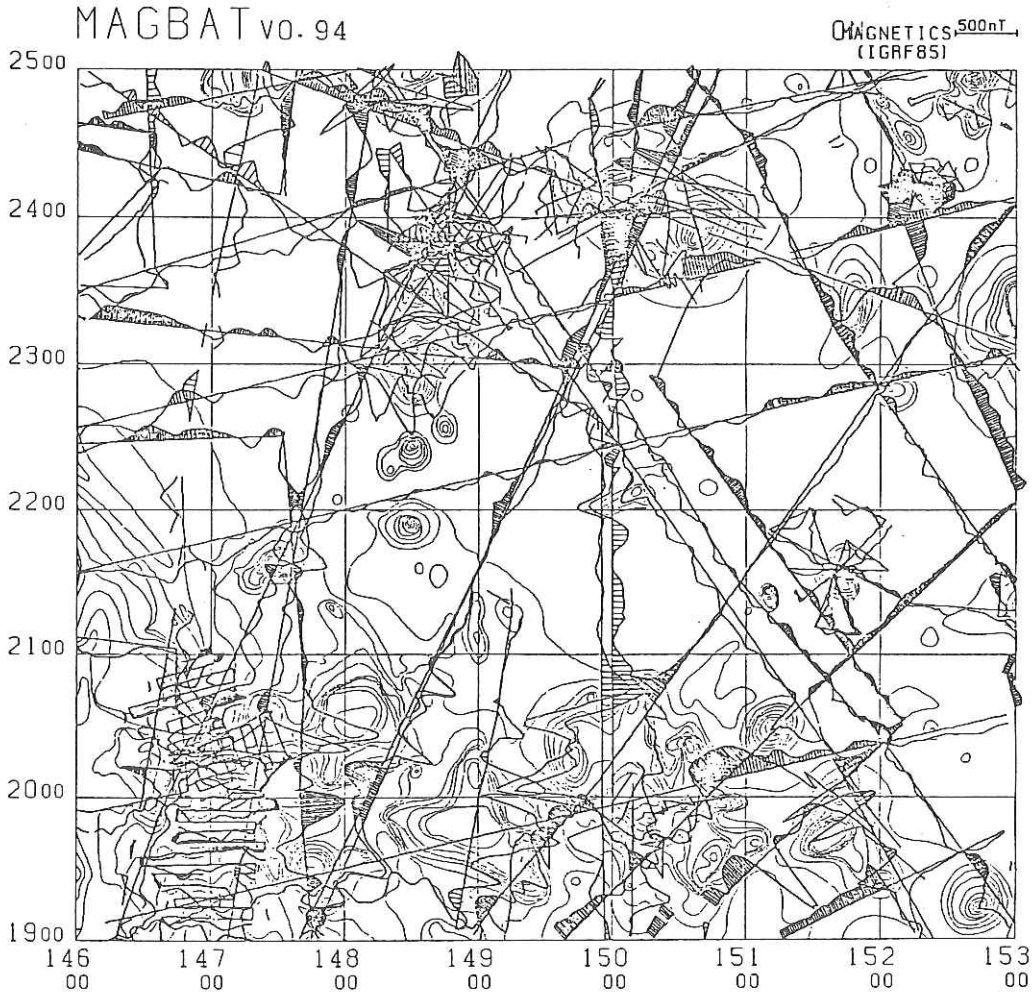

Fig. 6-2 Profiles of magenetic anomalies along tracks 1 to 3 of the KH 87-3 cruise in the northern part of the East Mariana Basin with their possible correlation.

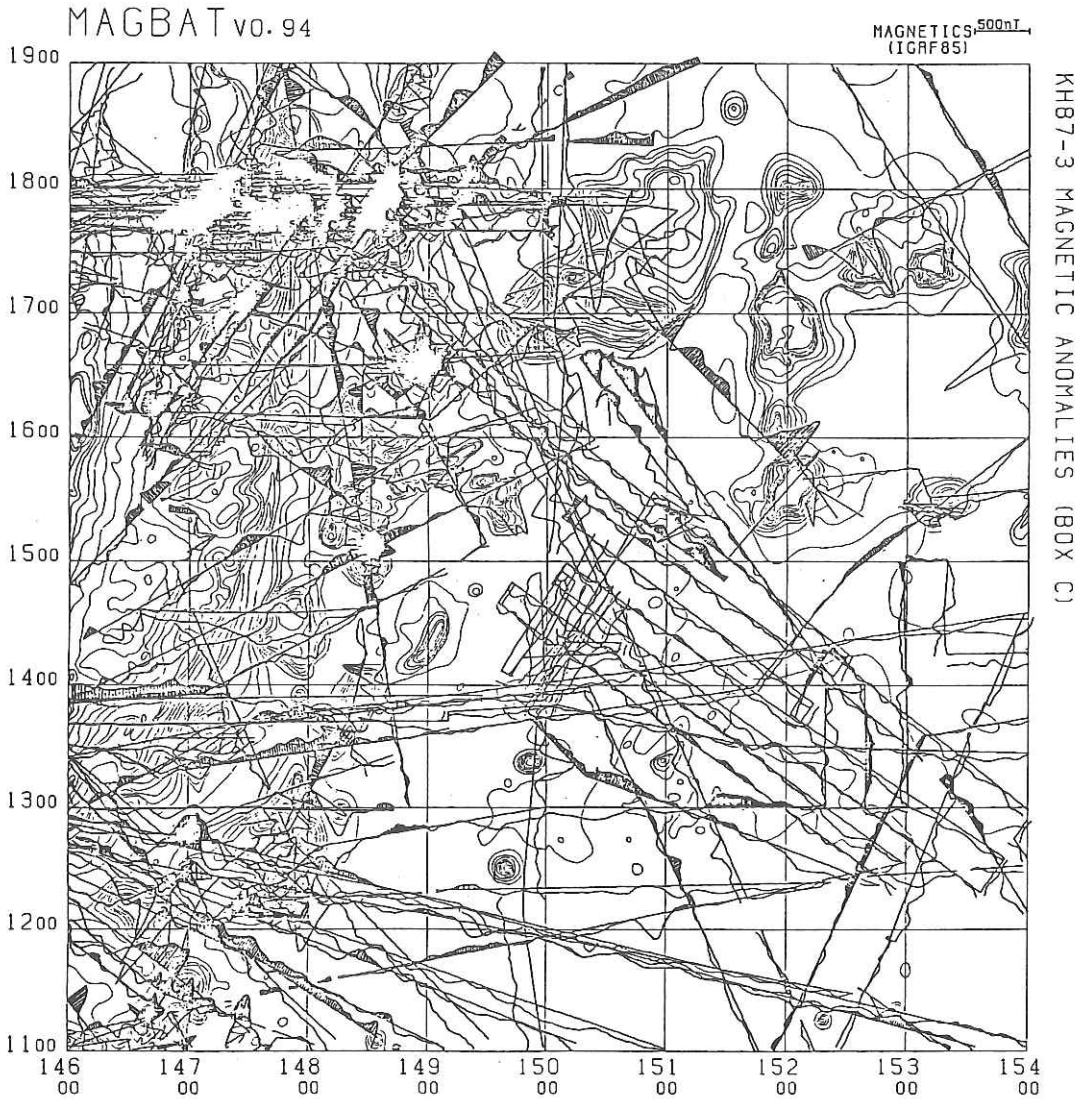

Fig. 6-3 Profiles of magenetic anomalies along tracks 4 to 7 of the KH 87-3 cruise in the southern part of the East Mariana Basin.

7. GEOMAGNETIC MEASUREMENTS ACROSS YAP ISLAND

M. Nakanishi and M. Watanabe

Geomagnetic total force was measured on the Yap Island by a proton magnetometer, OMNI IV during anchoring there. Number of measurement points were 43. We measured four or five times at a point until the measured value became stable. The points were chosen along roads so that the direction of the measurement line could be NW-SE across Yap Island. The direction is roughly perpendicular to the strike of geological structure of Yap Island. Magnetic measurement off the roads were difficult, because the land is very steep. Stability of our roadside data may be due to that roads are not paved and that there were few utility poles and electric wires which may disturbe ambient geomagnetic field.

One line of the measurement was completed in about two hours, so that the daily variation of geomagnetic field was not considered. The areas where measurements were carried out are shown in Fig. 7-1. The measurement points are shown Fig. 7-2 and data are shown in Table 7-1.

Acknowledgements

The authors thank the Kokusaidenshi Co. for permitting the use of a proton magnetometer, OMNI IV.

TABLE 7-1 Summary of measured values of the geomagnetic total force on the Yap Island.

Point No.	Latitude	Longitude	Total Force (nT)
1	9°32'50"N	138°6'22"E	35338.6
2	9°32'44"N	138°6'25"E	37343.2
3	9°32'43"N	138°6'28"E	37477.2
4	9°32'42"N	138°6'34"E	37546.4
5	9°32'41"N	138°6'40"E	37563.4
6	9°32'42"N	138°6'45"E	37553.3
7	9°32'38"N	138°6'52"E	37544.2
8	9°32'32"N	138°6'58"E	37556.3
9	9°32'28"N	138°7'02"E	37572.8
10	9°32'25"N	138°7'01"E	37543.2
11	9°32'20"N	138°6'58"E	37545.4
12	9°32'17"N	138°6'58"E	37542.3
13	9°32'10"N	138°6'59"E	37539.3
14	9°32'02"N	138°6'58"E	37496.9
15	9°32'01"N	138°7'04"E	37262.6
16	9°32'02"N	138°7'08"E	37343.3
17	9°32'03"N	138°7'12"E	37280.6
18	9°32'00"N	138°7'13"E	37315.1
19	9°31'59"N	138°7'16"E	37535.8
20	9°31'58"N	138°7'18"E	37534.6
21	9°31'58"N	138°7'22"E	37556.1
22	9°31'57"N	138°7'26"E	37514.3
31	9°32'48"N	138°9'53"E	37642.6
32	9°32'47"N	138°9'46"E	37704.6
33	9°32'39"N	138°9'37"E	37573.2
34	9°32'41"N	138°9'30"E	37586.8
35	9°32'46"N	138°9'16"E	37602.7
36	9°32'59"N	138°9'14"E	37618.9
37	9°33'04"N	138°9'13"E	37598.4
38	9°33'12"N	138°9'05"E	37597.2
39	9°33'19"N	138°9'02"E	37595.6
40	9°33'22"N	138°8'57"E	37606.0
41	9°33'29"N	138°8'50"E	37631.2

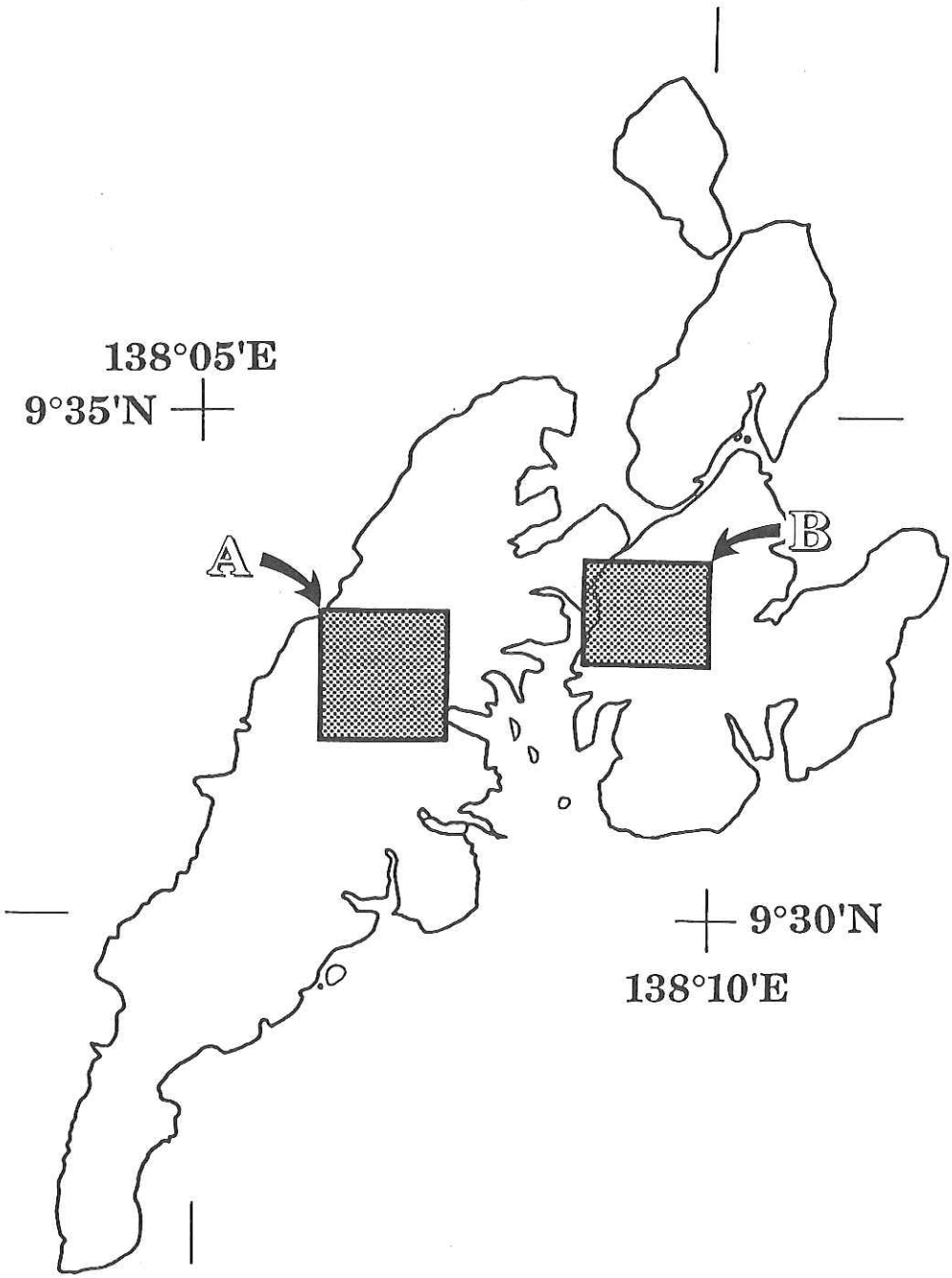

Fig. 7-1 Area of the geomagnetic total force measurement. Hatched zones; A, B, are that measurements were completed.

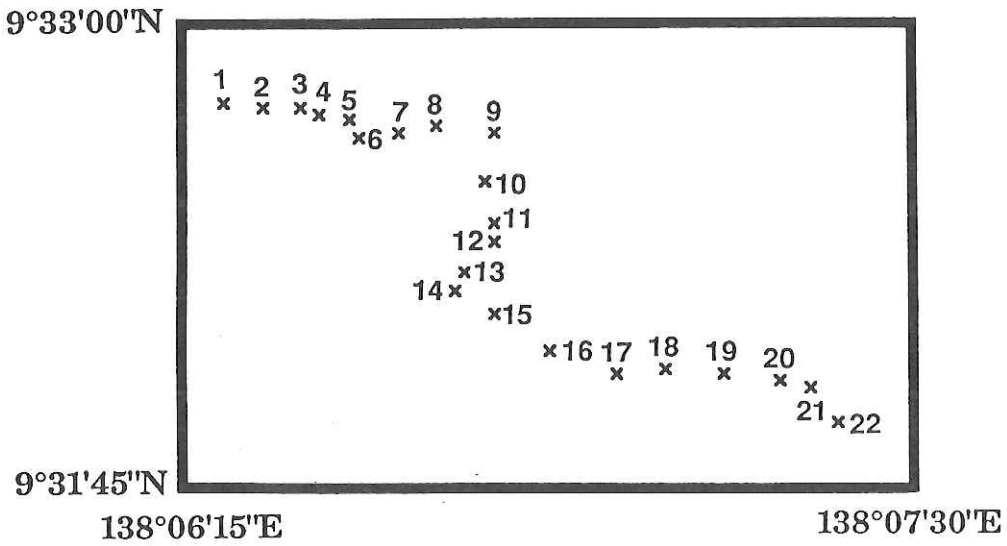

Fig. 7-2 Distribution of measured points in the area A. Numbers attached to the points are cited in Table 7-1.

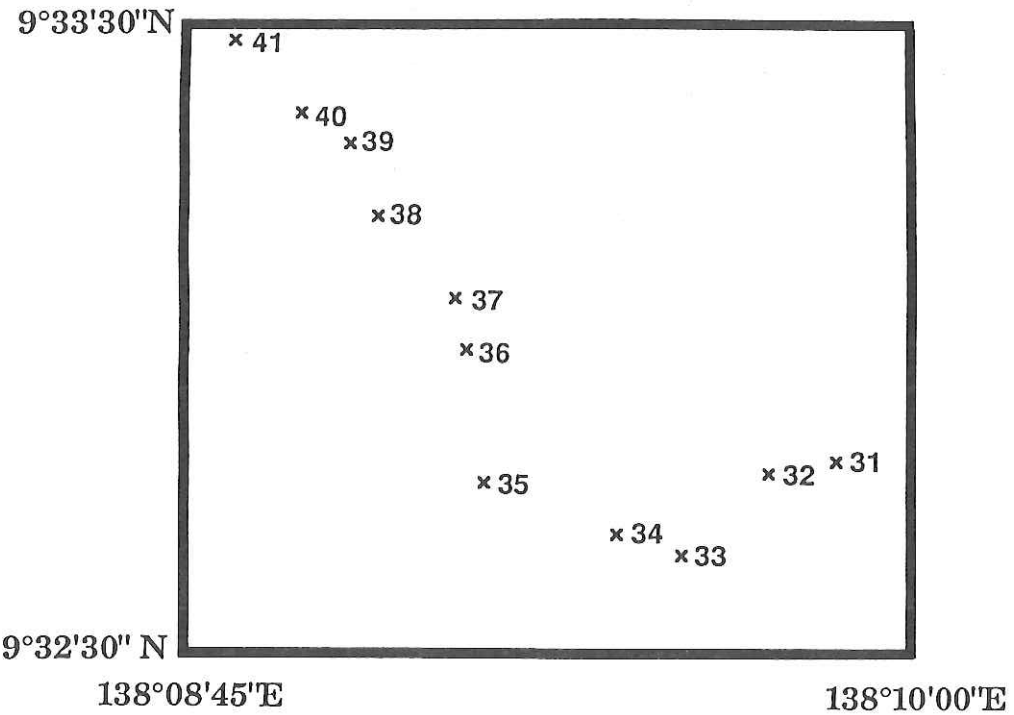

Fig. 7-3 Distribution of measured points in the are B.Numbersattached to the points are cited in Table 7-1.

8. GEOMAGNETIC SURVEY OF THE YAP ARC-TRENCH

K. Sayanagi and N. Nakanishi

The Yap arc-trench is a part of the Izu-Ogasawara-Mariana-Yap-Palau arc-trench system. The trench is bordered to the south by the Parece Vela Basin, and to the north by the West Caroline Basin. The geomagnetic survey was performed in the northern portion of the trench. In this section we report a summary of magnetic data collected by cruise KH 87-3, Legs 2 to 3 between 30th July and 7th August, 1987.

Fig. 8-1 shows ship's tracks for the survey in this area. The ship's positions were fixed by Loran C. The positions near Yap Islands, however, wereoften fluctuated, because one of three Loran C stations, the Yap Island station, is too close in relation to the remaining two stations. The heavy lines in Fig. 8-1 denote the ship's tracks on which total geomagnetic field was measured by a ship-towed proton precession magnetometer (Type O.R.I.). The detailed measurement system is described by Nakanishi et al. (in this volume). Data sampling interval was every 30 seconds. More than 2500 magnetic data points, more than 5000 magnetic values are included along the heavy track lines. The obtained data are of high quality.

Magnetic anomalies were derived by removing the International Geomagnetic Reference Field, Epoch 1985.0 from the total magnetic field measurements. Magnetic anomalies along the ship's tracks are shown in Fig. 8-2. The peak to peak amplitudes of the magnetic anomalies in this area were rather low, about 20 to 180 nT in the north of the trench, about 30 to 300 nT in the west, and less than about 250 nT in the east. The feature of low amplitude can also be seen over the entire Parece Vela Basin (Mrozowski et al., 1979).

Fig. 8-3 represents a compilation of marine magnetics data from this cruise and the previous surveys, plotted as magnetic anomalies along ship's tracks. The previous data were provided from the Hydrographic Department, Maritime Safety Agency of Japan and National Oceanic and Atmospheric Administration (NOAA). From the observation of magnetic anomalies, we could not identify magnetic lineations.

REFERENCE

Mrozowski, C. L., and D. E. Hayes: The evolution of the Parece Vela Basin, eastern Philippine Sea. Earth Planet. Sci. Lett., **46**, 49-67, 1979.

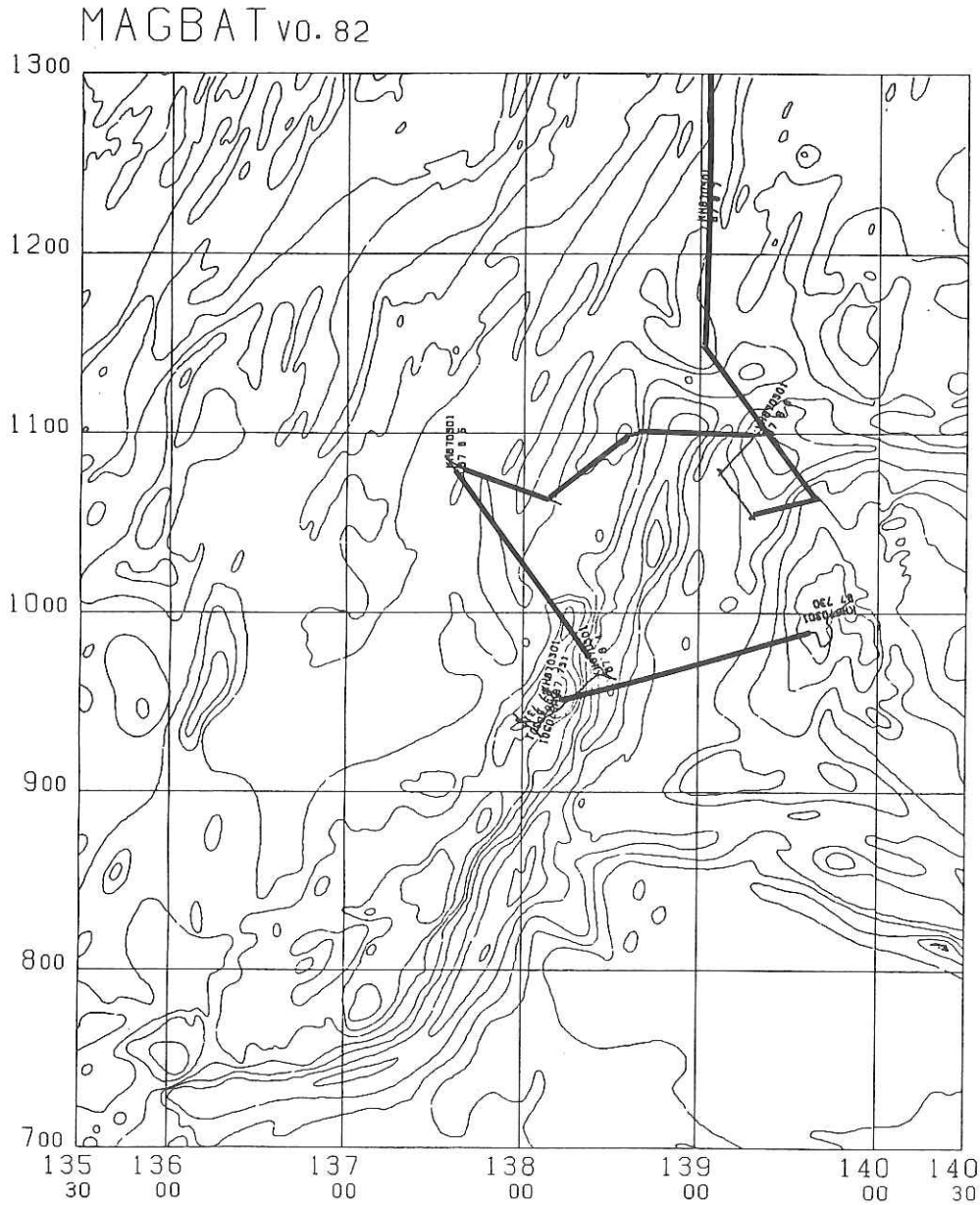

Fig. 8-1 Ship's tracks in the Yap arc-trench area. Tracks for magnetic survey are indicated with heavy lines.

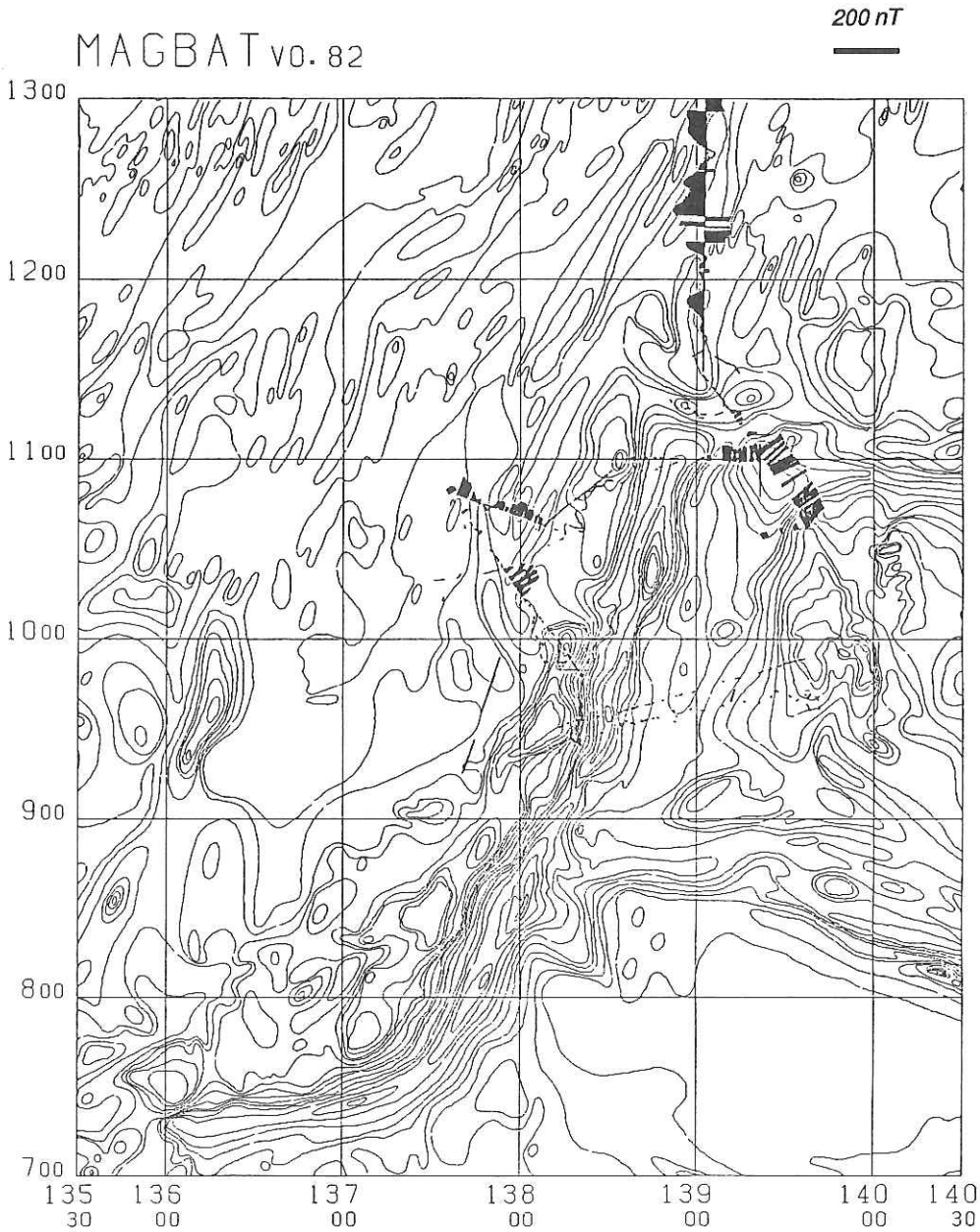

Fig. 8-2 Magnetic anomalies plotted along ship's tracks in the survey area. Positive anomalies are hatched.

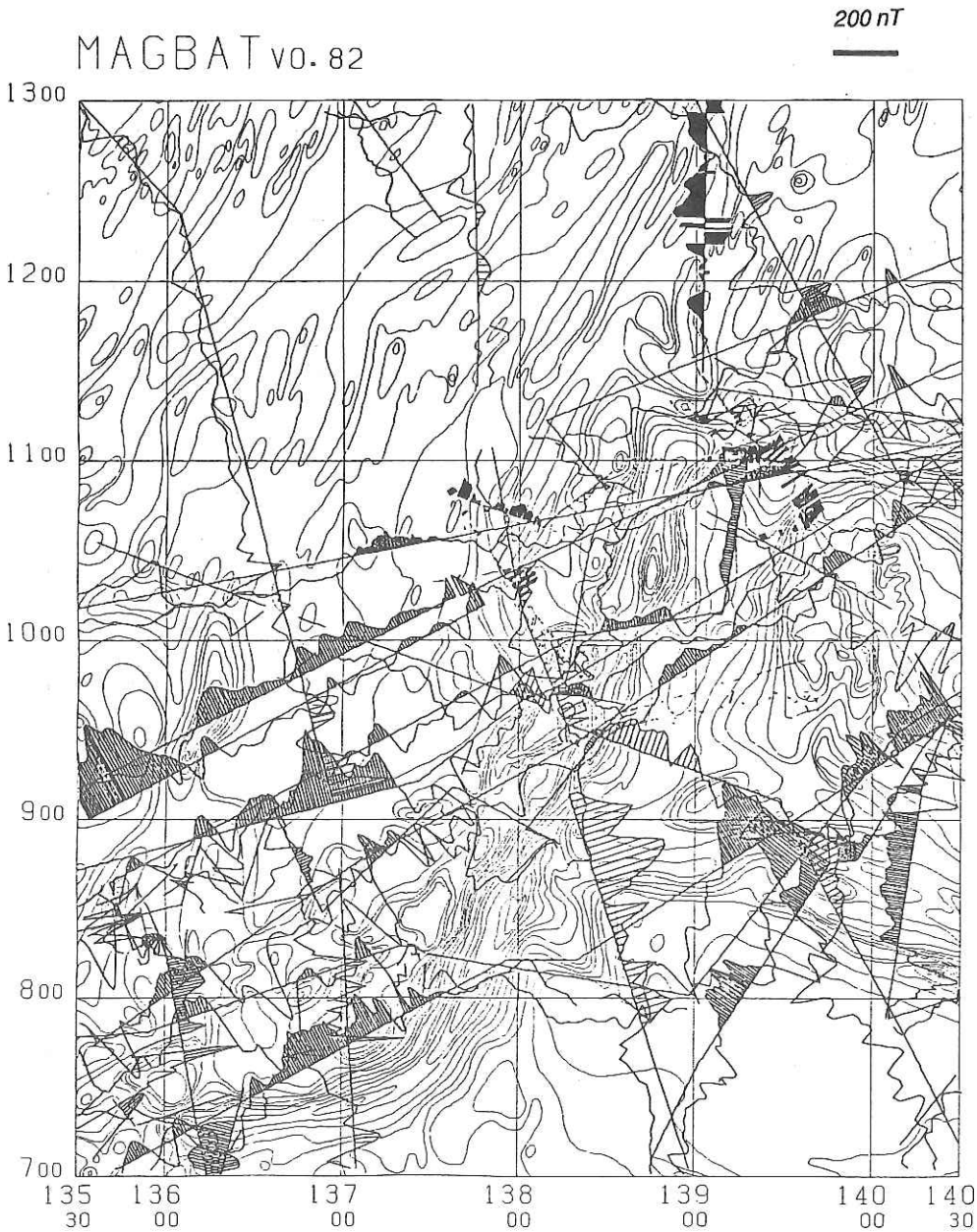

Fig. 8-3 Magnetic anomalies in the survey area compiled from available data along ship's tracks . The source of total field data is from the Hydrographic Department, Maritime Safety Agency of Japan and the National Oceanic and Atmospheric Administration (NOAA).

9. MEASUREMENT OF THE THREE COMPONENTS OF THE GEOMAGNETIC FIELD

Masako Miki and Yasuhisa Adachi

9-1. Introduction

During the KH 87-3 research cruise, magnetic surveys by STCM (Ship-board Three Component Magnetometer) were carried out in the East Mariana Basin and other northwestern Pacific regions. As this is the first time to measure three components of geomagnetic field in this area, we expect to obtain new information on the identification of magnetic anomaly in the northwestern Pacific. Particularly, in the East Mariana Basin, the data would help to solve the ambiguities on the origin of the Pacific Plate related to the R-R-R triple junction.

9-2. STCM

STCM measures intensities of three components of a geomagnetic field through flux gate sensors settled on the upper deck of the ship. The sensors were assembled rectangular to each other. In this cruise, they were fixed completely on the deck.

Three component geomagnetic anomalies give more information than total intensity anomalies usually measured by a proton magnetometer.For instance,

(1) Magnetic anomalies are easily examined whether they are lineated or not by a single anomaly profile.

(2) Near the geomagnetic equator like the East Mariana Basin, if magnetic anomaly trends NS, there occur eastward and vertical-down component anomalies. Because the main geomagnetic field is almost horizontal, no total intensity anomaly is observed. However, STCM can measure eastward and vertical-down component anomalies independently. For details about STCM, see Isezaki (1986).

9-3. Measurement

Data sampling was controlled by the microcomputer and observed values were stored in the minifloppy disk. Data sampling interval was one minute. We also measured the ship's heading and the rolling and pitching angles by a gyrocompass and a vertical gyroscope, respectively. The measurement was carried out throughout the cruise except while the ship was drifting.

The values measured by STCM are not real three components of the geomagnetic field, because they are influenced by the magnetic field induced by the ship's body. For removal of the components of the induced

field, a 360 degree rotation of the ship at a point where the three geomagnetic components are known is most convenient. During this cruise, rotating observation were carried out at 6 points. These points were chosen at various latitudes. They are listed in Table 9-1. Using these data sets, three components of geomagnetic field were calculated.

9-4. Results

The geomagnetic anomalies along track lines are shown in Figs. 9-1 to 9-4. Figs. 9-1, 9-2 and 9-3 show the anomalies of north, east and vertical components respectively. Fig. 9-4 shows the total intensity anomalies calculated from three components. The base lines of anomalies are calculatedfrom mean values of observed components on each segment of track lines. On a short segment, the base line is calculated to fit to the values of the adjacent segments.

The observed east components of geomagnetic anomaly are very noisy. It seems to be due to error (less than 1^{o}) of gyrocompass. The errors in the ship's heading are serious for the east component. In order to eliminate this noise, the anomalies of east component are smoothed by an operation of 29 minutes running mean. Anomalies of other two components and total intensity are smoothed by 7 minutes running mean. Figs. 9 -1 to 9-4 show the anomalies after this operation.

The anomaly pattern shows the characteristic feature that is obserbed near the geomagnetic equator as follows;

(1) The amplitudes both of north component and total intensity anomaly are small (less than 120 nT) except south-east portion in this area where anomalies of about 300 nT are observed.
(2) The amplitude of vertical component anomaly is large; it is about twice time as large as that of the total force.
(3) The anomaly curve of total force is similar to that of north component.

The anomalies with wave length of 30 km is observed between point A and point B.This pattern may be of anomaly lineations. The large magnetic anomalies between points C and D may be due to effect of topographic high.

Reference

Isezaki, N.: Newly designed shipboard three component magnetometer. Geophysics, **51**, 1992-1998, 1986.

TABLE 9-1. Points where the rotating observations were carried out.

	DATE (GMT)	LAT.	LONG.
1	JULY 6 87'	31° 0.19'	141° 24.00'
2	JULY 14 87'	16° 10.99'	147° 24.35'
3	JULY 22 87'	18° 49.38'	147° 43.38'
4	JULY 27 87'	12° 9.23'	151° 5.88'
5	AUG. 8 87'	21° 35.06'	139° 6.64'
6	AUG. 9 87'	26° 4.42'	139° 7.13'

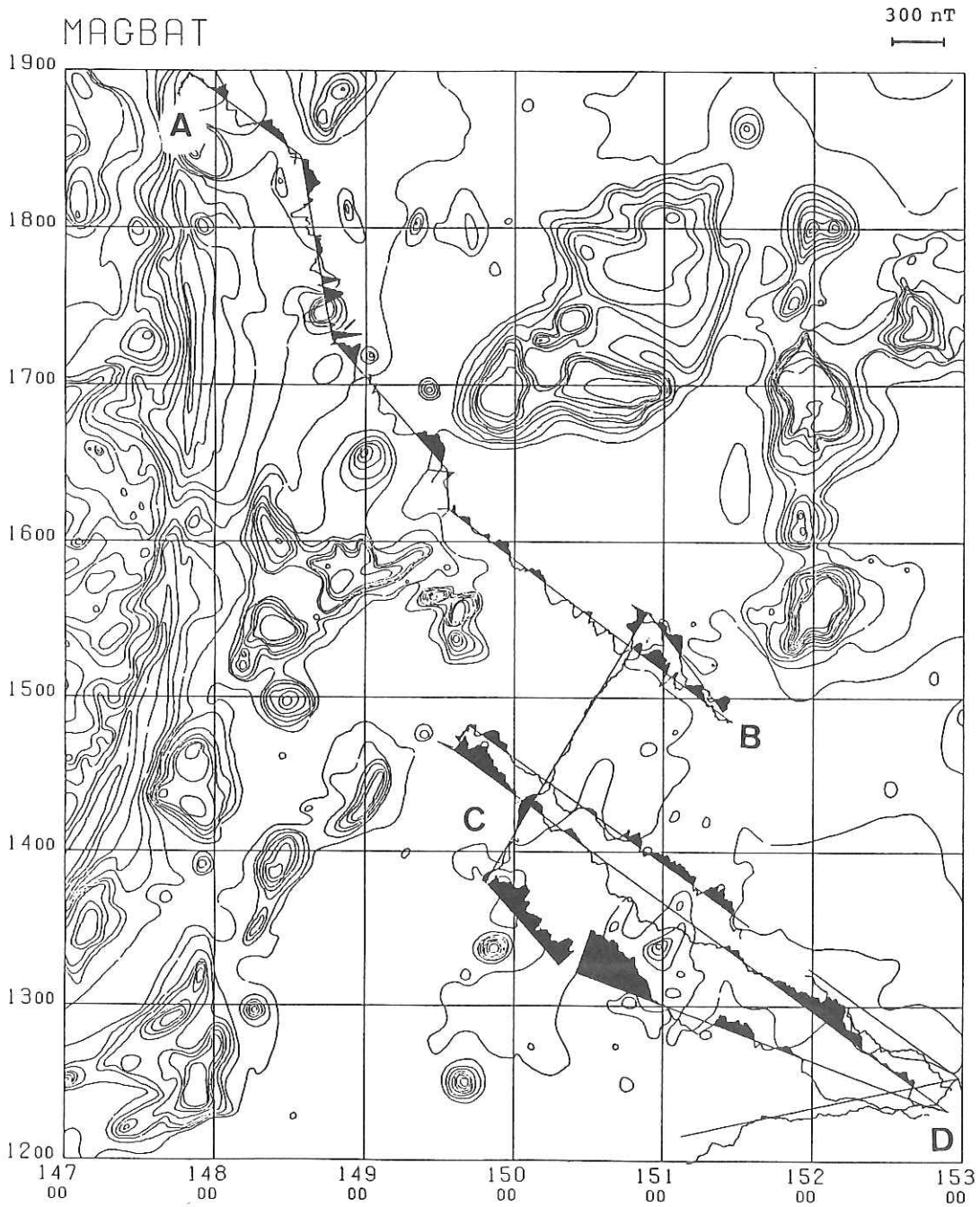

Fig. 9–1 The north component anomaly profiles projected on the ship's track. Positive anomalies are shaded.

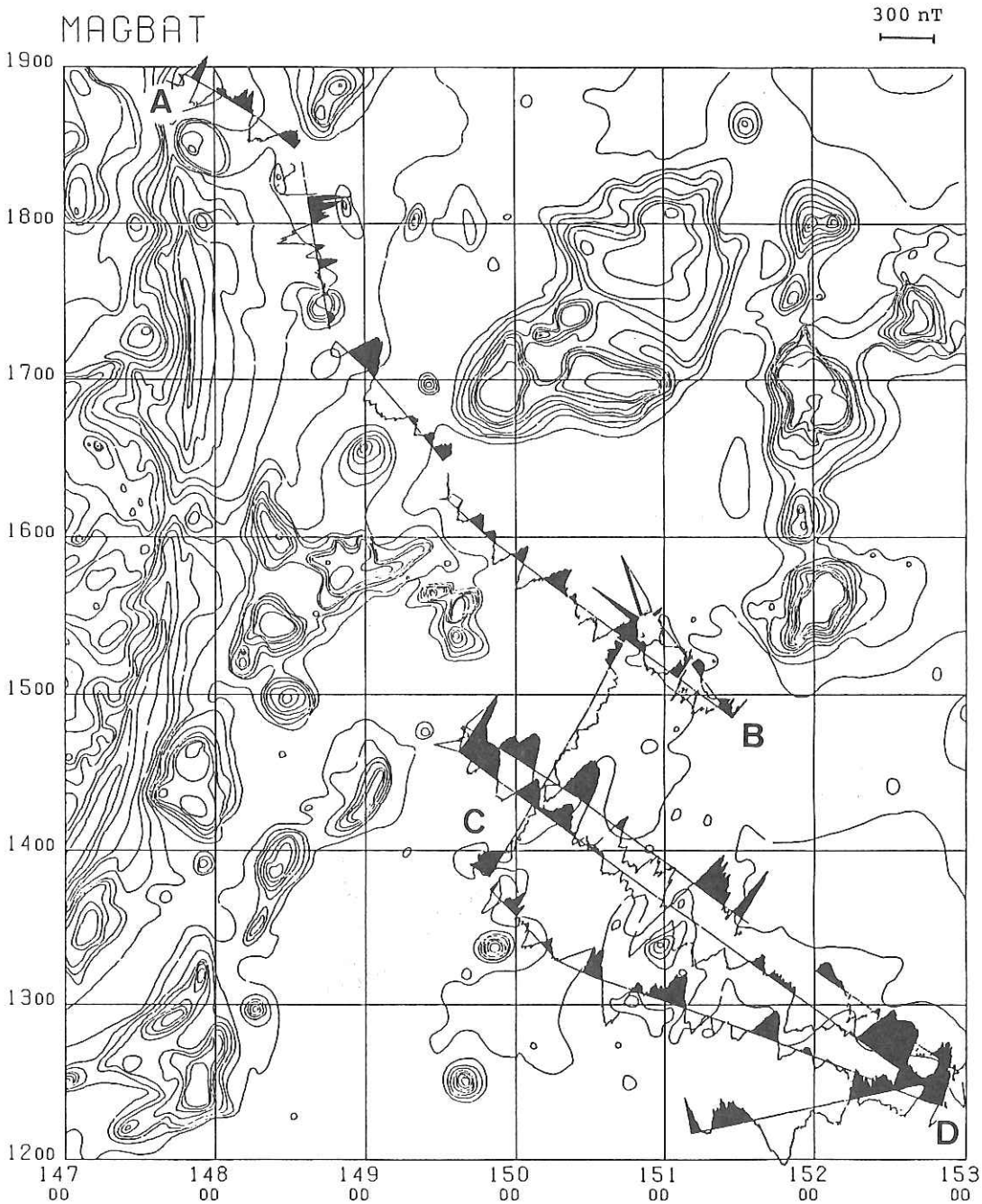

Fig. 9–2 The east component anomaly profiles projected on the ship's tracks. Positive anomalies are shaded.

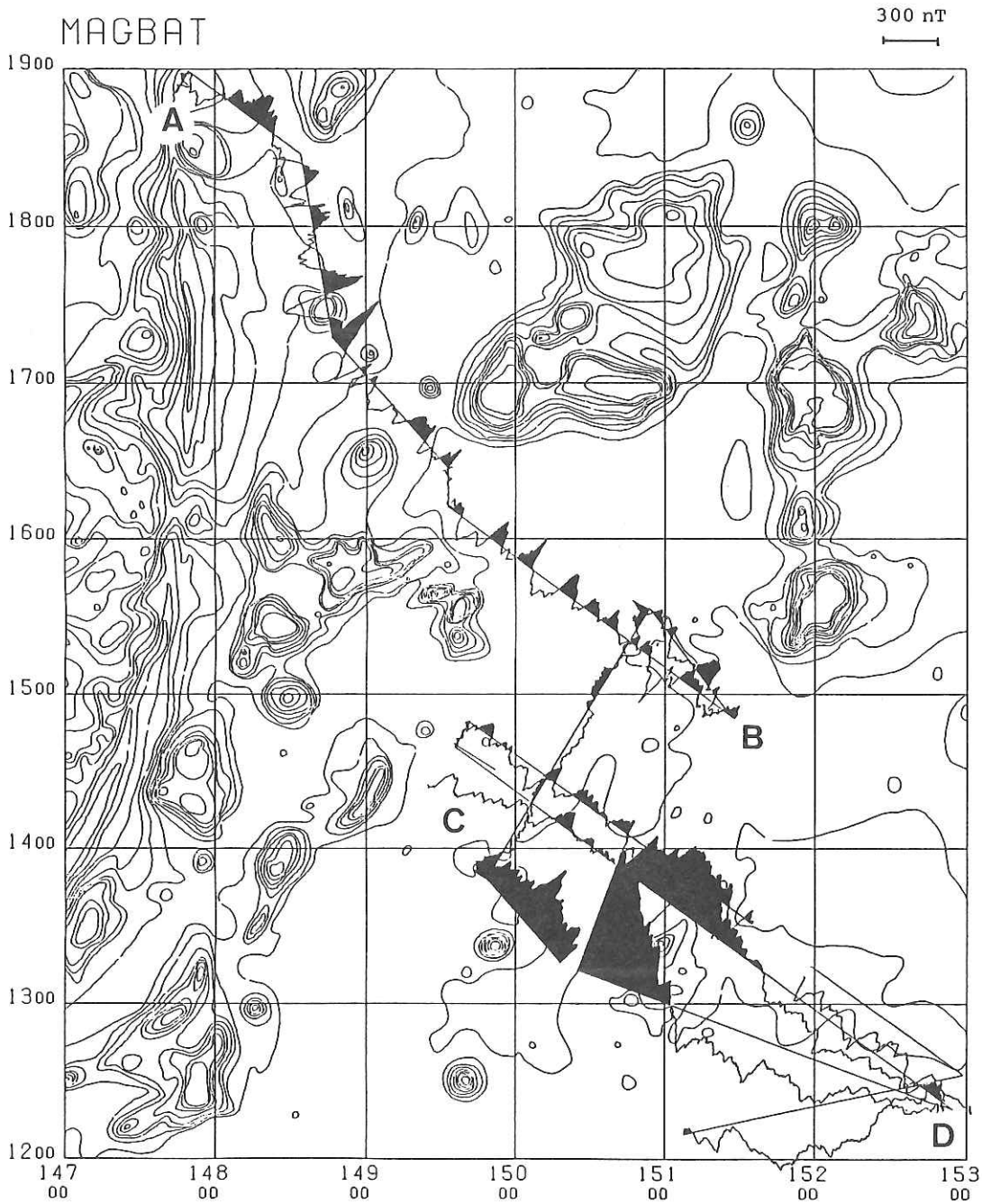

Fig. 9-3 The vertical component anomaly profiles projected on the ship's tracks. Positive anomalies are shaded.

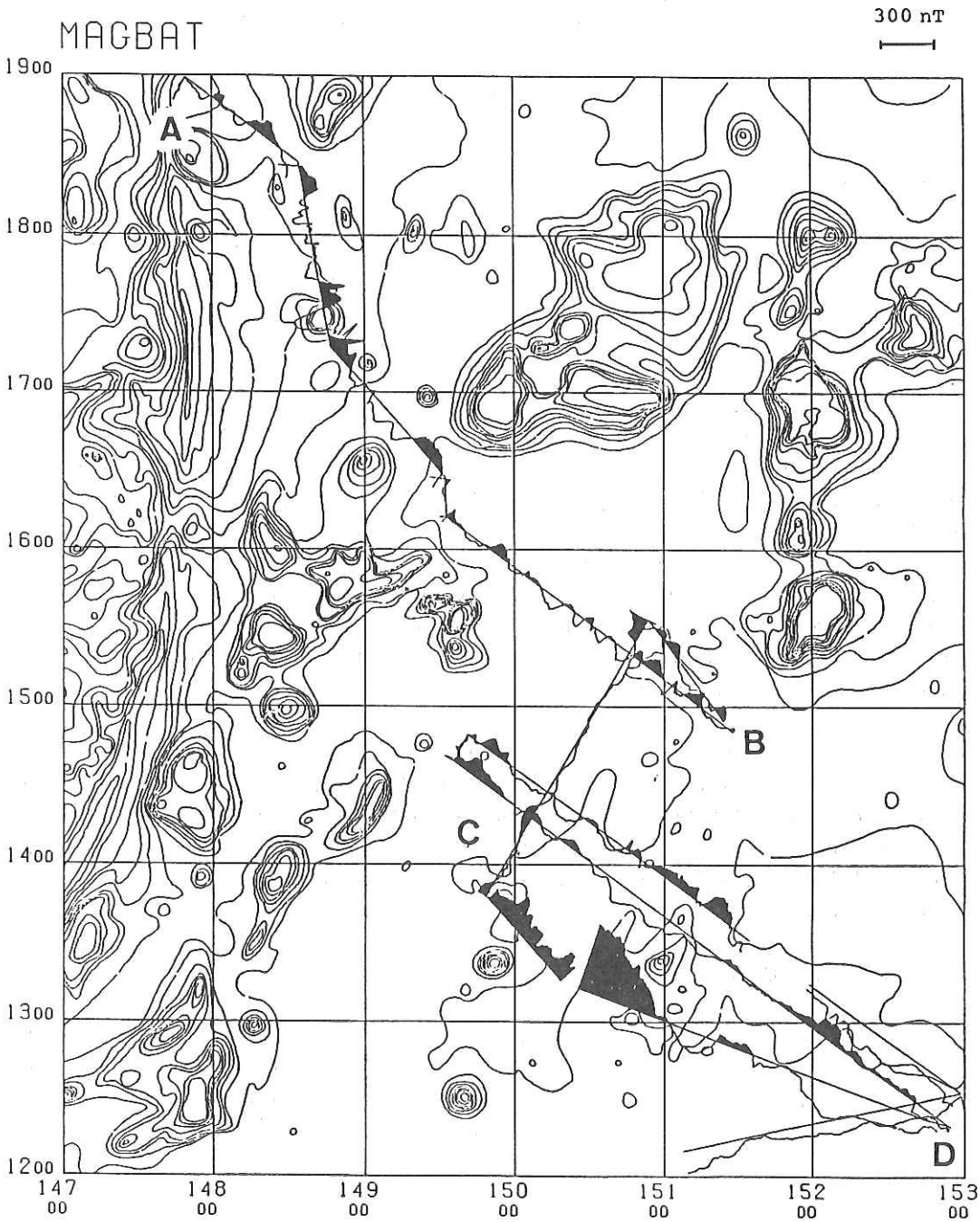

Fig. 9–4 The total intensity anomaly profiles projected on the ship's tracks. Positive anomalies are shaded. These anomalies are calculated from anomalies of three components.

10. COMPARISON MEASUREMENT OF GRAVITY BY USE OF JAPANESE AND CHINESE GRAVIMETERS

J. Segawa, H. Fujimoto, K. Koizumi, H. Toh and C.S. Yang (Japan Side)
C.J. Liang, X.Z. Pan and X.L. Zhang (China Side)

10-1. Japan-China Cooperative Program

In summer 1984 three staffs of the Institute of Geodesy and Geophysics Academia Sinica, Wuhan, China visited the Ocean Research Institute, University of Tokyo. On this occasion Prof. Li Xiqi, one of the Chinese visitors suggested that it would be useful to make a sea gravity comparison measurementusingboth the Japanese and Chinese ship-born gravimeters. In the next year a proposal on the Japan-China cooperative program was submitted to Academia Sinica under the agreement by Prof. Jiro SEGAWA of the Ocean Research Institute, Japan and Prof. Li Xiqi of the Institute of Geodesy and Geophysics, China. This proposal was formally accepted by Academia Sinica at the beginning of 1987, and soon after that the Japan Society for Promotion of Sciences also approved the program. It was decided that the comparison measurement of gravity would be conducted on board the R/V Hakuho-Maru of the Ocean Research Institute, University of Tokyo. Under the contract between Academia Sinica and Japan Society for Promotion of Science three Chinese scientists (Mr. Liang, Pan and Zhang) were invited to Japan.

The Chinese gravimeter was transported to Japan in May 1987 and the Chinese scientists came to Tokyo on June 15. On June 24 two Japanese gravimeters NIPR-ORI Model 2 and TSSG and a Chinese gravimeter CHZ (Ce di suo Hai yang Zhong li yi) were installed on R/V Hakuho-Maru to be prepared for the Hakuho-Maru KH 87-3 cruise. In this measurement a comparison of gravity among three gravimeters was successfully made.

10-2. NIPR-ORI Gravimeter Model 2

The NIPR-ORI (National Institute of Polar Research and Ocean Research Institute) gravimeter was first manufactured in 1980 and used on board the icebreaker Fuji during the 22nd Japan Antarctic Research Expedition. The NIPR-ORI Model 2 is a modified version which was completed this year and used in this cruise for the first time.

The NIPR-ORI gravimeter Model 2 is characterized by a servo gravity sensor, a Schuler-tuned vertical gyroscope and a 32-bit super mini-computer. The servo gravity sensor is a flexible-hinge type accelerometer with magnetic torquers and pick-up transformers. The magnets used are made of rare earth material which ensures highly stable magnetization and low

temperature effect. The sensor is installed in a vacuum housing which is regulated on a temperature 45 degrees C. The size of the sensor is 8 cm wide and 4 cm tall. This sensor measures the total gravity, i.e., the sensor has no mechanical compensator for gravity such as the helical spring. Compensation of gravity is conducted by subtracting a reference voltage from the output voltage of the sensor, and the fractional voltage resulted from subtraction is precisely measured by a digital voltmeter. The sensor responds to acceleration change from DC up to 30 Hz. Although the previous sensor was filled with viscous fluid for the sake of damping, such was not done with the new model. The fluid in which the sensor is dipped is likely to cause a significant change of buoyancy due to a slight temperature change and a convective motion which disturb the sensor output. The sensitivity of the sensor is 30 microvolt/mgal.

The vertical gyroscope is the Schuler-tuned gyro which is unaffected by ship's maneuvering. The gyro is made of an inertial grade, precisely tuned dry gyro with degrees of freedom. Verticality of this gyro is ± 1.5 minofarc. The platform of the sensor is separated from and remotely controlled by the gyro. The platform is drived by a pair of direct servo torquers which follow the roll and pitch signals from multi-synchroneous transmitters of the gyro.

The data processings are conducted by a super mini-computer ECLIPSE 4000DC (Data General, Inc.). Word length of this computer is 32 bits, processor cycle time 200 nsec, main memory 8 Mbytes, hard disc memory 70 Mbytes. The computer is accompanied by a printer and a magnetic tape driving unit (half size).

The relationship between the output voltage from the sensor and the vertical accelerationis linear. Gravity is expressed by thefollowing equation:

$$g = k_1 \bar{V} + k_2$$

where k_1 and k_2 are constants, $\bar{V}$ is a smoothed voltage output. Smoothing-out of the ship's disturbing acceleration is conducted by using a digital filter. Digital read-out of the output voltage is carried out with the intervals of 10, 50, 100 or 200 msec. The interval of 50 msec was selected for the present measurments. Digital filtering is conducted by taking a weighted average over a certain time interval. The weight function is of the error function type. This is a very effective filter and its filtering characteristics can be analytically expressed. The normalized weight function is expressed by

$$\phi(t) = \frac{1}{\sqrt{2\pi}\,\sigma} e^{-\frac{t^2}{2\sigma^2}}$$

Fourier transform of this function is

$$F(t) = \frac{1}{\sqrt{2\pi}} e^{-\frac{\sigma^2 w^2}{2}}$$

This weight function shows a good low-pass filtering effect. If is taken to be 30 sec, the disturbing acceleration with a period shorter than 30 sec is reduced to a degree less than -160 db. Although the g vs. V relationship is linear, it is desirable that the interval of data readout is as short as possible because of the Nyquist's criterion. In order to avoid short period vibrations the gravimeter is mounted on a shock absorbing steel board with a weight 250 kg, which is placed on air cushions. It seems, however, that such vibrations are slightly sensed by the gravity sensor and have an effect on the measurements to the order of magnitude of mgal. This problem was temporarily solved by adding a simple RC filter to the output from the sensor.

Fig. 10-1 shows the assembly of the NIPR-ORI gravimeter Model 2.

10-3. TSSG Gravimeter

The TSSG (Tokyo Surface Ship Gravimeter) gravimeter was first manufactured by the Institute of Geophysics, Faculty of Sciences, University of Tokyo in 1961.This meter is characterized by the sensor of vibrating string type, employment of gyro-stabilized platform and digital data processings.

The sensor of this gravimeter is of the size 3 cm x 3 cm x 4 cm approximately and a thin string made of beryllium copper vibrates at a frequency of about 2 kHz. Relationship between gravity and frequency of the string is

$$g = k_1 f^2 + k_2 f + k_3$$

where k_1, k_2 and k_3 are constants. This equation shows that the relationship is non-linear, and a high rate of sampling of the frequency change is required to reduce the non-linear rectification error. Filtering-out of the ship's movement is conducted by using a digital filter.

Gravity measurement was carried out throughout the cruise by use of a vibrating string sensor (No. 68-7-14) installed on a vertical gyroscope (Model 82-B). It was found in the inspection before the cruise that the amplitude of the vibration of the string was smaller than that during the KH 86-2 cruise (April 21 - May 15, 1986), and the feedback resistance was changed from 100 kiloohm to 95 kiloohm.

The real-time data processing was carried out by using the system developed before the KAIKO I cruise of the French R/V Jean Charcot in 1984. A 16-bit board computer measures the period of the vibration of the string and comverts it to the gravity value every 20 msec, filters off the effect of the ship's motion, and computes Eötvös corrections. A handheld personal computer was used as a keyboard of the board computer, and gravity values wererecordedin a floppy disc of the personal computer every lminute.

Observed gravity values and free-air anomalies were monitored on an analogue recorder.

Eötvös correction was computed with the ship's position given by a JRC JNA-760 Loran-C receiver. Ship's positions were calculated every 1 minute by overlapping mean of positions given every 4 sec. In the Mariana and Yap regions, navigation by Loran-C was not sufficiently good, especially at night, and Eotvos correction should be recalculated with the navigation data of the NNSS (Hokushin-Magnavox HX-1107) and GPS (JRC JLR-4000). The Loran-C station in Yap Island ceased to emit the wave on August 14, and a new station in Guam Island has become a permanent station"W" of 9970 chain.

An effect of a change of the room temperature on the observed gravity value was measured during the stay in Guam and Yap. The present exciting amplifier and the temperature regulation circuit for the gravity sensor were built up before the KAIKO I cruise in 1984. Fig. 10-2 shows variations of observed gravity values versus the room temperature. The temperature coefficient of the system is about -1 mgal/deg at temperature below 25°C. This value is about one order larger than that given by the previous temperature regulation unit. The present system should be re-examined and improved after the cruise is over. It must be also checked whether the temperature coefficient of the sensor (49 mgal/deg) remains unchanged or not. The effect of the temperature change of the exciting amplifier is shown in Fig.10-3. The temperature of the exciting amplifier is regulated at 32°C or 34.6°C.

Results of calibration of gravity values at ports of call are shown in Table 10-1. Gravity values (G Value) are determined by gravity measurements on the wharfs by using a Lacoste & Romberg gravimeter Model G (G-124). The drift of the gravimeter during 43 days was smaller than 0.1 mgal. Arrival, Leveling, and Departure show the observed gravity values on arrival, after releveling, and at departure, respectively. These values are corrected for the effect of the room temperature mentioned above.

TABLE 10-1 Calibration of gravity values at ports of call (TSSG)

Port	Date	G Value	Arrival	Leveling	Departure
Tokyo	87-7-01	979773.1			979773.1(0.0)
Guam	87-7-16	978527.6	978524.6(-3.0)	978528.0(+0.4)	
	87-7-21	978527.6			978527.6(0.0)
Yap	87-7-31	978467.6	978472.8(+5.2)	978474.5(+6.9)	
	87-8-03	978467.6			978467.6(0.0)
Tokyo	87-8-13	979773.1	979773.1(0.0)	979773.6(+0.5)	

10-4. CHZ Gravimeter

The CHZ sea gravimeter was developed by the Institute of Geodesy and Geophysics, Academia Sinica in 1985. This is an axially symmetric sea gravimeter. It is essentially unaffected by cross-coupling accelerations and can be operated in high sea states with vertical accelerations up to 500 gal and horizontal accelerations up to 200 gal. It was tested three times at sea. The results show that the CHZ meter has a high accuracy and performance when being operated at highly rough sea. The CHZ sea gravimeter comprises three units (Fig. 10-4);

Gravity sensor and gyro platform.
Electronic control unit.
Data acquisition unit.

The sensing system is of the force balanced type. The weight of the proof mass is balanced by pretension helical spring to maintain the mass at the original position where the output of the capacitive displacement transducer is zero. The gravity changes are detected by the transducer and compensated by electro-magnetic force generated in moving coil by P-1 (proportional integrator) feedback control current which is the measure of gravity variations.

Main Technical Data:

Dynamic accuracy 1-2 mgal
Measuring range 10000 mgal
Scale factor calibration standard 0.2 %
Response time 2 min
Platform freedom +-30 degrees

Design Features:

Exactly axial symmetry
Zero length spring suspension system
Silicon oil damping
High precision capacitance transducer and force-balanced feedback
Digital filter and programmable data aquisition system
Two thermostats and temperature compensator

Performance Features:

Highly accurate measurement
Operable under vertical accelerations up to 500 gal
Operation in different sea states is ensured by selection of appropriate filtering at the front panel
Automatic operation with three readout systems
digital printer, analog recorder and cassette tape recorder

Note:

1. CHZ: abbreviation of Chinese words [Ce di suo Hai yang Zhong li yi].
2. Gyro platform was developed by Hua Nan College of Technology, China.

10-5. Preliminary Result of Measurement

(1) Data of NIPR-ORI gravimeter at crossovers of the ship's tracks

The NIPR-ORI gravimeter is equipped with a device of automatic navigational data acquisition. Navigational data available are time, position from NNSS and LORAN C, ship's speed and heading, and water depth. This enablesone to get free-air and Bouguer gravity anomaliesinrealtime. However, since the navigational data are subject to errors, the EOTVOS correction and the calculated normal gravity are not always accurate. The NNSS and its dead reckoned positions are affected by water current, and LORAN C positions are affected by the condition of radio wave propagation or the geometrical relationship of the LORAN C stations. It is, therefore, unavoidable that the gravity data obtained in real time are adjusted by the later processings.

Comparison of gravity data obtained at crossover points was made at five different places in spite of the anxiety mentioned above. These five crossovers are all on the ship's tracks during LEG 2 from 21 to 31 July, 1987. Figs. 10-5 through 10-9 show the positions where the ship's tracks are crossed. It is evident that the crossover points estimated by NNSS and those by LORAN C are different. Since it is not known which site is a true crossing, both cases have been considered. Table 10-1 shows the numbers attached to the crossover points, time and positions for the two closest points, raw gravity g_1 and EOTVOS corrected gravity g_2, and water depth if available. These crossover points are listed up with NNSS and LORAN C positionings, respectively.

The absolute values of the differences between two EOTVOS corrected gravity g_2 are also listed in Table 10-2 with NNSS and LORAN C positionings, separately. The most important cause of the disagreement in gravity at crossovers are the inaccurate EOTVOS corrections. In the area concerned the positionings of LORAN C, in particular, were not good. The other causes may be some drift and temperature change of the gravity sensor. Therefore, if these causes are removed by post processings, better results may be reasonably expected.

TABLE 10-2

Navig.	NO	JST	LAT	LON	g_1 (mgal)	g_2 (mgal)	DEPTH (m)
	1	July 24					
		0614	15 21.65N	150 45.52E	978349.53	978418.17	5861
		1947	15 21.62N	150 45.47E	978462.43	978420.00	
	2	July 25					
		0057	14 28.48N	150 13.15E	978419.09	978379.44	5866
		July 27					
		0034	14 28.41N	150 13.13E	978308.73	978377.95	
NNSS	3	**********					
	4	July 25					
		2218	12 28.08N	152 36.08E	978200.08	978277.74	
		July 28					
		0000	12 28.01N	152 35.89E	978364.18	978278.32	
	5	July 26					
		0118	12 29.37N	152 42.45E	978345.15	978274.89	5928
		July 27					
		2330	12 29.37N	152 42.45E	978362.38	978277.64	5927
	1	July 24					
		0609	15 21.16N	150 44.61E	978350.64	978418.21	
		1958	15 21.11N	150 44.63E	978462.16	978412.40	
	2	July 25					
		0058	14 28.38N	150 13.17E	978419.02	978364.21	
		July 27					
		0034	14 28.40N	150 13.27E	978308.73	978377.99	
LORAN	3	July 25					
		0202	14 17.41N	150 06.56E	978408.46	978366.86	5930
		July 26					
		1656	14 17.43N	150 06.50E	978434.91	978358.44	
	4	**********					
	5	**********					

TABLE 10-2 (continued)

	Pt.NO	1	2	3	4	5	
Abs. Dif.	by NNSS	1.83	1.49	*****	0.58	2.75	(mgal)
	by LORAN	5.81	13.78	8.42	*****	*****	(mgal)

(2) Data of TSSG gravimeter at crossovers of the ship's tracks

TSSG's data are displayed on a strip-chart recorder for analog monitoring and printed in digital form every one minute as well as stored on a floppydisc. Theresult of comparison at crossover points are shown in Tables 10-3 and 10-4.

TABLE 10-3

Navig.	NO	JST	LAT	LON	g_1 (mgal)	g_2 (mgal)	DEPTH (m)
	1	July 24					
		0614	15 21.65N	150 45.52E	978344.8	978413.4	5861
		1947	15 21.62N	150 45.47E	978459.6	978417.2	
	2	July 25					
		0057	14 28.48N	150 13.15E	978416.1	978376.4	5866
		July 27					
		0034	14 28.41N	150 13.13E	978304.2	978373.6	
NNSS	3	**********					
	4	July 25					
		2218	12 28.08N	152 36.08E	978197.4	978275.1	
		July 28					
		0000	12 28.01N	152 35.89E	978364.4	978278.5	
	5	July 26					
		0118	12 29.37N	152 42.45E	978345.7	978275.4	5928
		July 27					
		2330	12 29.37N	152 42.45E	978362.1	978277.5	5927
	1	July 24					
		0609	15 21.16N	150 44.61E	978345.1	978412.7	
		1958	15 21.11N	150 44.63E	978459.5	978409.7	

	2	July 25				
		0058	14 28.38N	150 13.17E	978415.8	978361.0
		July 27				
		0034	14 28.40N	150 13.27E	978304.2	978373.5
LORAN	3	July 25				
		0202	14 17.41N	150 06.56E	978404.8	978363.3 5930
		July 26				
		1656	14 17.43N	150 06.50E	978432.9	978356.4
	4	**********				
	5	**********				

TABLE 10-4

	Pt.NO	1	2	3	4	5	
Abs. Dif.	by NNSS	3.8	2.8	*****	3.4	2.1	(mgal)
	by LORAN	3.0	12.5	6.9	*****	*****	(mgal)

(3) Data of CHZ gravimeter at crossovers of the ship's tracks

The CHZ gravimeter records the data on a strip-chart recorder, a small line-printer and a cassette tape recorder. The gravity profile recorded on a strip-chart recorder is mostly for monitoring the data, so that it is difficult to digitize it. The cassette tape recorder stores complete data sets of the measurement at the interval of 1 minute. However, this cannot be read until it is brought to China. The only data readable in a digital form on board are those printed on the small line printer. On this printer are recorded changeable fractions of gravity resding with a resolution of 1/100 mgal at the interval of 10 minutes.

In order to compare the measurements at crossover points the gravity values were estimated by interpolation using the neighboring 10 min data. Table 7-5 shows raw gravity values (fractional values) estimated for the time of crossing together with the neighboring 10 min data used for estimation. Table 7-6 shows the final results of comparison. Table 7-7 shows absolute differences of the two measurements at crossover points. It is seen that disagreement in gravity at crossovers is less than 1 mgal except for the point NO. 2. Crossing points obtained by LORAN C seem very erroneous also in this case.

TABLE 10–5

NNSS

NO.1	July 24	0610	905.27	July 24	1940	1017.42
		0620	905.34		1950	1015.91
		0614	905.30		1947	1016.36
NO.2	July 25	0050	973.63	July 27	0030	859.81
		0100	971.41		0040	860.36
		0057	972.07		0034	860.03
NO.4	July 25	2210	752.33	July 28	0000	915.90
		2220	751.62			
		2218	751.76			
NO.5	July 26	0110	898.07	July 27	2330	914.47
		0120	900.00			
		0118	899.61			

LORAN C

NO.1	July 24	0609	905.27	July 24	1950	1015.91
					2000	1015.75
					1958	1015.78
NO.2	July 25	0058	971.85	July 27	0034	860.03
NO.3	July 25	0200	961.69	July 26	1650	985.85
		0210	959.44		1700	987.09
		0202	961.24		1656	986.59

TABLE 10–6

Navig.	NO	JST	LAT	LON	g1 (mgal)	g2 (mgal)	DEPTH (m)
	1	July 24					
		0614	15 21.65N	150 45.52E	905.30	973.94	5861
		1947	15 21.62N	150 45.47E	1016.36	973.93	
	2	July 25					
		0057	14 28.48N	150 13.15E	972.07	932.42	5866
		July 27					
		0034	14 28.41N	150 13.13E	860.03	929.25	

NNSS	3	**********					
	4	July 25					
		2218	12 28.08N	152 36.08E	751.76	829.42	
		July 28					
		0000	12 28.01N	152 35.89E	915.90	830.04	
	5	July 26					
		0118	12 29.37N	152 42.45E	899.61	829.35	5928
		July 27					
		2330	12 29.37N	152 42.45E	914.47	829.73	5927
	1	July 24					
		0609	15 21.16N	150 44.61E	905.27	972.84	
		1958	15 21.11N	150 44.63E	1015.78	966.02	
	2	July 25					
		0058	14 28.38N	150 13.17E	971.85	917.04	
		July 27					
		0034	14 28.40N	150 13.27E	860.03	929.29	
LORAN	3	July 25					
		0202	14 17.41N	150 06.56E	961.24	919.64	5930
		July 26					
		1656	14 17.43N	150 06.50E	986.59	910.12	
	4	**********					
	5	**********					

TABLE 10-7

	Pt.NO	1	2	3	4	5	
Abs. Dif.	by NNSS	0.01	3.17	*****	0.62	0.38	(mgal)
	by LORAN	6.82	12.25	9.52	*****	*****	(mgal)

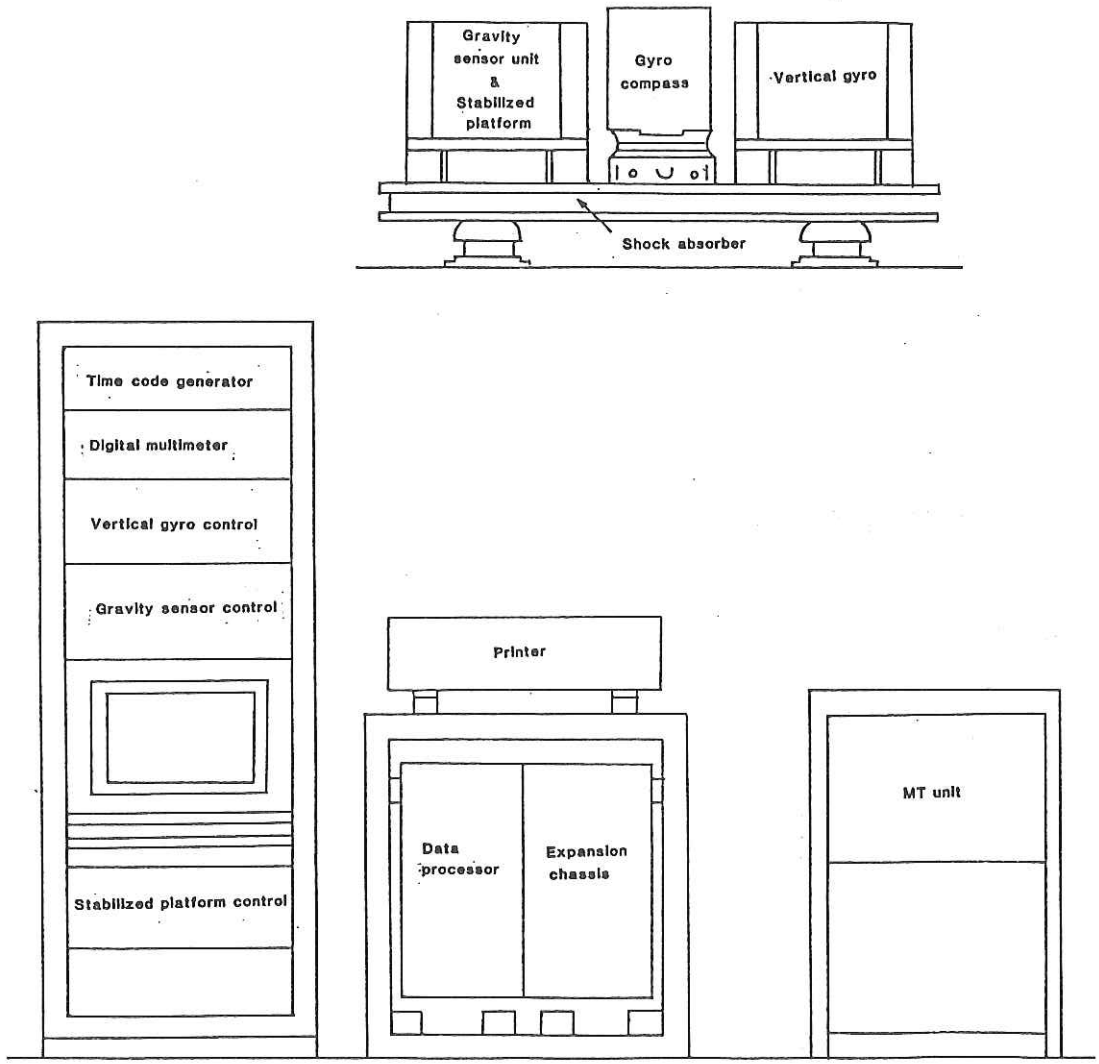

Fig. 10-1 General assembly of the NIPR-ORI Gravimeter.

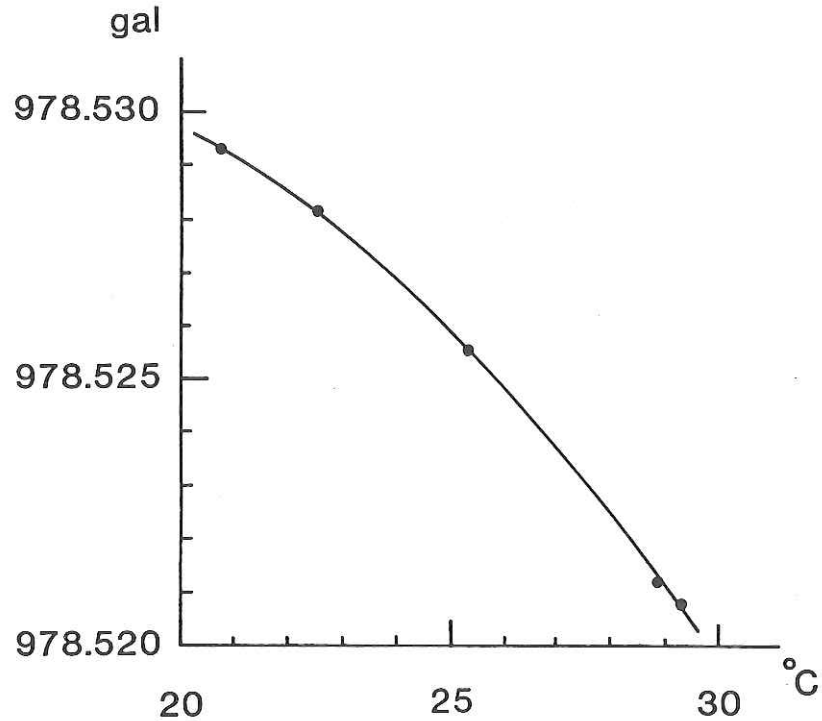

Fig. 10-2 Variations of observed gravity values with different temperatures

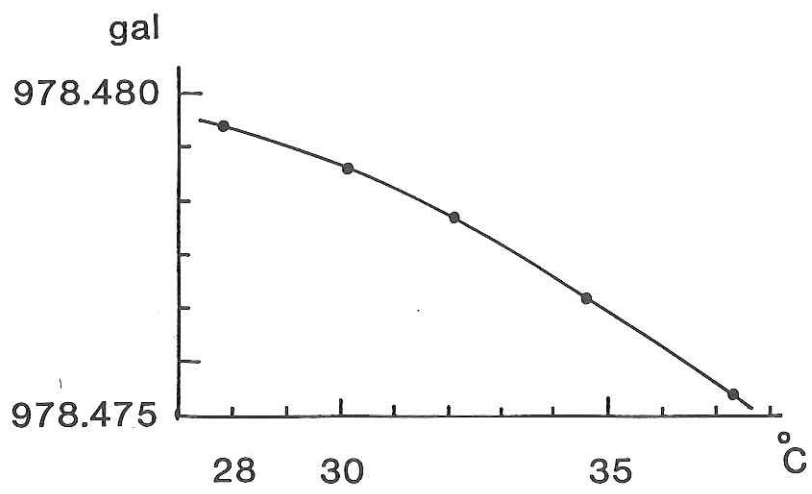

Fig. 10-3 Variations of observed gravity values with changes in temparature inside the exciting amplifier.

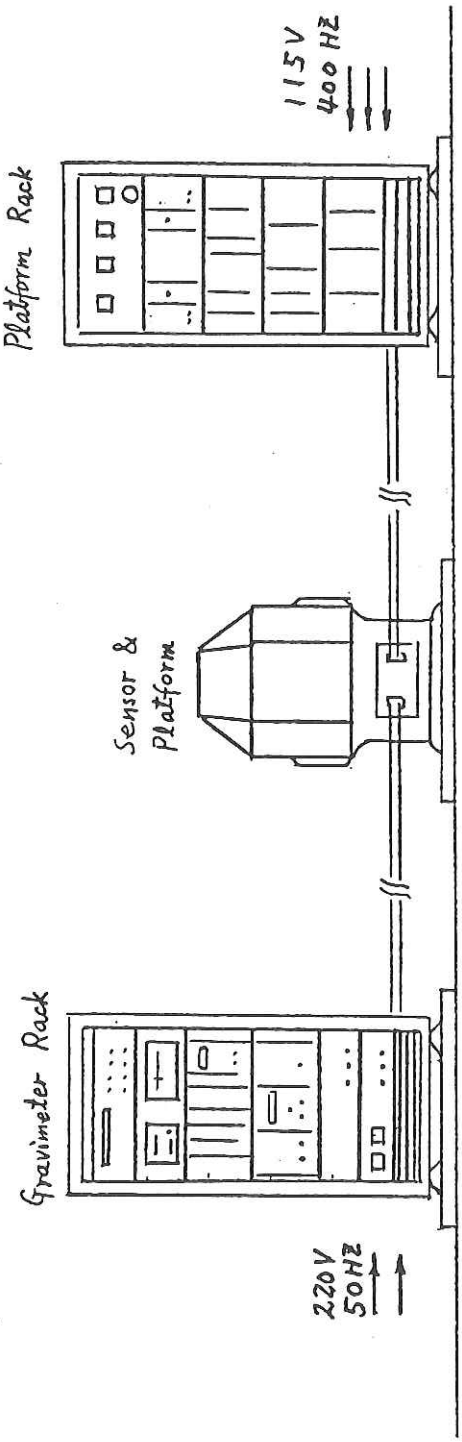

Fig. 10-4 Assembly of the CHZ Sea Gravimeter system.

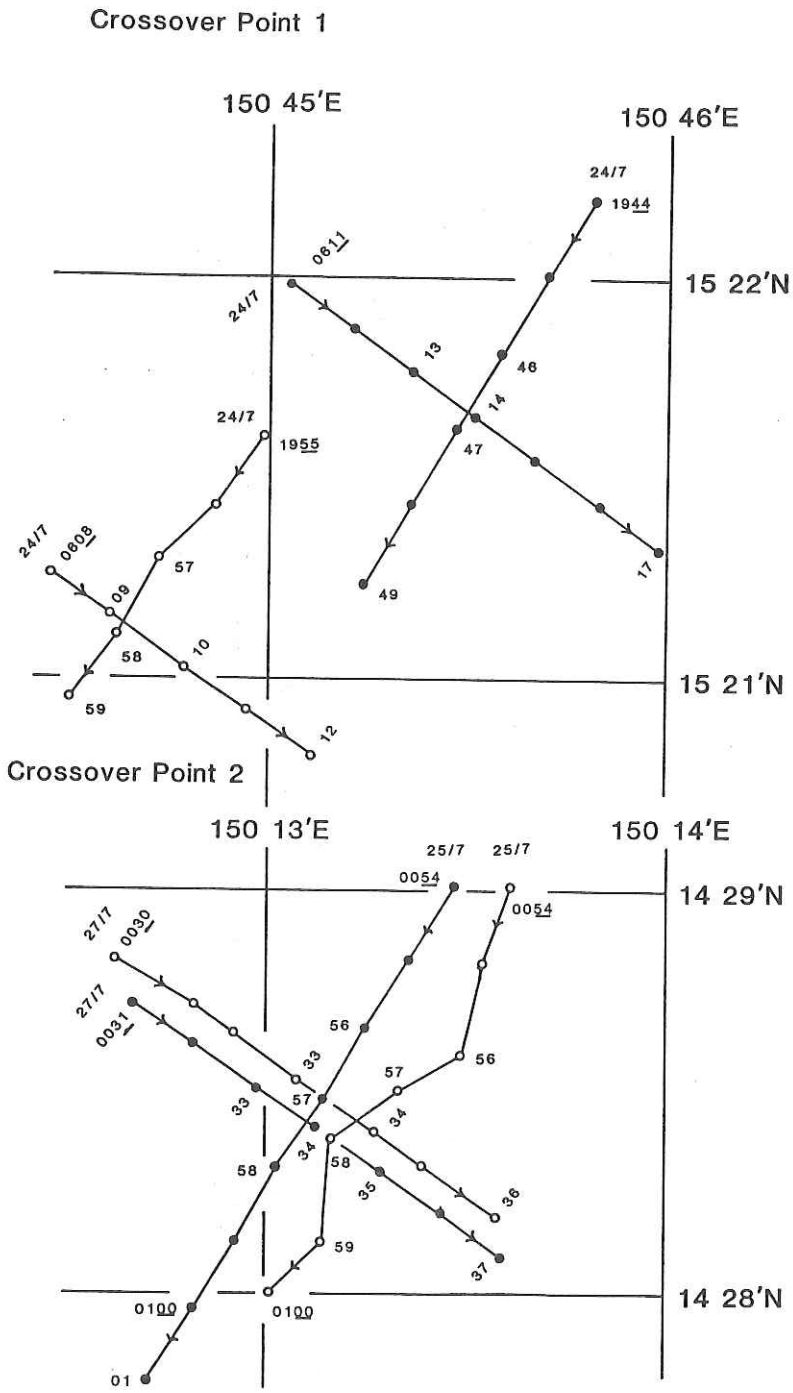

Fig. 10-5 Ship's positions at the crossover point 1. Numerical figures beside lines denote date, month, hour and minute (JST). Those beside dotts indicate minute.

Fig. 10-6 Ship's positions at the crossover point 2.

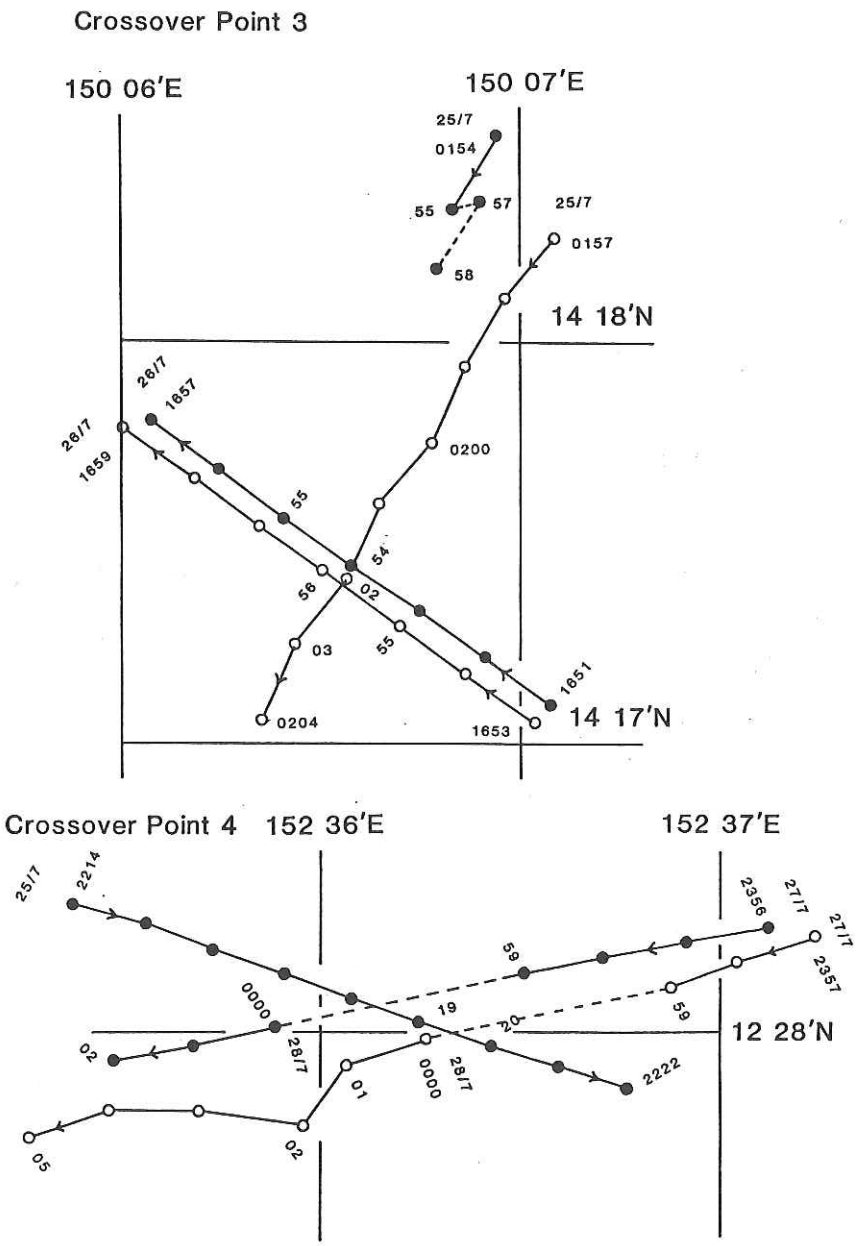

Fig. 10–7 Ship's positions at the crossover point 3.

Fig. 10–8 Ship's positions at the crossover point 4.

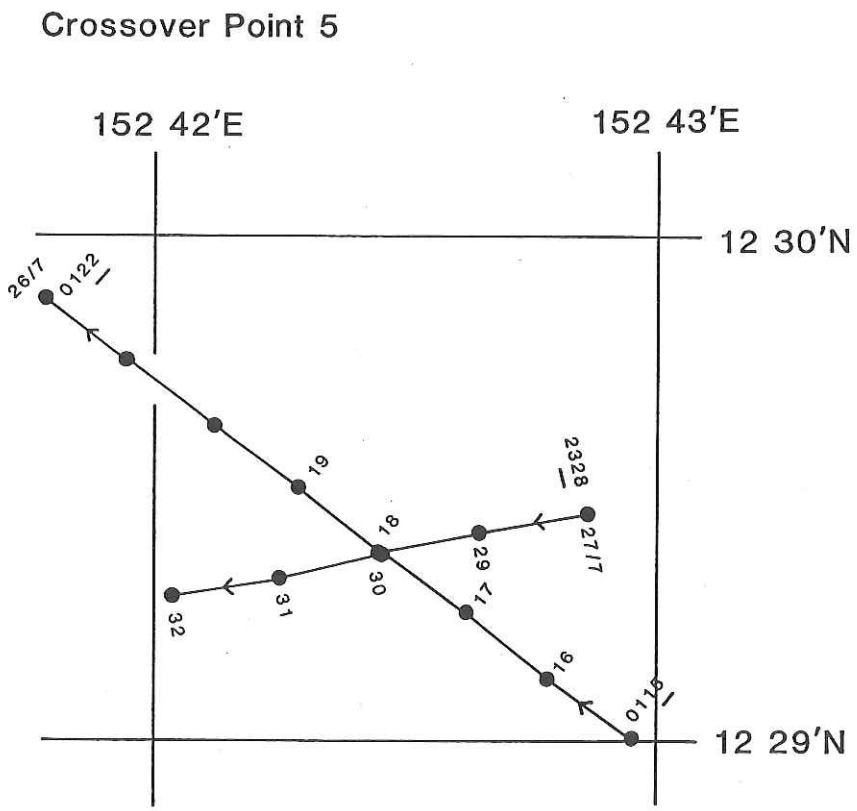

Fig. 10-9 Ship's positions at the crossover point 5.

11. ONBOARD PROCESSING SYSTEM FOR MARINE GEOPHYSICAL DATA

K. Sayanagi, N. Nakanishi, and K. Tamaki

Deep ocean surveys have been made by the R/V Hakuho-Maru since 1967. They produced large amounts of geophysical data of bathymetry, the earth's total magnetic field, and variations in the earth's gravity field. In addition, recent improvements of geophysical equipments tend to give us more numerous and more various data for geophysical properties. It is certain that the need of onboard data processing will increase with the progress of equipments.

During this cruise, we attempted to develop an onboard processing system for marine geophysical data. The block diagram of the system is presented in Fig.11-1. The data processing with the system consists of the following four components; 1) transferring data from a PC-9801 personal computer to an ECLIPSE S/120 mini-computer, 2) compiling bathymetry and total magnetic field data, 3) storing the data on a magnetic tape in the marine geophysical data exchange format - "MGD77" (Hittelman et al., 1981), and 4) plotting ship's tracks and geophysical data along the tracks in any selected area.

The onboard processing system is supported by an ECLIPSE S/120 computer system utilizing a Model mE674 CPU. The ECLIPSE S/120 is a 16-bit mini-computer system with 256 kilobytes of random-access memory (RAM) and assorted I/O cards. An additional memory is provided by a Model 6160N, 73 Megabytes of hard disk. The data collected from observations are transferred from a PC-9801 personal computer to an ECLIPSE S/120 via an RS-232 serial port. A magnetic tape subsystem (Model 6026) is used for storing the data. Another peripheral devices are a Model 5808 serial printer and a Model 5809 plotter.

A photographic view of the system is shown in Figs. 11-2 and 11-3. Fig. 11-2 shows an ECLIPSE S/120 computer system with a hard disk and a magnetic tape subsystem. A terminal display plus a keyboard (far left), a serial printer (center), and a plotter (right) are visiable in Fig. 11-3.

The first purpose of this system was to create cruise files in the MGD77 format from observed data. The data processing consisted of three steps, as follows;

(1) An ECLIPSE S/120 captured the observed data from a PC-9801 via an RS-232 serial port. The communication was controlled by softwares written in NEC Corporation's N88-BASIC for a PC-9801 and Data Genertal Generaleneral Corporation's FORTRAN 5 for an

ECLIPSE S/120. The data included ship positions by Loran C and total magnetic intensities. As a result, the preliminary data files were produced on a hard disk.

(2) Bathymetry data were added to the files produced in the step (1) by operators.

(3) Compiled data files in the previous step were reformatted into the MGD77 format and stored on a magnetic tape.

Another system was to plot the collected data (bathymetry, magnetics, and gravity) along ship's tracks. Two examples of magnetic anomalies plotted along ship's tracks in this cruise are given in Figs. 11-4 and 11-5.

The data plotting was done by using the "MAGBAT" (MArine Geophysical BAsic Tool) system (Nakanishi et al.,1987). The MAGBAT have been developed for the basic processing of marine geophysical data on an FACOM M-360AP computer system. The system program is written in Fortran 77. Note that main functions of the MAGBAT have been available on an ECLIPSE S/120 system too.

In this cruise we spent much time in developing an onboard data processing system. The main results are that the system was successful in two things onboard; 1) the cruise file storage on a magnetic tape and 2) the data plotting along ship's tracks.

It is thought that an onboard data processing system should play an important role in the entire ship's observation system in the near future. This attempt was the first step of development for the complete processing system. The better system should contribute more to the earth scientific observations by ships.

REFERENCES

Nakanishi, M., C. Park, K. Sayanagi, K. Tamaki, Y. Nakasa, A. Oshida, and N. Shima: Development of the basic processing system of marine geophysical data (MAGBAT). Geological Data Processing, **12**, 217-226, 1987 (in Japanese with English abstract).

Hittelman, A. M., R. C. Groman, R. T. Haworth, T. L. Holcombe, G. McHendrie, and S. M. Smith: The marine geophysical data exchange format - 'MGD77' (Bathymetry, Magnetics, and Gravity). Key to Geophysical Records Documentation, No. 10, 1-18, National Geophysical and Solar-Terrestrial Data Center, Boulder, Colorado, 1981.

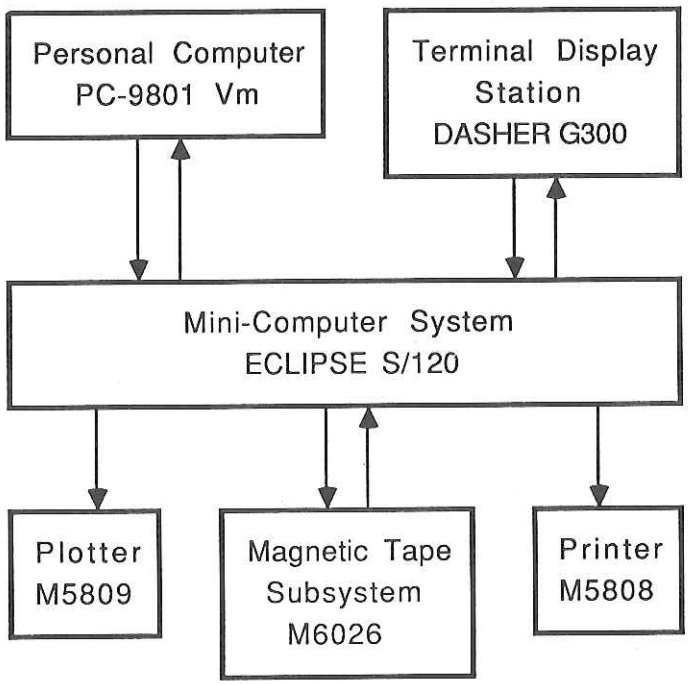

Fig. 11-1 Block diagram of the onboard processing system for marine geophysical data.

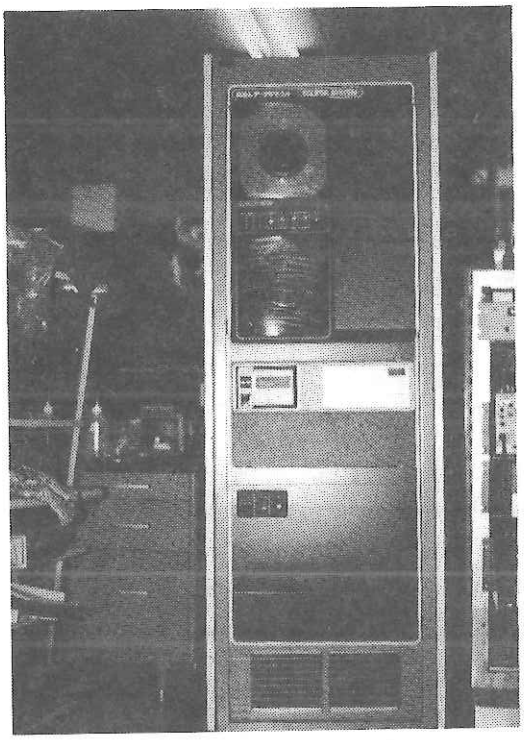

Fig. 11-2

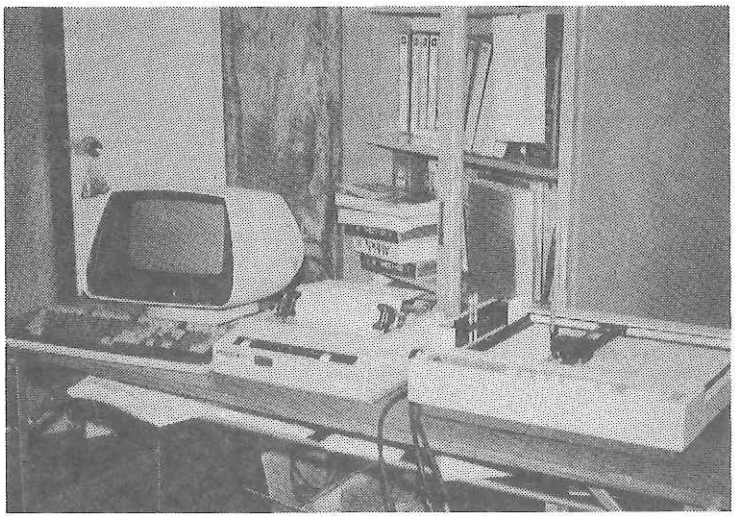

Fig. 11-3

Fig. 11-2 Photograph of an ECLIPSE S/120 computer system plus a Model 6160N hard disk (73 Mbytes) and a Model 6026 magnetic tape subsystem.

Fig. 11-3 Peripheral devices used in the system are (left to right): a terminal display plus a keyboard (DASHER G300), a Model 5808 serial printer, and a Model 5809 plotter.

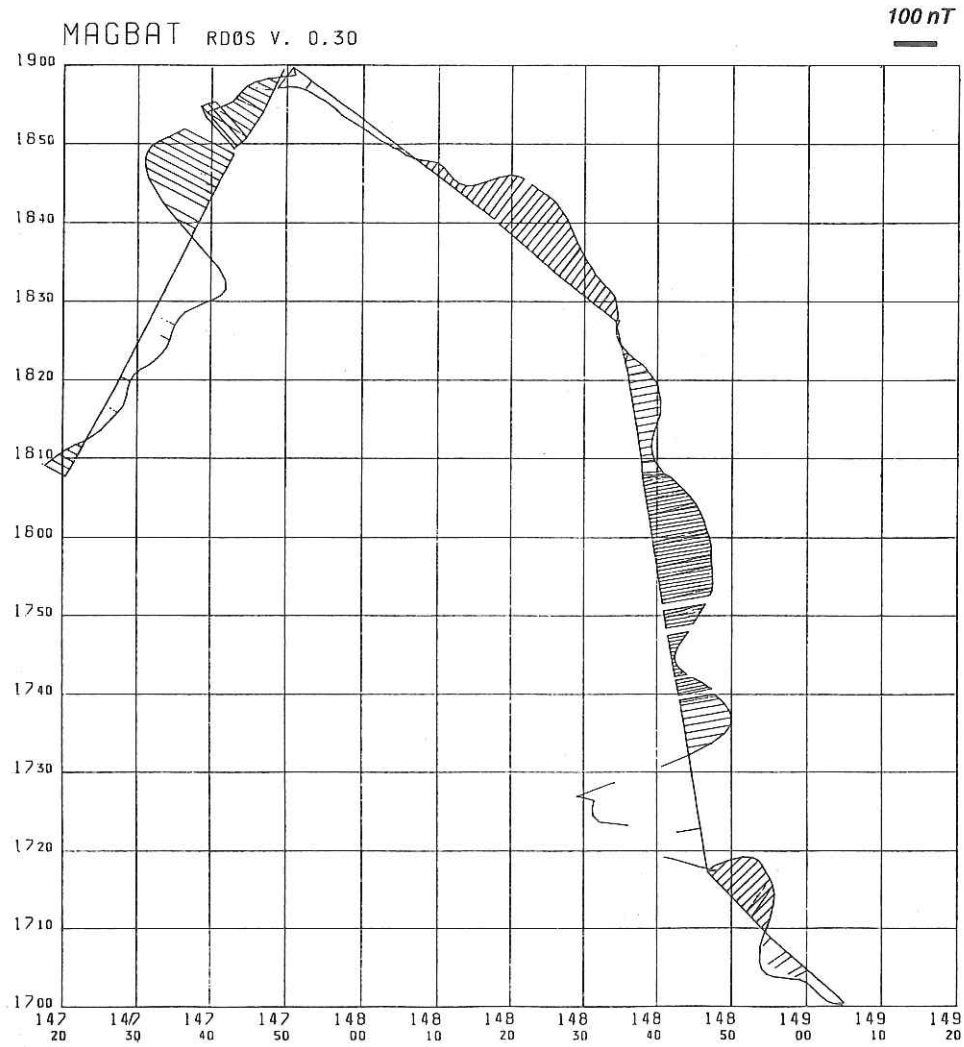

Fig. 11-4 Magnetic anomalies from this cruise plotted along ship's tracks. Example 1.

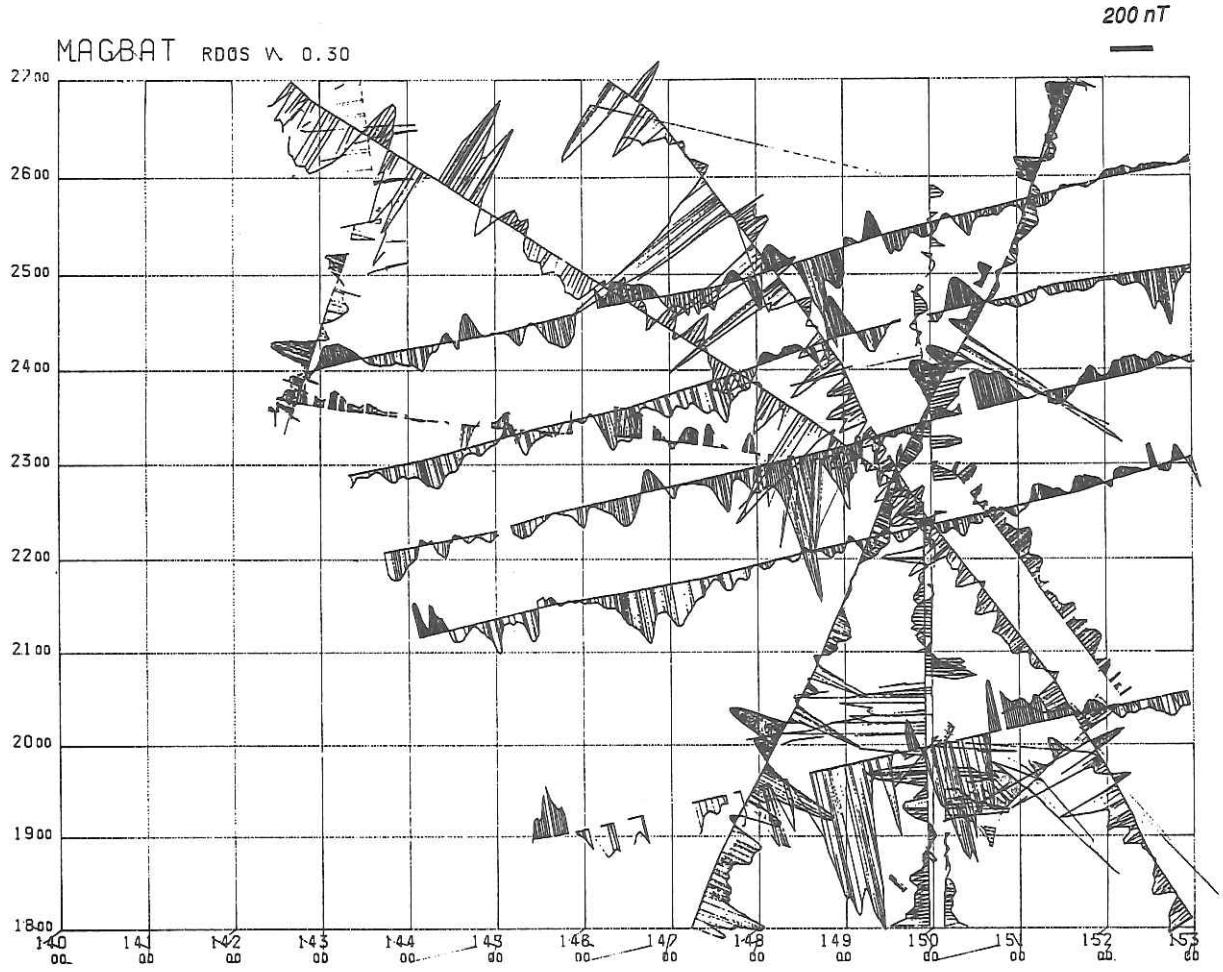

Fig. 11-5 Magnetic anomalies plotted along ship's tracks. The source of total field data is from this cruise and the National Oceanic and Atmospheric Administration (NOAA). Example 2.

12. PISTON CORING

12-1. OPERATION LOGS

Date Aug. 05,1987 Ship Hakuho Maru KH 87-3 Station 21 [P-3]
Latitude 10°46.6'N Longitude 137°35.9'E
Location Yap Trench Back Arc
Sea swell 2m Weather 6 m/s
Bottom Topography flat Profiler flat
Length of Core Pipe 12 m Wall Thickness mm Material Al
No. of pipe 1 ID of Pipe mm Core Head Wt. 450 kg Trigger Wt. 50 kg
Length Main Line m Length Trigger Line m Length Free Fall m
Response at Hit clear Response at Pull-out clear
Time Lowered 07 h 12 m; Uncorrected water Depth 4560 m
Time Hit 08 h 37 m; Uncorrected Water Depth 4807 m
Wire Angle at Hit Wire-out at Hit 4840 m
Time Surfaced 10 h 07 m Uncorrected Water Depth 4780 m
Cored Length 1017 cm
Trigger Cored Length cm
Method of Storage No. of Pipe filled 6
Length of Cores in Tray 1. 138 cm, 2. 189 cm, 3. 187 cm, 4. 193 cm, 5. 190 cm, 6. 114 cm.
No. of Cubic Samples for Paleomagnetism (No. No.)

Date Aug. 05, 1987 Ship Hakuho Maru KH 87-3 Station 22 [P-4]
Latitude 10°35.6'N Longitude 138°06.2'E
Location Yap Back Arc
Sea swell 2-3m Weather 9 m/s
Bottom Topography flat Profiler Thick sediments
Length of Core Pipe 8 m Wall Thickness mm Material Al
No. of pipe 1 ID of Pipe mm Core Head Wt. 600 kg Trigger Wt. 50 kg
Length Main Line m Length Trigger Line 12 m Length Free Fall 4 m
Response at Hit clear Response at Pull-out
Time Lowered 14 h 37 m; Uncorrected Water Depth 4330 m
Time Hit 16 h 00 m; Uncorrected Water Depth 4320 m
Wire Angle at Hit 0 °; Wire-out at Hit 4393 m
Time Surfaced 17 h 17 m; Uncorrected Water Depth 4780 m
Cored Length 298 cm
Trigger Cored Length 0 cm
Method of Storage No. of Pipe Filled 2
Length of Core in Tray 1. 102 cm, 2. 196 cm, 3. cm, 4. cm, 5. cm, 6. cm.
No. of Cubic Samples for Paleomagnetism (No. No.)

Date Aug. 06, 1987 Ship Hakuho Maru KH 87-3 Station 25 [P-5]
Latitude 10°58.4'N Longitude 139°19.6'E
Location Mariana & Yap Trench Junction
Sea Weather 8 m/s
Bottom Topography flat Profiler
Length of Core Pipe 8 m Wall Thickness 7.5 mm Material Al
No. of pipe 1 ID of Pipe mm Core Head Wt. 600 kg Trigger Wt. 50 kg
Length Main Line m Length Trigger Line 12 m Length Free Fall 4 m
Response at Hit unclear Lesponse at Pull-out
Time Lowered 07 h 20 m; Uncorrected Water Depth 7220 m
Time Hit 09 h 42 m; Uncorrected Water Depth 7330 m
Wire Angle at Hit Wire-out at Hit 7534 m
Time Surfaced 11 h 53 m; Uncorrected Water Depth 7500 m
Cored Length 0 cm
Trigger Cored Length 0 cm
Method of Storage 2 m No. of Pipe Filled
Length of Core in Tray 1. cm, 2. cm, 3. cm, 4. cm,
5. cm, 6. cm.
No. of Cubic Samples for Paleomagnetism (No. No.)

13. DREDGE HAULS

13-1. OPERATION LOGS

Date July 03-04, 1987 Ship Hakuho Maru KH 87-3 Station No. 1 [D-1]
Location Tori-Shima fore-arc seamount (150 km ENE from Tori-Shima)
Weather Cloudy Wind 8.5 m/sec W Sea Calm, small swell
Bottom Topography Western flank of seamount (toward crest)
Type of Dredge Nalwalk chain bag with backet Add.Wt. 100 kg+chain
Time lowered 20 h 36 m Uncorr. Water Depth 4530 m
Initial Time on Bottom 22 h 08 m Uncorr. Water Depth 4670 m
Wire Length 5082 m Wire Angle 0°
Ship Position Lat. 30°55.5'N Long. 141°45.3'E
Direction of Haul 110° Ship Speed 1.3 kt. (till 02 h 05 m)
Speed Wire-in 30 m/min (from 02 h 05 m) Winch No. 5
Final Time on Bottom 02 h 50 m Uncorr. Water Depth 4080 m
Wire Length 4200 m Wire Angle
Ship Position Lat. 30°55.7'N Long. 141°49.3'E
Time Surfaced 03 h 57 m
Dredged Materials Serpentinites (21) and related rocks (1), siltstones (147), pumices (14), scorias (2); total (186)

Date July 05-06, 1987 Ship Hakuho Maru KH 87-3 Station No. 2 [D-2]
Location Tori-Shima fore-arc seamount (same as KH 87-3-1)
Weather Cloudy, rainy Wind 12 m/sec WSW Sea Calm, swells
Bottom Topography Eastern flank of seamount (toward crest)
Type of Dredge Nalwalk chain bag with backet Add.Wt. 100 kg+chain
Time lowered 21 h 00 m Uncorr. Water Depth 4520 m
Initial Time on Bottom 22 h 41 m Uncorr. Water Depth 3970 m
Wire Length 5271 m Wire Angle 25°
Ship Position Lat. 30°54.9'N Long. 141°48.8'E
Direction of Haul 280° Ship Speed 1.1 kt. (till 23 h 50 m)
Speed Wire-in 30 m/min (from 23 h 50 m) Winch No. 5
Final Time on Bottom 00 h 22 m Uncorr. Water Depth 4250 m
Wire Length m Wire Angle
Ship Position Lat. 30°55.5'N Long. 141°46.8'E
Time Surfaced 01 h 32 m
Dredged Material Serpentinites (31) and related rocks (52), pumices (8), scorias (12); total (62)

Date July 06, 1987 Ship Hakuho Maru KH 87-3 Station No. 3 [D-3]
Location Tori-Shima fore-arc seamount (same as KH 87-3-1 & 2)
Weather Cloudy, rainy Wind 12 m/sec WSW Sea Calm, swells
Bottom Topography South-western flank of seamount (toward crest)
Type of Dredge Nalwalk chain bag with backet Add.Wt. 100 kg+chain
Time lowered 02 h 25 m Uncorr. Water Depth 4120 m
Initial Time on Bottom 03 h 59 m Uncorr. Water Depth 4170 m
Wire Length 4970 m Wire Angle 20°
Ship Position Lat. 30°53.4'N Long. 141°46.7'E
Direction of Haul 60° Ship Speed 1.0 kt. (till 06 h 10? m)
Speed Wire-in 30 m/min (from 06 h 10? m) Winch No. 5
Final Time on Bottom 06 h 47 m Uncorr. Water Depth 4100 m
Wire Length m Wire Angle
Ship Position Lat. 30°54.4'N Long. 141°49.6'E
Time Surfaced 08 h 07 m
Dredged Materials Serpentinites (41) and related rocks (3), green rocks (21), basalts (3), pumices (4), sediments (3); total (75)

Date July 08, 1987 Ship Hakuho Maru KH 87-3 Station No. 5 [D-4]
Location West part of Uyeda Ridge
Weather Fine Wind 2-3 m/sec S Sea Calm
Bottom Topography South slope of the ridge (toward crest)
Type of Dredge Nalwalk chain bag with backet Add.Wt. (200+50x3)kg+chain
Time lowered 08 h 28 m Uncorr. Water Depth 6450 m
Initial Time on Bottom 10 h 39 m Uncorr. Water Depth 6070 m
Wire Length 6274 m Wire Angle
Ship Position Lat. 27°08.3'N Long. 143°26.7'E
Direction of Haul 340° Ship Speed 0.75 kt. (till 13 h 15 m)
Speed Wire-in 15 m/min (from 13 h 15 m) Winch No. 1
Final Time on Bottom 13 h 51 m Uncorr. Water Depth 5820 m
Wire Length 5940 m Wire Angle
Ship Position Lat. 27°09.5'N Long. 143°26.3'E
Time Surfaced 16 h 09 m
Dredged Material Pieces of pillow basalt (805), hyaloclastites (40), sediments (19), phospholites (9), Mn-nodules (126), Mn-crusts (60), sponges (4); total (1063)
Note Dredge subnavigation transponder was installed at about 300 m above the 200 kg weight. 200 m wire was added to top of the No. 1 winch wire.

Date July 09, 1987 Ship Hakuho Maru KH 87-3 Station No. 7 [D-5]
Location Ogasawara Plateau (south)
Weather Rainy Wind 5 m/sec E Sea Calm, small swell
Bottom Topography Slope facing SW
Type of Dredge Nalwalk chain bag with backet Add.Wt. 100 kg+chain
Time lowered 13 h 20 m Uncorr. Water Depth 2000 m
Initial Time on Bottom 14 h 05 m Uncorr. Water Depth 1930 m
Wire Length 2290 m Wire Angle
Ship Position Lat. 25°26.4'N Long. 143°30.2'E
Direction of Haul 60° Ship Speed 1.1 kt. (till 15 h 17 m)
Speed Wire-in 30 m/min (from 15 h 17 m) Winch No. 5
Final Time on Bottom 15 h 36 m Uncorr. Water Depth 2090 m
Wire Length 2200 m Wire Angle
Ship Position Lat. 25°27.3'N Long. 143°31.0'E
Time Surfaced 16 h 10 m
Dredged Materials Pumice (23), scoria (28), siltstone (42), phospholite (16), Mn-nodule (20), sponge (22); total (157)

Date July 09, 1987 Ship Hakuho Maru KH 87-3 Station No. 8 [D-6]
Location Ogasawara Plateau (south)
Weather Partly coludy Wind 4 m/sec S Sea Calm
Bottom Topography Slope facing SW
Type of Dredge Nalwalk chain bag with backet Add.Wt. 100 kg+chain
Time lowered 16 h 57 m Uncorr. Water Depth 2700 m
Initial Time on Bottom 17 h 53 m Uncorr. Water Depth 2660 m
Wire Length 3415 m Wire Angle
Ship Position Lat. 25°31.6'N Long. 143°24.7'E
Direction of Haul 5° Ship Speed 1.0 kt. (till 16 h 32 m)
Speed Wire-in 18 m/min (from 16 h 32 m) Winch No. 5
Final Time on Bottom 18 h 54 m Uncorr. Water Depth 2670 m
Wire Length 3300 m Wire Angle
Ship Position Lat. 25°32.7'N Long. 143°24.8'E
Time Surfaced 19 h 50 m
Dredged Material No recovery, "break down" (lost dredge)
Note Dredge subnavigation transponder was installed at 500 m above the dredge.

Date Aug. 03, 1987 Ship Hakuho Maru KH 87-3 Station No. 13 [D-7]
Location Yap Fore Arc
Weather Wind 2 m/sec Sea
Bottom Topography Irregular rug. steep slope
Type of Dredge Cylindrical Chain with two small cylinders Add.Wt. 150 kg
Time lowered 17 h 12 m Uncorr. Water Depth 1870 m
Initial Time on Bottom 17 h 50 m Uncorr. Water Depth 1950 m
Wire Length 1975 m Wire Angle
Ship Position Lat. 9°19.0'N Long. 137°59.4'E
Direction of Haul Ship Speed (till h m)
Speed Wire-in m/min (from h m) Winch No. 5
Final Time on Bottom 18 h 17 m Uncorr. Water Depth 1880 m
Wire Length 2150 m Wire Angle
Ship Position Lat. 9°18.9'N Long. 137°58.7'E
Time Surfaced 18 h 54 m
Dredged Materials

Date Aug. 03, 1987 Ship Hakuho Maru KH 87-3 Station No. 15 [D-8]
Location Yap Fore Arc
Weather Wind 1 m/sec North Sea
Bottom Topography Steep irregular
Type of Dredge Add.Wt.
Time lowered 21 h 42 m Uncorr. Water Depth 1390 m
Initial Time on Bottom 22 h 07 m Uncorr. Water Depth 1400 m
Wire Length 1420 m Wire Angle 10°
Ship Position Lat. 9°20.6'N Long. 137°57.4'E
Direction of Haul Ship Speed (till h m)
Speed Wire-in m/min (from h m) Winch No. 5
Final Time on Bottom 22 h 52 m Uncorr. Water Depth 1210 m
Wire Length 1280 m Wire Angle 10°
Ship Position Lat. 9°20.5'N Long. 137°56.6'E
Time Surfaced 23 h 28 m
Dredged Material

Date Aug. 04, 1987 Ship Hakuho Maru KH 87-3 Station No. 16 [D-9]
Location Yap Ridge (Fore Arc)
Weather Fine Wind weak (N - S) Sea
Bottom Topography Steep slope and top step
Type of Dredge Cylindrical Chain with two small cylinders Add.Wt. 150 kg
Time lowered 00 h 19 m Uncorr. Water Depth 1240 m
Initial Time on Bottom 00 h 43 m Uncorr. Water Depth 1250 m
Wire Length 1270 m Wire Angle
Ship Position Lat. 9°21.5'N Long. 137°56.3'E
Direction of Haul Ship Speed kt. (till h m)
Speed Wire-in m/min (from h m) Winch No.
Final Time on Bottom 01 h 38 m Uncorr. Water Depth 940 m
Wire Length 1055 m Wire Angle
Ship Position Lat. 9°21.3'N Long. 137°55.8'E
Time Surfaced 02 h 02 m
Dredged Materials

Date Aug. 04, 1987 Ship Hakuho Maru KH 87-3 Station No. 18 [D-10]
Location Yap Trench Inner Slope
Weather Wind 2 m/sec Sea
Bottom Topography Steep slope with knob
Type of Dredge Cylindrical Chain with two cylinders Add.Wt. 100 kg
Time lowered 08 h 15 m Uncorr. Water Depth 6580 m
Initial Time on Bottom 10 h 28 m Uncorr. Water Depth 6200 m
Wire Length 6140 m Wire Angle 0°
Ship Position Lat. 9°36.9'N Long. 138°26.0'E
Direction of Haul Ship Speed kt. (till h m)
Speed Wire-in m/min (from h m) Winch No. 1
Final Time on Bottom 11 h 29 m Uncorr. Water Depth 6190 m
Wire Length 6236 m Wire Angle 15°
Ship Position Lat. 9°37.9'N Long. 138°25.5'E
Time Surfaced 13 h 15 m
Dredged Material

Date Aug. 04, 1987 Ship Hakuho Maru KH 87-3 Station No. 19 [D-11]
Location Yap Trench Inner Slope
Weather Wind 5 m/sec Sea
Bottom Topography
Type of Dredge Cylindrical Chain with two small cylinders Add.Wt.
Time lowered 13 h 35 m Uncorr. Water Depth 5450 m
Initial Time on Bottom 15 h 39 m Uncorr. Water Depth 5270 m
Wire Length 5273 m Wire Angle
Ship Position Lat. 9°40.3'N Long. 138°22.3'E
Direction of Haul Ship Speed kt. (till h m)
Speed Wire-in m/min (from h m) Winch No. 1
Final Time on Bottom 17 h 26 m Uncorr. Water Depth 4680 m
Wire Length 4946 m Wire Angle
Ship Position Lat. 9°41.6'N Long. 138°20.9'E
Time Surfaced 18 h 50 m
Dredged Materials

13-2. POSITIONS OF DREDGE HAUL

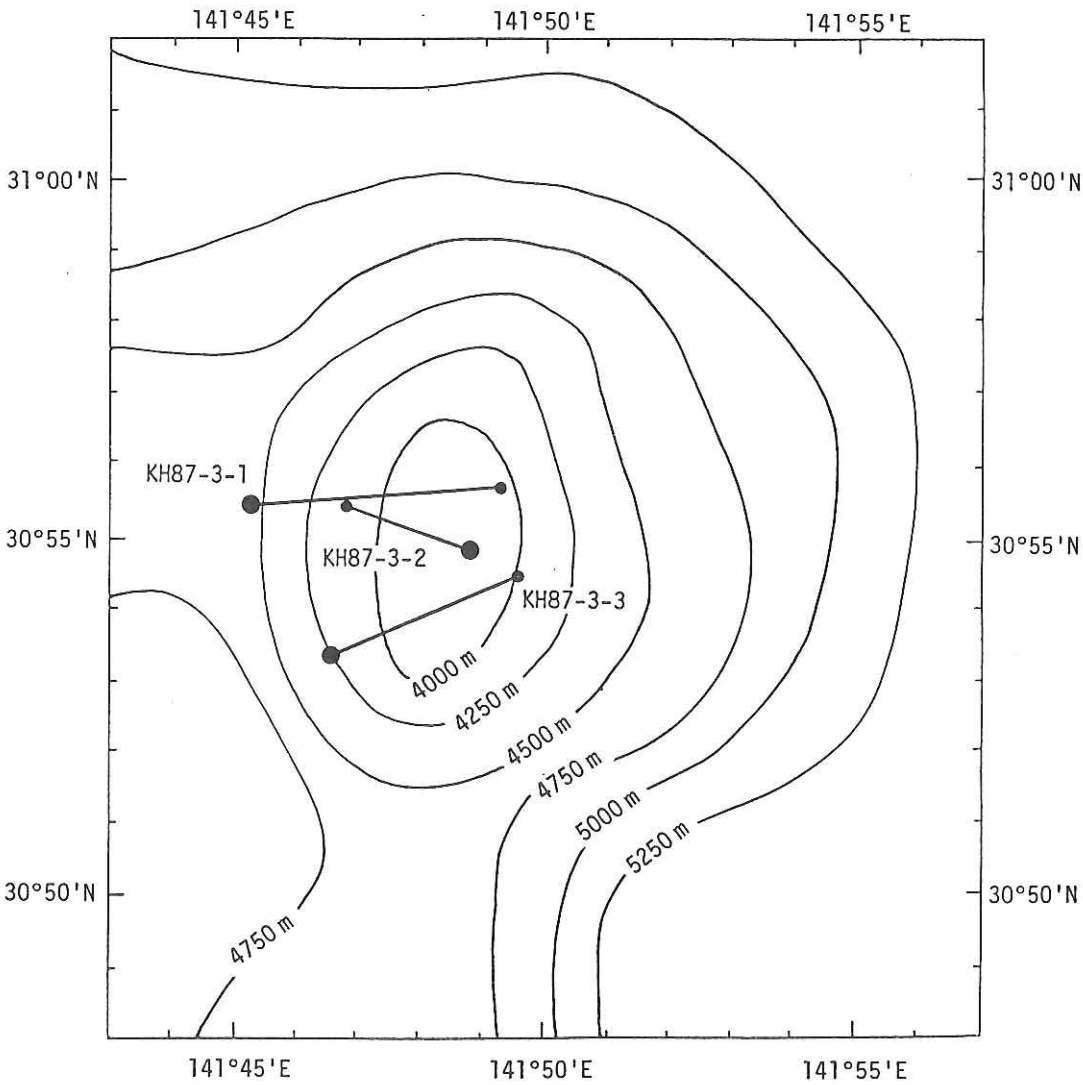

Fig. 13-2-1 Location of dredged hauls in Tori-Shima fore-arc seamount. Large and small circles indicate ship positions at the initial and final time on bottom of dredge, respectively.

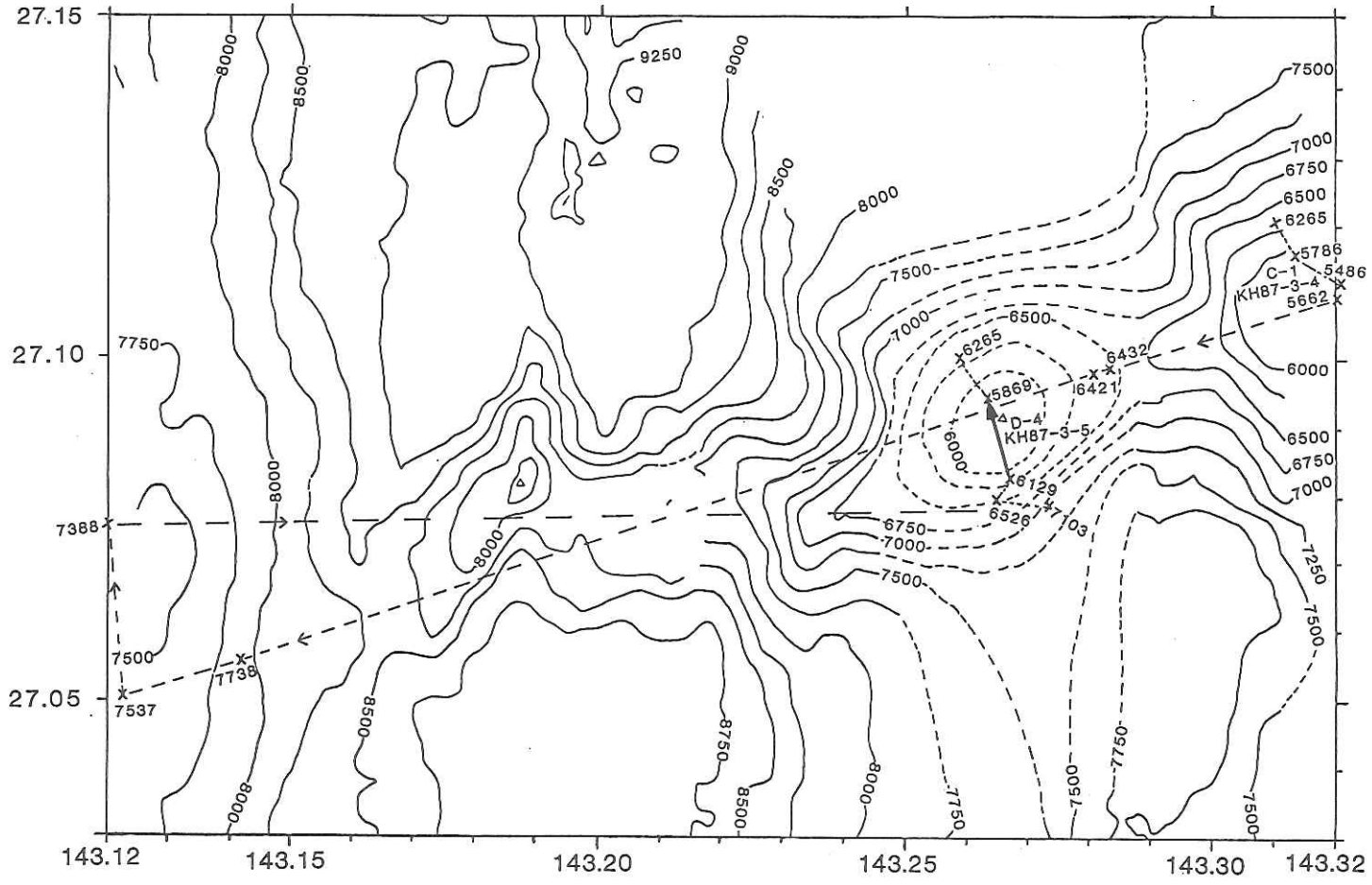

Fig. 13-2-2 Location of dredge hauls in the Uyeda Ridge during KH 87-3. Contours in the base map are taken from unpublished Seabeam data of Hydro-graphic Department, MSA Japan. Broken contours are obtained by PDR of the present cruise shown by dashed lines. C-1: Camera station KH 87-3-4.

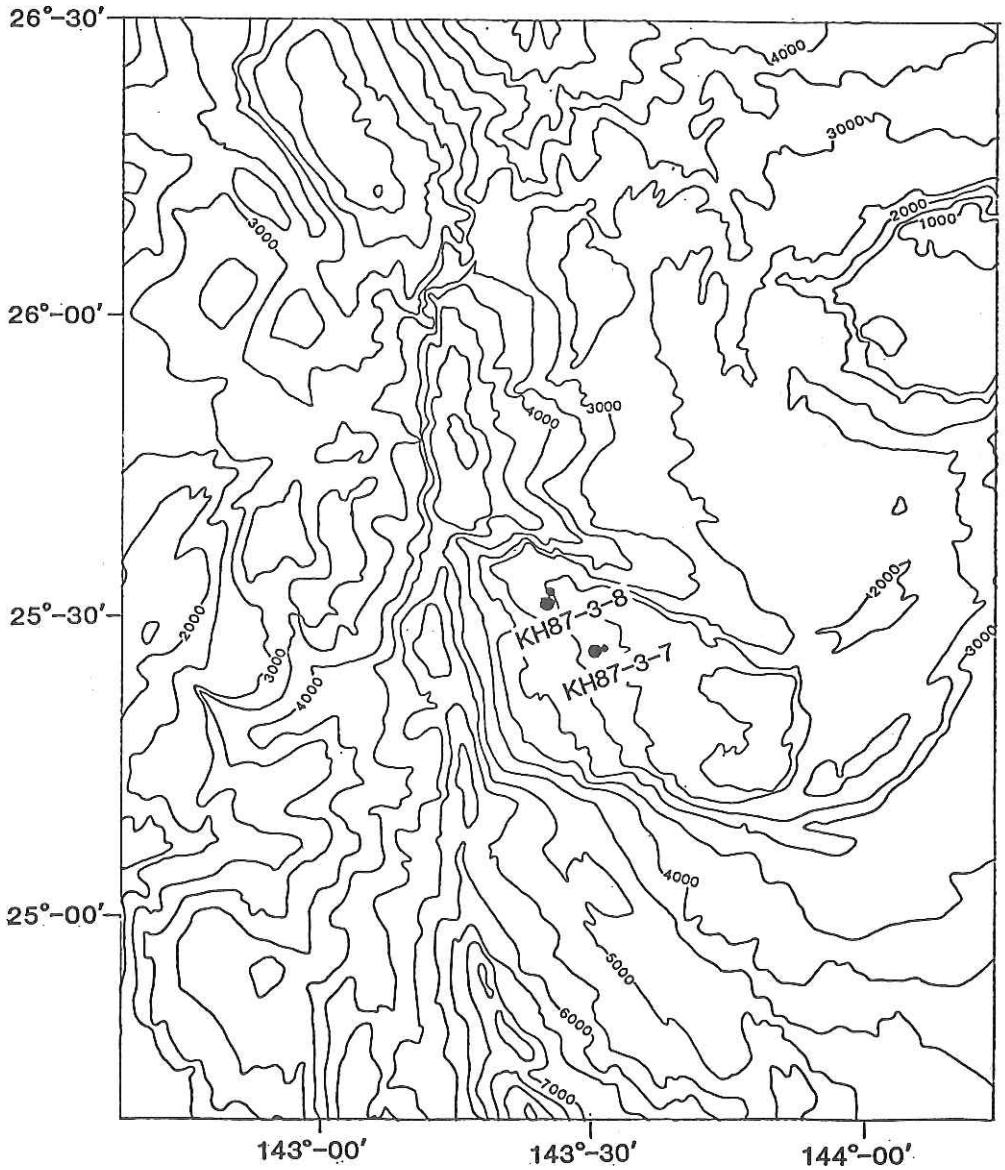

Fig. 13-2-3 Location of dredge hauls in the Ogasawara Plateau during KH 87-3. Contours in the base map are adopted from unpublished Seabeam data of Hydrographic Department, MSA Japan.

13-3. List of materials dredged during the first leg (Tokyo-Guam) of KH 87-3 cruise

TABLE 13-3-1(1). KH 87-3-1 (Tori-Shima fore-arc)

Sample No.	Diameter(mm) L	M	S	Round-ness	Wt(g)	Mn-coating(mm)	Lithology & Remarks
1-001	400	350	100	0.4	13810	PF	siltstone (biot., vein)
002	300	200	120	0.6	5250	PF	" (biot.)
003	250	100	110	0.6	2200	PF	" (")
004	180	160	100	0.4	1850	PF	" (")
005	200	130	90	0.4	1680	PF	" (")
006	160	120	80	0.6	1860	PF	" (bedded sand)
007	240	90	90	0.4	1650	PF	" (biot.)
008	220	140	100	0.4	2560	PF	" (")
009	250	200	110	0.4	3250	PF	" (")
010	170	140	80	0.4	1800	-	" (")
011	140	130	130	0.6	2250	PF	" (" , sandy)
012	220	140	100	0.4	1850	PF	" (")
013	150	120	80	0.4	1100	PF	" (" , sandy)
014	150	120	80	0.6	990	-	" (")
015	190	140	70	0.4	1140	PF	" (" , sandy)
016	190	150	60	0.4	1155	PF	" (" , frac.)
017	140	100	85	0.6	1070	-	" (")
018	160	100	80	0.4	1010	PF	" (" , sandy, frac.)
019	140	120	70	0.4	1000	PF	" (" , ")
020	110	100	60	0.4	525	PF	" (" , ")
021	150	100	60	0.4	575	-	claystone
022	120	100	80	0.4	630	PF	siltstone (biot., sandy)
023	180	90	40	0.3	490	PF	" (bedded sand)
024	130	100	60	0.3	430	PF	" (frac.)
025	140	90	50	0.4	450	-	"
026	100	80	70	0.6	435	PF	"
027	100	100	60	0.4	635	PF	" (biot., sandy)
028	150	120	90	0.6	930	PF	"
029	160	100	70	0.6	765	PF	"
030	140	90	40	0.4	460	PF	"
031	140	90	40	0.4	470	PF	" (biot., sandy)
032	140	90	60	0.6	620	PF	claystone
033	120	90	80	0.4	510	PF	siltstone (biot., sandy)
034	110	100	60	0.4	475	PF	" (")
035	130	90	70	0.4	465	PF	" (" , sandy)
036	140	60	50	0.4	355	-	claystone
037	130	90	60	0.4	390	PF	siltstone (biot.)
038	130	60	60	0.4	275	PF	" (vein)
039	110	70	35	0.4	240	PF	" (biot., sandy)
040	130	60	40	0.4	245	PF	" (")
041	100	70	30	0.4	195	PF	" (frac.)
042	140	100	70	0.3	415	PF	claystone (frac.)
043	90	90	60	0.6	405	-	siltstone (biot., sandy)
044	120	70	60	0.6	485	-	claystone (biot.)
045	80	80	70	0.6	365	-	siltstone (biot., sandy)
046	140	90	50	0.3	400	PF	" (vein)
047	120	80	70	0.4	430	PF	" (biot.)

Sample No.	Diameter(mm) L	M	S	Round-ness	Wt(g)	Mn-coating(mm)	Lithology & Remarks
1-048	120	80	50	0.6	270	PF	siltstone
049	120	50	40	0.4	180	PF	" (vein)
050	80	70	50	0.6	220	-	" (biot.)
051	90	70	40	0.4	190	-	"
052	110	80	40	0.3	210	PF	" (biot., sandy)
053	100	100	40	0.4	240	-	(" , ")
054	110	80	40	0.4	230	PF	" (sandy)
055	100	65	40	0.3	210	PF	" (biot.)
056	90	60	40	0.4	170	PF	(")
057	70	70	40	0.6	175	PF	"
058	100	70	50	0.4	240	PF	" (biot., sandy)
059	70	70	25	0.4	110	-	(" , ")
060	100	60	35	0.4	185	-	(" , ")
061	80	60	60	0.4	165	-	(" , vein)
062	80	50	30	0.6	125	PF	"
063	70	40	40	0.6	150	-	" (sandy)
064	60	60	40	0.6	150	-	" (biot., sandy)
065	70	70	40	0.4	170	-	"
066	90	80	50	0.3	240	PF	" (sandy)
067	90	80	40	0.3	215	-	" (vein)
068	100	70	40	0.6	190	-	" (sandy)
069	90	60	30	0.4	145	PF	" (yellow)
070	110	70	40	0.4	220	PF	"
071	80	70	50	0.4	185	-	" (biot., sandy)
072	100	70	45	0.4	250	-	claystone
073	100	90	40	0.4	275	-	siltstone (vein)
074	110	70	60	0.4	315	PF	" (sandy)
075	75	65	40	0.6	165	PF	"
076	100	70	40	0.4	195	PF	"
077	80	60	50	0.4	140	PF	" (biot.)
078	85	70	50	0.6	215	-	" ?, sandy)
079	90	60	40	0.4	160	-	" (sandy)
080	90	55	40	0.6	120	-	" (")
081	80	80	50	0.3	170	PF	" (" , biot.)
082	80	60	50	0.3	155	PF	"
083	70	60	40	0.6	125	PF	"
084	100	50	40	0.3	150	PF	" (sandy)
085	70	70	30	0.6	120	-	" (")
086	110	55	25	0.4	110	-	" (")
087	80	60	40	0.4	120	PF	" (frac.)
088	70	60	60	0.6	145	PF	" (sandy)
089	80	50	40	0.4	130	-	"
090	80	65	30	0.4	150	PF	"
091	90	60	30	0.3	120	-	" (sandy)
092	80	60	20	0.4	95	-	" (" , biot.)
093	70	60	30	0.4	100	PF	"
094	75	40	40	0.6	110	PF	" (sandy)
095	70	50	30	0.3	105	PF	"
096	70	50	30	0.6	95	PF	"
097	70	50	30	0.6	100	-	" (vein)
098	70	50	30	0.3	95	PF	"
099	80	50	40	0.6	150	-	" (sandy, biot.)

Sample No.	Diameter(mm) L	M	S	Round-ness	Wt(g)	Mn-coating(mm)	Lithology & Remarks
1-100	70	50	30	0.4	105	PF	siltstone
101	70	50	35	0.4	120	-	" (sandy)
102	70	60	20	0.6	90	PF	" (" , biot.)
103	70	40	30	0.4	85	-	" (biot.)
104	70	50	30	0.3	80	-	" (sandy)
105	65	50	30	0.4	85	PF	" (" , biot.)
106	70	50	40	0.3	95	PF	"
107	80	40	25	0.3	65	PF	"
108	80	50	30	0.4	100	-	"
109	70	45	30	0.4	75	PF	"
110	80	40	25	0.4	70	-	" (sandy)
111	55	40	35	0.3	50	-	"
112	60	50	30	0.4	60	-	" (sandy)
113	60	50	25	0.3	55	PF	"
114	60	40	20	0.4	50	-	" (sandy)
115	80	50	40	0.4	100	PF	" (" , biot.)
116	70	50	50	0.4	100	-	" (biot., vein)
117	65	60	30	0.4	80	-	" (sandy, biot.)
118	60	45	25	0.4	85	PF	"
119	50	50	30	0.4	80	-	" (biot.)
120	70	45	25	0.3	70	-	" (sandy)
121	65	50	20	0.4	50	PF	claystone
122	60	40	35	0.4	90	-	siltstone (sandy)
123	65	45	20	0.4	60	-	" (biot.)
124	70	50	50	0.3	125	PF	"
125	80	50	30	0.3	70	PF	" (sandy, biot.)
126	50	50	30	0.6	75	-	" (")
127	50	50	45	0.4	80	-	"
128	70	40	15	0.3	50	PF	"
129	65	45	25	0.3	55	PF	" (sandy, biot.)
130	65	40	30	0.4	80	-	" (" , ")
131	60	55	25	0.4	45	-	" (")
132	70	40	30	0.4	70	PF	" (")
133	70	40	30	0.4	70	-	" (" , biot.)
134	50	35	30	0.4	50	PF	" (" , ")
135	60	45	25	0.4	50	PF	" (")
136	70	45	30	0.4	80	PF	" (")
137	60	45	20	0.3	45	-	"
138	60	50	35	0.3	70	-	" (sandy, biot.)
139	50	45	25	0.4	55	-	sandstone (silty)
140	45	40	25	0.6	50	-	siltstone (vein)
141	90	90	70	0.3	320	PF	" (biot.)
142	95	50	25	0.4	140	-	" (sandy)
143	80	45	30	0.4	110	PF	" (" , biot.)
144	100	50	35	0.3	145	-	" (" , ")
145	50	40	30	0.4	60	-	" (")
146	70	45	40	0.3	80	-	"
147	55	45	30	0.3	60	PF	" (sandy)
148	60	45	30	0.4	65	PF	" (")
181					1750		others (siltstone etc.)
182					1515		" (")

Sample No.	Diameter(mm) L	M	S	Round-ness	Wt(g)	Mn-coating(mm)	Lithology & Remarks
1-183					400		others (siltstone etc.)
201	70	45	45	0.3	140	PF	serpentinite
202	70	50	50	0.3	150	PF	"
203	50	50	30	0.3	120	PF	"
204	60	50	20	0.3	70	PF	"
205	70	55	35	0.3	100	PF	" (sandstone)
206	50	35	30	0.3	50	PF	"
207	75	50	30	0.3	90	PF	"
208	60	50	40	0.3	100	PF	"
209	45	30	25	0.3	40	PF	"
210	40	35	10	0.3	18	PF	"
211	20	20	10	0.3	6	-	"
212	110	70	60	0.3	440	PF	"
213	70	50	40	0.3	100	PF	"
214	70	40	40	0.3	110	F	"
215	60	50	40	0.3	80	PF	"
216	20	20	10	0.3	6	-	"
217	20	25	10	0.3	6	0.5	"
218	20	20	10	0.3	4	F	"
219	20	20	10	0.3	6	-	"
220	15	15	10	0.3	3	-	"
221	20	20	15	0.3	4	PF	"
222	20	17	10	0.2	3	PF	"
301	60	50	40	0.3	45	PF	pumice
302	40	30	30	0.3	27	F	"
303	80	50	40	0.6	83	-	"
304	50	40	30	0.4	27	-	"
305	45	25	25	0.3	11	-	scoria
306	40	30	20	0.6	9	-	pumice
307	30	20	20	0.6	10	-	"
308	20	10	10	0.4	6	-	"
309	20	20	20	0.6	6	-	scoria
310	20	20	10	0.4	5	PF	pumice
311	30	20	15	0.4	4	-	"
312	30	20	15	0.4	4	-	"
313	20	15	10	0.4	4	F	"
314	20	15	15	0.6	4	-	"
315	30	20	10	0.3	4	PF	"
316	20	20	10	0.3	4	-	"
317					36		others (pumice+scoria)
401					3200		soft sediments (mud)
402					3650		" (")
403					3100		" (coaise)
404					2800		"

Note
biot. : bioturbation
F : filmed
frac. : fracture
PF : partly filmed

TABLE 13-3-1(2). KH 87-3-2 (Tori-Shima fore-arc)

Sample No.	Diameter(mm) L	M	S	Round-ness	Wt(g)	Mn-coating(mm)	Lithology & Remarks
2-001	180	120	90	0.2	3450	PF	serpentinite (harzburgite)
002	100	80	50	0.3	640	PF	" (foliation)
003	140	80	50	0.3	440	0.3	"
004	130	90	70	0.1	515	-	" (massive+sandy)
005	120	70	45	0.2	415	PF	" (foliation)
006	120	120	20	0.4	250	0.1	"
007	100	100	60	0.4	460	-	" (+serpentine clay)
008	75	70	50	0.4	335	-	" (massive+sandy)
009	90	70	50	0.2	295	-	" (slicken side)
010	80	70	70	0.2	330	-	" (")
011	70	60	45	0.3	205	0.1	" (sands. like)
012	60	45	30	0.4	200	PF	" (foliation)
013	70	60	35	0.3	185	0.1	" (sands. like, polyhed.)
014	70	65	30	0.4	130	-	" (mud. like)
015	100	50	35	0.3	155	0.1	" (")
016	80	50	40	0.3	120	0.1	" (foliation, polyhed.)
017	75	70	25	0.4	115	-	" (mud. like)
018	70	65	25	0.4	125	0.1	" (mud. like, calsite?)
019	75	50	30	0.6	120	0.1	" (sand. like)
020	70	65	30	0.4	140	-	"
021	60	45	35	0.1	80	PF	" (foliation)
022	65	40	30	0.4	100	0.1	" (mud. like)
023	70	50	40	0.3	115	0.1	" (")
024	95	40	30	0.3	120	0.1	" (mud. like, polyhed.)
025	70	40	35	0.4	95	-	" (" , calsite?)
026	50	40	40	0.3	90	PF	" (mud. like)
027	75	55	25	0.3	105	0.1	" (")
028	50	45	40	0.3	90	-	"
029	60	40	25	0.3	60	-	" (mud. like)
030	70	60	25	0.3	70	0.1	" (")
031	60	50	20	0.2	70	0.1	"
032	70	35	15	0.3	55	-	"
033	55	40	25	0.4	75	-	" (polyhedral)
034	50	40	30	0.3	90	0.1	" (")
035	55	45	20	0.2	80	-	" (with vein)
036	40	40	35	0.3	65	PF	"
037	60	35	10	0.3	29	-	" (calsite?)
038	40	30	25	0.4	34	-	" (polyhedral)
039	50	35	15	0.3	31	PF	" (mud. like)
040	40	35	15	0.3	26	PF	" (polyhedral)
041	45	30	25	0.4	36	-	"
042	45	35	15	0.3	25	0.2	"
043	40	30	30	0.3	33	0.1	" (slicken side)
044	40	30	30	0.3	27	-	"
045	35	25	20	0.4	23	-	"
046	30	25	25	0.2	23	-	" (slicken side)
047	30	25	20	0.4	22	-	" (calsite?)
048	25	25	8	0.3	12	-	" (")
049	35	25	8	0.3	13	-	" (")
050	30	20	20	0.4	17	-	"

Sample No.	Diameter(mm) L	M	S	Round-ness	Wt(g)	Mn-coating(mm)	Lithology & Remarks
2-051	55	20	10	0.3	21	0.1	serpentinite
052	40	30	10	0.3	20	-	"
053					300		others (serpentinites)
054					110		" (")
101	80	60	50	0.4	130	PF	pumice
102	70	70	35	0.3	130	-	"
103	80	60	40	0.4	165	PF	scoria
104	50	60	30	0.4	60	-	pumice
105	70	50	35	0.2	55	PF	"
106	50	40	40	0.4	50	-	"
107	40	35	20	0.4	25	-	scoria
108	50	35	20	0.3	26	-	pumice
109	35	30	25	0.3	22	0.1	"
110	35	30	20	0.3	19	0.2	"
201					4250		soft sediments (mud)
202					4600		" (")
203					3600		" (")
204					4170		" (")
205					1880		" (")
206					1450		" (")
207					2050		" (sand)
208					2050		serpentine clay (+pebble)
209					505		"

Note

F : filmed
PF : partly filmed
muds. : mudstone
polyhed. : polyhedral
sands. : sandstone

TABLE 13-3-1(3). KH 87-3-3 (Tori-Shima fore-arc)

Sample No.	Diameter(mm) L	M	S	Round-ness	Wt(g)	Mn-coating(mm)	Lithology & Remarks
3-001	280	250	160	0.4	15000	0.1	green rock(gabbro?,polyhed.)
002	190	90	80	0.2	1550	0.1	" (dolerite?,with vein)
003	120	110	90	0.4	1100	-	serpentinite (polyhedral)
004	100	80	50	0.4	575	PF	" (")
005	110	90	80	0.4	705	PF	" (")
006	160	90	80	0.3	1190	PF	"
007	140	130	40	0.2	635	PF	"
008	90	60	60	0.3	330	PF	" (zeolite?)
009	120	80	70	0.3	375	PF	serpentinite sandstone
010	80	55	55	0.6	420	PF	green rock(dolerite?,polyhed.)
011	130	70	50	0.3	450	PF	serpentinite (polyhedral)
012	110	60	45	0.4	310	-	" (")
013	90	50	50	0.2	235	-	basalt (polyhedral)
014	110	90	60	0.2	450	-	green rock
015	90	60	45	0.3	230	-	"
016	60	50	50	0.3	130	-	"
017	100	70	50	0.3	280	PF	"
018	75	50	45	0.4	215	PF	serpentinite(harz.,polyhed.)
019	85	50	40	0.2	180	0.2	" (polyhed., C.V.)
020	80	50	40	0.3	140	1.0	conglomerate(polyhed.,slick.s.)
021	60	60	40	0.6	125	0.2	green rock
022	60	50	30	0.3	120	-	" (slicken side)
023	55	35	30	0.3	75	-	serpentinite (white vein)
024	60	45	35	0.4	75	-	" (polyhedral)
025	110	45	25	0.1	75	-	" (conglomerate?)
026	45	40	40	0.4	90	-	green rock(polyhed.,slick.s.)
027	60	40	40	0.3	85	-	"
028	50	40	40	0.3	60	-	serpentinite
029	70	60	40	0.4	125	0.1	green rock (polyhedral)
030	80	45	20	0.3	65	0.1	"
031	70	50	40	0.4	120	PF	" ?
032	55	40	40	0.2	105	-	green rock + zeolite
033	70	50	25	0.3	90	0.1	serpentinite
034	60	50	30	0.3	105	0.1	basalt
035	55	35	20	0.3	40	-	serpentinite
036	70	45	20	0.3	75	0.1	green rock
037	55	45	30	0.4	70	-	serpentinite ?
038	50	30	30	0.3	70	PF	serpentinite (slicken side)
039	50	40	30	0.4	95	PF	" (polyhedral)
040	70	50	35	0.2	90	-	basalt (slicken side)
041	50	40	30	0.2	75	0.1	serpentinite ?
042	50	40	40	0.3	84	-	green rock(polyhed.,slick.s.)
043	50	40	25	0.3	60	-	serpentinite (slicken side)
044	45	45	20	0.4	55	-	green rock(polyhed.,slick.s.)
045	70	50	15	0.3	59	PF	serpentinite ?
046	60	40	15	0.3	43	0.1	serpentinite
047	60	60	15	0.3	51	PF	"
048	50	35	15	0.4	37	-	"
049	55	40	25	0.3	49	-	" (polyhedral)
050	55	25	25	0.3	41	0.1	serpentinite

Sample No.	Diameter(mm) L	M	S	Round-ness	Wt(g)	Mn-coating(mm)	Lithology & Remarks
3-051	50	25	20	0.3	51	PF	serpentinite (slicken side)
052	45	35	30	0.3	48	-	green rock (slicken side)
053	35	35	30	0.3	49	F	serpentinite ?
054	60	40	20	0.3	41	-	serpentinite
055	50	30	10	0.4	22	-	"
056	50	30	20	0.3	26	0.1	" ? (polyhedral)
057	70	40	25	0.3	40	PF	" ?
058	50	35	30	0.2	41	PF	" ? (white vein)
059	45	35	30	0.2	48	-	serpentinite sandstone
060	55	40	25	0.1	49	PF	serpentinite (polyhedral)
061	50	50	15	0.3	39	0.1	"
062	60	35	20	0.3	30	-	"
063	50	25	25	0.4	30	-	"
064	35	35	30	0.4	41	PF	"
065	45	30	25	0.3	35	-	"
066	40	40	35	0.3	58	-	"
067	40	35	25	0.4	36	0.1	green rock (polyhedral)
068	50	45	15	0.2	35	PF	serpentinite (white vein)
069	65	35	25	0.3	28	PF	" ? (polyhedral)
070					460		others - 1
071					725		others - 2
072					810		others - 3
3-201	60	50	40	0.4	52	0.1	pumice
202	60	30	20	0.4	18	0.1	"
203	70	40	40	0.3	79	PF	"
204	60	40	30	0.3	46	PF	"
3-301	240	120	100	0.4	1960	PF	mudstone (bioturbation)
302	30	20	15	0.6	20	-	"
3-401					6000		soft sediments (mud)
402					4950		" (")
403					4700		" (")
404					4950		" (sand)
405					2300		" (serpentine clay?)
406					2600		" (sand)

Note

C.V.	: carbonate vein
F	: filmed
harz.	: harzburgite
PF	: partly filmed
polyhed.	: polyhedral
slick. s.	: slicken side

TABLE 13-3-1(5). KH 87-3-5 (Uyeda Ridge)

Sample No.	Diameter(mm) L	M	S	Round-ness	Wt(g)	Mn-coating(mm)	Lithology & Remarks
5-001	280	150	130	0.4	4350	PF	pillow lava
002	200	170	110	0.4	2650	PF	"
003	190	140	120	0.4	1870	F	" (fresh)
004	130	110	100	0.3	1600	PF	"
005	230	100	90	0.3	1750	PF	"
006	180	120	90	0.4	1750	F	" (fresh)
007	160	120	90	0.4	1650	F	"
008	130	110	70	0.6	1060	4.0	"
009	170	90	90	0.3	855	PF	"
010	110	96	60	0.3	560	PF	"
011	140	120	80	0.3	1460	PF	" (pl,g-Ti-aug,xth,fr)
012	120	90	90	0.4	1330	F	" (ol with sp, fr)
013	120	100	90	0.4	990	PF	"
014	110	100	100	0.3	1195	PF	"
015	100	100	90	0.4	1100	F	" (fresh)
016	200	90	60	0.3	1000	PF	"
017	120	110	80	0.3	935	PF	"
018	110	100	70	0.4	530	PF	"
019	160	60	50	0.3	585	PF	"
020	90	90	60	0.4	740	3.0	"
021	110	110	70	0.3	845	4.0	"
022	130	100	75	0.4	830	6.0	"
023	120	80	60	0.3	620	PF	" (fresh)
024	100	100	60	0.3	685	PF	"
025	140	110	90	0.3	900	F	"
026	120	110	60	0.3	890	PF	"
027	120	90	90	0.4	1055	20.0	"
028	110	80	50	0.4	390	7.0	"
029	90	60	60	0.3	535	PF	"
030	110	90	55	0.4	710	10.0	"
031	110	80	65	0.4	630	PF	" (ol, g-Ti-aug, fr)
032	130	100	70	0.3	990	4.0	"
033	130	80	60	0.3	655	2.0	"
034	100	75	60	0.3	500	10.0	"
035	160	90	55	0.3	825	PF	" (ol,pl,g-Ti-aug,fr)
036	120	90	40	0.3	425	PF	"
037	120	80	50	0.3	710	PF	" (ol, g-Ti-aug)
038	150	90	70	0.3	855	PF	"
039	130	70	60	0.3	370	PF	"
040	110	70	70	0.4	590	PF	"
041	110	90	80	0.3	865	PF	" (ol with sp, fr)
042	110	100	90	0.4	900	F	"
043	100	90	70	0.4	575	PF	"
044	180	90	60	0.2	620	PF	"
045	120	100	50	0.4	780	PF	"
046	160	120	100	0.3	2400	PF	" (ol with sp,pl,fr)
047	140	70	70	0.3	680	PF	"
048	110	80	70	0.3	510	PF	"
049	80	70	70	0.4	565	PF	"
050	100	70	50	0.3	300	PF	"

Sample No.	Diameter(mm) L	M	S	Round-ness	Wt(g)	Mn-coating(mm)	Lithology & Remarks
5-051	110	90	70	0.4	590	1.0	pillow lava
052	120	70	70	0.3	415	PF	"
053	110	50	25	0.2	120	PF	"
054	90	80	70	0.3	525	PF	"
055	90	70	70	0.3	440	PF	"
056	100	80	55	0.4	495	2.0	"
057	90	85	60	0.3	425	PF	"
058	80	70	60	0.4	350	PF	"
059	90	55	50	0.4	225	PF	" (plagioclase rich)
060	120	70	70	0.3	390	PF	" (ol with sp,g-Ti-aug,fr)
061	120	60	50	0.3	430	1.0	"
062	120	80	60	0.2	605	PF	" (plagioclase rich)
063	120	90	60	0.3	650	PF	"
064	90	90	60	0.3	490	1.0	"
065	110	80	50	0.3	485	PF	"
066	120	70	55	0.3	450	F	"
067	90	70	50	0.2	535	PF	"
068	100	80	70	0.3	640	PF	"
069	140	60	50	0.3	350	-	"
070	130	50	40	0.3	445	PF	"
071	100	70	60	0.3	380	PF	" (plagioclase-rich)
072	130	100	50	0.3	490	PF	"
073	160	60	50	0.3	500	PF	" (plagioclase-rich)
074	110	70	50	0.3	365	PF	"
075	100	70	50	0.3	430	F	"
076	130	90	50	0.2	640	PF	"
077	120	120	70	0.3	625	PF	"
078	130	60	50	0.3	410	PF	"
079	90	90	60	0.4	525	F	"
080	130	80	60	0.4	570	4.0	" (ol, pl, fr)
081	140	70	60	0.2	530	PF	"
082	110	80	70	0.2	555	PF	"
083	140	70	60	0.3	620	PF	"
084	130	70	55	0.3	475	PF	"
085	100	90	70	0.3	820	PF	"
086	120	70	70	0.3	725	PF	" (ol with sp,pl,fr)
087	100	80	70	0.3	535	PF	"
088	100	60	60	0.3	455	PF	"
089	90	70	40	0.3	320	PF	"
090	110	70	70	0.3	415	2.0	"
091	110	70	60	0.4	480	7.0	"
092	100	60	60	0.3	400	2.0	" (fresh)
093	130	90	60	0.3	620	F	"
094	120	100	80	0.3	995	0.5	" (fresh)
095	90	80	60	0.3	360	PF	"
096	120	60	60	0.3	485	PF	" (plagioclase-rich)
097	100	65	50	0.3	320	F	"
098	100	70	50	0.4	305	2.0	"
099	100	70	70	0.2	290	PF	"
100	90	90	70	0.3	415	F	" (ol with sp, pl)
101	110	60	60	0.3	360	PF	"
102	90	90	70	0.3	445	F	"

Sample No.	Diameter(mm) L	M	S	Roundness	Wt(g)	Mn-coating(mm)	Lithology & Remarks
5-103	140	50	45	0.3	350	PF	pillow lava
104	110	50	50	0.4	295	1.0	"
105	80	80	60	0.3	415	PF	"
106	110	50	50	0.4	280	5.0	"
107	130	90	70	0.3	610	PF	"
108	140	80	50	0.3	475	PF	"
109	100	70	50	0.4	370	PF	"
110	120	60	50	0.3	340	PF	"
111	130	70	60	0.3	425	PF	"
112	110	50	40	0.3	270	PF	"
113	110	60	50	0.2	260	1.0	"
114	110	60	50	0.3	305	PF	"
115	90	60	60	0.3	230	PF	"
116	90	70	60	0.4	375	F	"
117	100	60	60	0.4	415	8.0	"
118	120	50	40	0.3	260	PF	"
119	90	75	70	0.3	370	PF	" (plagioclase rich)
120	130	50	50	0.3	360	PF	"
121	110	60	50	0.3	265	PF	" (fresh)
122	80	60	40	0.3	195	PF	"
123	80	70	60	0.3	285	PF	" (fresh)
124	90	70	60	0.2	240	PF	"
125	70	65	50	0.3	220	F	"
126	80	50	50	0.3	200	2.0	"
127	80	70	35	0.4	180	F	"
128	90	70	60	0.3	290	F	"
129	100	60	60	0.2	275	PF	" (+phosphorite)
130	90	60	60	0.3	255	F	"
131	105	65	50	0.3	310	PF	"
132	110	80	50	0.3	465	PF	" (pl-rich, fresh)
133	90	80	45	0.3	270	PF	" (" , ")
134	70	70	70	0.3	315	PF	"
135	100	70	50	0.3	275	PF	" (plagioclase rich)
136	110	70	50	0.4	430	PF	"
137	125	60	40	0.3	215	PF	"
138	120	65	50	0.3	395	PF	"
139	110	80	45	0.3	340	-	"
140	120	70	45	0.3	400	F	"
141	128	80	55	0.3	515	PF	" (fresh)
142	120	65	40	0.3	335	F	"
143	110	60	60	0.3	360	F	"
144	80	70	40	0.3	230	PF	"
145	110	40	30	0.3	170	1.0	"
146	70	50	35	0.3	205	PF	"
147	60	60	40	0.3	165	PF	"
148	70	60	35	0.3	170	F	"
149	75	60	50	0.3	245	F	"
150	85	60	45	0.3	225	F	" (fresh)
151	65	60	35	0.3	185	PF	"
152	100	50	45	0.3	210	PF	"
153	90	55	35	0.3	155	F	"
154	100	60	60	0.3	295	PF	"

Sample No.	Diameter(mm) L	M	S	Round-ness	Wt(g)	Mn-coating(mm)	Lithology & Remarks
5-155	75	60	40	0.3	170	PF	pillow lava
156	105	35	35	0.2	140	PF	"
157	90	70	60	0.4	385	F	"
158	110	55	55	0.3	320	PF	"
159	75	55	55	0.3	270	PF	"
160	80	60	45	0.3	225	2.0	"
161	90	60	55	0.3	325	PF	"
162	90	65	45	0.3	230	PF	" (pl-rich, fresh)
163	140	55	55	0.3	395	F	"
164	110	70	60	0.3	455	F	"
165	90	70	65	0.3	515	PF	" (fresh)
166	120	60	45	0.3	350	PF	"
167	100	85	70	0.3	615	F	"
168	120	45	45	0.3	310	F	" (plagioclase-rich)
169	130	80	70	0.3	570	F	"
170	90	80	70	0.4	450	F	"
171	110	80	80	0.4	585	F	"
172	100	65	65	0.3	420	PF	" (plagioclase-rich)
173	85	55	35	0.3	145	PF	"
174	85	70	65	0.3	340	PF	" (fresh)
175	95	65	35	0.3	300	PF	"
176	100	70	60	0.3	345	PF	" (fresh)
177	90	65	60	0.3	255	PF	" (plagioclase-rich)
178	90	60	50	0.4	350	1.0	" (fresh)
179	85	85	55	0.3	290	PF	"
180	100	75	50	0.3	365	PF	" (fresh)
181	100	60	55	0.3	340	PF	"
182	75	75	50	0.4	280	PF	"
183	80	60	40	0.3	175	PF	"
184	60	60	60	0.3	245	PF	"(ol with sp,pl-rich,xth,fr)
185	70	70	50	0.3	225	PF	"
186	130	70	40	0.3	290	PF	"
187	100	80	60	0.3	290	PF	"
188	90	75	50	0.3	335	PF	" (fresh)
189	60	60	60	0.4	250	PF	"
190	80	70	60	0.3	415	PF	"
191	90	65	60	0.3	320	4.0	"
192	60	55	55	0.4	155	PF	"
193	90	65	50	0.3	205	PF	"
194	80	60	45	0.3	140	PF	"
195	100	50	45	0.3	185	PF	"
196	70	55	40	0.3	240	F	"
197	100	65	55	0.4	400	F	" (pl-rich, fresh)
198	80	80	60	0.3	325	PF	" (" , ")
199	65	65	65	0.3	190	F	"
200	100	50	50	0.3	225	F	"
201	130	55	45	0.3	285	PF	"
202	90	75	65	0.4	355	PF	"
203	110	70	30	0.3	190	PF	" (pl-rich, fresh)
204	95	65	40	0.3	255	PF	" (pl-rich, fresh)
205	80	60	45	0.3	260	PF	"
206	90	60	45	0.3	270	PF	"

Sample No.	Diameter(mm) L	M	S	Round-ness	Wt(g)	Mn-coating(mm)	Lithology & Remarks
5-211	110	65	50	0.3	290	-	pillow lava (fresh)
212	95	70	65	0.3	325	PF	"
213	60	60	60	0.3	180	PF	"
214	90	50	30	0.3	195	PF	"
215	80	60	40	0.3	175	PF	"
216	65	50	50	0.3	180	PF	" (fresh)
217	90	65	45	0.3	250	2.0	"
218	80	55	35	0.4	235	PF	"
219	85	70	30	0.3	210	PF	" (fresh)
220	95	70	60	0.3	300	F	"
221	110	50	45	0.4	245	F	"
222	90	60	50	0.3	240	F	"
223	100	60	50	0.3	345	PF	"
224	80	60	35	0.3	120	4.0	"
225	90	60	55	0.4	360	F	"
226	90	35	30	0.3	215	F	"
227	95	55	50	0.4	225	1.0	" (fresh)
228	70	50	45	0.3	150	F	"
229	70	40	30	0.3	105	F	"
230	70	50	40	0.4	145	1.0	"
231	60	60	60	0.3	190	PF	"
232	60	55	30	0.4	150	F	" (plagioclase-rich)
233	90	50	50	0.3	185	F	"
234	80	50	40	0.3	170	F	"
235	70	50	50	0.4	155	5.0	"
236	55	50	50	0.3	115	12.0	"
237	70	65	60	0.3	190	PF	"
238	60	60	50	0.3	165	PF	"(ol with sp,pl,xth,fr)
239	100	40	30	0.4	160	2.0	"
240	90	60	40	0.3	245	PF	"
241	60	50	40	0.4	120	PF	"
242	70	40	30	0.3	120	F	"
243	75	45	40	0.3	110	F	"
244	80	45	40	0.3	140	PF	"
245	80	60	60	0.3	260	PF	"
246	65	45	45	0.4	125	PF	"
247	80	60	40	0.3	205	F	"
248	80	55	50	0.3	190	PF	" (fresh)
249	70	65	50	0.3	205	PF	"
250	90	60	50	0.3	250	4.0	"
251	70	45	40	0.3	175	F	"
252	60	50	35	0.4	180	3.0	" (white)
253	55	55	55	0.4	140	PF	"
254	80	70	55	0.4	300	4.0	"
255	90	70	50	0.3	200	4.0	" (+mud)
256	70	40	40	0.3	120	PF	"
257	65	50	40	0.3	130	PF	"
258	50	50	40	0.3	125	PF	"
259	85	45	45	0.3	170	PF	"
260	80	75	25	0.4	270	2.0	"
261	90	60	60	0.3	255	F	"
262	75	65	40	0.3	300	F	"

Sample No.	Diameter(mm) L	M	S	Round-ness	Wt(g)	Mn-coating(mm)	Lithology & Remarks
5-263	80	70	70	0.3	365	5.0	pillow lava (fresh)
264	90	70	60	0.3	335	PF	" (+hyaloclastite)
265	60	60	40	0.3	190	PF	"
266	80	70	50	0.3	255	F	" (plagioclase-rich)
267	110	65	60	0.3	335	PF	"
268	70	60	60	0.3	200	PF	" (plagioclase-rich)
269	80	40	35	0.3	120	-	" (fresh)
270	70	60	45	0.3	235	F	"
271	85	50	40	0.4	210	6.0	" (fresh)
272	70	50	50	0.4	205	PF	"
273	90	70	50	0.4	255	-	"
274	75	70	40	0.4	230	2.0	"
275	70	65	40	0.4	195	PF	"
276	90	50	40	0.3	180	1.0	" (fresh)
277	65	60	50	0.4	175	PF	"
278	105	40	30	0.4	185	PF	"
279	80	50	50	0.4	210	3.0	"
280	80	60	45	0.3	185	PF	"
281	75	70	40	0.4	200	F	"
282	90	65	50	0.4	270	PF	"
283	80	50	40	0.3	190	PF	"
284	100	50	50	0.3	185	PF	"
285	110	50	50	0.3	210	F	"
286	90	60	50	0.3	225	PF	"
287	80	70	50	0.3	275	0.5	"
288	90	55	50	0.3	230	4.0	" (fresh)
289	80	60	50	0.3	300	PF	"
290	90	70	60	0.4	430	PF	" (fresh)
291	120	60	40	0.3	300	PF	" (")
292	70	50	45	0.3	155	2.0	"
293	90	50	40	0.3	235	PF	" (pl-rich, fresh)
294	60	30	30	0.3	80	PF	"
295	110	50	50	0.3	235	10.0	" (phosporite?)
296	95	60	60	0.3	270	PF	"
297	100	60	50	0.3	255	PF	"
298	80	50	50	0.3	190	PF	"
299	105	60	60	0.3	180	PF	"
300	60	60	50	0.4	130	PF	" (fresh)
301	70	60	40	0.4	150	PF	"
302	90	70	50	0.3	290	F	" (fresh)
303	90	50	50	0.3	315	PF	"
304	75	50	50	0.4	220	1.0	"
305	80	70	50	0.3	280	F	" (pl-rich, fresh)
306	100	60	50	0.3	230	PF	"
307	65	65	65	0.3	265	2.0	"
308	70	50	50	0.3	235	PF	" (fresh)
309	80	60	60	0.3	320	PF	"
310	80	60	50	0.3	145	PF	"
311	75	70	40	0.4	200	2.0	"
312	95	65	35	0.4	235	5.0	" (fresh)
313	90	70	40	0.4	225	F	" (")
314	105	50	50	0.4	235	PF	"

Sample No.	Diameter(mm) L	M	S	Round-ness	Wt(g)	Mn-coating(mm)	Lithology & Remarks
5-315	80	70	60	0.4	240	F	pillow lava (ol with sp,pl,g-Ti-aug,fr)
316	100	50	30	0.3	220	F	pillow lava (fresh)
317	95	50	45	0.3	220	-	"
318	90	70	60	0.3	235	1.0	"
319	85	50	30	0.3	150	F	"
320	75	70	50	0.3	295	F	" (fresh)
321	80	60	40	0.4	180	PF	"
322	90	70	50	0.3	260	F	"
323	80	60	50	0.3	220	0.5	"
324	80	50	50	0.3	235	F	"
325	80	70	40	0.4	240	F	"
326	80	70	40	0.4	220	2.0	"
327	95	60	50	0.4	225	F	"
328	70	70	60	0.3	215	0.5	" (fresh)
329	70	60	40	0.3	160	-	"
330	85	65	60	0.3	165	F	" (plagioclase-rich)
331	70	50	40	0.3	210	PF	"
332	100	50	40	0.3	300	F	" (ol with sp,pl,g-Ti-aug,xth,fr)
333	100	60	50	0.3	210	5.0	pillow lava
334	80	60	50	0.4	295	2.0	" (fresh)
335	80	80	50	0.4	290	4.0	" (")
336	120	70	40	0.3	335	1.0	" (+hyaloclastite,fresh)
337	80	80	50	0.3	260	1.0	"
338	90	80	50	0.3	330	F	" (fresh)
339	90	90	70	0.3	490	10.0	"
340	115	45	30	0.3	200	F	"
341	60	50	50	0.4	160	2.0	"
342	80	70	50	0.3	230	-	"
343	90	80	60	0.3	300	F	" (plagioclase-rich)
344	80	50	45	0.4	185	2.0	"
345	60	50	40	0.4	115	4.0	"
346	60	40	40	0.3	150	-	"
347	80	65	30	0.3	130	F	"
348	70	60	50	0.3	205	F	"
349	60	60	40	0.4	155	F	" (pl-rich, fresh)
350	70	55	50	0.3	220	1.0	"
351	50	50	40	0.2	140	F	"
352	90	60	50	0.4	205	2.0	"
353	80	50	30	0.3	155	F	"
354	90	70	45	0.3	255	1.0	"
355	70	60	35	0.3	170	-	"
356	80	70	40	0.2	255	F	" (white)
357	100	60	50	0.3	170	PF	"
358	70	60	50	0.3	245	3.0	"
359	90	60	40	0.2	160	PF	"
360	70	50	40	0.3	145	PF	"
361	90	60	60	0.4	320	PF	" (fresh)
362	90	60	40	0.4	285	PF	"
363	70	60	30	0.3	200	F	" (ol with sp,pl,g-Ti-aug,fr)

Sample No.	Diameter(mm) L	M	S	Round-ness	Wt(g)	Mn-coating(mm)	Lithology & Remarks
5-364	70	60	40	0.3	195	PF	pillow lava
365	90	70	40	0.3	280	5.0	"
366	80	40	40	0.4	160	PF	"
367	60	50	45	0.4	140	-	"
368	80	60	30	0.4	135	PF	"
369	80	60	50	0.3	190	F	" (fresh)
370	100	60	30	0.3	235	F	"
371	110	60	50	0.3	230	F	" (fresh)
372	80	60	40	0.3	205	F	"
373	80	50	40	0.2	210	1.0	" (white)
374	70	45	40	0.3	145	1.0	"
375	60	55	30	0.3	130	F	"
376	60	55	50	0.2	185	F	"
377	75	40	40	0.3	190	1.0	"
378	60	60	60	0.3	215	F	"
379	80	60	50	0.2	160	1.0	"
380	90	70	60	0.3	280	F	"
381	60	60	50	0.3	155	4.0	"
382	100	50	50	0.3	260	PF	" (fresh)
383	100	50	50	0.3	210	1.0	"
384	100	60	40	0.3	215	F	" (plagioclase-rich)
385	70	60	40	0.3	185	F	" (xenolith?)
386	80	60	50	0.3	285	2.0	"
387	80	55	40	0.3	200	1.0	"
388	100	50	30	0.3	160	F	"
389	90	50	40	0.3	155	1.0	"
390	70	60	60	0.3	200	5.0	"
391	80	50	45	0.3	195	F	"
392	65	50	50	0.3	155	F	"
393	100	70	50	0.2	230	F	"
394	65	60	50	0.3	145	PF	"
395	70	60	45	0.3	150	3.0	"
396	90	60	45	0.3	215	F	"
397	90	70	40	0.3	245	F	"
398	100	60	50	0.3	200	PF	"
399	60	40	40	0.3	115	F	"
400	100	50	50	0.3	260	0.5	" (pl-rich, fresh)
401	70	50	40	0.3	120	PF	"
402	80	50	50	0.3	225	PF	"
403	90	70	70	0.3	300	1.0	" (fresh)
404	70	50	40	0.3	135	PF	"
405	65	65	50	0.3	180	F	"
406	60	50	50	0.3	150	F	"
407	80	60	40	0.3	175	F	"
408	70	60	40	0.3	150	F	"
409	80	70	50	0.3	210	F	"
410	70	70	50	0.3	190	F	"
411	90	60	50	0.4	180	F	" (fresh)
412	60	60	50	0.3	135	F	"
413	80	50	40	0.3	150	F	"
414	100	50	40	0.3	165	F	"
415	80	50	40	0.4	175	F	"

Sample No.	Diameter(mm) L	M	S	Round-ness	Wt(g)	Mn-coating(mm)	Lithology & Remarks
5-416	90	60	35	0.4	200	PF	pillow lava (fresh)
417	90	50	50	0.3	150	PF	"
418	80	50	40	0.3	130	PF	"
419	70	50	50	0.3	175	1.0	"
420	80	60	40	0.2	150	-	"
421	70	60	50	0.2	140	1.0	"
422	70	60	40	0.4	180	2.0	"
423	70	70	50	0.3	175	F	"
424	70	50	50	0.3	210	3.0	"
425-444	(20)				2480		" (pl-poor)
445-464	(20)				2530		"
465-484	(20)				2140		"
485-504	(20)				1260		"
505-524	(20)				2270		"
525-544	(20)				1700		"
545-564	(20)				1028		"
565-584	(20)				2150		"
585-604	(20)				2150		"
605-624	(20)				1590		"
625-644	(20)				1720		"
645-664	(20)				1920		"
665-684	(20)				2250		"
685-704	(20)				1407		"
705-724	(20)				2180		" (pl-rich)
725-744	(20)				1285		"
745-764	(20)				2400		"
765-784	(20)				2130		"
785-801	(20)				1950		"
802					200		" (ol, pl)
803					200		" (aphyric)
804	150	100	80	0.4	1460	F	"
805	90	60	60	0.3	420	F	"
806					1730		others
1000	730	530	280	0.3	74000	35.0	Mn-nodule (c., conglomerate)
1001	300	260	130	0.2	7500	30.0	" (")
1002	300	230	100	0.2	4900	30.0	" (")
1003	180	140	110	0.4	2280	30.0	" (c., pillow lava)
1004	230	150	110	0.3	3380	60.0	" (c., phosphorite)
1005	230	200	130	0.3	3150	40.0	"
1006	360	180	80	0.3	5250	2.0	phosphorite
1007	260	180	90	0.2	3070	30.0	Mn-nodule (c., conglomerate)
1008	250	140	90	0.2	1860	30.0	" (")
1009	230	140	60	0.2	1700	1.0	conglomerate
1010	230	140	100	0.3	1890	5.0	Mn-nodule (c., pillow lava)
1011	210	110	70	0.3	1210	-	conglomerate(with Mn-nodule)
1012	260	200	100	0.2	4800	3.0	phosphorite
1013	230	160	90	0.2	3220	PF	"
1014	210	160	90	0.3	2380	-	conglomerate (Mn-nd.+phsph.)
1015	180	100	70	0.2	900	-	" (with Mn-nodule)
1016	190	160	60	0.2	1420	PF	phosphorite

Sample No.	Diameter(mm) L	M	S	Roundness	wt(g)	Mn-coating(mm)	Lithology & Remarks
5-1017	190	130	100	0.3	2450	PF	hyalocasdtite
1018	160	150	60	0.3	1030	10.0	conglomerate
1019	180	110	70	0.2	1040	PF	phosphorite
1020	140	135	110	0.4	1850	50.0	Mn-nodule (c., pillow lava)
1021	190	140	80	0.3	1760	30.0	" (c., chert+phsph.)
1022	170	130	70	0.3	710	65.0	"
1023	180	80	80	0.4	1180	15.0	" (c., pillow lava)
1024	120	110	90	0.4	705	50.0	" (c., red chert+?)
1025	120	100	80	0.4	790	15.0	"
1026	110	80	50	0.4	310	30.0	"
1027	120	80	80	0.3	530	70.0	" (c., chert)
1028	110	75	70	0.3	585	8.0	" (c., pillow lava)
1029	90	80	80	0.4	550	25.0	" (c., lava)
1030	120	100	70	0.4	540	12.0	" (c., pillow lava)
1031	90	70	70	0.3	280	15.0	"
1032	110	70	70	0.3	295	-	mudstone (with Mn-nodule)
1033	110	70	70	0.4	430	15.0	Mn-nodule (c., lava)
1034	130	90	90	0.3	690	PF	mudstone
1035	210	120	60	0.4	945	PF	mudstone
1036	90	90	80	0.2	575	20.0	phosphorite
1037	120	70	70	0.3	440	PF	conglomerate
1038	120	100	80	0.4	585	-	mudstone
1039	120	100	60	0.2	545	PF	conglomerate
1040	130	90	50	0.3	440	PF	hyaloclastite
1041	150	110	30	0.2	425	F	phosphorite
1042	140	90	50	0.3	465	PF	mudstone
1043	90	90	60	0.2	385	-	hyaloclastite
1044	90	80	60	0.2	290	PF	"
1045	170	130	50	0.3	1075	PF	phosphorite
1046	100	100	80	0.2	565	F	hyaloclastite
1047	120	110	90	0.2	890	F	phosphorite
1048	170	130	50	0.2	1300	PF	"
1049	150	100	50	0.2	675	PF	"
1050	90	90	80	0.2	500	-	conglomerate(with Mn-nodule)
1051	130	100	55	0.3	475	F	phosphorite
1052	120	100	30	0.2	280	F	"
1053	120	100	70	0.2	455	20.0	"
1054	120	90	80	0.4	650	40.0	Mn-nodule (c., pillow lava)
1055	110	80	35	0.2	335	PF	hyaloclastite
1056	110	80	70	0.2	300	PF	"
1057	80	60	50	0.3	210	PF	"
1058	80	80	80	0.3	415	F	phosphorite
1059	80	70	60	0.2	210	PF	hyaloclastite
1060	100	70	70	0.3	395	PF	"
1061	110	70	30	0.3	200	PF	phosphorite
1062	110	70	50	0.3	255	PF	hyaloclastite
1063	90	60	50	0.3	210	PF	"
1064	110	80	25	0.3	160	4.0	phosphorite
1065	70	60	50	0.3	205	1.0	"
1066	90	70	80	0.3	185	1.5	"
1067	90	60	20	0.3	210	F	"
1068	80	60	30	0.3	190	PF	"

Sample No.	Diameter(mm) L	M	S	Roune-ness	wt(g)	Mn-coating(mm)	Lithology & Remarks
5-1069	110	80	35	0.4	245	4.0	Mn-nodule (c., phosphorite)
1070	90	90	40	0.3	240	2.0	phosphorite
1071	70	70	30	0.3	200	PF	"
1072	80	40	40	0.3	185	PF	"
1073	80	60	50	0.3	190	PF	"
1074	90	70	40	0.3	195	PF	"
1075	130	100	50	0.3	325	PF	conglomerate
1076	120	60	40	0.2	260	PF	phosphorite
1077	100	100	40	0.3	430	3.0	"
1078	100	60	45	0.4	240	4.0	Mn-nodule
1079	90	80	35	0.2	260	PF	phosphorite
1080	90	70	50	0.3	335	PF	"
1081	90	70	30	0.2	240	PF	"
1082	60	60	25	0.4	105	8.0	Mn-nodule
1083	65	40	30	0.4	65	10.0	"
1084	80	60	40	0.3	115	-	mudstone
1085	80	50	30	0.3	110	F	phosphorite
1086	110	80	50	0.3	395	1.0	"
1087	80	70	50	0.3	285	5.0	Mn-nodule (c., lava)
1088	50	50	50	0.3	190	25.0	"
1089	70	50	30	0.4	55	PF	mudstone
1090	90	70	50	0.2	255	PF	phosphorite
1091	70	60	35	0.2	235	PF	"
1092	70	50	40	0.2	135	PF	" (white)
1093	70	70	50	0.3	150	PF	hyaloclastite
1094	50	40	30	0.3	95	20.0	Mn-nodule
1095	110	55	40	0.4	155	PF	mudstone
1096	70	70	50	0.2	270	PF	phosphorite
1097	70	50	40	0.3	135	15.0	Mn-nodule
1098	80	50	40	0.3	110	PF	hyaloclastite
1099	100	70	50	0.2	150	PF	"
1100	100	65	30	0.2	145	PF	phosphorite
1101	100	60	40	0.3	210	PF	"
1102	90	60	30	0.3	90	PF	mudstone
1103	70	40	20	0.3	75	PF	phosphorite
1104	110	50	40	0.2	170	PF	"
1105	80	60	40	0.3	205	PF	"
1106	110	80	25	0.3	295	1.0	"
1107	60	60	50	0.3	160	F	"
1108	90	60	30	0.3	160	PF	"
1109	80	50	50	0.3	145	15.0	Mn-nodule
1110	110	70	20	0.3	195	PF	phosphorite
1111	85	50	40	0.2	150	PF	"
1112	60	40	40	0.3	75	PF	hyaloclastite
1113	85	60	30	0.3	140	PF	"
1114	100	70	50	0.4	355	20.0	Mn-nodule
1115	100	80	50	0.3	215	-	conglomerate
1116	100	80	50	0.3	230	15.0	phosphorite
1117	80	70	40	0.4	160	PF	"
1118	60	60	40	0.3	135	2.0	Mn-nodule
1119	110	80	20	0.2	280	F	phosphorite
1120	80	70	40	0.2	145	PF	"

Sample No.	Diameter(mm) L	M	S	Round-ness	wt(g)	Mn-coating(mm)	Lithology & Remarks
5-1121	95	40	40	0.3	150	10.0	phosphorite
1122	60	60	60	0.3	140	PF	sandstone
1123	70	60	30	0.2	190	PF	phosphorite
1124	50	50	50	0.3	95	-	conglomerate
1125	80	70	50	0.3	255	50.0	Mn-crust
1126	80	60	50	0.2	295	F	phosphorite
1127	80	80	50	0.3	290	40.0	Mn-nodule (c., phosphorite)
1128	70	50	30	0.3	125	PF	phosphorite
1129	80	70	70	0.4	265	10.0	Mn-nodule
1130	60	50	50	0.4	145	40.0	Mn-crust
1131	60	60	40	0.4	140	10.0	Mn-nodule
1132	60	50	30	0.2	110	PF	phosphorite
1133	80	40	25	0.2	80	PF	"
1134	80	50	40	0.2	145	PF	conglomerate
1135	70	60	30	0.3	110	PF	phosphorite
1136	80	50	40	0.4	100	-	conglomerate
1137	100	70	40	0.2	195	F	phosphorite
1138	110	80	60	0.2	345	PF	hyaloclastite
1139	70	70	40	0.3	115	5.0	Mn-nodule
1140	35	35	25	0.2	55	10.0	phosphorite
1141	70	50	25	0.3	60	PF	"
1142	50	50	25	0.2	85	F	"
1143	45	45	45	0.3	80	PF	"
1144	60	50	40	0.3	80	-	"
1145	75	40	40	0.2	95	PF	"
1146	70	50	20	0.4	55	PF	sandstone
1147	60	50	40	0.3	70	PF	phosphorite
1148	50	40	20	0.2	50	PF	"
1149	60	45	30	0.3	85	PF	"
1150	60	40	30	0.2	60	PF	"
1151	70	60	30	0.2	110	PF	phosphorite
1152	70	50	50	0.2	85	5.0	"
1153	60	40	35	0.4	80	PF	"
1154	65	40	30	0.3	50	PF	conglomerate
1155	70	60	20	0.3	100	5.0	phosphorite
1156	60	30	30	0.3	40	PF	hyaloclastite
1157	75	40	30	0.2	125	5.0	phosphorite
1158	75	60	35	0.3	90	5.0	Mn-nodule
1159	60	50	35	0.2	55	F	phosphorite
1160	65	55	30	0.4	115	5.0	Mn-nodule
1161	60	50	40	0.4	100	10.0	"
1162	60	60	30	0.4	95	30.0	Mn-crust
1163	30	30	20	0.2	35	PF	hyaloclastite
1164-1183			(20)		1050		hyaloclastite
1184-1207			(24)		1085		sandstone and mudstone
1208-1227			(20)		1190		phosphorite
1228-1247			(20)		1600		"
1248-1257			(10)		790		"
1258-1278			(21)		1210		Mn-nodule

Sample No.	Diameter(mm) L	M	S	Round-ness	wt(g)	Mn-coat-ing(mm)	Lithology & Remarks
5-1301					1280		others
1302					2500		"
1303					3050		"
1304					2530		"
1305					2250		"
1306					2400		"
1307					50		"
1401					920		pebbles
1402					780		soft sediments (sand)
1403					1450		" (mud)
1404					2950		" (")

TABLE 13-3-1(7). KH 87-3-7 (Ogasawara Plateau)

Sample No.	Diameter(mm) L	M	S	Round-ness	wt(g)	Mn-coating(mm)	Lithology & Remarks
7-001	300	170	150	0.4	4950	1.0	mudstone
002	280	200	170	0.3	10600	50.0	phosphorite
003	300	170	140	0.6	6600	70.0	"
004	220	180	150	0.4	4700	30.0	"
005	250	180	170	0.3	4550	5.0	conglomerate (with phsph.)
006	210	160	60	0.4	2150	0.4	mudstone
007	250	200	40	0.3	1650	2.0	"
008	190	110	70	0.3	2620	5.0	phosphorite (with Mn-nd.)
009	200	110	110	0.3	1280	2.0	mudstone
010	170	130	100	0.4	2200	15.0	Mn-nodule
011	360	240	30	0.3	2320	0.4	mudstone
012	260	120	100	0.4	1880	10.0	"
013	160	150	50	0.4	915	1.0	"
014	160	100	80	0.3	1000	1.0	"
015	230	100	80	0.3	1250	5.0	"
016	180	120	90	0.2	1600	2.0	" (partly congl.)
017	160	80	80	0.3	920	30.0	Mn-nodule (c., phosphorite)
018	160	110	70	0.2	1020	55.0	"
019	140	100	60	0.2	520	50.0	"
020	140	110	80	0.4	745	2.0	mudstone
021	135	90	60	0.4	690	5.0	"
022	120	100	60	0.3	470	0.2	"
023	100	100	80	0.4	560	7.0	"
024	120	80	50	0.3	495	7.0	Mn-nodule (c., phosphorite)
025	100	90	50	0.4	410	10.0	mudstone
026	100	70	50	0.3	360	2.0	phosphorite
027	160	140	30	0.2	500	2.0	conglomerate (with phsph.)
028	110	90	50	0.1	395	1.0	phosphorite
029	90	50	30	0.2	225	2.0	mudstone (with sponge)
030	100	90	30	0.3	165	2.0	" (")
031	100	90	40	0.1	220	3.0	phosphorite
032	70	60	40	0.2	200	2.0	"
033	90	60	40	0.2	160	2.0	mudstone
034	70	60	50	0.3	140	30.0	Mn-nodule
035	100	60	40	0.2	115	3.0	mudstone
036	80	40	40	0.2	90	20.0	Mn-nodule
037	70	45	35	0.2	70	1.0	phosphorite
038	90	60	40	0.1	130	2.0	"
039	80	60	40	0.3	190	30.0	Mn-nodule (c., phosphorite)
040	70	45	40	0.4	100	3.0	" (")
041	45	45	30	0.4	50	3.0	" (")
042	85	50	45	0.1	90	1.0	phosphorite
043	70	60	40	0.4	165	F	"
044	75	60	30	0.3	65	5.0	mudstone
045	80	60	60	0.2	150	2.0	phosphorite
046	80	40	30	0.4	95	2.0	mudstone
047	65	40	25	0.4	75	2.0	"
048	60	60	20	0.4	90	4.0	Mn-nodule
049	60	60	20	0.3	50	3.0	mudstone
050	80	50	30	0.2	75	2.0	conglomerate

Sample No.	Diameter(mm) L	M	S	Round-ness	wt(g)	Mn-coating(mm)	Lithology & Remarks
7-051	75	65	20	0.3	95	3.0	sandstone
052	50	45	25	0.4	60	2.0	phosphorite
053	60	30	30	0.4	70	15.0	Mn-nodule
054	55	40	40	0.6	90	20.0	"
055	65	40	30	0.4	110	3.0	" (c., phosphorite)
056	60	40	40	0.2	80	PF	mudstone
057	60	50	30	0.4	65	2.0	"
058	60	45	40	0.4	60	PF	"
059	80	60	50	0.4	140	2.0	"
060	70	60	30	0.4	100	2.0	phosphorite
061	80	55	30	0.4	120	2.0	mudstone
062	94	40	25	0.4	95	2.0	"
063	80	40	40	0.4	90	PF	"
064	55	45	40	0.4	95	2.0	"
065	60	50	40	0.4	85	2.0	"
066	80	40	40	0.2	70	PF	"
067	80	50	35	0.2	140	2.0	"
068	70	60	20	0.4	70	2.0	"
069	60	50	50	0.4	115	30.0	Mn-nodule
070	55	40	30	0.4	70	6.0	"
071	50	25	25	0.3	30	-	phosphorite
072	40	40	40	0.6	45	2.0	mudstone
073	60	30	30	0.3	40	-	" (with sponge)
074	45	30	30	0.4	45	2.0	"
075	65	40	30	0.4	50	-	"
076	65	40	30	0.3	55	3.0	phosphorite
077	55	35	20	0.3	35	0.2	mudstone
078	50	45	30	0.4	50	2.0	"
079	55	40	30	0.3	30	20.0	Mn-nodule
080	50	50	25	0.3	30	4.0	"
081	45	40	25	0.4	45	3.0	mudstone
082	45	25	20	0.2	20	12.5	Mn-nodule
083	45	35	30	0.2	35	5.0	sandstone
084	55	50	25	0.3	75	0.2	" (tuffaceous)
201	250	170	150	0.4	3270		scoria
202	220	180	130	0.4	3020	PF	pumice
203	240	140	100	0.3	3000	PF	"
204	140	130	70	0.2	730	PF	"
205	150	100	70	0.3	770		scoria
206	80	70	60	0.4	135	PF	pumice
207	120	90	70	0.3	370	PF	"
208	100	90	60	0.4	27		scoria
209	95	70	55	0.4	160	-	pumice
210	90	60	50	0.2	160		scoria
211	90	85	60	0.1	165		"
212	90	75	60	0.3	225		"
213	80	70	50	0.3	225		"
214	100	70	55	0.1	80	-	pumice
215	90	60	40	0.3	170		scoria
216	90	70	45	0.3	140	PF	pumice
217	80	70	60	0.4	175		scoria

Sample No.	Diameter(mm) L	M	S	Round-ness	wt(g)	Mn-coating(mm)	Lithology & Remarks
7-218	90	65	50	0.3	135		scoria
219	60	60	45	0.3	55	PF	pumice
220	70	40	40	0.4	65		scoria
221	55	50	40	0.2	70		"
222	60	50	40	0.3	55	PF	pumice
223	75	65	50	0.4	100	-	"
224	60	50	40	0.3	65		scoria
225	60	60	40	0.4	55	-	pumice
226	50	50	40	0.2	70	PF	"
227	75	55	50	0.2	125		scoria
228	60	50	50	0.2	100	PF	pumice
229	70	55	35	0.2	65		scoria
230	55	45	30	0.2	40		"
231	55	35	30	0.2	40		"
232	65	40	20	0.3	30		"
233	50	40	30	0.3	25	-	pumice
234	55	35	30	0.4	25	PF	"
235	50	35	35	0.3	30		scoria
236	60	35	30	0.4	55		"
237	50	40	30	0.2	30		"
238	50	40	30	0.3	35	PF	pumice
239	55	45	30	0.4	45		scoria
240	35	30	25	0.3	25	PF	pumice
241	60	40	30	0.1	40		scoria
242	60	50	30	0.4	40		"
243	50	40	30	0.4	35		"
244	50	25	25	0.4	20	-	pumice
245	50	40	25	0.4	35	PF	"
246	50	30	30	0.3	25		scoria
247	60	35	30	0.2	30	PF	pumice
248	50	40	35	0.3	30	PF	"
249	70	55	35	0.3	40		scoria
250	75	50	25	0.4	60	PF	pumice
251	55	45	30	0.3	65		scoria
301					530		others
302					655		"
501-510			(10)		2500		sponge
511-522			(12)		1900		"
523					2000		" (others-1)
524					1200		" (" -2)
525					900		" (" -3)
526					450		" (" -4)

Note:

c.	: core	phsph.	: phosphorite
congl.	: conglomerate	pl	: plagioclase
F	: filmed	PF	: partly filmed
fr	: fresh	xth	: xenolith
g-Ti-aug	: groundmass titanaugite	ol	: olvine
Mn-nd	: Mn-nodule	ol with sp	: olvine with spinel inclusion

13-4. DESCRIPTION OF DREDGED SAMPLES FROM OPHIOLITIC SEAMOUNT (IN TORI-SHIMA FORE-ARC), UYEDA RIDGE AND OGASAWARA PLATEAU, DURING THE FIRST LEG (TOKYO TO GUAM) OF KH 87-3 CRUISE

T. Ishii, H. Maekawa, H. Ozawa, J. Ashi,
H. Matsuoka, K. Konishi and K. Kobayashi

More than one thousand and five hundred rocks (about 650 kg weight in total) were dredged during the first leg (Tokyo to Guam) of KH 87-3 cruise. Three sites (Stations KH87-3-1, -2 and -3), one site (Station KH87-3-5) and two sites (Stations KH87-3-7 and -8) were selected for the investigation of an ophiolitic seamount in Tori-Shima (Izu Islands) fore-arc, Uyeda Ridge and Ogasawara Plateau, respectively. Precise position, depth of each station and relevant information are given at the operation logs of dredge hauls (13-1), and position of each station is shown in the bathymetric charts (Figs. 13-2-1, 13-2-2 and 13-2-3).

Improved Nalwalk chain-bag dredges with backet (Ishii et al., 1985) were used to collect boulder to granule rock samples as well as psammitic to pelitic soft sediments. Newly prepared dredge pinger-transponder (DPT-1030) (Ishii et al., 1988) was installed at 200-500 meters above the dredge to confirm for dredge hitting sea bottom. Because most of the dredged rock-samples were more or less covered with soft sediments and/or Mn-coating, these rocks were at first separated from soft sediments by washing. They were cut by a diamond saw into two or more pieces for observation and description of visual features inside each sample. Washed samples were classified into several groups according to their lithologic characteristics.

After numbering the samples (in the order of size), diameter (L, M and S), roundness, weight and thickness of Mn-coating, lithology and remarks of each sample were observed on board as well as in the shore-based laboratory and described in Table 13-3-1 except for data on soft sediments. Lithologic distribution of each station was summarized in Fig. 13-4-1 (a)-(e) and Table 13-4-1. In Tables 13-3-1, roundness is described after the Powers' system (Powers, 1953), that is 0.10=very angular, 0.20=angular, 0.30=sub-angular, 0.40=subrounded, 0.60=rounded and 0.85=well-rounded. Representative bulk chemical analyses of dredged igneous rocks as well as Mn-nodules are shown in Table 13-4-2a and -2b, respectively.

OPHIOLITIC SEAMOUNT IN TORI-SHIMA FORE-ARC

Many topographic highs are recognized along the Izu-Ogasawara-Mariana

fore-arc region in the detailed bathymetric charts. Ophiolitic rocks were dredged from sone of those seamounts (Bloomer 1983, Ishii 1985). One of those seamounts in Tori-Shima fore-arc is located about 145 km northeast by east from the Tori-Shima (tori=bird, shima=island in Japanese) and 40 km west from the axis of the Ogasawara Trench. This seamount is 30 km in diameter of the base and 1400 m in height from the base. The crest is 3750 m deep (Fig. 13-2-1).

More than 140 ophiolitic rocks including serpentinized peridotites, metamorphosed basic rocks (gabbroes, dolerites and basalts) and their derivatives were collected by three dredge hauls from the seamount (Table 13-3-1, Figs. 13-4-1a, b & c). Bulk chemistry of those rocks is shown in Table 13-4-2a. Dredged ultramafic and mafic rocks from the seamount are described more in detail by Maekawa et al. in this volume (Chapt. 13-5).

UYEDA RIDGE

More than one thousand samples including about 800 pieces of basic pillow lava, 40 hyaloclastites, Mn-oxides, phosphorites and sedimentary rocks (Table 13-3-1, Fig. 13-4-1d) were obtained from the southern slope of Uyeda Ridge(Fig. 13-2-2). Each piece of basalt lavas shows beautiful pillow structure, having trancated long-pyramidal shape, with altered chilled glass zone. Those rocks are divided into three groups according to those phenocrysts assemblages, that is, olivine phyric, plagioclase phyric and olivine-plagioclase phyric basalts. Relatively fresh rocks were selected for detailed petrological studies as well as K-Ar age determinations. Bulk chemistry of these Mn-oxides is shown in Table 13-4-3b. Precise petrological studies on the above volcanic rocks are reported by Ozawa et al. in this volume (Chapt. 13-6).

OGASAWARA PLATEAU

Ogasawara Plateau has been surveyed by many research vessels. Several basal volcanic rocks were reported from the northern Ogasawara Plateau (Smoot's Broken-Top Seamount) (Ishii et al.,1985, Naka, 1985), but there is no report on dredged igneous rocks from the southern part of the plateau. Two dredge hauls were operated to collect basal volcanic rocks in the southern Ogasawara Plateau. About one-hundred sixty samples (excluding basal rocks) including phospholites, Mn-oxides, sedimentary rocks and pumices + scorias were collected (Table 13-3-1, Fig. 13-3-1e) from steep slope along assumed strike slip fault with WNW direction (Fig. 13-2-3). Bulk chemistry of Mn-oxides are characterized by high Pt (platinum) content up to 0.60 ppm (Table 13-4-2b). Precise studies on the above rocks are reported by Konishi et al. in this volume (13-6). Detailed prtrological

and geochemical investigation have been in progress to understand the geological history and petrogenesis of each area.

ACKNOWLEDGEMENTS

We thank Mr. H. Haramura for his wet chemical analyses on igneous rocks, and Nippon Kokan K. K. for chemical analyses of Mn-oxides. Thanks are due to Dr. T. Hiroi for computer programs, Ms. A. Hatanaka in preparation of polished thin sections, and Ms. T. Mizutani in typewriting.

REFERENCES

Bloomer, S. H.: Distribution and origin of igneous rocks from the landward slopes of the Mariana trench: implications for its structure and evolution. J. Geophys. Res., **88**, 7411-7428, 1983.

Ishii, T.: Dredged samples from the Ogasawara fore-arc seamount or "Ogasawara Paleoland"-"fore-arc ophiolite". In Formation of Active Ocean Margins (eds. Nasu, N. et al.), Terr Scientific Publishing Company, Tokyo, 307-342, 1985.

Ishii, T., Furuta, T., Watanabe, M. and Nakanishi, M.: First trial use of Dredge Pinger-Transponder (DPT-1030) for dredge hauls during KH 86-2. In Preliminary Report of the Hakuho-Maru Cruise KH 86-2, Ocean Research Institute, University of Tokyo, 1988.

Ishii, T., Kobayashi, K., Shibata, T., Naka, J., Johnson, K., Ikehara, K., Iguchi, M., Konishi, K., Wakita, H., Zhang, F., Nakamura, Y. and Kayane, H.: Description of samples from Ogasawara fore-arc. Ogasawara Plateau and Mariana Trough, during KH 84-1 Cruise. In Preliminary Report of the Hakuho-Maru Cruise KH 84-1 (Ocean Research Institute, University of Tokyo), 105-165, 1985.

Naka, j.: Volcanic rocks dredged from the Ogasawara Plateau. ibid., 196-201, 1985.

Powers, M.C.: A new roundness scale for sedimentary particles. J. Sed. Pet., **23**, 117-119, 1953.

TABLE 13-4-1 Summary of lithologic composition of samples dredged during the first leg (Tokyo to Guam) of KH 87-3 cruise.

Location	Tori-Shima fore-arc			Uyeda Ridge	Ogasawara Plateou
Station Number	KH87 3-1	KH87 3-2	KH87 3-3	KH87 3-5	KH87 3-7
Serpentinite	21	31	41	-	-
Harzburgite	-	1	-	-	-
Serpentine breccia	-	4	1	-	-
Serpentine sandstone	1	4	2	-	-
Serpentine mudstone	-	12	-	-	-
Green rock	-	-	21	-	-
Basic lava	-	-	3	-	-
Pillow lava	-	-	-	805	-
Hyaloclastite	-	-	-	40	-
Pumice	14	8	4	-	23
Scoria	2	2	-	-	28
Conglomelate	-	-	1	3	3
Sandstone	1	-	-	14	3
Mudstone	147	-	2	2	42
Phospholite	-	-	-	9	16
Mn-nodule	-	-	-	126	20
Mn-crust	-	-	-	60	-
Sponge	-	-	-	4	22
Total Number (1543)	186	62	75	1063	157
Total Weight (652.3 kg)	91.5	35.9	57.0	381.0	86.9

TABLE 13-4-2a Wet chemical analyses of igneous rocks collect during the first leg (Tokyo to Guam) of the KH 87-3 cruise (Analyst: H. Haramura).

	Serpentinite		Green-rock				Alkali-basalt?
	Harzb.	Harzb.	Gabbro	Dolerite		Dolerite	
Anal.No.	1	2	3	4	5	6	7
Sample No.	KH87-3 2-01	KH87-3 3-18	KH87-3 3-01	KH87-3 3-2A	KH87-3 3-2B	KH87-3 3-10	KH87-3 3-13
SIO2	35.22	38.26	38.51	46.31	39.52	40.00	47.56
TIO2	.00	.00	.06	1.61	1.11	.54	3.70
AL2O3	.71	.40	15.20	14.75	17.31	14.33	19.13
FE2O3	4.21	5.79	1.10	2.97	5.14	1.50	5.71
FEO	2.54	2.14	1.02	4.72	3.46	5.83	2.64
MNO	.10	.10	.26	.17	.22	.31	.17
MGO	37.48	36.30	23.93	7.34	5.91	17.86	4.78
CAO	1.73	.52	9.62	13.97	19.90	11.15	5.20
NA2O	.02	.00	.12	2.69	1.05	.18	4.55
K2O	.02	.00	.02	.47	.18	.03	1.11
P2O5	.00	.05	.00	.11	.12	.07	.74
NIO	.22	.26	-	-	-	-	-
CR2O3	.25	.30	-	-	-	-	-
H2O+	15.53	14.29	9.36	4.49	6.18	7.77	3.69
H2O-	1.68	2.10	.58	.40	.40	.58	1.23
TOTAL	99.71	100.51	99.78	100.00	100.50	100.15	100.21
NI(ppm)	-	-	172	66	53	82	132
CR(ppm)	-	-	753	335	242	180	113
CIPW NORM							
Q	-	-	.00	.00	.00	.00	.70
OR	-	-	.13	2.92	.00	.19	6.88
AB	-	-	.46	17.98	.00	1.66	40.40
AN	-	-	45.50	28.16	44.70	41.62	22.00
NE	-	-	.37	3.22	5.12	.00	.00
WO	-	-	3.18	18.35	17.06	7.57	.00
EN	-	-	2.70	13.66	14.24	5.66	.00
FS	-	-	.06	2.89	.66	1.16	.00
EN	-	-	.00	.00	.00	4.88	12.49
FS	-	-	.00	.00	.00	1.00	.00
FO	-	-	44.59	3.90	1.00	26.57	.00
FA	-	-	1.11	.91	.05	6.02	.00
MT	-	-	1.78	4.53	7.94	2.37	.00
IL	-	-	.13	3.22	2.24	1.12	6.23
AP	-	-	.00	.27	.30	.18	1.80
C	-	-	.00	.00	.00	.00	2.90
HM	-	-	.00	.00	.00	.00	5.99
OT	-	-	.00	.00	12.47	.00	.60

Note ; Harzb. = harzburgite, OT = others.

	Uyeda Ridge				Ogasawara Plateau			
Sample No.	KH87-3 5-1000 -	KH 87-3-5 1005A Inner	1005B Middle	1005C Outer	KH87-3 7-2 -	KH87-3 7-3A Inner	KH87-3 7-3B Middle	KH87-3 7-3C Outer
Anal.No.	1	2	3	4	5	6	7	8
SiO2	16.78	11.68	12.61	20.99	9.11	7.69	10.13	5.75
TiO2	1.77	1.93	2.27	1.74	1.31	1.83	2.19	1.50
Al2O3	3.75	2.64	2.62	5.25	3.08	2.09	2.97	1.60
Fe2O3	28.75	21.51	27.51	26.45	14.04	20.19	25.14	25.96
MnO2	21.33	32.87	30.35	21.43	31.92	39.05	30.79	35.32
MgO	1.18	1.21	1.65	1.87	2.08	1.88	1.69	1.83
CaO	3.12	3.15	2.66	2.82	11.72	4.55	3.01	3.18
Na2O	3.34	2.88	2.66	2.86	2.75	2.67	2.60	2.67
K2O	.77	.80	.65	.96	.48	.45	.60	.36
P2O5	1.10	.92	.86	.84	5.81	1.72	1.21	1.33
BaO	.11	.14	.14	.10	.14	.15	.13	.11
Igloss	15.17	19.22	17.34	14.15	16.27	18.66	19.40	20.94
Total	97.17	98.95	101.32	99.46	98.71	100.93	99.86	100.55
Ni(wt%)	.15	.43	.30	.20	.68	.50	.31	.35
Cu	.08	.14	.11	.12	.14	.08	.04	.05
Co	.21	.41	.45	.23	.34	.48	.39	.79
Cr	tr.	tr.	tr.	tr.	tr.	tr.	tr.	tr.
Pb	.02	.04	.05	.02	.04	.10	.06	.09
Zn	.02	.03	.03	.02	.06	.04	.03	.03
Pt(ppm)	.08	.33	.12	.13	.60	.47	.18	.23

TABLE 13-4-2b Chemical analyses of Mn-oxides collected during the first leg (Tokyo to Guam) of the KH 87-3 cruise (Analyst: Nippon Kokan K. K.).

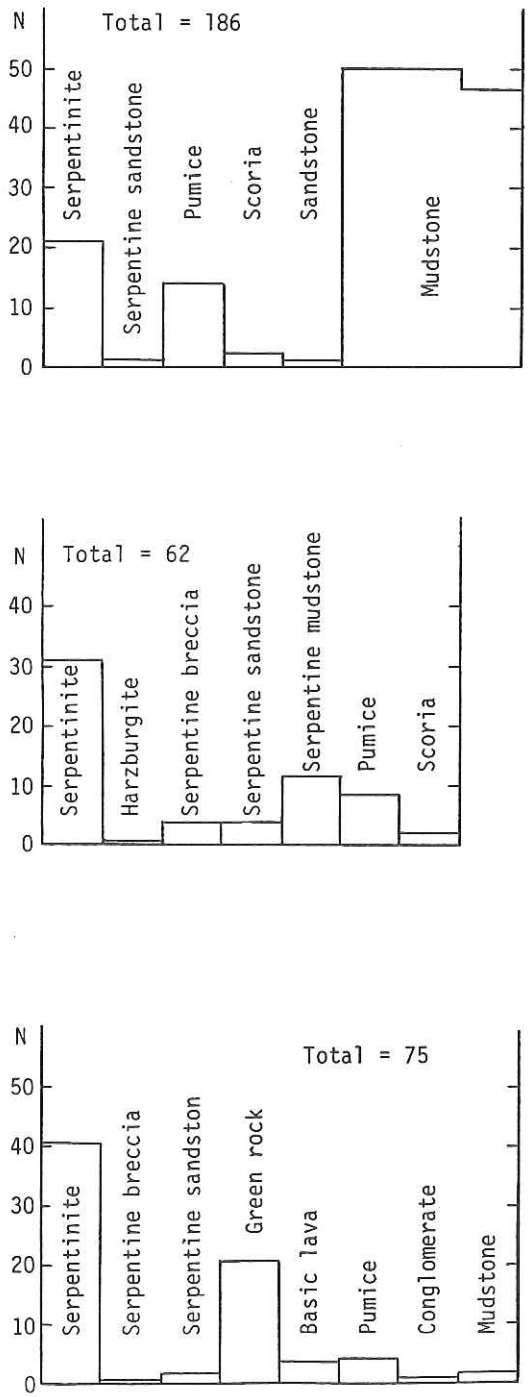

Fig. 13-4-1 Block diagrams showing lithologic composition of samples dredged from ophiolitic seamount in Tori-Shima fore-arc (a; above, b; middle, c; below).

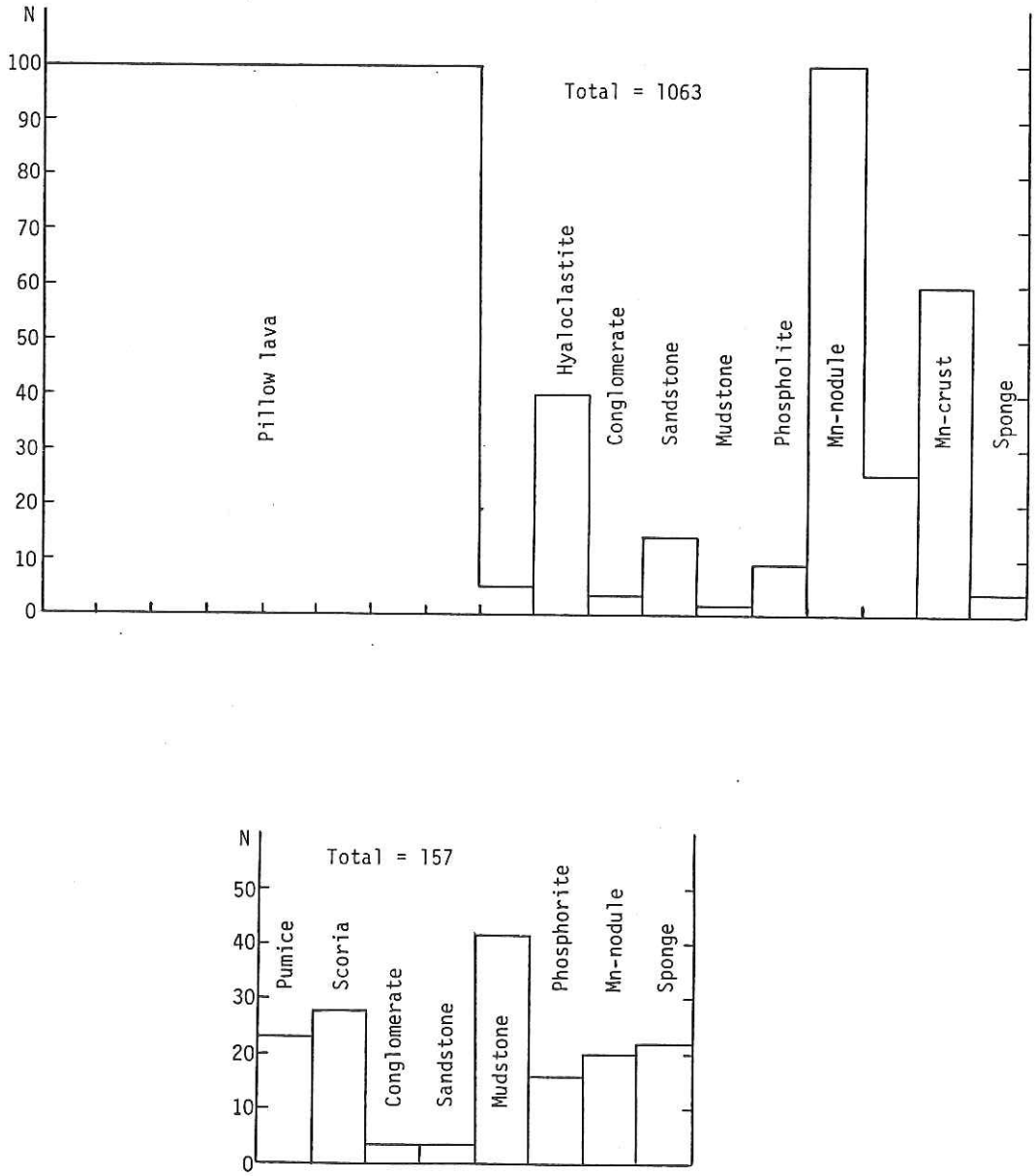

Fig. 13-4-1 Block diagrams showing lithologic composition of samples dredged from Uyeda Ridge (d; above) and the southern Ogasawara Plateau (e; below).

13-5. ULTRAMAFIC AND MAFIC ROCKS DREDGED FROM AN OPHIOLITIC SEAMOUNT IN TORI-SHIMA (IZU ISLANDS) FORE-ARC DURING KH 87-3 CRUISE

H. Maekawa, T. Ishii and H. Ozawa

Many ophiolitic rocks including serpentinite, gabbro, and green rocks, were obtained from a fore-arc seamount, located 30°55'N, 141°50'E, east of the Tori-Shima. Rock association suggests that the seamount is a newly discovered fore-arc ophiolite, similar to the ophiolites distributed along the Ogasawara-Mariana Trench landward slope (Bloomer, 1983; Ishii, 1985; Hussong and Fryer, 1985). Most of the specimens are ellipsoidal, and each sample is surrounded by several fault planes, their edges and corners being more or less rounded. Such a feature suggests that the rocks have undergone fracturing, i.e., each sample was detached from its source along faults, and their corners and edges were rounded off by later flow. In this section, we will summarize petrographical features of the representative samples. Wet chemical analyses of bulk rocks (shown by * and ** in the following list) are reported by Ishii et al. in this volume (13-4).

A. Serpentinite (KH 87-3-2-1* -5, -12, -13, -16, -19, -20, -21, -24, -26, -31, -32, -33, -34, KH 87-3-3-5, -6, -7, -8, -9, -11, -15, -18*, -21, -24, -28, -29, -31, -39, -50)

Most of the ultramafic rocks are fully or considerably serpentinized harzburgite and dunite. They consist of serpentine, clay and relict chromite. In most specimens, serpentine is partly or fully altered to brownish clay. Orthopyroxene and olivine are well retained in the specimens KH 87-3-1 and -18. Mesh and bastite textures are commonly observed. The specimens KH 87-3-3-9 and -31 consist of 5 to 0.1 mm serpentinite fragments and clay matrix. These specimens seem to have been serpentinite sandstone or serpentinite affected by cataclastic deformation.

B. Gabbro (KH 87-3-3-1*)

The gabbro consists of clinopyroxene, chlorite and dusty clay minerals. No other minerals remain. Gabbro was intensely sheared, and have well developed foliation (Fig. 13-5-1). Boudinage structure is common. Gabbroic texture, however, is observable in small pods which escaped the deformation. Clinopyroxene is commonly deformed, and always has closely spaced cleavages.

C. Green rocks (KH 87-3-2-37, KH 87-3-3-2**, -10*, -12, -17, -22, -26, -27, -32, -38, -42, -44, -52, -67)

Green rocks are mainly basalt and/or dolerite origin. They consist of clinopyroxene, chlorite, clay and calcite. Clinopyroxene is frequently replaced by aggregates of acicular green hornblende in the specimen KH 87-

3-3-10. These aggregates frequently show weak kinking. Pumpellyite occurs in vein and matrix in the specimens KH 87-3-3-2, -10 and -44. Ophitic, subophitic and intergranular textures are common. The specimens KH 87-3-52 and -67 are glassy and have many varioles. The green rocks show abundant shearing and pulverization.

References

Bloomer, S. H.: Distribution and origin of igneous rocks from the landward slopes of the Mariana trench: implications for its structure and evolution. J. Geophys. Res., **88**, 7411-7428, 1983.

Hussong, D. M. and Fryer, P.: Fore-arc Tectonics in the Northern Mariana Arc. In Formation of Active Ocean Margins (eds Nasu, N. et al.), Terra Scientific Publishing Company, Tokyo, 273-290, 1985.

Ishii, T.: Dredged samples from the Ogasawara fore-arc seamount or "Ogasawara Paleoland" - "fore-arc ophiolite". In Formation of Active Ocean Margins (eds Nasu, N. et al.), Terra Scientific Publishing Company, Tokyo, 307-342, 1985.

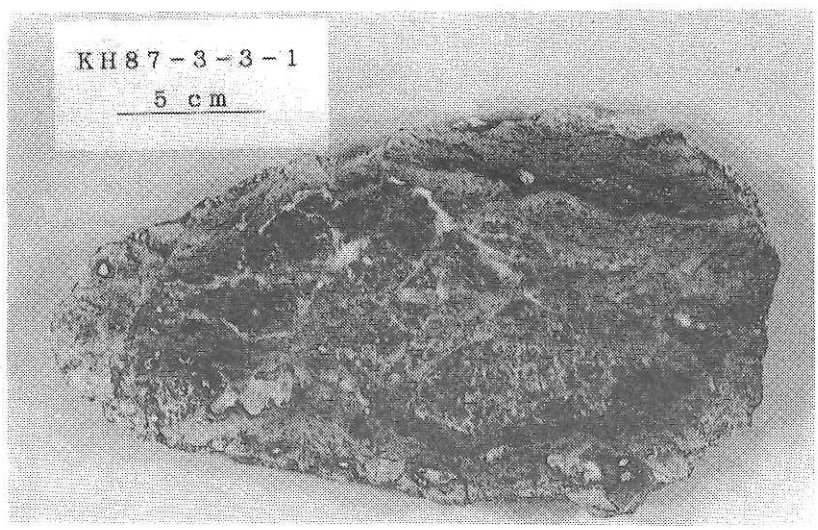

Fig. 13-5-1 Photograph of sheared gabbro (KH 87-3-3-1).

13-6. PILLOW LAVAS DREDGED FROM "UYEDA RIDGE" DURING KH 87-3 CRUISE

H. Ozawa, T. Ishii, H. Maekawa and K. Konishi

Introduction

The Uyeda Ridge is located around 27°20'N and 144°00'E. It is approximately 148 km long, and 18 km wide in average (36 km at its greatest width) and has a strike of 070°. The Uyeda Ridge is thought to be a part of an extinct remnant of spreading center or of a product of the magma leakage through a transform fault (Smoot & Heffner, 1986). However, for lack of petrological data, their discussion has not yet been confirmed. During this cruise, we have obtained some rock samples from the ridge by dredge hauls at site KH 87-3-5. In this report, we present the petrological description of these samples.

Petrography

Almost all of the dredged igneous rocks are fragments of pillow lavas and small amounts are hyaloclastite. Pillow lavas have chilled margins about 1 cm thick and the pillow's assumed original diameter is 20 to 50 cm. Generally they have small amounts of vesicles. Manganese coating can be seen in most of the samples. Some sample are altered to crystallize phosphate minerals.

These rocks consist of olivine and Ca-plagioclase as phenocryst. Olivine phenocrysts are about 2 mm across showing euhedral shape and are completely altered to clay minerals. Usually, olivine phenocrysts include euhedral spinel grains which are 100 μm in diameter. Plagioclase phenocrysts show euhedral lath shape and are about 2 mm across. Twinning and oscillatory zoning are common in plagioclase. Some of the plagioclase phenocrysts are altered to K-feldspar. Three types of phenocryst assemblage are as follows;

i) olivine, ii) olivine + plagioclase and iii) plagioclase.

Groundmasses of these rocks consist of olivine, clinopyroxene, plagioclase and magnetite. Plagioclase in the groundmass shows lath shape and intersertal texture. Clinopyroxene in the groundmass occurs as fibrous-shaped spherical aggregates. Most of them are altered, but some still preserve the original composition and show the original purple color.

Chemical Composition of Minerals

Mineral compositions are determined by electron probe microanalysis using the JEOL JCXA-733 of the Ocean Research Institute, University of

Tokyo, with the Bence and Albee (1968) correction procedure and using the JEOL JSM840 with the LINK AN10/50 of the Geological Institute, University of Tokyo, with the ZAF correction procedure.

Representive electron probe microanalyses of minerals are shown in Table 13-6-1. An content of core of plagioclase phenocryst varies 76 - 70, which is not so different from that of its rim. Clinopyroxenes in the groundmass show high TiO_2 content (> 2 wt%). Spinels show low Cr / (Cr + Al) ratios (=0.424 - 0.304), low Fe^{3+} / [Fe^{3+} + Cr + Al] ratios (=0.121 - 0.082) and high Mg / [Mg + Fe^{2+}] ratios (=0.642 - 0.586). They are shown in Figs. 13-6-1 and 13-6-2.

These rocks are probably classified into alkaline rock affinity, because of presence of olivines in groundmass and high TiO_2 content of clinopyroxenes in groundmass. Spinel compositions are plotted in "MORB" region shown by Crawford et al. (1986). Detailed petrological and geochemical investigations have been in progress to understand the petrogenesis of the Uyeda Ridge.

Reference

Bence, A.E. and Albee, A.L.: Emprical correction factors for the electron microanalysis of silicates and oxides. J. Geol., **76**, 382-403, 1968.

Crawford, A.J., Beccaluva, V., Serri, G. and Dostal, J.: Petrology, geochemistry and tectonic implications of volcanics dredged from the intersection of the Yap and Mariana trenches. Earth Planet Sci. Lett., **80**, 265-280, 1986.

Smoot, N. C. and Heffner, K. J.: Bathymetry and possible tectonic interaction of the Uyeda Ridge with its environment. Tectonophysics, **124**, 23-36, 1986.

TABLE 13-6-1 Selected analyses of plagiocalse (pl), Ti-augite (Cpx) and Cr-spinel (Sp) in pillow lava from the Uyeda Ridge (KH 87-3-5).

	Pl-1	Pl-2	Cpx-1	Cpx-2	Sp-1	Sp-2
SiO2	49.146	49.849	46.053	45.590	-----	0.054
TiO2	0.027	0.042	3.021	3.452	0.885	0.882
Al2O3	31.505	31.163	6.557	4.804	35.616	36.865
FeO*	0.390	0.443	10.952	16.007	23.853	23.285
MnO	0.005	0.012	0.231	0.330	0.171	0.183
MgO	0.185	0.172	11.033	8.322	14.509	14.308
CaO	15.578	14.696	21.193	20.178	0.014	0.007
Na2O	2.694	3.269	0.471	0.626	-----	0.019
K2O	0.037	0.057	0.025	0.018	0.018	-----
Cr2O3	0.029	0.005	0.144	0.191	24.484	24.128
V2O3	-----	-----	0.074	0.168	0.206	0.214
NiO	0.065	0.048	-----	-----	0.174	0.172
Total	99.660	99.806	99.755	99.686	99.806	100.188

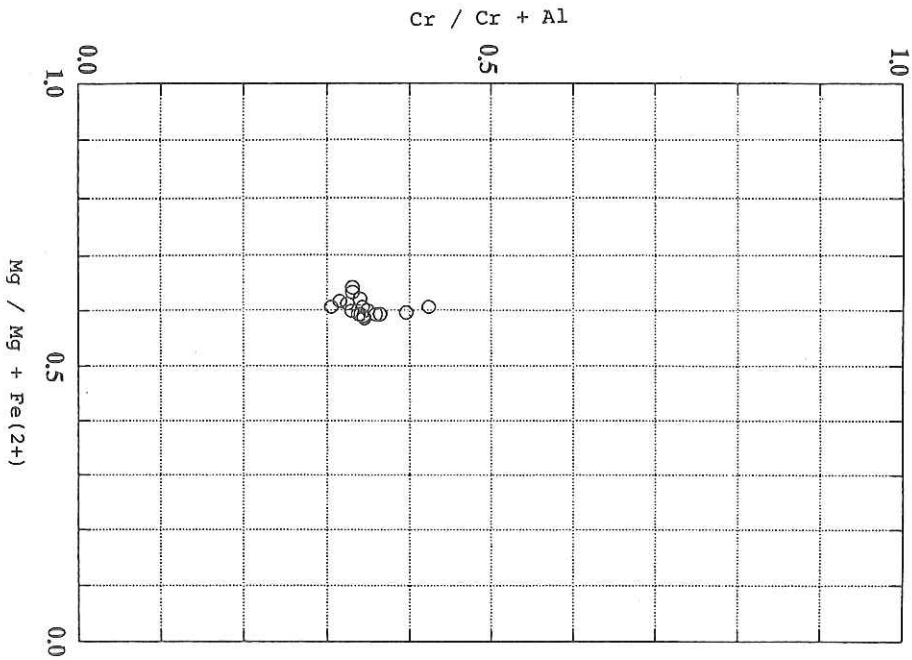

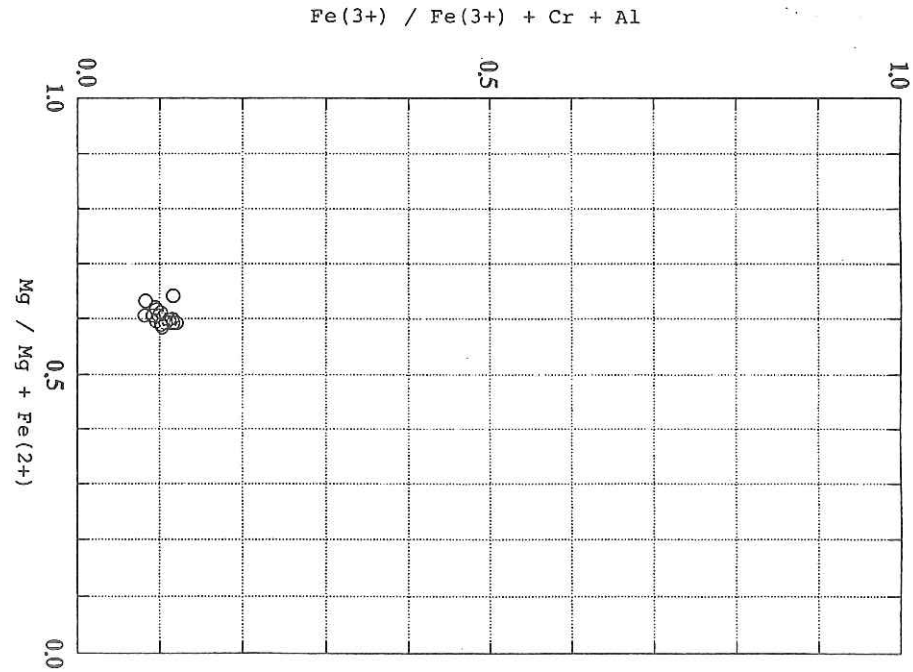

Fig. 13-6-1 Cr/Cr+Al versus Mg/Mg+Fe^{2+} for spinels

Fig. 13-6-2 Fe^{3+}/Fe^{3+}+Cr+Al versus Mg/Mg+Fe^{2+} for spinels

13-7. SEDIMENTARY TEXTURES OBSERVED IN THE SILTSTONES DREDGED FROM THE SEAMOUNT IN THE TORI-SHIMA FORE-ARC

J. Ashi

One hundred and eighty three (183) semi-consolidated siltstones were obtained by a dredge haul at station KH87-3-1. These samples are dark yellow to light gray tuffaceous siltstones occasionally intercalated with thin sandstone beds, some of which are intensely bioturbated. In sliced sections, light colored spots which are disturbed beds or burrows filled by tuffaceous materials are found. In this report, precise sedimentary textures observed in these samples will be presented.

Burrows:

Burrow fillings are generally semi-consolidated sediments the same as the surrounding materials, but are composed of soft-sediments in a few cases. The former is smaller than the latter in diameter. The latter is 1 cm in diameter. It exists at a high angle to bedding, and branches (Fig. 13-7(a)). This is similar to Thalassinoides.

Faults and folds:

Faults and folds are observed in one sample (Fig. 13-7(b)). Fault is healed one and partly causes the drag structure. This fault divides a part of flow folds from chaotic part. The faults and folds are thought to be derived from slumping.

Vein structure:

The structure which comprises parallel sets of dark colored discontinuities spaced nearly constant apart is observed in 16 samples (Fig. 13-7(b)). Similar structures are reported in the inner slope section of the oceanic active margins, for example, observed in the IPOD Legs 56 and 57 areas of the Japan Trench (Arthur et al.,1980) and Leg 67 area of the Middle America Trench off Guatemala (Cowan, 1982) and called "veins" and "vein structure", respectively. Moreover, this structure is recognizable on land (Ogawa, 1980) and in piston core samples at the junction area between the Mariana and Yap trenches (Fujioka et al., 1986). The origin of vein structure is generally thought to be layer-parallel extension fracture before tilting, although several hypotheses are existing.

Vein fillings are darker in color and finer in grain size than the surrounding matrix. No difference was observed between vein fillings and surrounding materials in characteristic Properties such as composition. Finer materials in the veins are interpreted to be selectively intruded from the surrounding matrices (Cowan, 1982). Vein structure is nearly

perpendicular to the bedding. In the section sliced normal to the bedding, width of vein is maximum in the central part. Vein structure is not developed in the coarse or tuffaceous beds so well. Vein structure-bearing zone is parallel to bedding. Spacing between adjacent veins is 1 mm to 1 cm and very uniform within one veined zone (Fig. 13-7(c)). In coarser grained samples, vein structure is developed sparsely, although the length of each vein is long (Fig. 13-7(d)). Veins often cut burrows but individual veins show no offset or small offsets less than 1 mm. Shape of vein is usually planar. Curved or sigmoidal planar veins are probably caused by soft-sedimentary deformation after vein formation (Fig. 13-7(e)). On the contrary, Cowan (1982) attributed the sigmoidal veins to layer-parallel shear such as downslope creep. The same material as vein fillings is disturbed as plane parallel to the bedding (Fig. 13-7(e)) or clod of 1 cm in diameter (Fig. 13-7(f)).

Fracture:

Fractures are recognizable in most of the samples and dominantly were caused during operation of dredge hauls. In the case of existence of vein structure, fractures are well developed along the vein walls (Fig. 13-7(c)). On the other hand, open fractures, which occur regularly and have a preferred orientation in spite of outline of samples' shape, suggest in situ deformation (Fig. 13-7(a)). This structure consists of open fractures, spaced 2 to 3 mm, and is intersected with the bedding at an angle of forty-five degree.

References

Arthur, M.A., B., Carson, and R., von Huene, Initial tectonic deformation of hemipelagic sediments at the leading edge of the Japan convergent margin. Initial Repts. Deep Sea Drilling Project, **57**, 569-613, 1980.

Cowan, D.S., Origin of vein structure in slope sediments on the inner slope the Middle America trench off Guatemala. Initial Repts. Deep Sea Drilling Project, **67**, 645-649, 1982.

Fujioka, K., T., Furuta, G., Kimura, K., Kodama, K., Koga, S., Kuramoto, H., Matsugi, T., Seno, A., Takeuti, M., Watanabe, and S., Yamamoto, Sediments and Rocks in and around the Palau and Yap Trenches. Preliminary Report of the Hakuho Maru Cruise KH 86-1, Ocean Research Institute Univ. Tokyo, 147, 1986.

Ogawa, Y., Beard-like veinlet structure as fracture cleavage in the Neogene siltstone in the Miura and Boso Peninsula, central Japan. Sci. Rep. Fac. Sci., Kyushu Univ., **13**, 321-327, 1980.

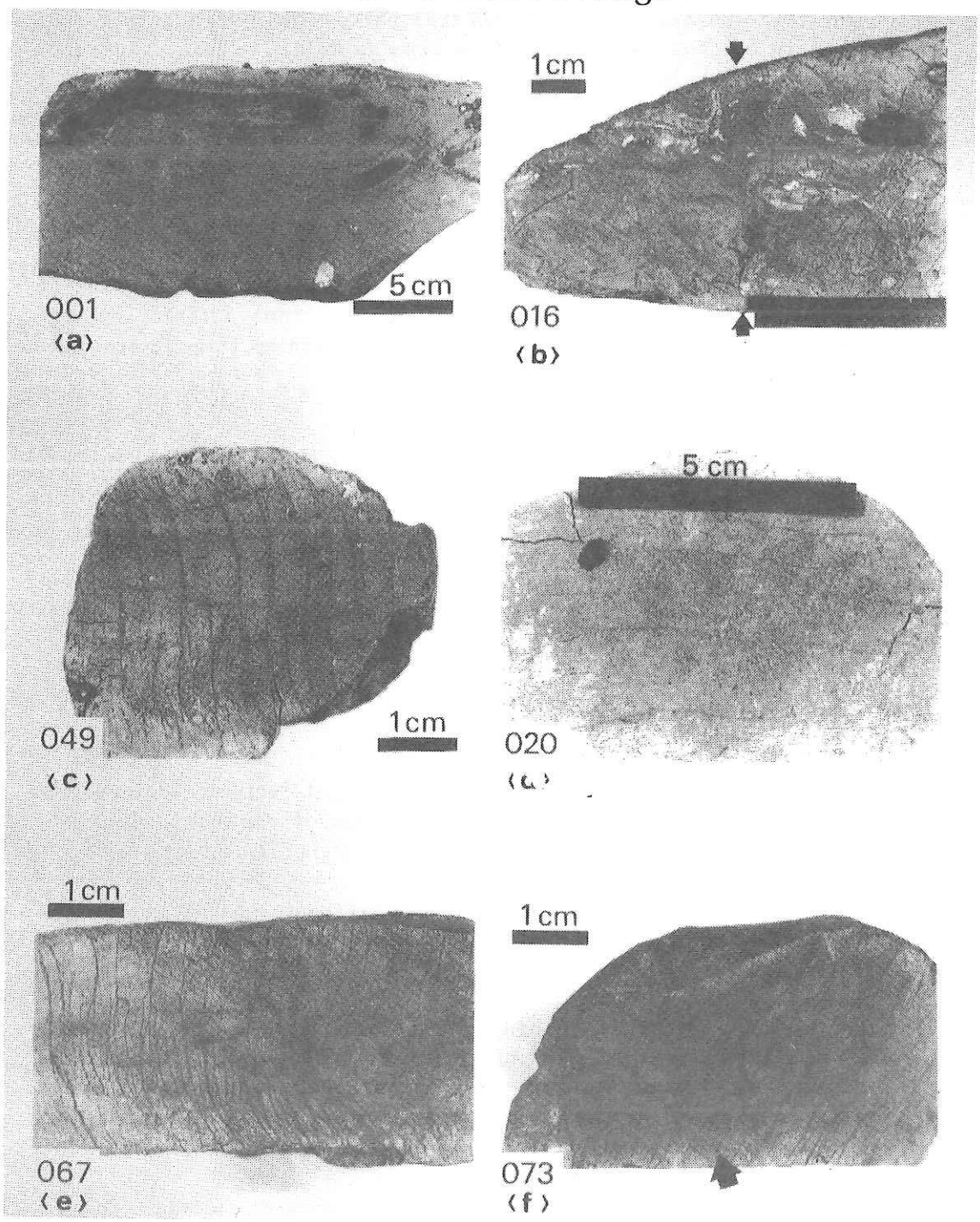

Fig. 13-7 Typical siltstone samples recovered by dredge haul at station KH 87-3-1 in a fore-arc seamount near Tori-shima Island.

14. SEA FLOOR GEOMAGNETIC OBSERVATION

J. Segawa, H. Fujimoto, K. Koizumi, C. Yang and H. Toh

14-1. Purpose of Observation

Electrical conductivity structure beneath the sea floor can be determined by making use of the OBM's through geomagnetic depth sounding method (GDS). Depth sounding is carried out by spectral analysis of sampled geomagnetic time series. The electric current induced by geomagnetic variations of external origin has 'skin depth' depending on the frequency of source geomagnetic variation. The lower the frequency is, the deeper the electric current penetrates into the earth. Therefore, analysis of geomagnetic variations whose angular frequency is ω shows the averaged conductivity structure as deep as its skin depth. The skin depth is given by the following formula:

$$\delta = (2 / \mu\omega\sigma)^{1/2}$$

where μ and σ denote magnetic permeability and electrical conductivity, respectively.

Band limitation of frequency is one of the characteristics of geomagnetic variations at the sea floor. Upper limit of geomagnetic variations observed at the sea floor is caused by rapid decay of high frequency components because of the existence of conductive ocean. This limitation occurs around 0.01 Hz. Lower limit is caused by the oceanic induction which is brought about by motions of sea water under geomagnetic field. The lower limit in frequency is about 10^{-4}Hz. Consequently, effective geomagnetic signals for GDS lies between several minutes and several hours in period. From this band limitation it is obvious that geomagnetic storms are the most useful phenomenon of external origin. In order to record geomagnetic storms, at least a few month duration of observation is needed. All the equipments installed at the beginning of this cruise, July 03,'87 - July 05, '87, will be retrieved in the middle of next September. The total length of the time series amount to as long as 75 days, which is considered to be long enough to apply the GDS method.

Transfer function is preliminary result of the GDS method, which shows lateral contrast of conductivity structure. In case of the previous cruise KT 86-12, on which 5 ocean bottom magnetometers were installed along the latitude of 32° N, it was revealed that there are two main characteristics in regard to the calculated transfer function of the northern Izu-Bonin

Ridge. One is the coast effect of the ridge observed at the sites on the foot of the ridge. The other is some strange induction vectors which are oriented toward SSE, although one of them was located on the very axis of the ridge. The latter characteristic has not been well interpreted.

To solve this problem is the main purpose of the present observation, i. e., to find out whether or not the existence of curious induction vectors continues to the south. All the sites of this cruise are situated on about 31° N, 120km south of the previous observation. The second purpose is to ensure the coast effect on the fore-arc side of the ridge where the data obtained in the previous cruise was so short due to some unfortunate reason that the estimation error of transfer function was relatively large. The authors expect that the sea floor geomagnetic observation along east-west transverse section of the Izu-Bonin Ridge will prove the conductivity structure of another type of arc which originated from the interaction of two oceanic plates in contrast to the case of the Japan-arc.

Improvement of accuracy is added to the purpose of this observation. Two instruments were used for this sake this time. One is a fluxgate type three-component ocean bottom magnetometer called OBM-C3 (Fig. 14-1) and the other is an ocean bottom proton magnetometer called OBP. Through simultaneous use of these two instruments, a fluxgate type OBM can be calibrated by taking advantage of OBP data. The authors think that the attempt to make a more accurate measurement will lead to a long-term absolute geomagnetic observation at the ocean bottom. Specifications of these instruments will be given briefly in the next section.

14-2. Instruments

Six ocean bottom magnetometers were prepared for this cruise. They consist of 5 fluxgate-type three-component ocean bottom magnetometers (OBM's) and 1 ocean bottom proton magnetometer (OBP). The OBM's used here were able to be sorted into two types: spherical, rather small and light ones (OBM-S's) and cylindrical, large and heavy one which has better accuracy in stead. The former include OBM-S1, OBM-S3, OBM-S5 and OBM-SMZ, each of which weighs 80 kg in air and has 60cmx60 cm for the maximum size. The latter include OBM-C3. OBM-C3 is a newly developed meter for the sake of long-term accurate measurement. It is 2 m tall so as to get a proper distance between the sensor and other electronics. And it weighs as heavy as 350 kg in air when fully mounted. Its life-time is extended to half a year by 2 minutes samplings at the cost of handiness.

OBP is also a cylindrical type magnetometer that weighs 250 kg in air and is 2 m in height. The sensor is placed at a higher position than the

other electronics. The role of OBP is not only to measure geomagnetic total force at the sea floor but also to make calibration of the fluxgate type three-component OBM installed at a nearby station.

Every OBM and OBP was equipped with a beacon, a flasher and an acoustic release system.

14-3. Installation of Instruments

The experiment was made on the east-west transverse section of the Izu-Bonin Ridge at 31° N. The west end of the section is 138° 5.4' E and the east end is 141° 20.6' E. The transverse section has about 160 nautical miles in length. Water depth varies from 2000 m to 4000 m at this latitude. As for the detailed information of installation, refer to the map of installation points (Fig. 14-2) and the observation log table (Table 14-1). Both OBM-C3 and OBP were installed toghther at site JK13 to improve the accuracy of the whole measurement.

Thanks to the calm weather, the actual operation of installation ended in success. In installation, we kept staying on the installation spot and followed the down-going instrument by acoustic method until we made sure its arrival at the sea floor.

Acknowledgements

We are grateful, from the bottom of our hearts, to all the crew on Hakuho-maru. We acknowledge the profound understanding of Professor K. Kobayashi who was the chief scientist of this cruise.

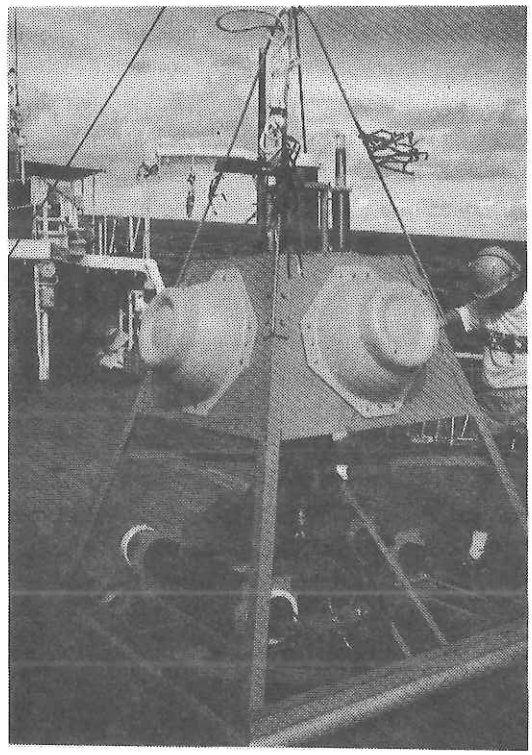

Fig. 14-1 Fluxgate-type three-component Ocean Bottom Magnetometer (OBM-C3) prepared on board the Hakuho Maru.

TABLE 14-1 Observation Log of OBM and OBP in the Cruise KH 87-3

Observation Log Table of Cruise KH87-3

	Site	Position Ship's Loran-C	Depth (m)	Code	Beacon (MHz)	Flasher	Start Time	Sampling Rate	Installation Date
OBM-S5-ORI	JK10	3(° 51.1′ N 138° 05.4′ E	4020	3A	TM 43.528	TM	6th/JUL 02:40	2min.	5th/JUL 00:17 Arrival 01:57
OBM-S3	JK11	30° 53.0′ N 139° 01.3′ E	2000	3A	ORI 27.045	TM	4th/JUL 10:28	2min.	4th/JUL 18:04 Arrival 18:57
OBM-S1	JK12	30° 56.0′ N 139° 52.7′ E	2280	3C	OAR 26.995	TM	2nd/JUL 22:30	2min.	3rd/JUL 08:27 Arrival 09:37
OBProton	JK13 -1	30° 57.1′ N 140° 39.1′ E	2380	3B	TM 43.528	TM	4th/JUL 15:50	2min.	5th/JUL 12:52 Arrival 13:38
OBM-C3	JK13 -2	30° 57.3′ N 140° 39.3′ E	2370	1B	TM 43.528	TM	6th/JUL 00:00	2min.	5th/JUL 13:45 Arrival 14:40
OBM-SMZ	JK14	30° 59.7′ N 141° 20.6′ E	3100	2C	TM 43.528	TM	4th/JUL 00:00	2min.	3rd/JUL 16:54 Arrival 17:55

Notes :

* OBM-S3 carries out full recording until 5th/JUL 07:50.
* OBM-S1 carries out 16 bit recording until 3rd/JUL 15:33.

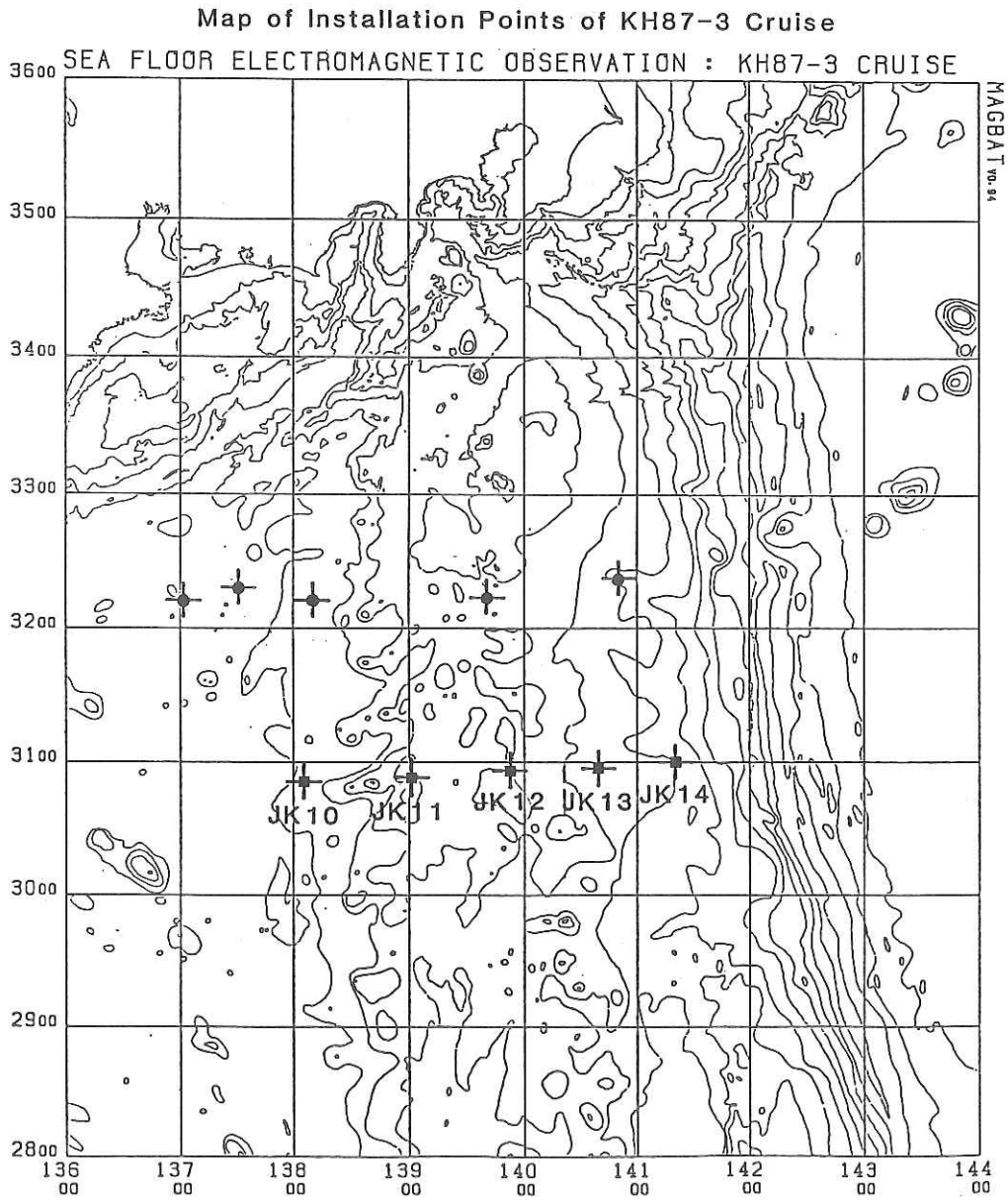

Fig. 14-2 Map indicating the installation points of OBM and OBP. See Table 14-1 for details of the sites. Five marks without site names denote observation points of KT 86-12 cruise.

15. SEISMIC REFLECTION SURVEY

S. Abe, K. Tamaki, T. Asanuma and Y. Kasumi

15-1. CONFIGURATION OF SINGLE CHANNEL SEISMIC REFLECTION SURVEY SYSTEMS

Single-channel seismic reflection survey was carried out at a speed of 6 kt or 10 kt, using BOLT 1500C type (Fig. 15-1-1) or BOLT 1900C type (Fig. 15-1-2) airguns. When we used air gun of BOLT 1500C type, the ship speed was set at 6 kt, whereas the speed was 10 kt for 1900C type. An air gun was fired at about 1240 psi. The shot interval was 20.0 seconds, and it was controlled by an electrical pulse fed to the solenoid valve. The towing depth of the air gun was about 10 meters. A hydrophone streamer cable was composed of 150 meters lead-in cable, a weighted section of approximately 3 meters followed by the streched, active and dead sections of 25 meters each with approximately 30 meters of dummy rope. The streched section was provided to improve S/N ratio. We used the No. 6 winch installed on the Hakuho Maru for towing operation. During this cruise, we recorded reflection data with two different types of recording systems. One is a digital and the other is an analog recording system. Digital recording system was NE128 system belonging to Ocean Research Institute, University of Tokyo.

Field data were fed to preamplifier, filter, main amplifier and A/D converter, and then recorded in magnetic tapes and after D/A conversion the output is displayed on an on-board monitor to check the system. Recording density of magnetic tapes are 1600 BPI. Usually digital sampling rate is 4 ms, and recording length is 8 seconds. During this cruise, however, we performed the survey with sampling rate of 2 ms and recording length of 4 seconds to gain the higher density of recording data.

Analog recording was performed by a NE102 deep sea crustal structure recording and playback system belonging to Department of Earch Sciences, Chiba University. It is composed of an NE-91A signal recording controll unit (amplifier and filter) and an NE-17B delay signal generator. The data were output to on-board monitor, and recorded with 4 channels FM recorder (SONY). Signal was input to NO. 1 channel, and shot pulse was input to NO. 3 channel. Figs. 15-1-3 and 15-1-4 show on-board equipments of the digital and analog recording systems.

15-2. SINGLE CHANNEL SEISMIC REFLECTION SURVEY OF LEG-1AROUND THE OGASAWARA PLATEAU

During KH 87-3 cruise, single-channel seismic reflection survey was performed around the Ogasawara Plateau and the northern Mariana Arc in Leg 1, and the East Mariana Basin in Leg 2. We totally obtained five lines in Leg 1, and the lines around the Ogasawara Plateau were L-1, L-2, L-3, L-4. L-1 was a line crossing the Ogasawara trench parallel to the Uyeda ridge. L-2 was a line crossing the southern part of the Ogasawara trench and ended at the northern part of the Ogasawara Plateau. L-3 was a long line starting at the southern part of the Ogasawara Plateau, passing through the Mariana trench and ending at the northern part of the Mariana Arc. L-4 was a line to decide the point of pistone coring survey. Fig.15-2-1 shows track lines of single channel seismic reflection survey in Leg-1. Table 15-2-1 represents locations of starts and end points in Leg 1. Bathymetry around the Ogasawara Plateau was provided by multi-narrow beam echo sounder data (Smoot, 1983). Hydrographic Department, Maritime Safety Agency of Japan also extensively surveyed this area in 1987-1988. Multi-channel seismic reflection explorations were already carried out by Ocean Research Institute, University of Tokyo in the cruise KT 86-9.

The recorded data during Leg 1 of the present cruise was relatively noisy possibly owing to the following reasons;

1. Complex bathymetry around the Ogasawara Plateau.
2. The ship speed was too fast to catch the seismic wave signal.
3. The power of airgun was low.
4. The oil leakage of hydrophone streamer cable.

TABLE 15-2-1. Air gun lines in Leg 1, KH 87-3

KH 87-3-1	Start	27° 9.34'	-	27° 8.16'
	End	143°25.82'	-	143°27.21'
KH 87-3-2	Start	26°46.01'	-	25° 2.60'
	End	143°29.82'	-	143°45.59'
KH 87-3-3	Start	25°31.29'	-	23°28.85'
	End	143°23.90	-	142°39.27'
KH87-3-4	Start	23°33.84'	- 23°39.30' -	23°34.86'
	End	142°41.45'	- 142°26.06' -	142°40.52'
KH 87-3-5	Start	20°49.94'	-	20°32.61'
	End	151°54.30'	-	152° 9.47'

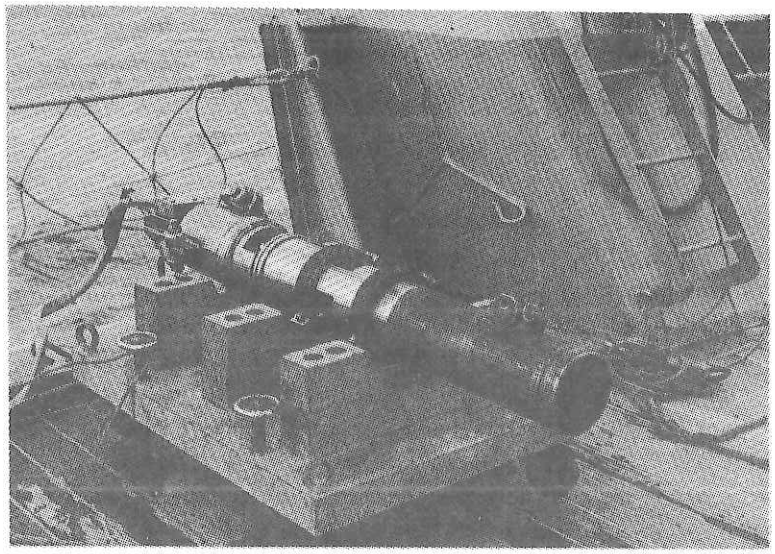

Fig. 15-1-1 Airgun of BOLT 1500C type (above)

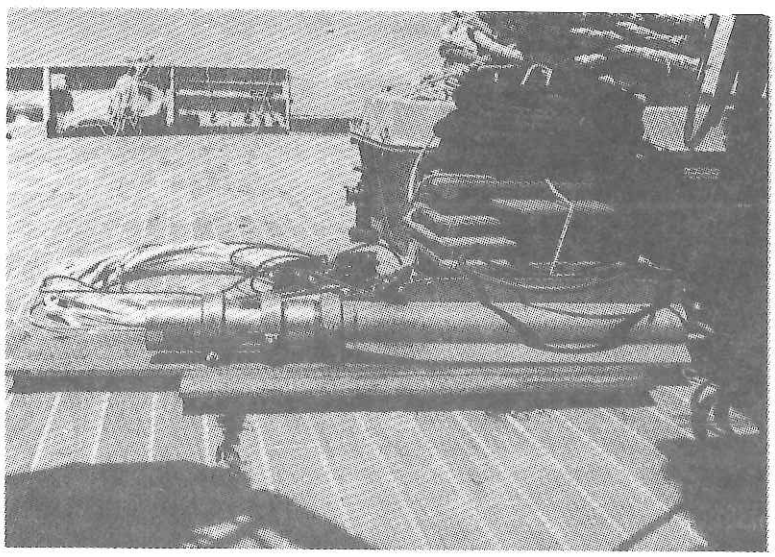

Fig. 15-1-2 Airgun of BOLT 1900C type (below)

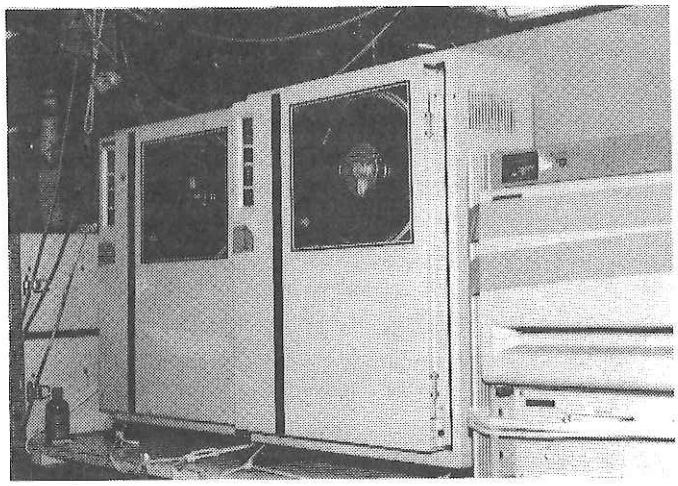

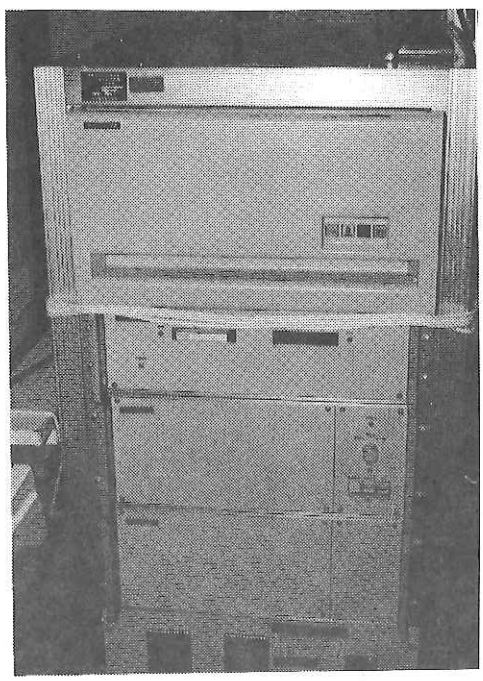

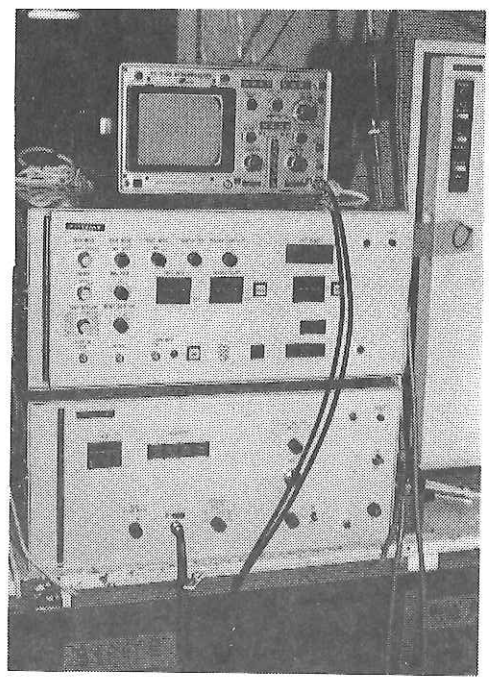

Fig. 15-1-3 Digitalrecording system for seismic reflection survey in KH 87-3.

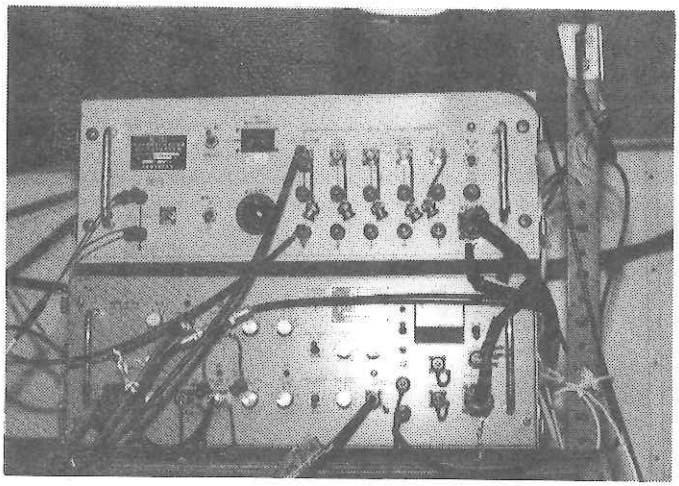

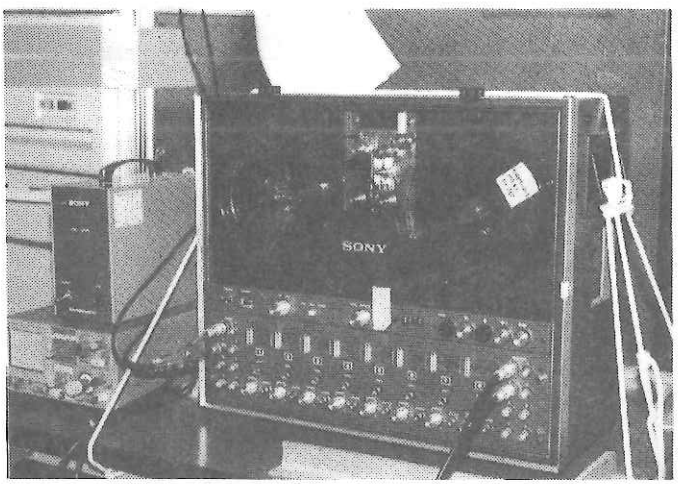

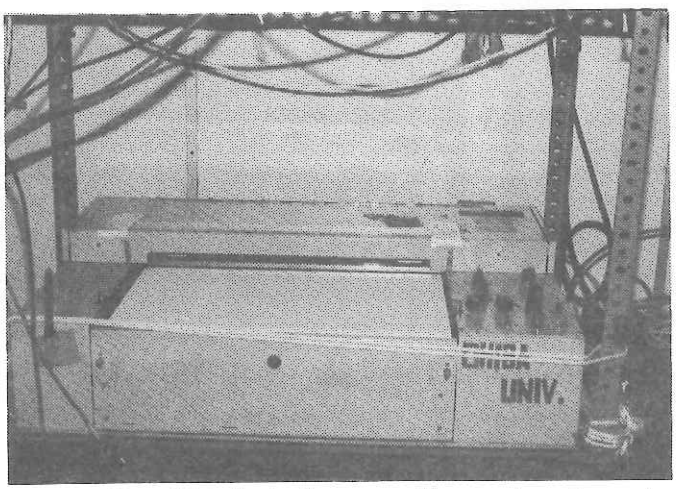

Fig. 15-1-4 Analog recording system for seismic reflection survey in KH 87-3.

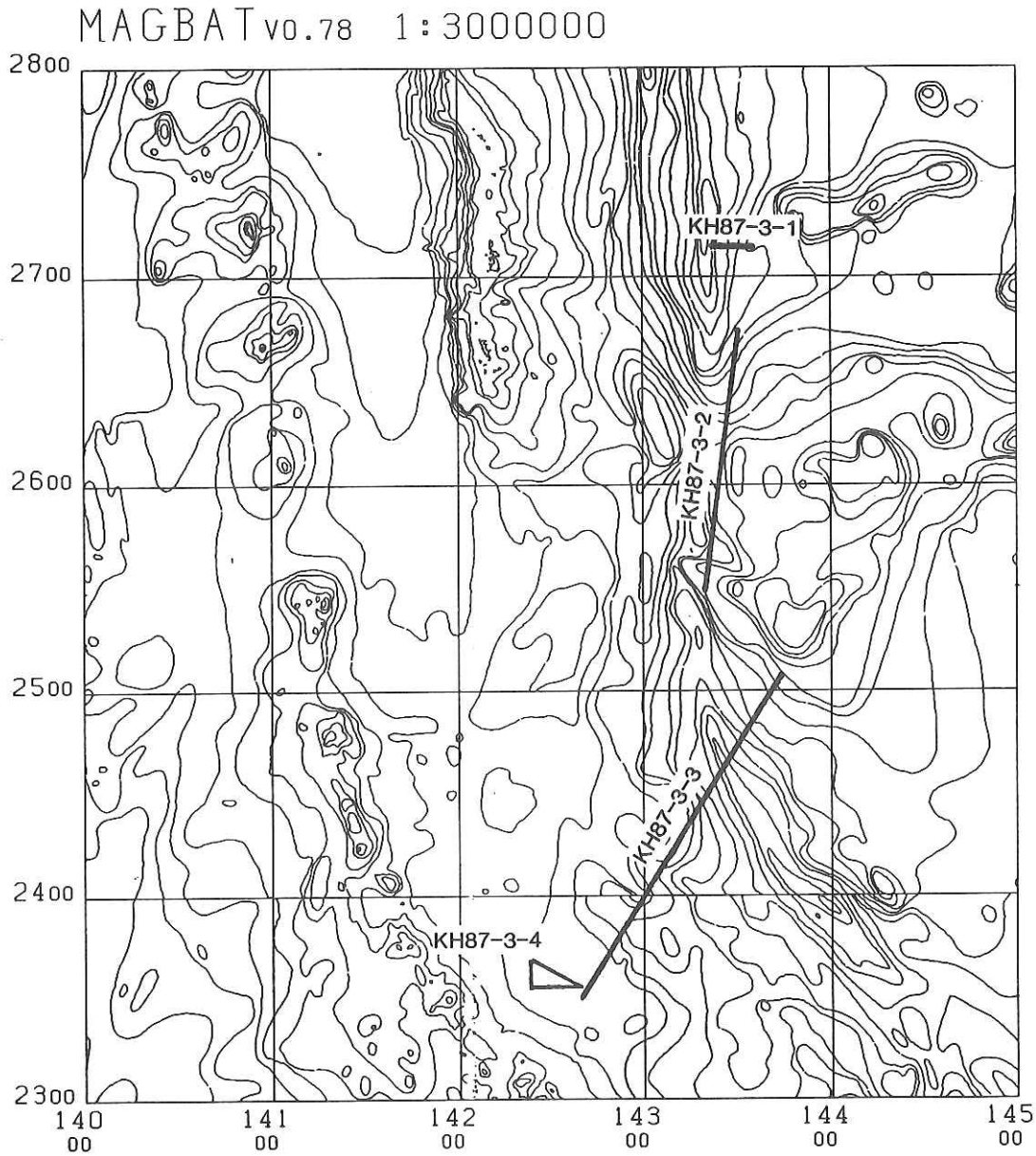

Fig. 15-2-1 Track lines of single-channel seismic survey in Leg 1, KH 87-3

15-3. SEISMIC REFLECTION SURVEY OF THE EAST MARIANA BASIN

K. Tamaki, S. Abe, Y. Kasumi, and T. Asanuma

Seismic reflection survey of the East Mariana Basin was carried out during Leg 1 and Leg 2 of the KH 87-3 cruise (Fig. 15-3-1). The instrumentation for the survey is described by Abe and others (15-1, this volume). Four lines of profiles with a length of 33 mile each were obtained. Line 1 (Fig. 15-3-2) is on magnetic anomaly M34, Line 2 (Fig 15-3-3) is on M23, Line 3 (Fig. 15-3-4) is on M29, and Line 4 (Fig 15-3-5) is on M33. The principal objective of this seismic survey was site survey of ODP drilling sites that are planned to be proposed by Tamaki and Kobayashi.

All the profiles show a similar stratigraphy with banded basement signals overlain by stratified sediments with a thickness of 0.1 - 0.3 sec. The banded basement signals suggest that the acoustic basement of the East Mariana Basin is composed of a sill complex as observed in the Nauru Basin by Larson and Schlanger(1981), although thickness of the sill complex of the East Mariana Basin appears to be thinner than that of the Nauru Basin.

Reference

Larson, R. L. and Schlanger, S. O.: Geological evolution of the Nauru basin and regional implications. In: Larson, R. L., Schlanger, S. O. et al., Initial Reports of the Deep Sea Drilling Project, U. S. Government Printing Office, Washington, D.C., **61**, 841-862, 1981.

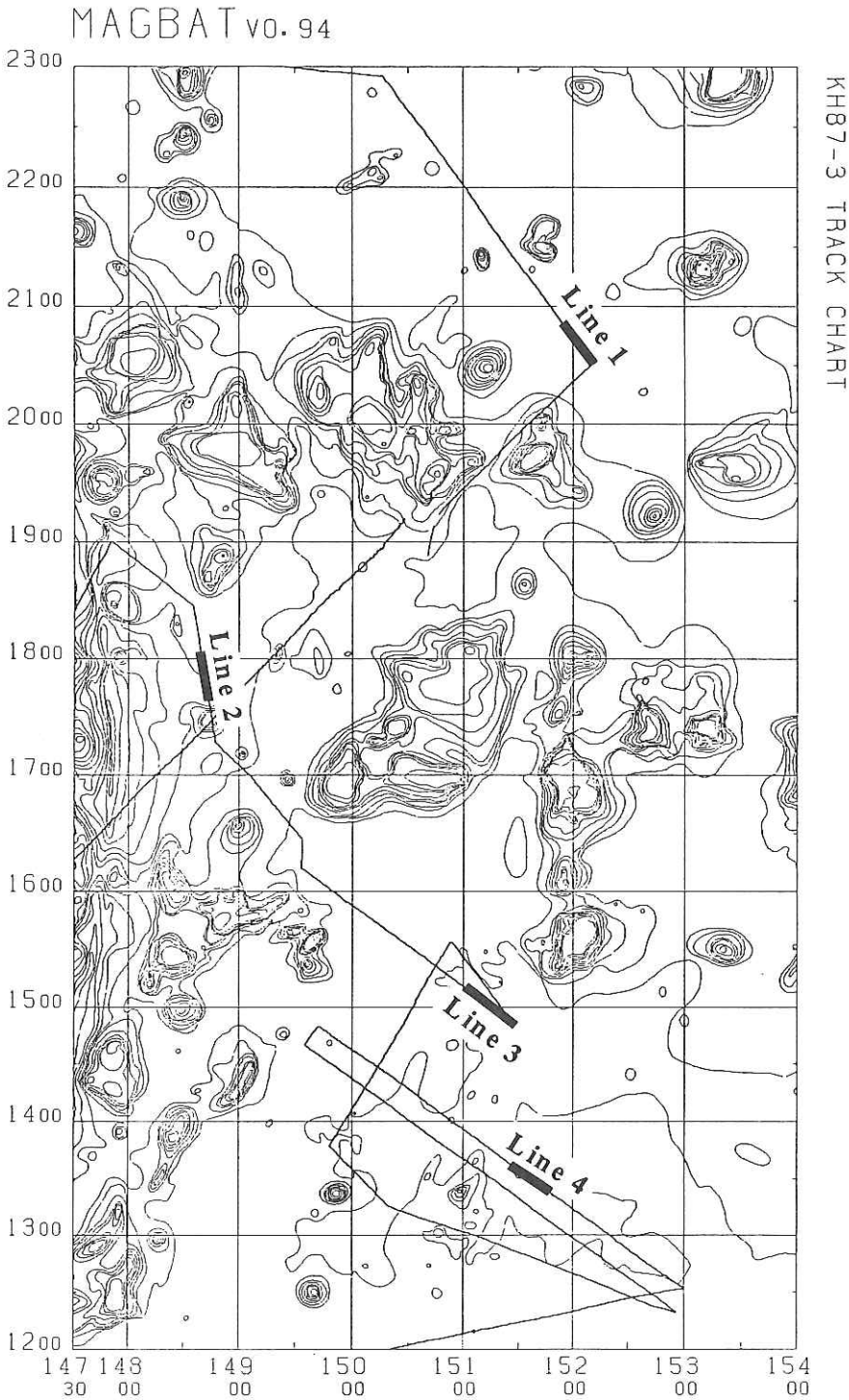

Fig. 15-3-1 Track lines for the seismic reflection survey of KH 87-3, Legs 1 and 2.

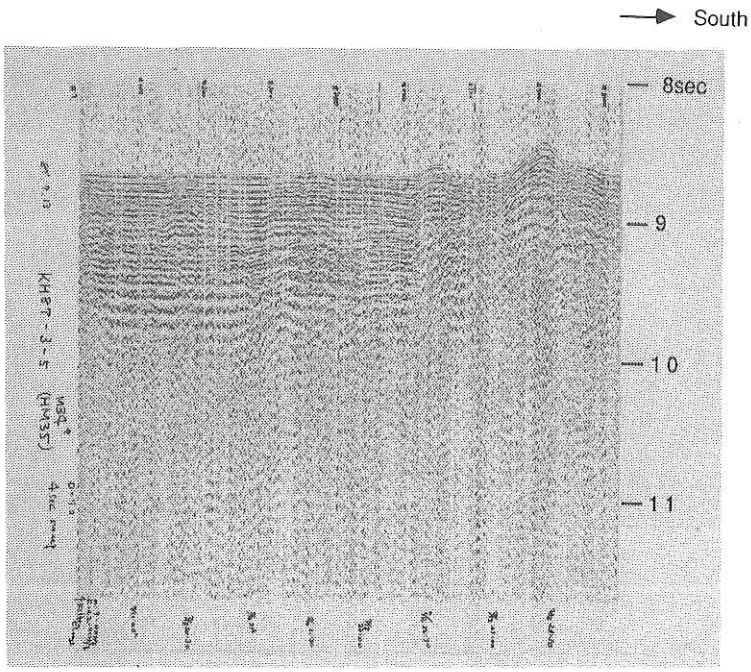

Fig. 15-3-2 On board monitor record of Line 1, East Mariana Basin.

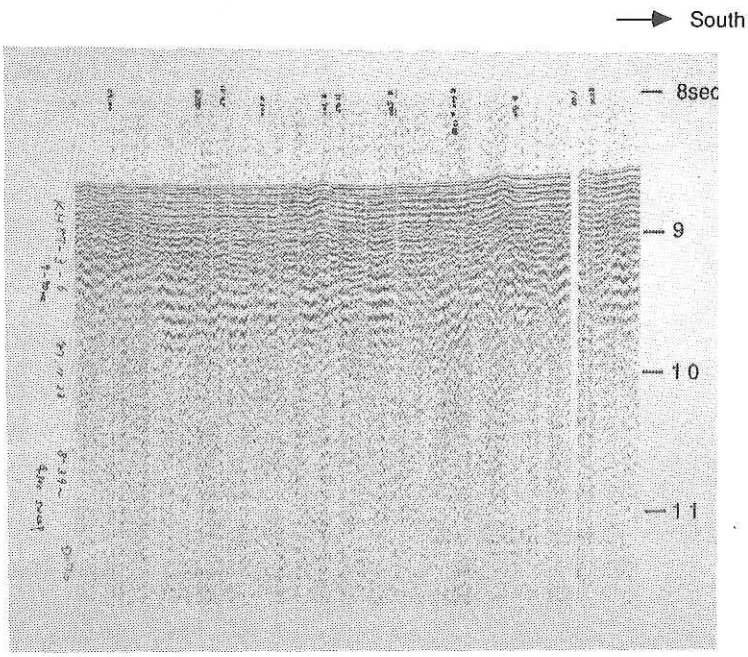

Fig. 15-3-3 On board monitor record of Line 2, East Mariana Basin.

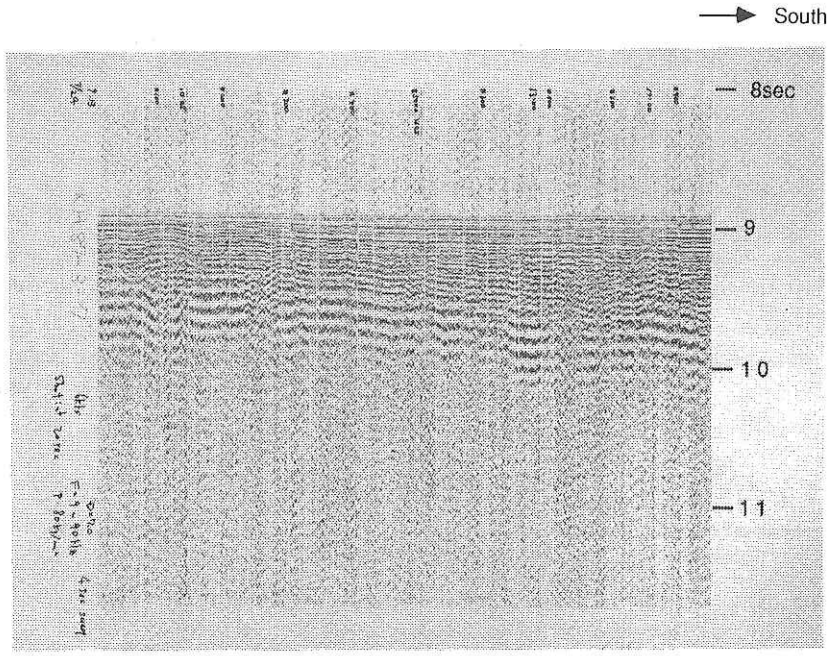

Fig. 15-3-4 On board monitor record of Line 3, East Mariana Basin.

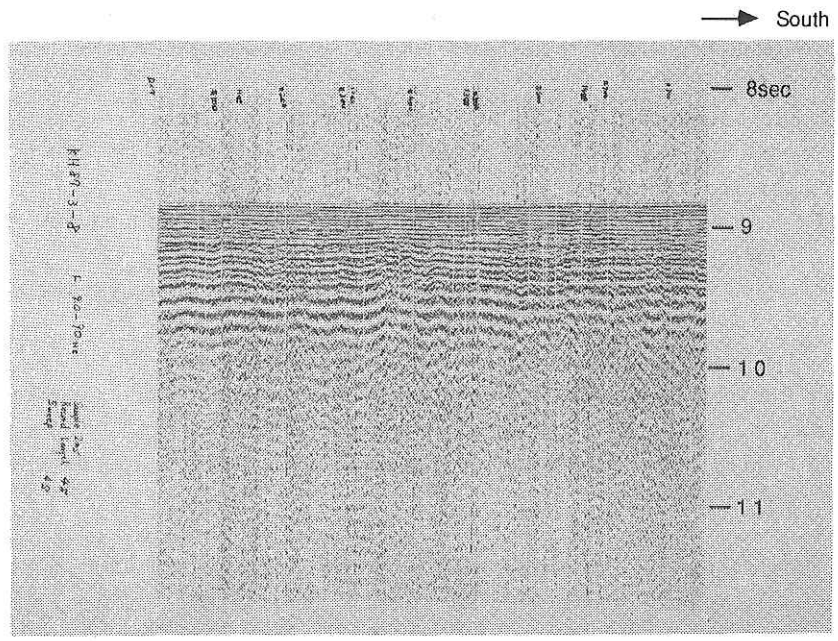

Fig. 15-3-5 On board monitor record of Line 4, East Mariana Basin.

16. SUBNAVIGATION BY A LONG-BASELINE TRANSPONDER SYSTEM

T. Furuta, H. Fujimoto and H. Murakami

16-1. Transponder Subnavigation System

A long base-line acoustic transponder system capable of subnavigation in water as deep as 6000 meters has been developed in these severalyears. Thesystemis compact in size, easy to handle and reliable inrecovery. Positioning by this system was evaluated to be as accurate as a few meters in a sea trial in this cruise. Software for the system was improved during the cruise. Judging from data obtained in this cruise and in the previous cruise (KH87-2), it can be said that the system has almost been completed.

Fig. 16-1 shows a simplified block diagram of the system. A personal computer system is used for the processing and logging of the data. A block digram of the ultrasonic unit of the system is shown in Fig. 16-2. The mooring system for each transponder is shown in Fig. 16-3.

16-2. Software for the Transponder Navigation System

Software for playback of the transponder navigation data was newly developed in this cruise. The software is written in BASIC language and consists of the following four routines;

(1) Calculation of the average acoustic velocities corresponding to depths of the transmitter and the receiver based on the observed XBT data or on the Carter's echo-sounding correction table.
(2) Error detection routine which distinguishes errors in the slant range measurements from the systematic errors caused by wrong estimate of positions of the transponders on the ocean floor.
(3) Iterative procedure for relocation of three transponders on the ocean floor.
(4) Playback of the acoustic navigation data obtained by this system.

Fig. 16-4 shows the track chart of the ship and the Unit D transponder which was set up at the end of a wire 3000 meters long. Fig. 16-5 shows the estimated errors of the ship's positions obtained by the transponder navigation system before relocation. Crosses indicate errors in the slant range measurements.

Positions of the three transponders are recalculated to minimize the systematic errors shown in Fig. 16-5. Positioning errors after the relocation procedure are shown in Fig. 16-6. Root mean square of the fluctuation of the data in Fig. 16-6 is 2.4 m, so that accuracy of the ship's positions by this system is estimated to be a few meters.

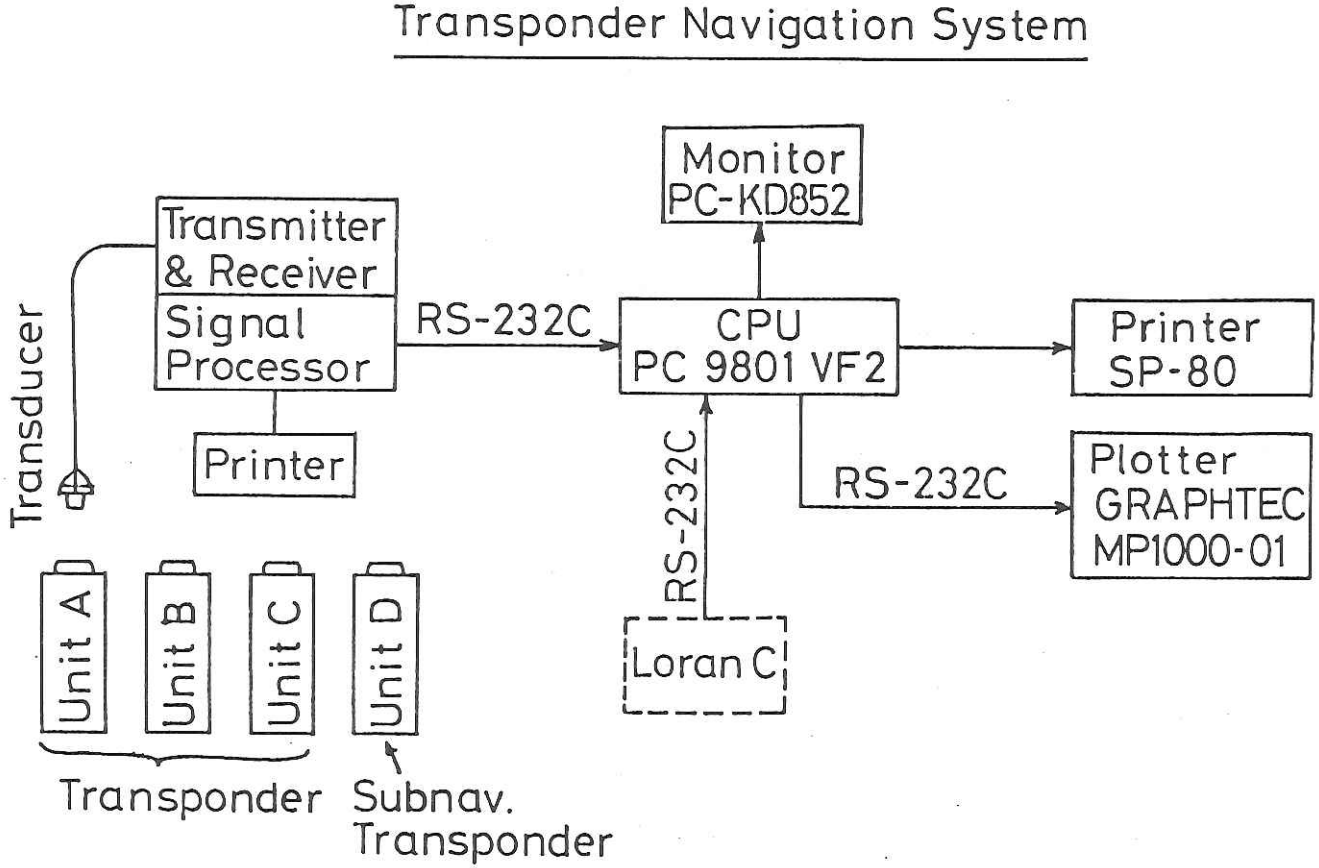

Fig. 16-1 Block diagram of the long base-line acoustic transponder system.

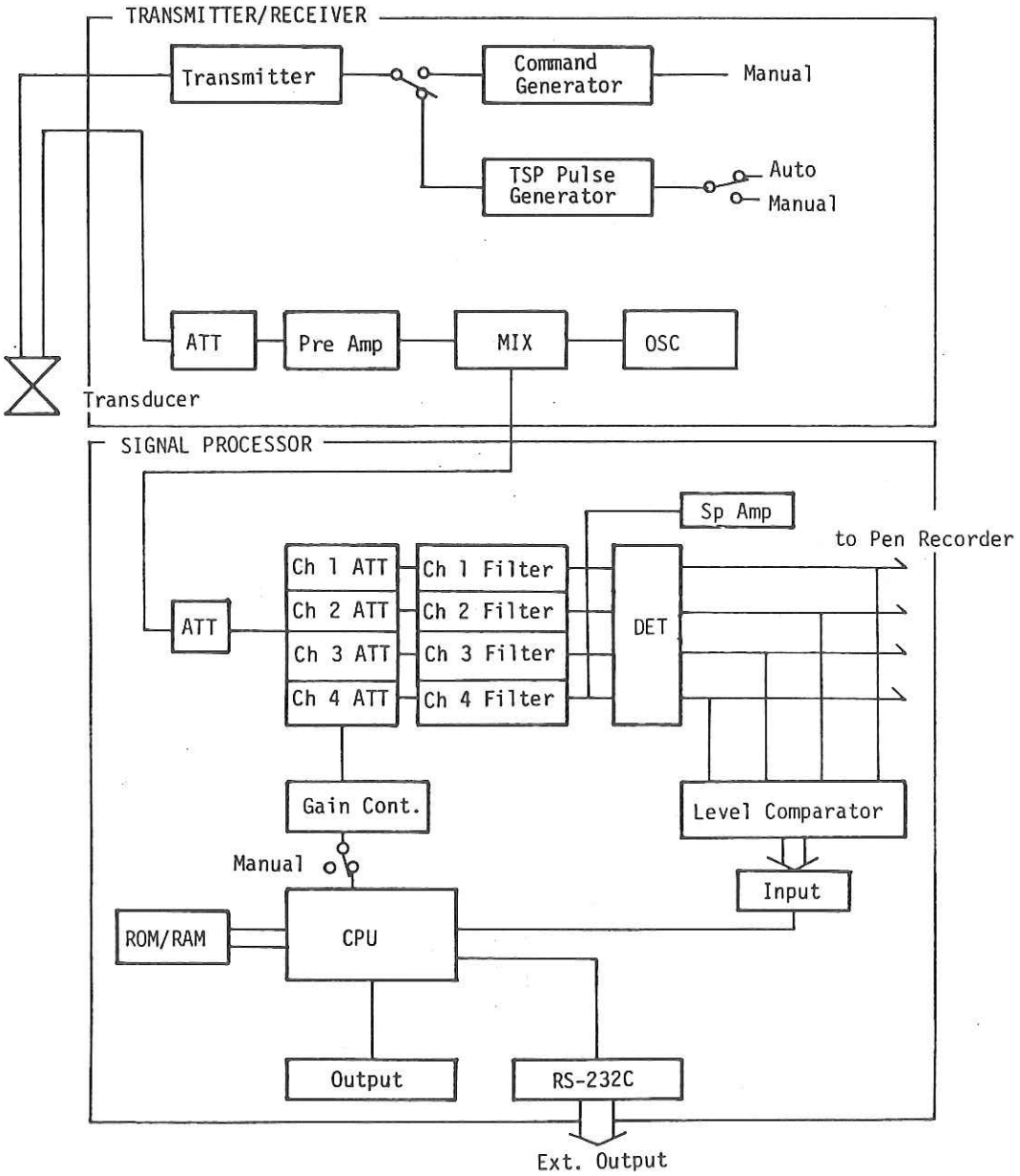

Fig. 16-2 Block diagram of an onboard acoustic processing system. Digitized data are transmitted to a microcomputer through RS232C interface.

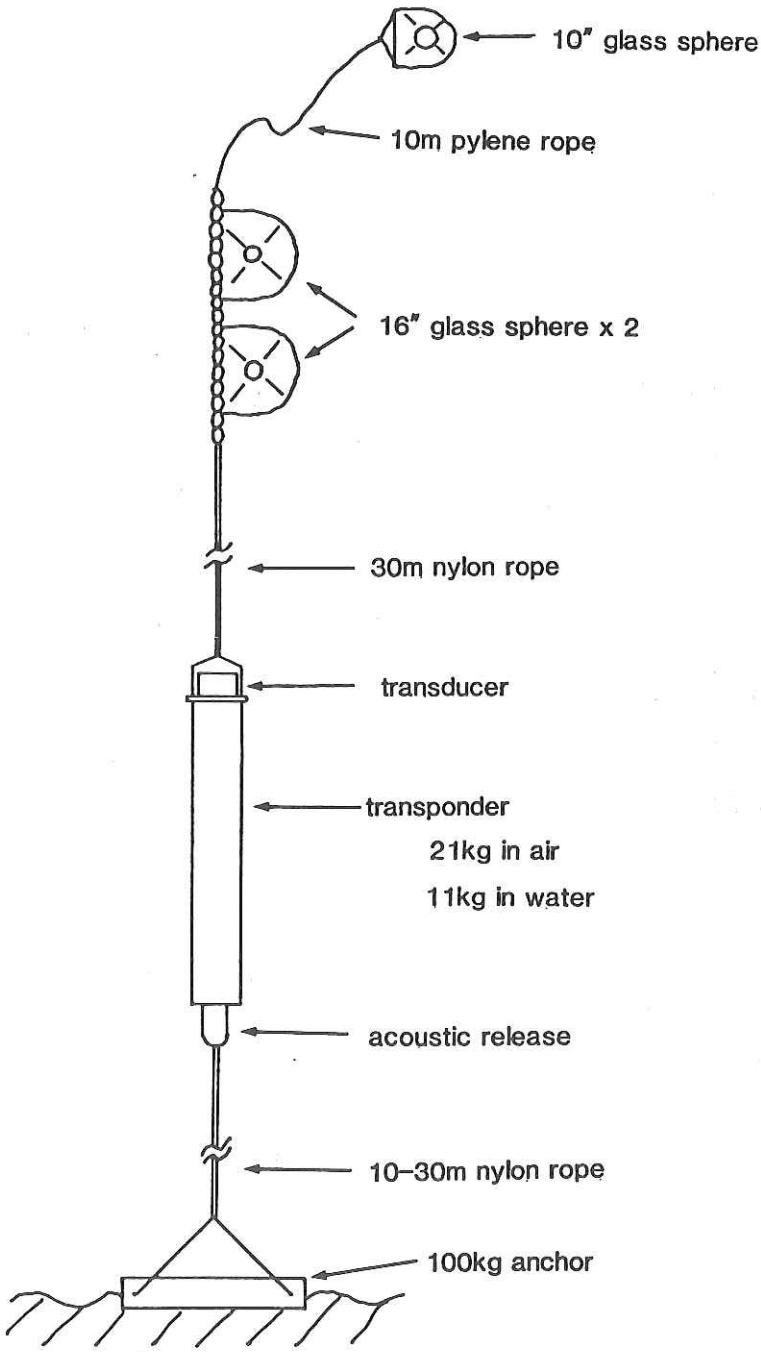

Fig. 16–3 Mooring system of the transponder.

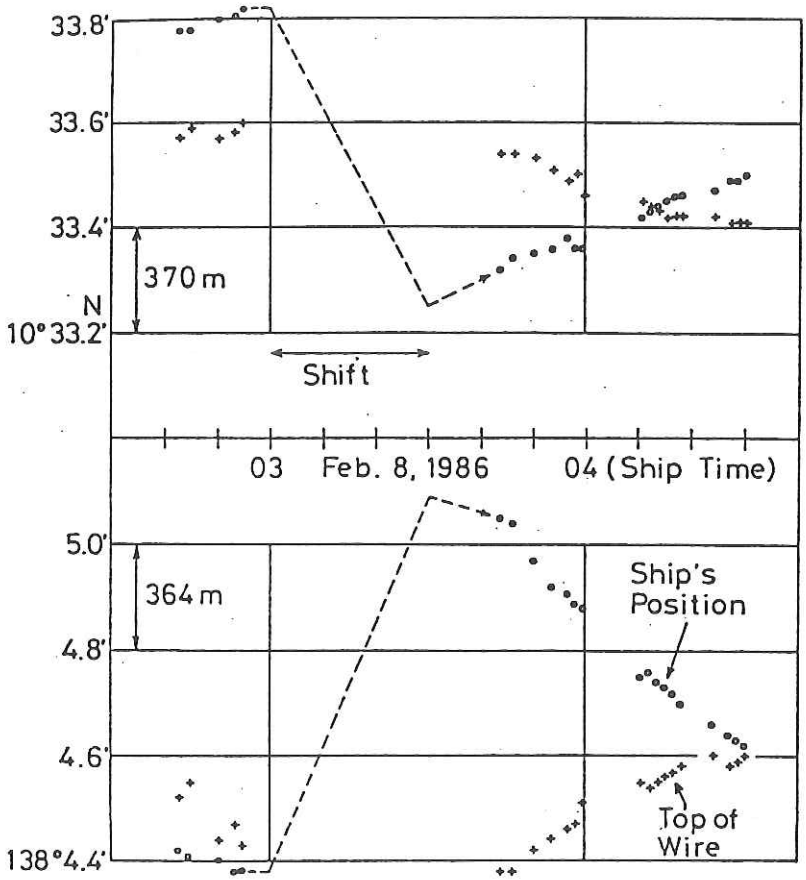

Fig. 16–4 Tracks of the ship and subnavigation transponder.
+: ship's position, square: subnavigation transponder position.

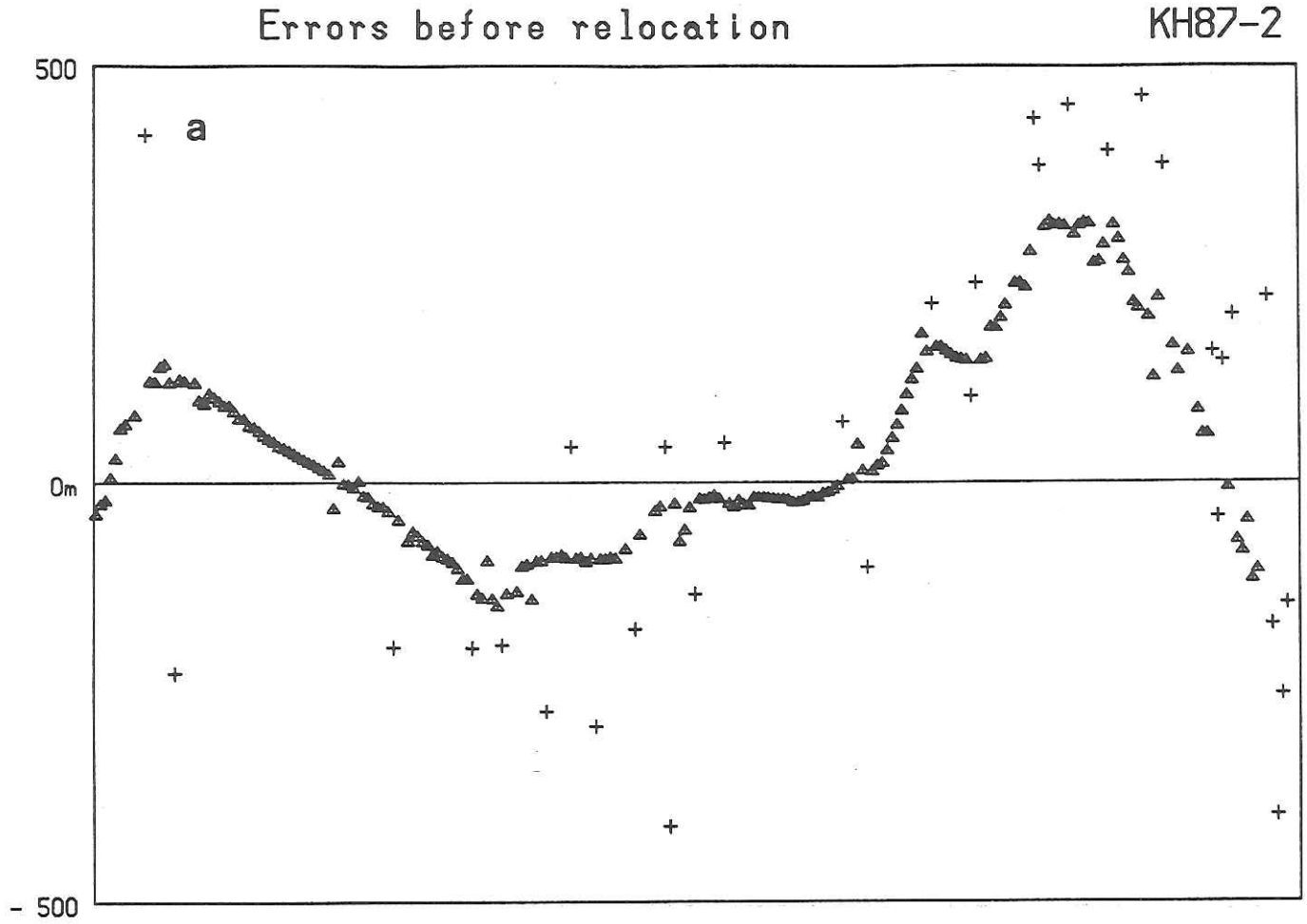

Fig. 16-5 Estimated errors before relocation of each transponder.

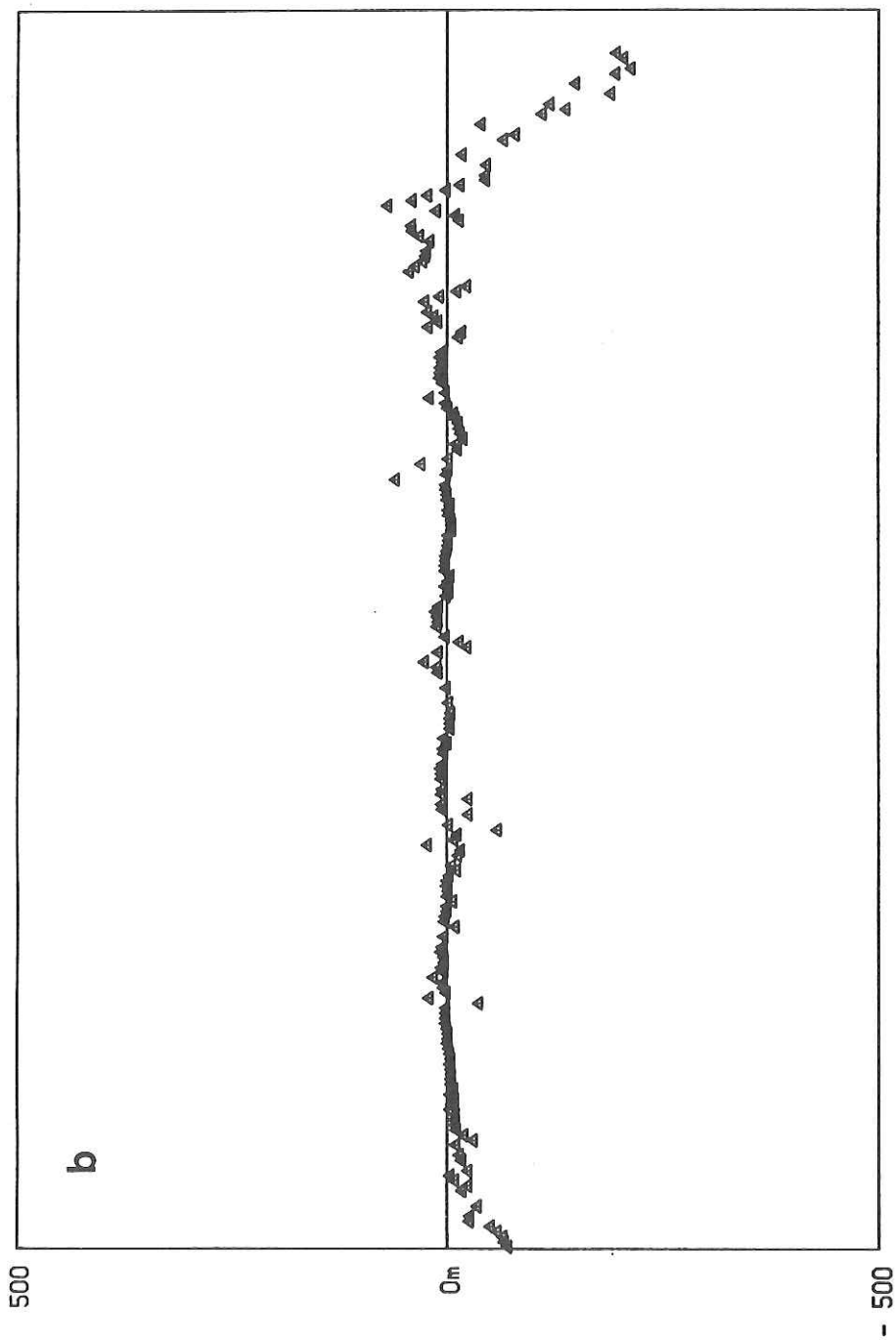

Fig. 16-6 Errors after relocation.

17. SOUND PROPAGATION EXPERIMENTS IN THE SEA FOR MEAN CURRENT VELOCITY MEASUREMENT

T. Takeuchi

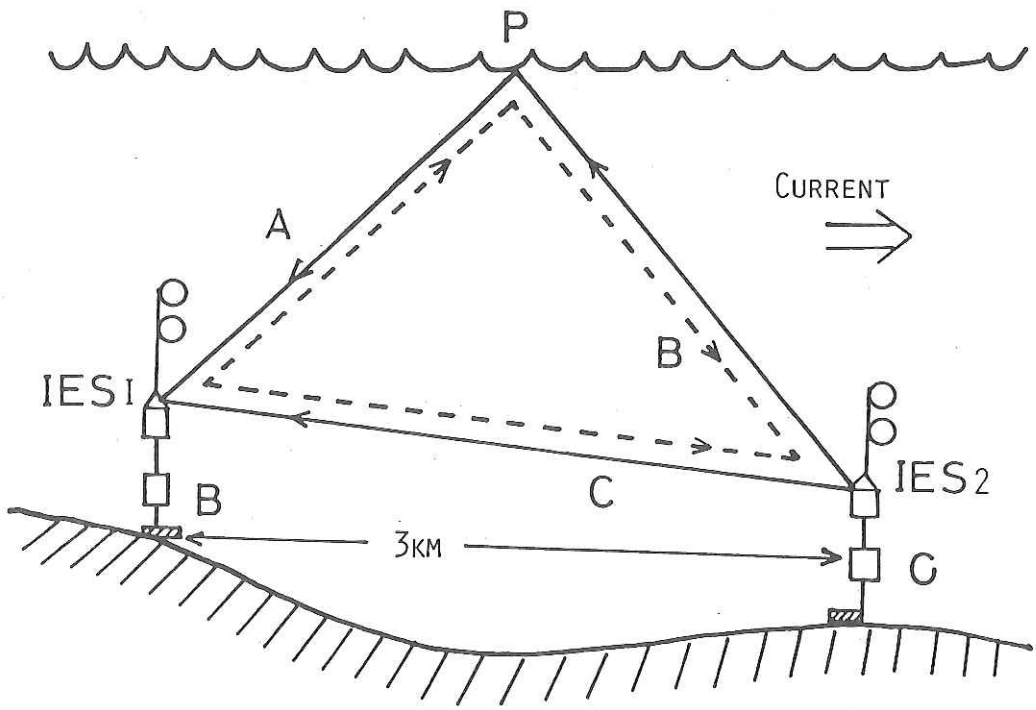

Fig. 17-1 Illustration showing a principle of the mean current velocity measurement using two Inverted Echo Sounders, IES1 + IES2 and P; surface.
Sound wave propagates along paths as follows;

A: IES1-IES2-P-IES1
B: IES1-P-IES2-IES1
C: IES1-IES2-IES1

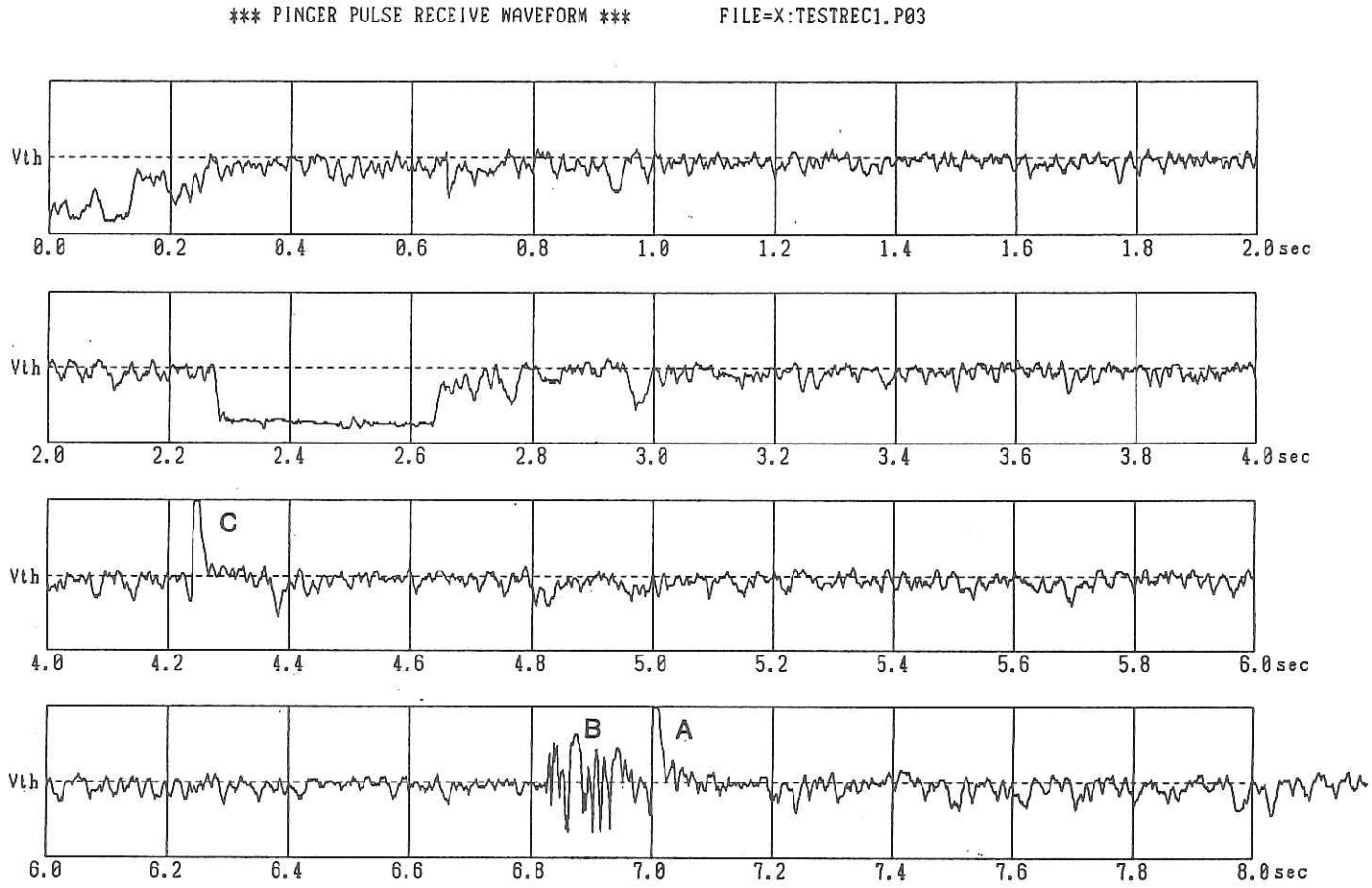

Fig. 17-2 A result of IES pulses form recorded in IES1 receiver. Small difference in arrival times between A and B denotes the mean current vetor.

18. HEAT FLOW MEASUREMENT

18-1. HEAT FLOW MEASUREMENT IN THE MARIANA TRENCH

Y. Kasumi and M. Kinoshita

During leg 1 of the cruise KH 87-3 of the R. V. Hakuho-maru, heat flow in the ocean floor was measured twice at sites HF-1 and -2 in stations KH 87-3-10 in the northern fore-arc region of the Mariana Trench. In this area number of the previous heat flow data had been very few, although a high heat flow value (140mW/m^2) was observed near these sites. The thermal conductivity was measured at station KH 87-3-9 (P-1).

[1]. Method of observation

<Temperature gradient>

At HF-1 and -2, the Ewing type heat flow probe developed at Chiba University was used. It weighs about 250kg and the probe is about 4m long on which six sensors are equipped (outriggered) at intervals of 60cm. One of the sensors is attached with the heating wire for in-situ thermal conductivity measurements. Using this probe, the thermal conductivity data are obtained from the observation of the thermal decay after transient heating (pulse-probe method). This instrument permits multiple penetrations.

<Thermal conductivity>

The thermal conductivity was measured on the pilot core sample taken at KH 87-3-9 (P-1) by the needle probe method (Von Herzen and Maxwell, 1959). Obtained sample was stored for one day in order to equilibrate to the room temperature. A good care was taken not to lose the interstitial water. At HF-1 and HF-2, in-situ thermal conductivity measurements were attempted.

[2]. Measurements

HF-1 and HF-2

They were located in the northern fore-arc region of the Mariana Trench. They were very close to each other. We made them by POGO penetrations. No penetrations were successful, because of sandy sediments.

TABLE 18-1-1. List of Heat Flow Measurements in KH 87-3-10

Stn	Site	Latitude (N)	Longitude (E)	Depth (m)	PEN	dT/dz (mK/m)	K (W/m/K)	Q (mW/m^2)
KH 87-3								
10-1	HF-1	23°37.3'	142°43.1'	3200	0		1.09	
10-2	HF-2	23°37.5'	142°43.3'	3200	0		1.09	

Depth: the corrected water depth, PEN: number of thermistors in the mud, K:measured thermal conductivity from P-1 sample; Q: heat flow value.

TABLE 18-1-2. List of Piston Coring Site at which thermal conductivity was measured.

Stn	Site	Latitude (N)	Longitude (E)	Depth (m)
KH 87-3-9	P-1	23°34.8'	142°41.1'	3180

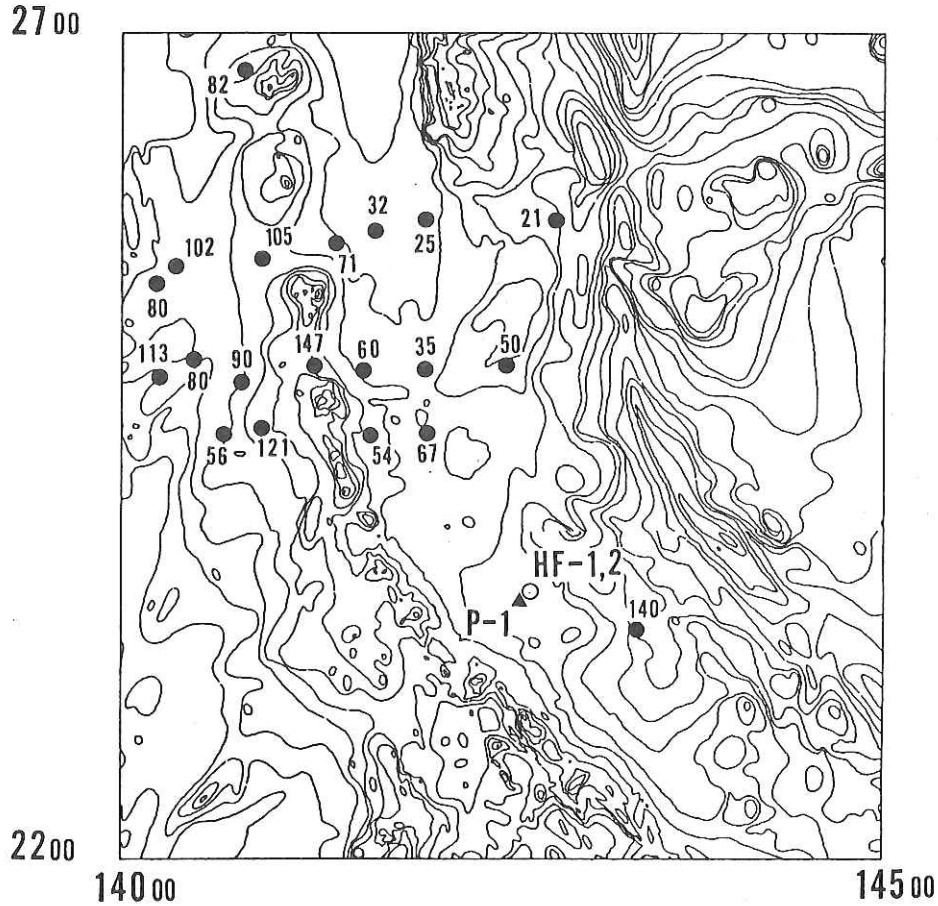

Fig. 18-1-1 Heat flow value in mW/m^2 around the Ogasawara Plateau. Closed circles are the previous stations. Open circle is the station KH 87-3-10 of this cruise. Triangle indicates sampling site KH 87-3-9 by a piston corer.

18-2. HEAT FLOW MEASUREMENTS IN THE YAP TRENCH AREA

M. Kinoshita and Y. Kasumi

[1]. Introduction

During leg 3 of KH 87-3 cruise, heat flow was measured in the northern part of the Yap Trench. In this area, number of the previous heat flow data had been very few before the KH 86-1 cruise. During that cruise a lot of heat flow data were obtained across the northern part of the Yap Trench (five measurements on the western side of trench and two on the eastern side). During the KH 87-3 cruise, measurements were attempted at two stations: KH 87-3-20 (HF-3) and KH 87-3-23 (HF-4) in the backarc area and at two stations: KH 87-3-26 (HF-5) and -27 (HF-6) on the seaward side where the Caroline Ridge seems to abut the Yap Trench.

[2]. Method

<Temperature gradient>

At site HF-3, the violin bow type marine geothermal probe developed by the Applied Microsystems Limited (AML) was used. It weighs about 150kg and the sensor probe is 2m long and 8mm in diameter in which seven thermistors are installed at intervals of every 45cm. This sensor probe is held by the strong steel rod, and therefore it enables multiple penetrations. It is called the AML-POGO instrument.

At sites HF-4 and HF-6, the Bullard type probe developed also by the AML was lowered. The sensor probe is about 3m long and 16mm in diameter in which seven thermistors are installed, and weighs about 100kg. As recognized from the shape of the sensor probe, it is easy to penetrate in the sediment. However, it was usually bent when pulled out from the sea bottom and did not allow multiple penetrations.

At site HF-5, the Ewing type heat flow probe developed at Chiba University was used. It weighs about 250kg and the probe is about 4m long on which six sensors are equipped (outriggered) at intervals of every 60cm. One of the sensors is equipped with the heating wire for in-situ thermal conductivity measurements. This instrument permits multiple penetrations.

<Thermal conductivity>

Thermal conductivities were measured on samples taken by the piston corer at stations KH 87-3-21 and -22 (P-3, P-4) by the needle probe method (von Herzen and Maxwell, 1959). Obtained samples were laid down without cutting for one day in order to equilibrate to the room temperature. A good care were taken not to lose the interstitial water.

At HF-5 (Chiba Univ. system), in-situ thermal conductivity measurement by the pulse probe method (Lister, 1979) was attempted. This method is to obtain the thermal conductivity by the observation of the thermal decay after transient heating. The result obtained at HF-5-B is possibly less than the true value by a few percent depending on the method (Boh, 1986).

[3]. Measurements and Results

<HF-3> [AML-POGO]

It was located in the northern part of the backarc area. The probe penetrated three times, but due to the leakage of water into the pressure vessel the data was lost before the first penetration. Judging from the tensionmeter record, the probe penetrated rather deeply in the mud. The thermal conductivity was measured on samples taken by the piston corer KH 87-3-21 (P-3) located very close to HF-3. The result is shown in Fig. 18-2-2.

<HF-4> [AML-Bullard]

This was also situated in the backarc area, between HF-3 and the trench axis. The station HF-1 of KH 86-1 was located close to this station. Three of seven thermistors were in the mud. The piston core KH 87-3-22 (P-4) was also located close to HF-4, where the thermal conductivity was measured on the obtained core samples. Results are shown in Figs. 18-2-1 and -2-2. The determined heat flow value is 102mW/m^2, which seems to be practically the same as the result at site HF-1 of KH 86-1.

<HF-5> [Chiba Univ.]

This was located on the outer swell of the trench. At HF-5-B, one of six sensors seems to have penetrated in the mud. At HF-5-A and -C, their penetrations were unsuccessful. The lowermost sensor with the heating wire was broken and the other three sensors were bent, probably due to rocks on the sea floor or because the probe had fallen obliquely.

<HF-6> [AML-Bullard]

HF-6 was located just east of HF-5. Three thermistors were in the sediment. The probe bent so much. The result (see Fig. 18-2-1) indicates low heat flow (29mW/m^2), and the temperature versus depth profile seems to be somehow concave.

[4]. Preliminary interpretation of the results

Measured heat flow values are listed in Table 18-2-1, and presented in Fig. 18-2-3 together with previous ones. The heat flow profile across the Yap Trench is shown in Fig. 18-2-4. A general feature indicates lower heat flow on the eastern side of the Yap Arc and higher on the western side. This pattern is similar to those in the ordinary trench-arc systems, as mentioned by Nagihara et al. (1986).

On the landward side of the trench, the peak of heat flow values appear a few tens of kilometers west of the Yap Arc. The maximum value ($168mW/m^2$) is abnormally high and the mean value (around $120mW/m^2$) is still higher than the average heat flow in the Parece Vela Basin ($88mW/m^2$). Except for these high values, other heat flow value coincide with this average. Therefore, the high heat flow represents some thermal anomaly on the western side of the Yap Arc, and it possibly indicates recent or present volcanic activity. The abnormally high heat flow of $168mW/m^2$ (this site was very close to others where heat flow values ranging from 107 to $118mW/m^2$ were observed) may reflect hydrothermal activities related with this volcanic activity.

As to the eastern side of the trench, heat flow value at HF-6 is consistent with the theoretical value in the Pacific Ocean estimated from its age. However, other values (the previous data observed to the south of HF-6) are higher, which may be under the effect of the Sorol Trough and the Caroline Ridge that are younger than the Pacific Ocean. Moreover, the temperature versus depth profile of HF-6 seems concave, which may indicate either the sediment downwarping due to the penetration of the probe or the downward pore water flow.

References

Boh, R.: graduate thesis. 1986.

von Herzen, R. P., and A. E. Maxwell: The measurement of thermal conductivity of deep-sea dediments by a needle-probe method. J. Geophys. Res., **64**, 1557-1563, 1959.

Lister, C. R. B.: The pulse-probe method of conductivity measurement. Geophys. J. R. astr. Soc., **57**, 451-461, 1979.

Nagihara, S., M. Kinoshita and H. Kinoshita: Heat flow measurements around the Yap Trench. Programme and Abstracts, Seismol. Soc. Japan, 1986(2), 9, 1986.

TABLE 18-2-1. List of Heat Flow Measurements in Leg 3 of KH 87-3 Cruise

Stn	Site	Latitude (N)	Longitude (E)	Depth (m)	PEN (m)	N	G (mK/m)	K (W/m/K)	Q (mW/m^2)
KH87-3									
20	HF3-A	10°46.9'	137°35.7'	4800	-	-	-	-	-
	-B	10°46.9'	137°35.4'	4800	-	-	-	-	-
	-C	10°47.2'	137°35.5'	4800	-	-	-	-	-
23	HF4	10°35.5'	138°06.0'	4350	1.5	3	132	0.77	102
26	HF5-A	10°45.3'	139°05.2'	4100	-	-	-	-	-
	-B	10°45.2'	139°05.3'	4100	-	-	-	0.761	-
	-C	10°45.1'	139°05.3'	4100	-	-	-	-	-
27	HF6	10°29.0'	139°15.7'	5150	1.5	4	38	0.761*	29
21	P-3	10°46.9'	137°35.9'	4800				0.74 0.03	
22	P-4	10°35.5'	138°06.0'	4350				0.77 0.02	

Notes:
Depth is the uncorrected water depth,
PEN: length of the probe in the sediment,
N: number of thermistors used for the calculation of G,
G: temperature gradient calculated with the least square method,
K: thermal conductivity (*represents values measured at nearby stations),
Q: heat flow value as the product of G and K.

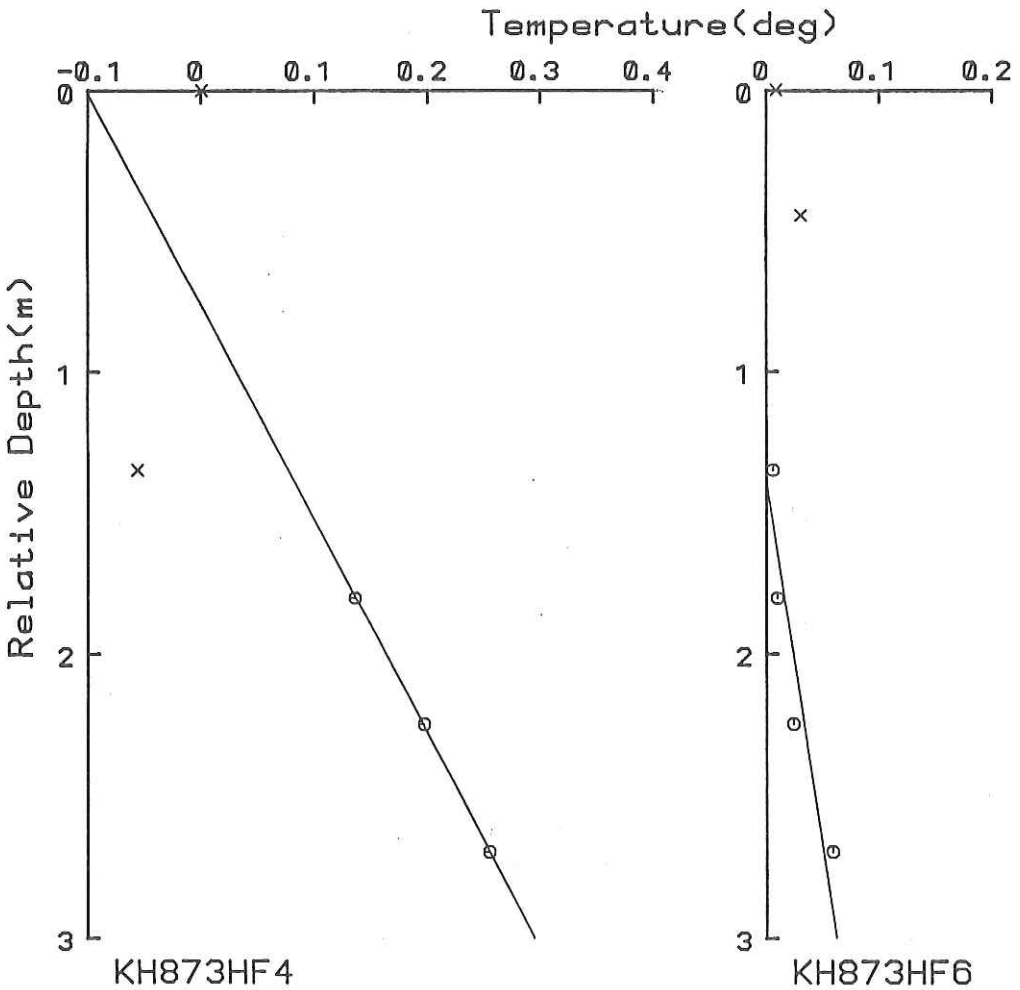

Fig. 18-2-1 Temperature versus depth profiles for HF-4 and HF-6. The depth is taken relative to the position of the topmost sensor. Temperature indicates difference between the equilibrium temperature and reference temperature.

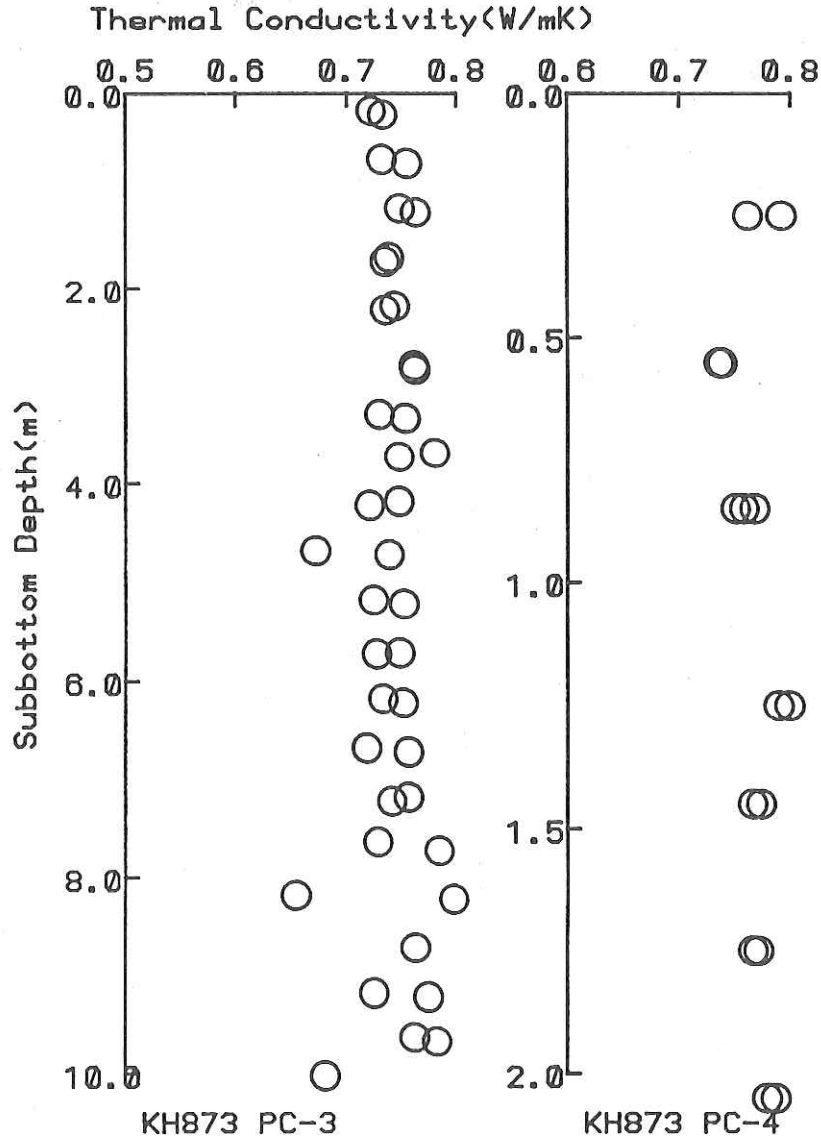

Fig. 18-2-2 Thermal conductivity versus depth profiles measured on samples taken at P-3 and P-4. The column is the depth from the sea floor.

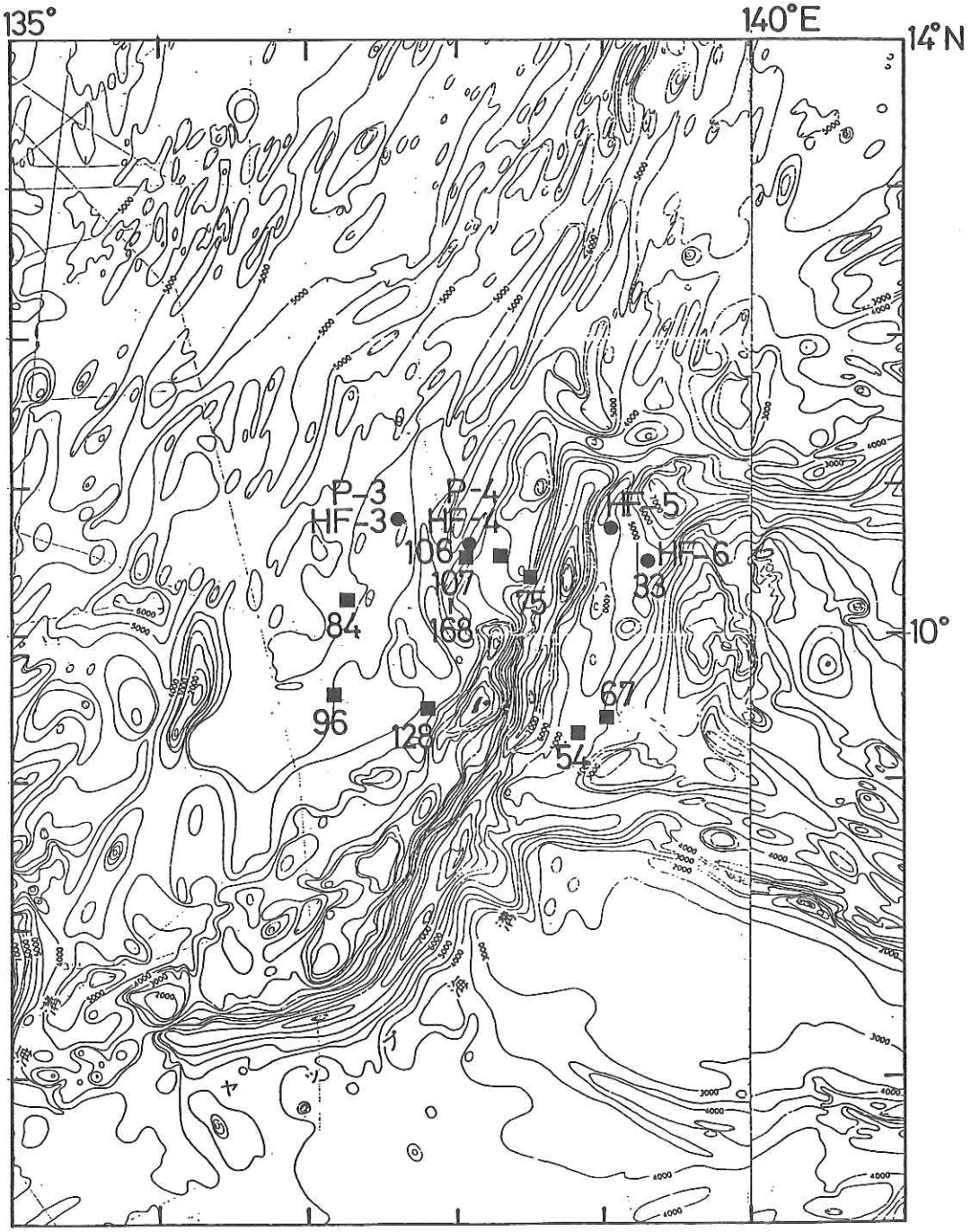

Fig. 18-2-3 Heat flow stations and data around the Yap Trench. Closed squares are the previous data whereas closed circles represent newly obtained stations. The unit of heat flow values is mW/m^2.

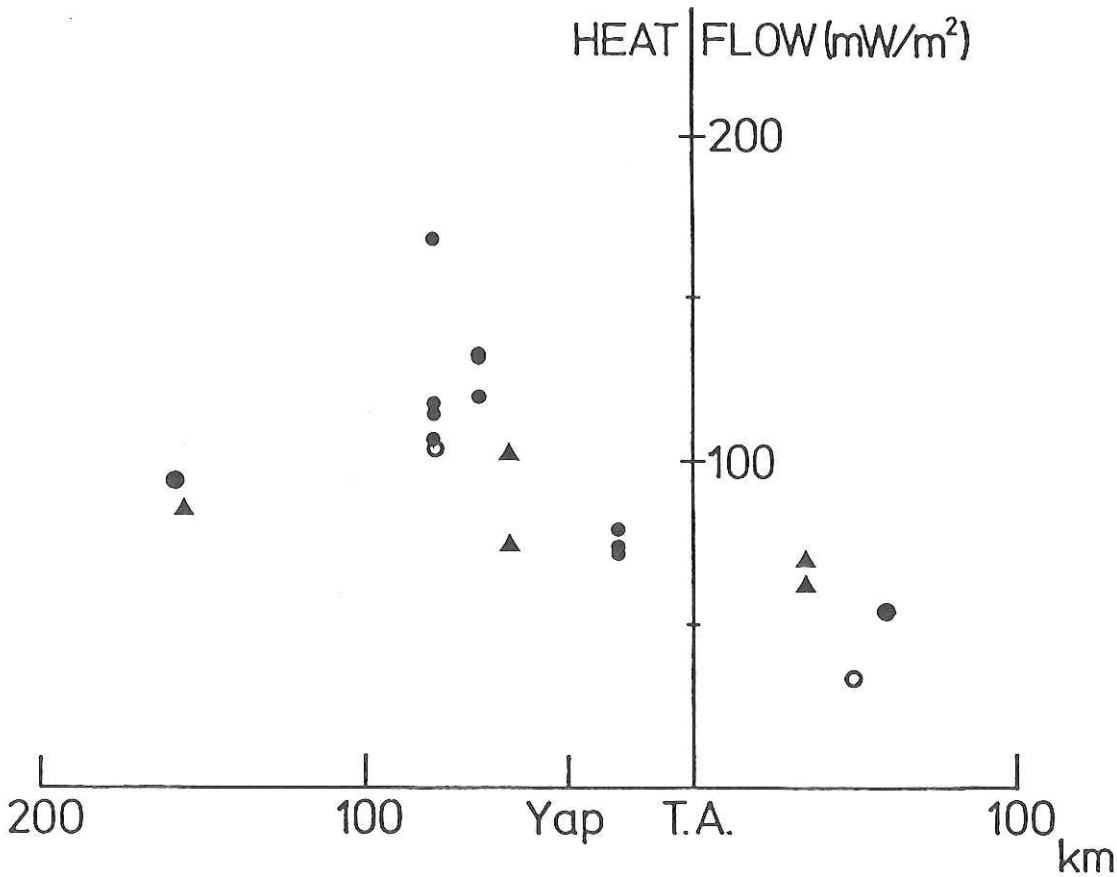

Fig. 18-2-4 Heat flow profile across the Yap Trench. Closed circles are the previous data, triangles indicate the previous but less reliable one and open circles the newly obtained data.

19. CALCAREOUS NANNOFOSSILS FROM THE YAP ARC-TRENCH SYSTEM

H. Matsuoka

In order to know the geological age, the calcareous nannofossils were examined with two cores (PC-3 and PC-4) and sediments collected by five dredge hauls (D-7,-8, -9, -10, -11), both of which were recovered from the Yap arc-trench system in Leg 3 of the cruise KH 87-3. Twenty eight samples were prepared at an interval of about 50cm from the cores and twenty three samples from the dredges. The nannofossils were analyzed by using an optical microscope. The nannofossil zonation proposed by Okada and Bukry (1980) was adopted to assign age of the nannoflora.

P - 3 (KH 87-3-21)

Nannofossils were absent in the samples taken from the upper part (0-700 cm) of this core. The nannoflora partially dissolved was observed in the samples from the lower part (750-1000cm). Samples from 900, 950 and 1000cm in the core yield commonly Discoaster pentaradiatus and Discoaster surculus, but lack Discoaster tamalis and Sphenolithus spp. and, therefore, are assignable to Zone CN12b. The Sample from 850cm of the core may belong to Zone CN12c, because D.surculus does not occur.

The sample from 800cm of the core lacks D.pentaradiatus and seems to fit into the CN12d. The acme of Discoaster triradiatus is a typical marker of the latest Pliocene age, and its abundant occurrence in the Sample from 750cm indicates the top of Zone CN12d. Consequently, these samples, as a whole, belong to the Upper Pliocene.

P - 4 (KH 87-3-22)

As there is no Pseudoemiliania lacunosa, but Gephyrocapsa oceanica in the sample from 15cm, it is assigned to the Zone CN14b. The presence of G.oceanica shows that the Sample CC is assigned to CN14. Accordingly this core seems to correspond to the Pleistocene. However, it is not possible to assign this core to nannofossil zone in any further detail, because of the severe dissolution and reworking of nannofossils.

Dredge Samples

Fig. 19-1 shows the observation on the samples from the dredge hauls. Diagenetic overgrowth and reworking of coccoliths were observed in many samples. No nannofossils were observed from the Samples D-8-003, 138, D-9-102, D-10-000 and D-11-000. Positions of the dredge hauls are given in Table of Chapter 3 as D-7 = KH 87-3-13, D-8 = KH 87-3-15, D-9 = KH 87-3-16, D-10 = KH 87-3-18 and D-11 = KH 87-3-19.

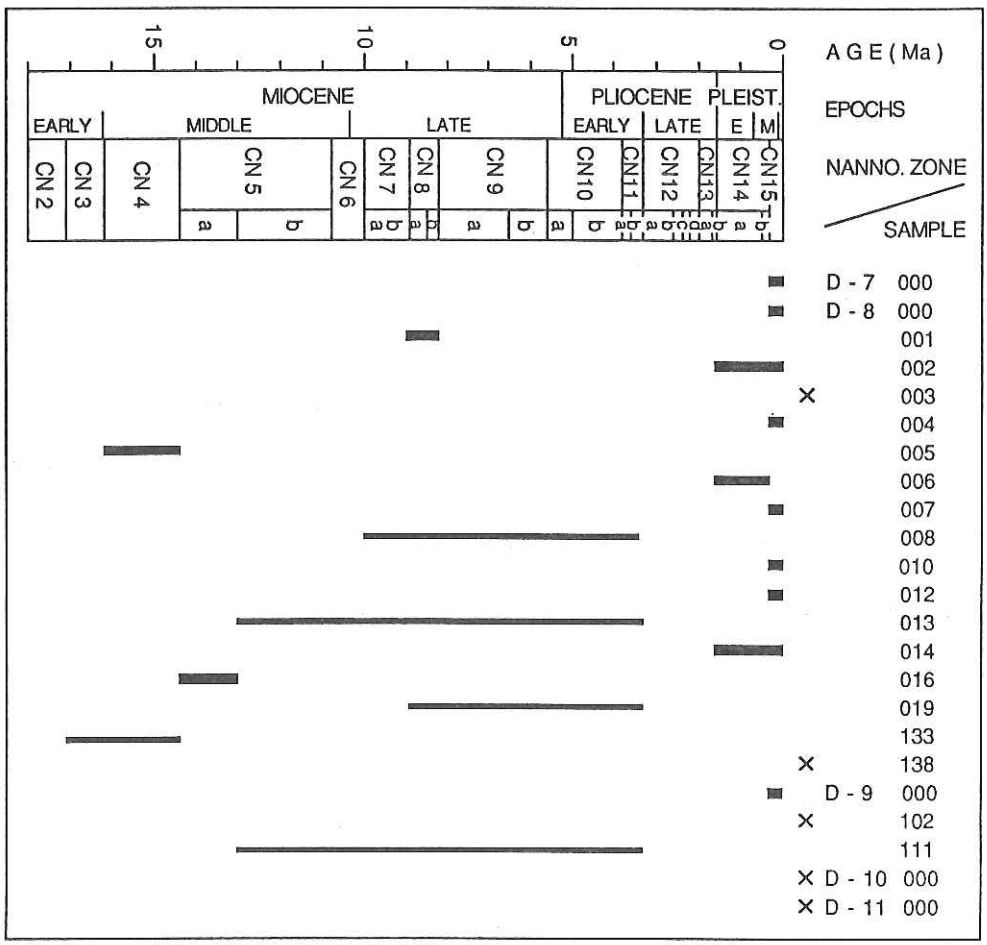

Fig. 19-1 Age assignment of dredge samples. Age data for Zones are based on the work of Berggren et al (1985).

20. SEDIMENTS AND ROCKS AROUND THE YAP TRENCH

K. Fujioka, A. Takeuchi, G, Kimura,
J. Ashi, S. Kuramoto, H. Matsuoka and M. Watanabe

20-1. INTRODUCTION

[1]. Introduction

The expedition to the Yap Islands and their adjacent areas started on August 3, 1987 in order to gather further evidence about marine geophysical and geological phenomena which may form this anomalous island arc; the Yap arc-trench system. The Yap Island Arc-trench system consists of metamorphic and ultramafic rocks, whereas common arc-trench systems are composed mostly of volcanic rocks with active volcanicity and seismicity. In the early 20th century, scientific investigation on the geology and geophysics of the Yap islands was done by many foreign scientists, chiefly by German scientists. Late Dr. R. Tayama visited the Yap islands in 1934, as the first Japanese researcher who visualized geologic outline of the islands (Tayama, 1935).

Recently geologic evolution of the arc-trench systems in the world has been made clear by the plate tectonic framework. However, the Yap islands, which are mostly composed of high grade metamorphic rocks such as greenschists and amphibolites, are still enigma for many earth scientists as for the mechanism forming them (Hawkins and Batiza,1977; Shiraki, 1971; Shiraki and Maruyama, 1978).

Last year, we had the first expedition to the Yap and Palau arc-trench systems and obtained geological and geophysical data both on lands and sea areas to solve the problems concerning the origin and tectonic evolution of the Yap arc-trench systems. Leg 3 of the present cruise was the second expedition to further extend the previous efforts at the same region. The major problems on the Yap Islands are as follows;

1. Why is there no Quaternary volcanism in the arc, although the islands are accompanied by a deep trench?
2. Why does the high-grade metamorphic rocks such as greenschists and amphibolites crop out on the Yap islands?
3. How and why are such kinds of rocks emplaced on the Yap islands?

To solve these questions stated above, we intended to survey the whole area on the Yap islands as well as the adjacent seas in the southern parts of the Philippine Sea. In this cruise, we had the topographic survey by a deep-sea wide-beam echo sounder and 3.5 KHz subbottom profiler. We collected rocksand sediment samples by dredge hauls, piston corings and grab sampler as well as took photographs by deep sea camera. Fig. 20-1 shows

ship's tracks and the sites for the sampling and measurement. The station works done during Leg 3 of the KH 87-3 are listed in a table of Chapter 3.

We will present here the geophysical and geological data concerning the Yap area obtained during Leg 3 of the Hakuho-maru cruise of KH 87-3. Although our idea for the origin and tectonic evolution of the Yap arc trench system is still immature, we will propose a short discussion on the origin of the arc-trench system (this section was written by K. Fujioka).

[2]. Previous works

Historical review of the previous works on the geological study of the Yap Islands will be briefly summarized here. Before the 20th century, geology of the Yap Islands was poorly known except that Graffe (1873) reported geographic and geologic outline of the Islands. Until 1935 when Tayama (1935) published the topographic and geological description of the whole islands, several mineralogical and petrological works on greenstones exposed on the Islands were carried out mainly by German and Japanese scientists (Velkens, 1901; Kaiser, 1902:1903, Iwasaki, 1915; Ohtsuki, 1915; Mizusawa, 1915; Koert and Finch, 1920; Tsuboya, 1932).

Tayama (1935) stayed in the Yap Islands for more than 20 days and made geologic survey on the whole islands. He divided the rocks distributing on land into seven geologic units; Yap formation, Map formation, Tomil agglomerate, Garim limestone, Terrace deposits, Beach deposits and Recent coral reef in the ascending order. This article introduced, for the first time, various kinds of rocks which crop out on the Yap Islands with geologic succession. He emphasized the geomorphological change of the Yap Islands and their adjacent areas. Shiraki (1971) described metamorphosed mafic igneous rocks of the Yap Islands with special emphasis to the major element chemistry of these rocks. Some of the greenstones have chemical composition similar to those composing the Mid-Atlantic Ridge; abyssal tholeiite (MORB). Ito et al. (1972) and Aoki et al.(1976) petrographically described the granitic rocks which are included in the Map formation of Tayama (1935) and demonstrated that these granites were the products resulting from the oceanization. Later, Fujita (1975) proposed the "Bonin Orogenesis and Yap disturbance"based on existence of these granitic rocks in the oceanic area.

On the other hand, Hawkins and Batiza (1977) proposed the obduction model for emplacement of the ophiolitic rock assemblage of the Yap Islands using the terms of the plate tectonics as Dewey (1976) explained the origin of ophiolites by obduction process. Hamilton (1979) summarized morphologic and tectonic characteristics of various island arcs distributing around the Indonesian region. He briefly showed the diagnostic features of the metamorphic rocks of the Yap Islands. Shiraki and Maruyama (1978) examined the

low grade metamorphic rocks of the Yap Islands and draw the isotherm of the metamorphic conditions by using the peristerite solvus of plagioclase. They concluded that type of metamorphism of these rocks is low pressure intermediate group like the Abukuma metamorphic belt, Japan (Miyashiro, 1961) and showed that the metamorphic grade is higher northeastward from greenschist to amphibolite facies. In 1971, Russian Research Vessel Vityaz attempted to survey the Marianas, Yap, Palau and Philippine area in order to understand the ophiolitic rocks distributing onshore islands as well as offshore area (Bagdanov, 1977).

An AGU meeting concerning the origin of the marginal seas such as the south China Sea, Philippine Sea and Banda Sea was held with hot discussions on theorigin of the marginal seas. A lot of papers dealing withthe southern margins of the Philippine Sea as the plate boundaries have been published (e.g.,Cardwell et al., 1980). Configuration of the plate boundaries in this area is so complicated that many debates about the southern margin of the Philippine Sea plate are still underway. In 1986, a marine research cruise was held around the Yap, Palau and Philippine Islands in order to gather the fundamental data for geophysical and geological nature of these islands and their adjacent areas (Fujioka et al., 1986). During the cruise, it has been clear that the metamorphic rocks crop out further northeast of the Yap Islands. Marbles which do not exist onshore Yap Islands were discovered from the forearc region of the Islands. Piston core was taken from the junction area between Mariana and Yap Trenches. Sediments existing several centimeters below the ocean bottom represents strong dehydration and deformation structure (Fujioka et al., 1986; Koga et al.,in press). It was the first discovery of highly deformed sediments from anomalously shallow part in the landward slope of the trench in the world.

Ages of some rocks exposed both in onshore and offshore areas of the Yap Islands have been reported (Tsunakawa, 1985). Beccaluva et al.(1980) compiled K-Ar ages of volcanic rocks dredged from the Philippine Sea area. They obtained K-Ar ages around 7 Ma and 11 Ma but Tsunakawa (1985) pointed out that these radiometric ages are possibly the ages of Caroline Ridge. Fujioka and Takigami (in prep.) are now continuing analysis of the metamorphic ages of the greenstones and amphibolite on the Yap Islands. Tayama (1935) reported several fossils from the limestone beds as well as the sandstone belonging to the Map formation. During the field survey onshore Yap Islands, we discovered calcareous nannofossils from the Yap formation intercalated in the debris flow deposits consisting chiefly of amphibolites (Fujioka et al., 1986), although their paleontological zonation has not been done. Based upon these available data in the Yap Islands, Fujioka et al.(in press) proposed a new model for the tectonic history of the southern tip of the Philippine-Sea plate (written by K. Fujioka).

20-2. TOPOGRAPHY

[1]. General remarks

(a). Morphology in and around the Yap arc-trench system

The Yap Island arc-trench system fringes a southern and eastern margin of the southwestern tip of the Parece Vela basin between the West Mariana and Kyushu-Palau Ridges in the Philippine Sea Plate. The Yap arc-trench system has no clear Quaternary volcanic front but has a deep trench, whose arcuate configuration connects the Marianas with the Palau arc-trench systems. Fig. 20-1 shows the ship's tracks during Leg 3 around the Yap region.

Topographic cross-sections of the Yap arc-trench system are shown in Fig. 20-2. Along the arc, six geomorphologic domains or segments are identified in terms of its structural trend and configuration of the inner trench slope as well as in relation to the Mariana and Palau arc systems, based on the trench topographic map of the western Pacific region (Fujioka et al.,1986). They are, from north to south, a junction between Mariana and Yap(JM), northern(N), north-central(NC), south-central(SC), southwest(SW) domains and a junction between Palau and Yap (JP), as shown in Fig. 20-3. The arc system is about 710 km long, trending N30°E in the northern two third portion (N, NC, SC) and E-W in the rest, southwestern domain. Trench topography is quite comprehensive and its maximum depths are approximately 8500 m, which are located in the south-central and northern domains.

The northwestern tip of Caroline Ridge is morphologically terminated by the Yap trench, where the ridge collides with the Mariana arc to choke the southern Mariana Trench. Width of the Cretaceous Caroline Ridge is equivalent to the northern two third length of Yap Trench. Morphology of the Yap ridge and trench seems to be affected by structural relieves of the Caroline Ridge, especially by the Sorol Trough. Namely, the highest portion of Yap Ridge,i.e. the north-central domain, is located just in front of the Sorol Trough across the trench. Caroline Ridge must have played a great role to commence the Miocene and later backarc spreading along the Yap arc, i.e. formation of the Parece Vela Basin and Mariana Trough.

(b). Trench morphology

Parallelism between Yap trench and Yap Ridge continues through the whole area along the arc. Topographic cross-sections Yap-1, -2, -3, M1, M2 + M3 and M5 shown in Fig. 20-2 together with seismic profiler records described in the previous reports (Tokuyama et al.,1985; Fujioka et al.,1986) provide evidences on the common morphologic features of the Yap arc.

In the seaward side of the arc-trench system a conspiceous topographic high called 'outer swell' with a group of horsts and grabens which resulted

from normal faulting is clearly seen. Trench axis has a diagnostic V shape structure which seems to be lack of sediments in some parts and covered with thick trench-fill sediments in the others. Along the landward slope of the Yap Trench, three conspicuous topographic features are seen and can be classified into the Upper, Middle and Lower slopes. Each portion is connected with thrust faults gently dipping landward which form structural notches near the underlying faults. Water depths of the notches between the Upper and Middle slopes are 5.3 sec on Line Yap-1, 4.3 sec on Yap-2, 5.3 sec on Yap-3 and 5.2 sec on M-5, respectively. Those between Middle and Lower are 8.3 sec on Yap-1, 8.3 sec on Yap-2, 8.0 sec on Yap-3 and 7.9 sec on M-5, respectively. These water depths of notches are quite uniform, suggesting that the three morphologic units are distributed all over the areas and each unit consists of the same materials.

(c). Trench Termination

Both the northern and southern tips of Yap Trench are not directly conjuncted with the neighboring trenchs but are suddenly terminated. The Yap Ridge(Yap arc and its northern continuation) and the West Mariana Ridge are joined together in the northern junction. The WNW-ESE linear depression connecting the Yap trench with the deepest Mariana trench is expected to be atransform fault, or a zone of highly oblique subduction. However, the northernmost Yap Trench and the southwestern extention of the West Mariana Ridge are terminated in the tectonic zone constituting a remnant portion of the backarc spreading of the Parece Vela Basin.

According to the Scrips Chart No. 2303N, it is possible to recognize that the 6,000 m deep linear depression is derived from the northern tip of the Yap Trench and runs north-northeastward along the Yap Ridge, being traced in the Parece Vela basin with the same trend as the elongation of Yap Ridge (see domain JM in Fig. 20-3). Looking at the JODC Chart No. 143, however, an E-W trending barrier appears to connect the West Mariana and the Yap Ridges. The problem whether or not such a barrier does exist, may remain unsolved until precise Seabeam bathymetric maps become available in the study area, in the near future.

On the basis of Seabeam bathymetry, it can be said that the northern tip of Palau Trench is terminated by a transform fault (Kato et al., 1986). In a manner similar to the case of the westernmost portion of the Mariana Trench, the southern tip of Yap Trench does not seem to be connected directly to the Palau Trench, but jumps to it (see domains SW and JP in Fig. 20-3). Although no linear structure as the one in the Mariana-Yap junction area is morphologically recognized, either transform fault or collion zone is expected between the West Caroline Basin and the southern continuation of Yap arc sliver to bound the northwestern margin of Caroline

plate. Based on the regional topograpgic maps, a NE to NNE trending ridge (thick broken line in Fig. 20-3) is terminated by a tectonic zone striking a NW-SE direction from the western end of Yap Trench to the northern tip of Palau arc, along the domain boundary between JP and SW in Fig. 20-3. Across the northeastern portion of the ridge, single-channel seismic profile Line S-9 (KH86-1, 1986) shows a symmetrical spreading-center topography in the southernmost Parece Vela Basin, suggesting that the backarc region of the Yap arc system once spread to form the southernmost Parece Vela basin.

These geomorphologic features constrain the idea for origin of the Yap island arc system and the southernmost Parece Vela basin and their evolution as follows;

(1) Spreading of the Parece Vela basin is suppressed or aborted by the existence (or collision) of Caroline Ridge during the end of Oligocene when a high grade metamorphism occurred which was followed by uplifting to form the upper Map formation in Yap Islands characterized by melange-like facies of meta-volcaniclastics and their clastic sediments due to some synsedimentary tectonic disturbances.

(2) Topographically, the Yap ridge is clearly a forearc in the Yap arc-trench system which existed at least during the period when the Parece Vela Basin opened as the Mariana arc was moving eastward. The northern continuation of Yap Ridge seems to join the central axis of the Parece VelaBasin possibly by ridge-trench transform.

(3) The northern part of Yap-Palau trench junction area (JP in Fig. 20-3) does not belong to the West Caroline Basin but to the Yap arc system. It seems likely that a backarc basin of the Yap system behaved as a part of the Caroline plate to be subducted into the Palau Trench, as a result of oceanic collision or aborted subduction (written by A. Takeuchi and K. Fujioka).

[2]. 12 kHz wide-beam echo sounder (PDR)

Water depths around Yap and Mariana trenches were measured by a 12 kHz echo sounder (PDR). These profiles are taken between survey sites (dredge hauls, deep sea camera, piston coring, heat flow) and divided into eleven lines as shown in Fig. 20-1. Lines PDR2 (Fig. 20-4(b)) and PDR5 (Fig. 20-4(e))roughly correspond to the multichannel seismic profiler lines, Line M5 and Line M3 obtained by the KH 86-1 cruise. On the JODC topographic map, there are three remarkable morphological domains along the ship's tracks.

(a). Yap arc-trench system

Line PDR1 to Line PDR4 (Figs. 20-4 (a)to (d)) and Line PDR7(Fig. 20-(g)) show the characteristic morphology. North-central and northern domains which are defined by the former survey of KH 86-1 cruise correspond to the PDR1-PDR4 and the PDR7 lines, respectively.

North-central part

The morphology of the forearc region of the Yap arc-trench system has a steep slope with several inflection points. On the Line PDR3, there are four major inflection points whose depths are 2,100, 2,800, 4,200, 6,000 m and the depth of the trench axis is 8,800 m. These four inflection points are obtained by the survey of the previous cruises (KH 84-1, KH 86-1). By comparing these profiles, it is obvious that the depth of inflection point is in proportional to the depth of trench axis itself (Fig. 20-2). Morphology of the inflection shows steps or notches where horizontally deposited sediment is often observed (Line PDR3, 6,050 m).

North part

There are rather flat topographies at water depths of 2,000, 3,000 and 4,000 m on the Line PDR6 (Fig. 20-4(f)) and these profiles are consistent to the bathmetric map (JODC). The topography from Yap to Caroline Ridges (Line PDR7) shows one step at a water depth of 4,400 m and these profiles show the landward dipping reflectors which are interpreted to be faults.

(b). Back-arc

The back-arc area shows considerably rough topography in spite of its small depth change. Many steps are found on slopes and interpreted to be faulted notches which are filled by trapped sediment. A broad basin is found at 4,400 m depth. Line PDR5(Fig. 20-(e)) is similar to the profile of subparallel line M5 (KH 86-1). In this profile depths of depressions become shallower eastward. Amplitude of roughness is smaller eastward.

(c). Mariana trench

Morphology of the landward dipping slope at Mariana trench is rougher than the seaward slope at Yap trench. Line PDR8 shows two steps and slope inclination of which is more gentle westward. Line PDR9 (Fig. 20-(i)) shows an interesting depression at 5,400 m depth and their morphology looks like levee and channel. The western flank of Caroline Ridge is more rough topography in comparison with its eastern flank (Line PDR10, Fig. 20-(j)).

At the seaward slope inclination of the slope below 5,900m is not smooth, but more gentle than at shallower depths. As compared with seaward slope the profile of landward slope is very steep and rough. PDR11 to PDR13 (Figs. 20-4,(k) to (m)) show topography along the ship's tracks going back to Tokyo (written by J. Ashi and K. Fujioka).

[3]. 3.5 kHz Subbottom Profiling Survey

3.5 kHz subbottom profiling survey was carried out during Legs 1, 2 and 3 of KH-87-3 cruise. In Leg 3 around the Yap arc-trench system, 3.5 kHz subbottom profiles were observed to reveal distribution, thickness and

processes of sediments for the following two purposes. One is the precise survey for operations of piston corings, heat flow measurements and deep-sea cameras, and the other is for understanding of the geological processes which took place in this area.

The subbottom profiling survey system is composed of 3.5 kHz transducers, PTR 105B transceiver, CESP II correlation echo sounder processor and UGR recorder of the Raytheon Co.. Ship's speeds on the survey lines were about 10-12 knots, partially being reduced to 5 knots. The vertical exaggeration is about 50 times at the ship's speed of 10 knots. The subbottom profiles continuously obtained in Leg 3 were not so good because of rough sea conditions and steepness of topography. Some profiles (ie., D-7, 8 and 9, C-3 and 4, HF-3, P-3 areas) were recorded relatively clearly.

D-7, 8 and 9, C-3 and 4 line: nearly on the multichannel seismic line M5 of KH86-1 cruise from east to west (Fig. 20-5(a)). Three dredge sites are so steep cliffs as fault scarps. Step-like topography is recognized which may be covered by some sediments. Echoes are very dispersed and not penetrated into deeper part of the sediments.

D-10 and 11 line: no profiles obtained due to mechanical troubles.

HF-3, P-3 line: nearly on the line M3 of KH86-1 cruise from west to east (Fig. 20-5(b)). This area is divided into two layers based on the acoustic features. The upper one is transparent layer that has 0.02 sec (two-way travel time) thickness from the sea bottom, and the lower is opaque layer more than 0.04 sec thick from the bottom of transparent layer. These layers have continuous and intense reflectors.

P-4, HF-4 line: continuing to the HF-3 + P-3 line and on the line M3 of KH-86-1 cruise (Fig. 20-5(c)). The record is not sufficiently good for precise interpretation.

C-5 line: showing very irregular topography with dispersed reflections. We can not interpret the subbottom features.

P-5 line and HF-5 line: topography of cliff is very steep and many hyperbolic echoes are visible. Because of them, we can not interpret the subbottom features. According to the deep sea photograph, bared metamorphic rocks are cropping out in this region (Fig. 20-5(d)).

HF-6, lines: Thin opaque layer is only visible that has roughly flat topography (Fig. 20-5(e)). (written by S. Kuramoto and K. Fujioka).

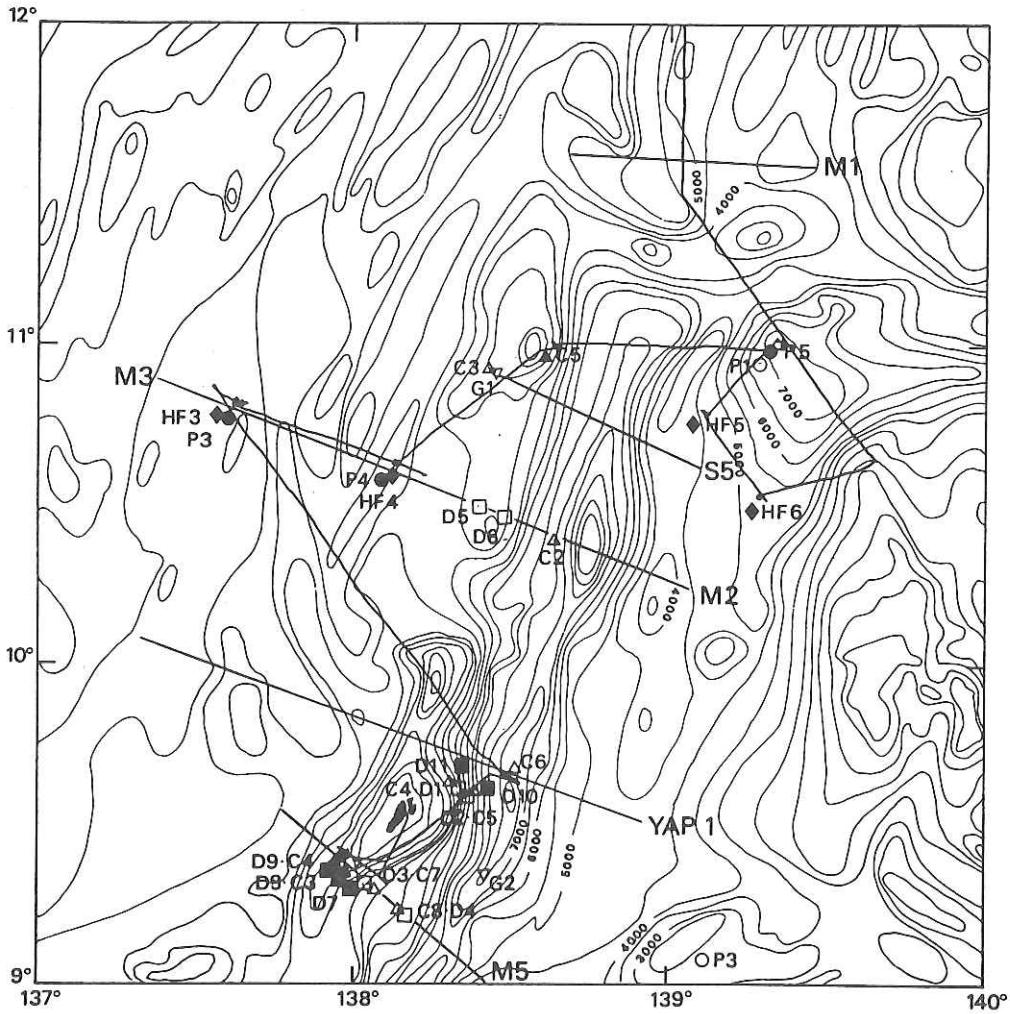

Fig. 20-1 Ship's tracks and sampling stations in Leg 3 of cruises KH 87-3 and KH 86-1 around the Yap Islands. :Piston Coring, :Dredge Haul, :Camera, :Grab Sampler, :Heat Flow
(Solid marks: KH 87-3, Hollow marks: KH 86-1)
Symbols beside stations are explained in the text.

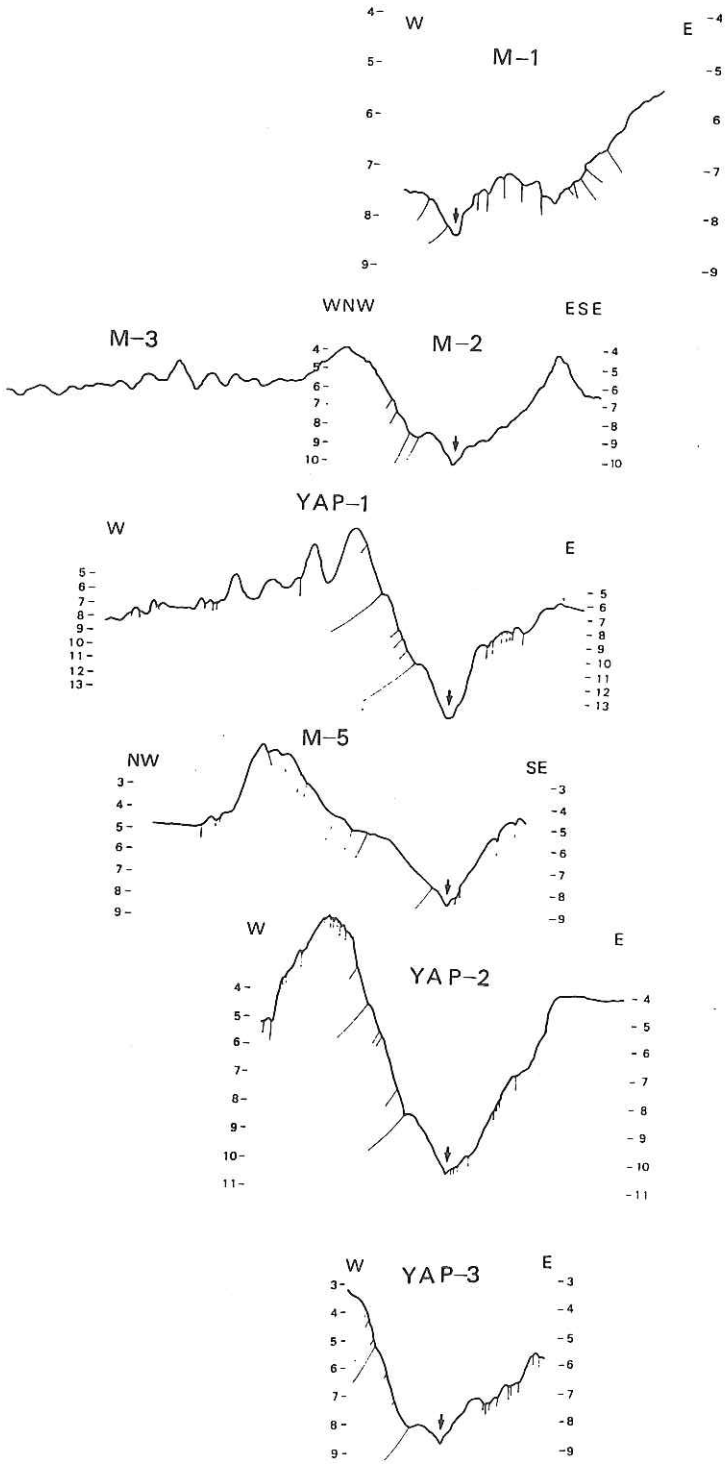

Fig. 20-2 Topographic cross-sections of the Yap arc-trench system nearly perpendicular to the trench. Positions are indicated in Fig. 20-1.

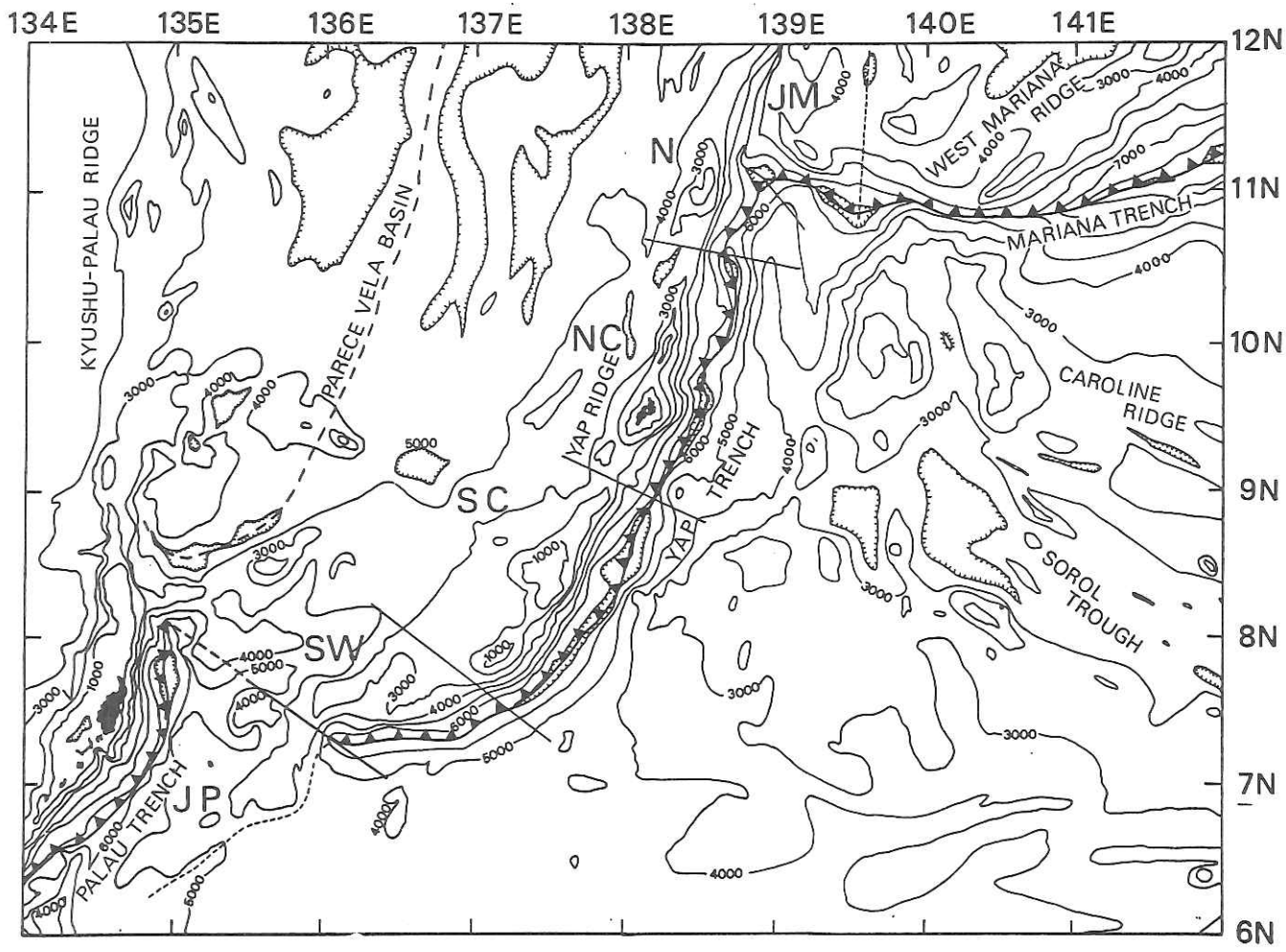

Fig. 20-3 Morphological divisions of the Mariana, Yap and Palau arc-trench systems.

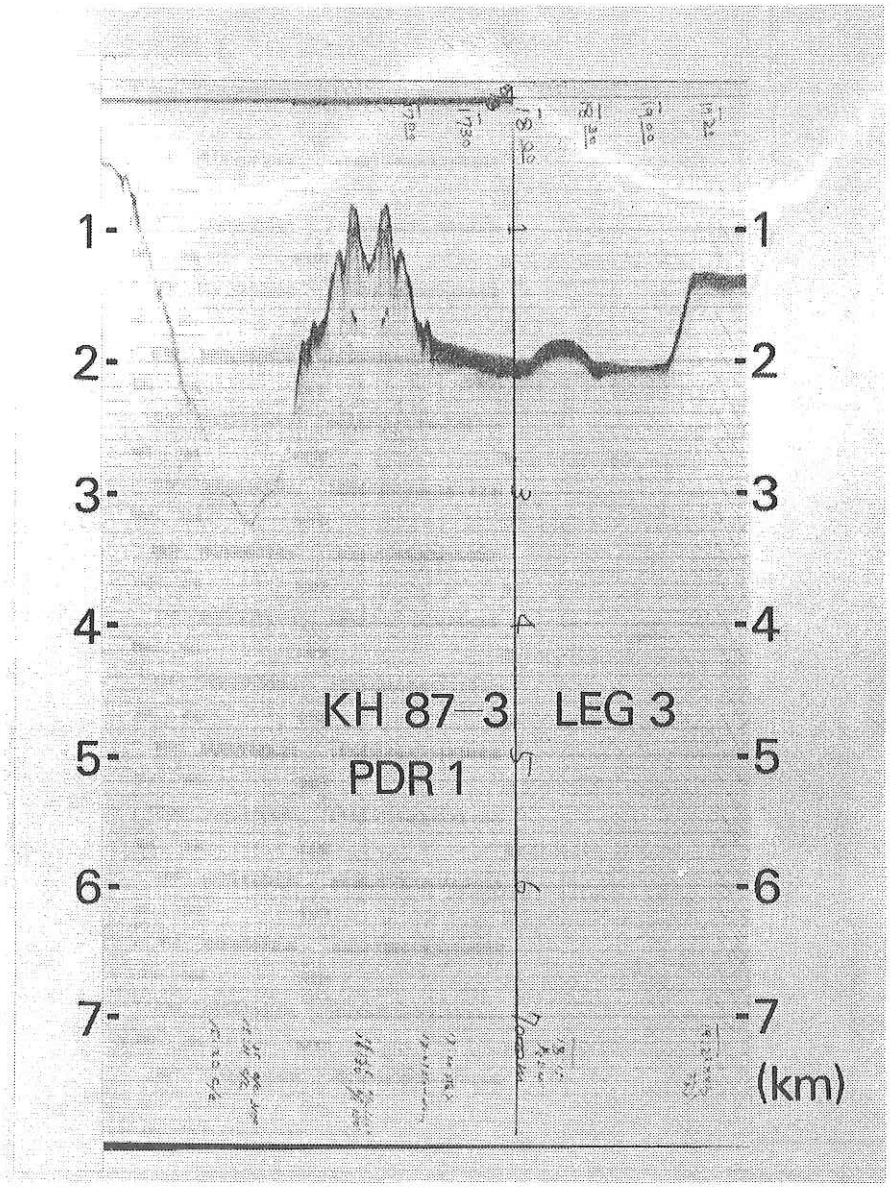

Fig. 20-4(a) Topographic cross-section revealed by echo sounder; line PDR-1

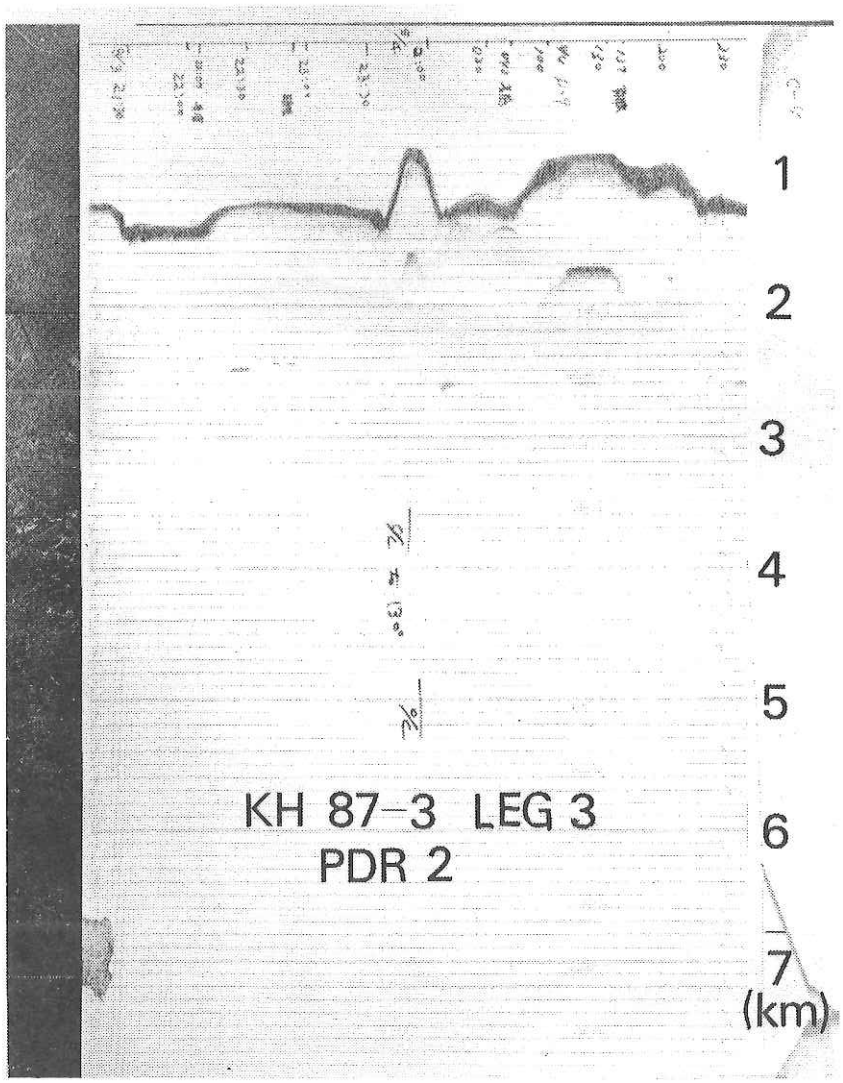

Fig. 20-4(b) Topographic cross-section revealed by echo sounder; line PDR-2

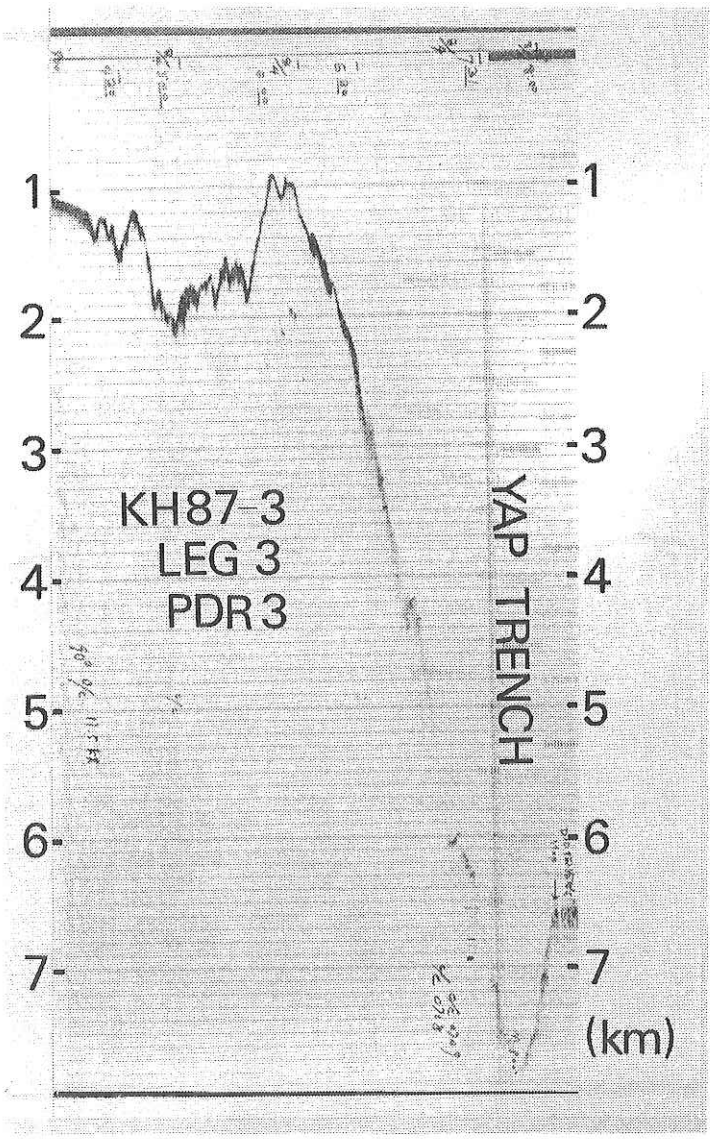

Fig. 20-4(c) Topographic cross-section revealed by echo sounder; line PDR-3

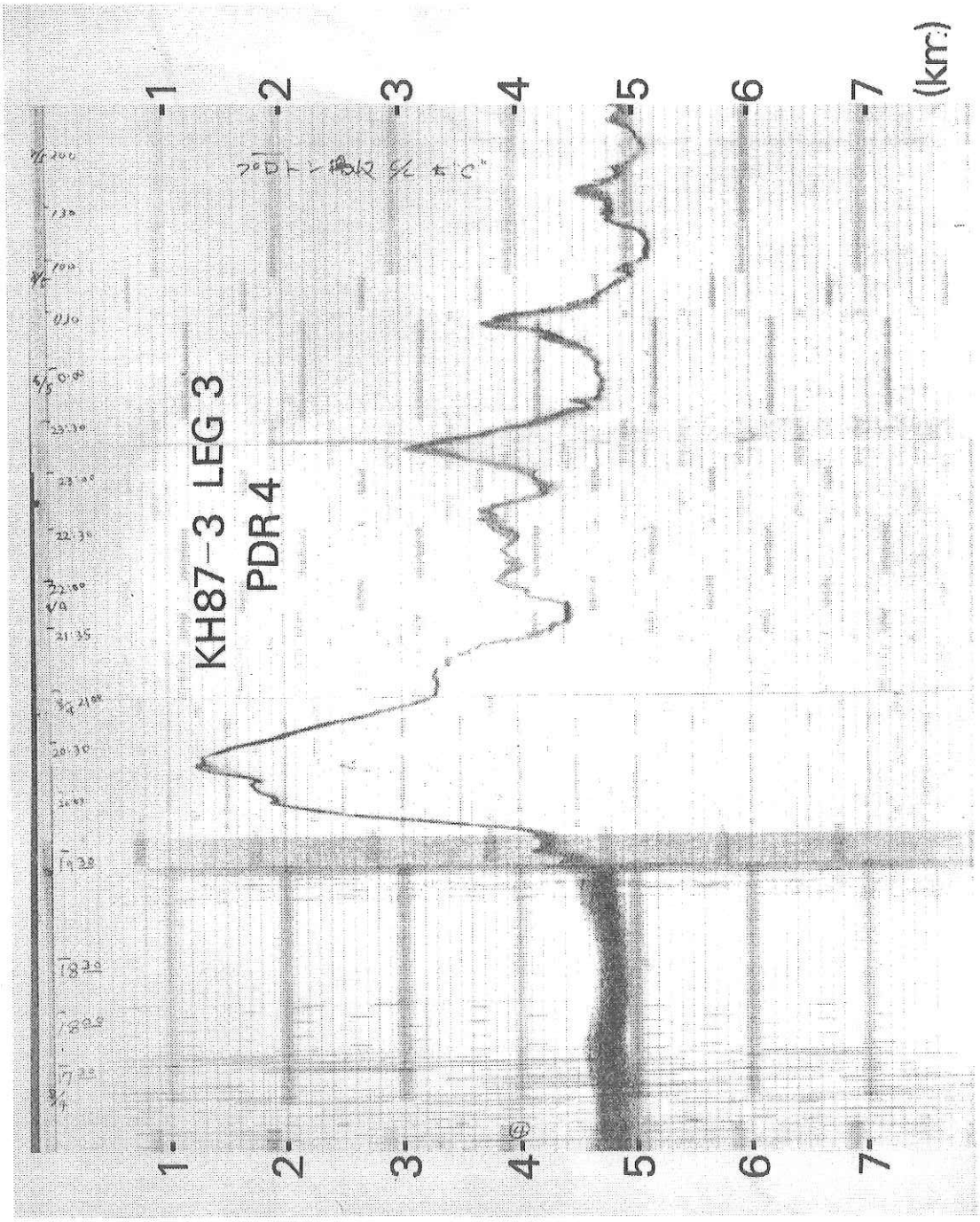

Fig. 20-4(d) Topographic cross-section revealed by echo sounder; line PDR-4

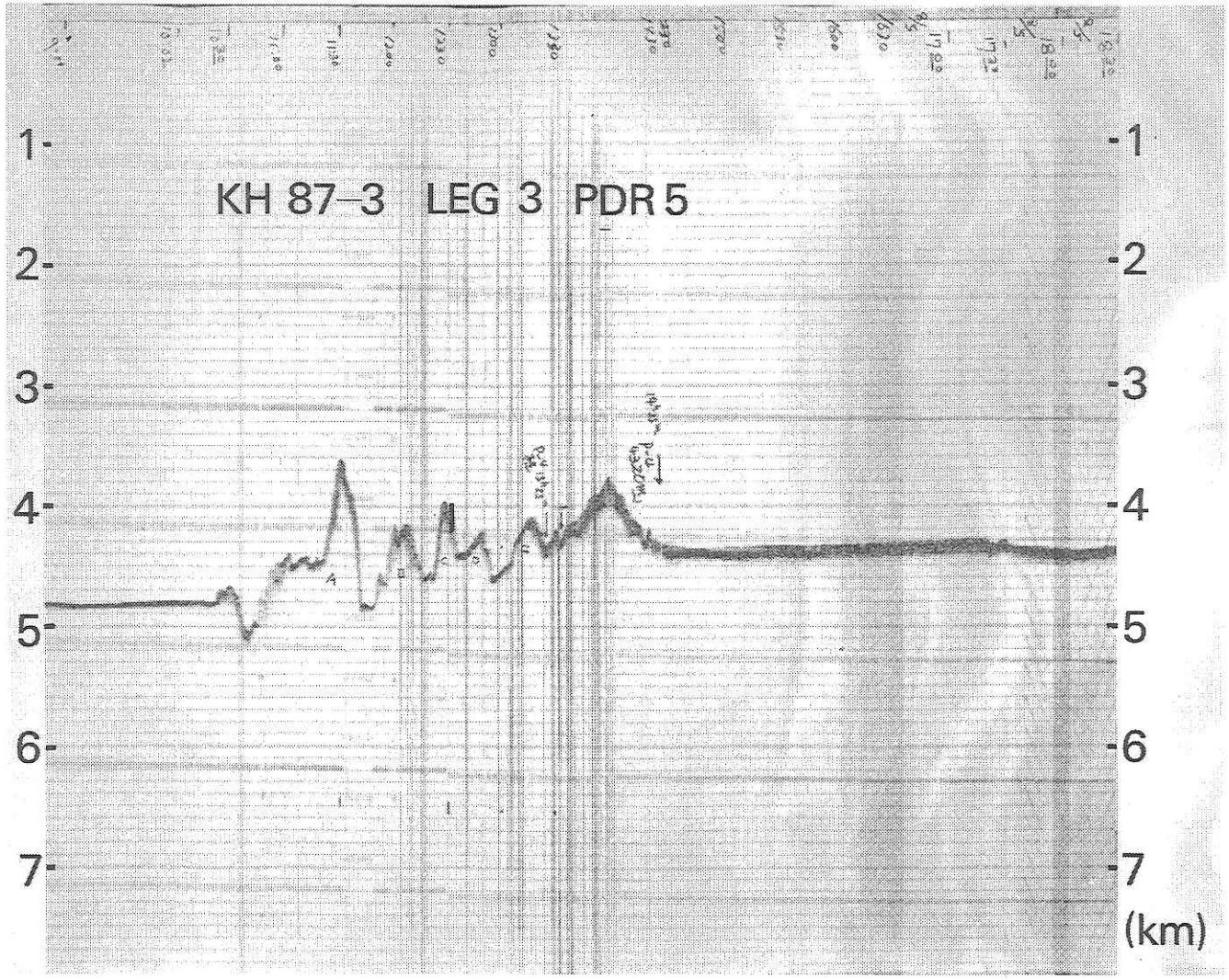

Fig. 20-4(e) Topographic cross-section revealed by echo sounder; line PDR-5

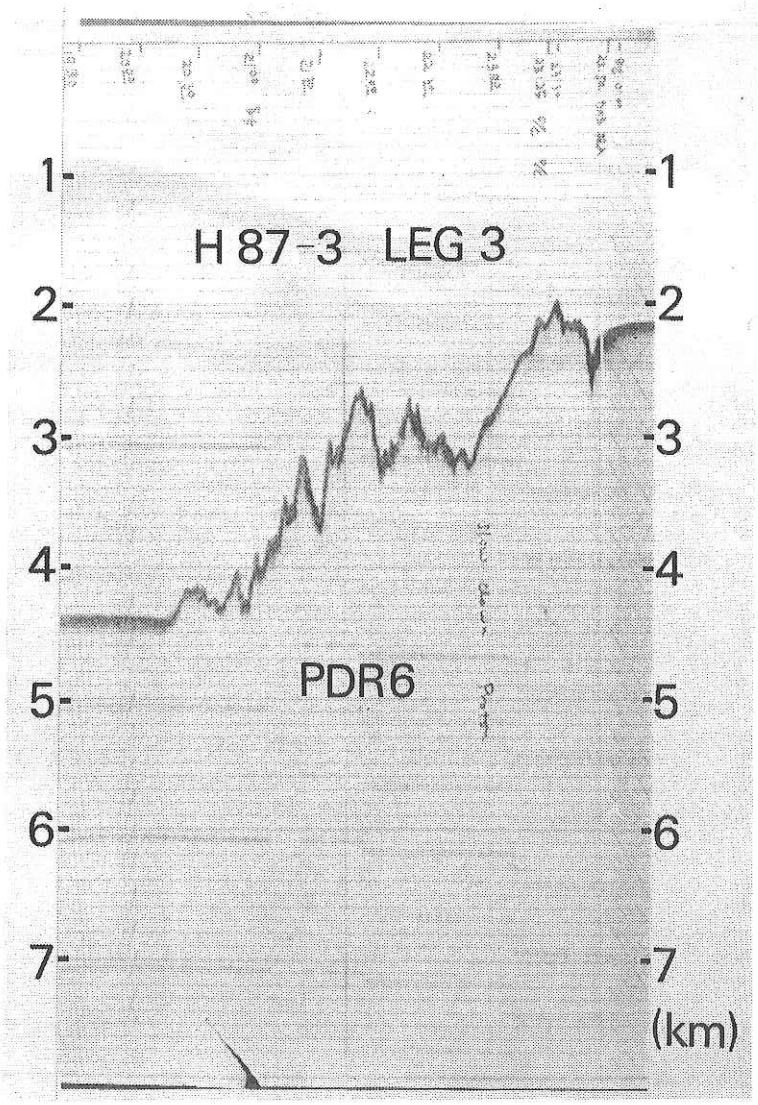

Fig. 20-4(f) Topographic cross-section revealed by echo sounder; line PDR-6

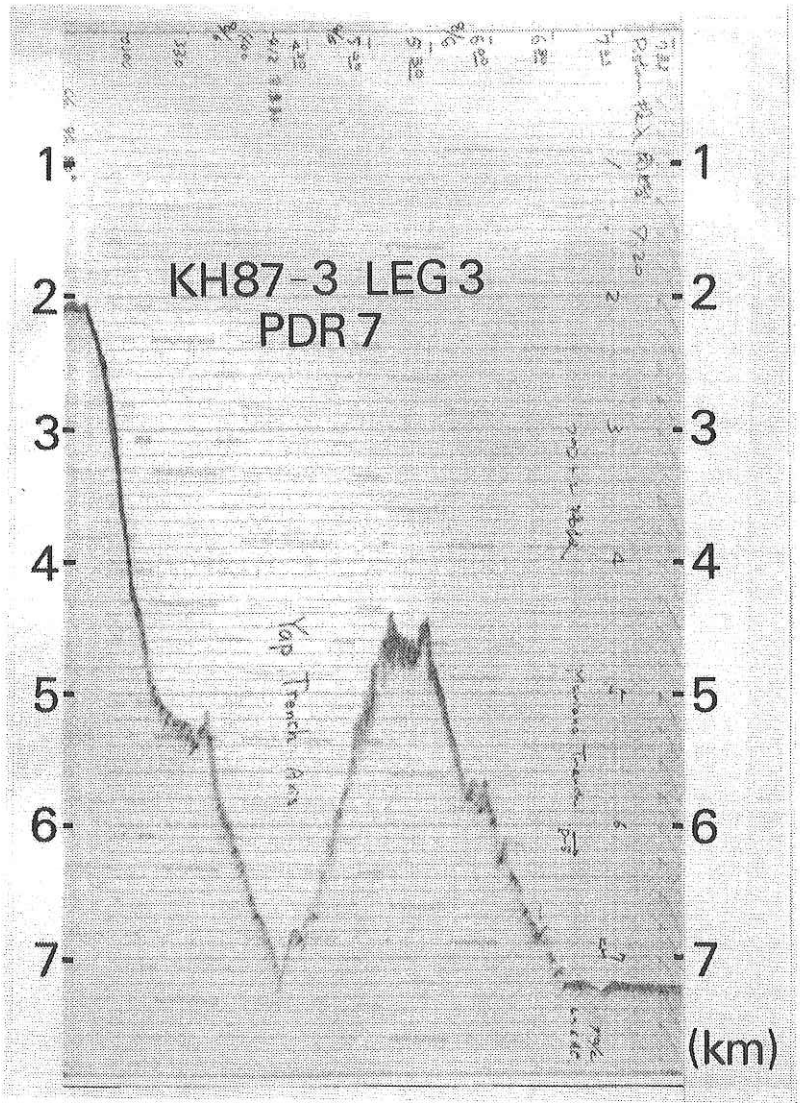

Fig. 20-4(g) Topographic cross-section revealed by echo sounder; line PDR-7

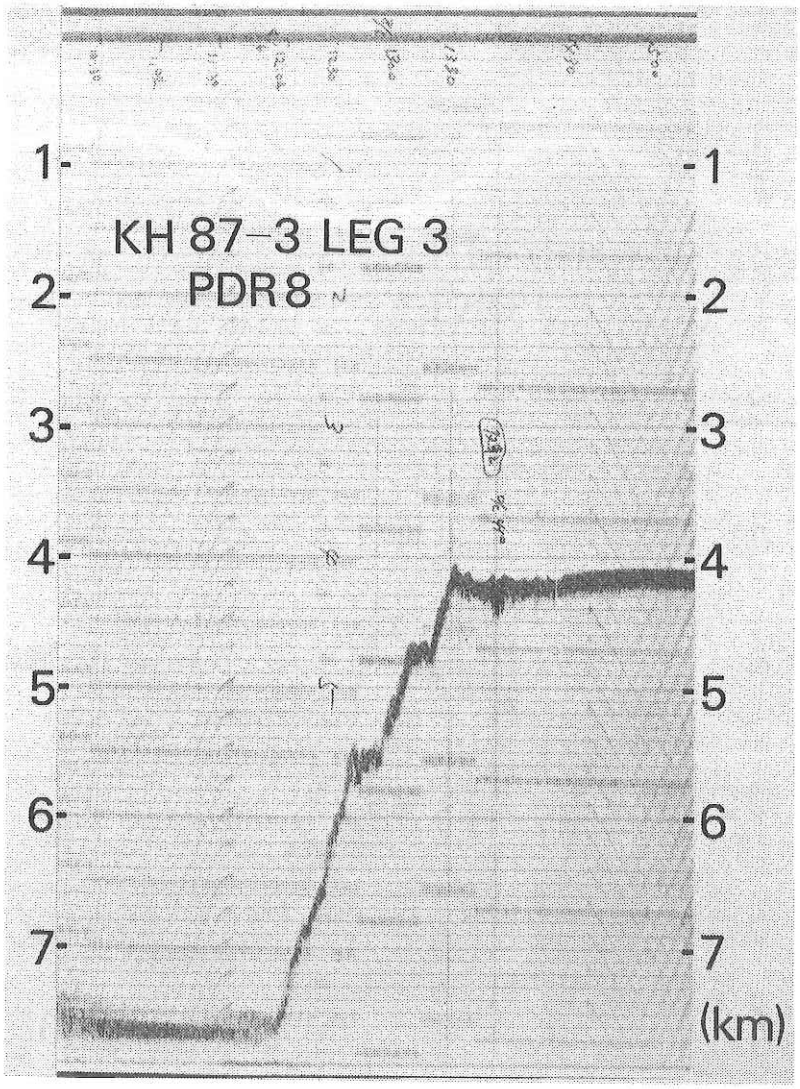

Fig. 20-4(h) Topographic cross-section revealed by echo sounder; line PDR-8

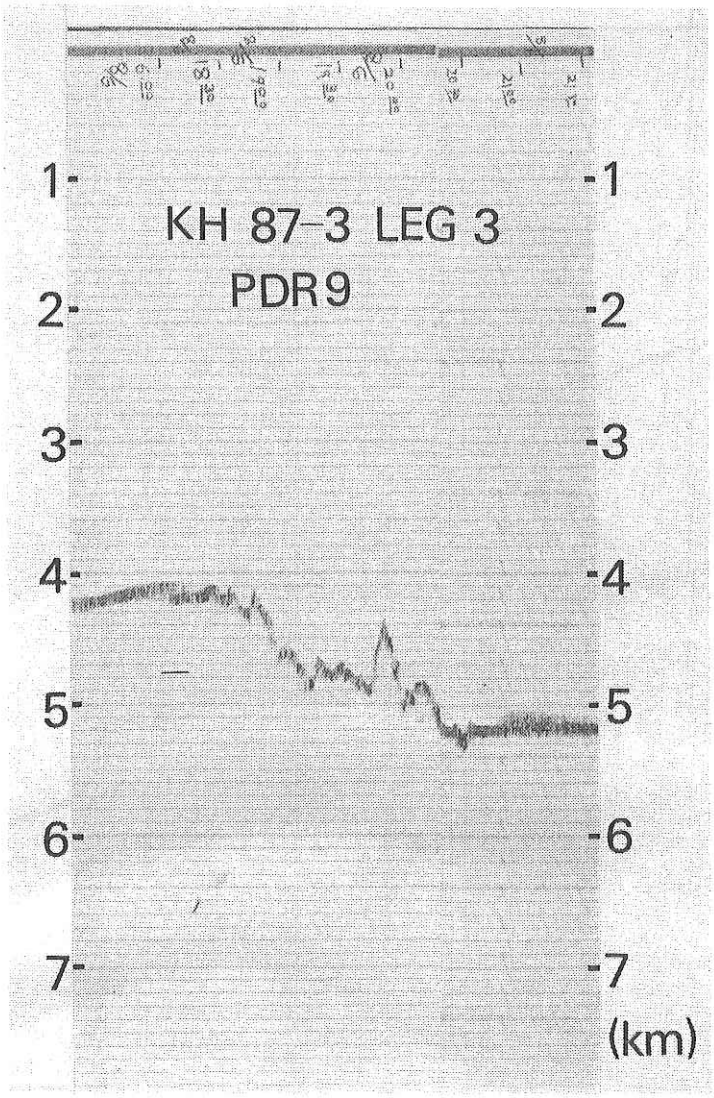

Fig. 20-4(i) Topographic cross-section revealed by echo sounder; line PDR-9

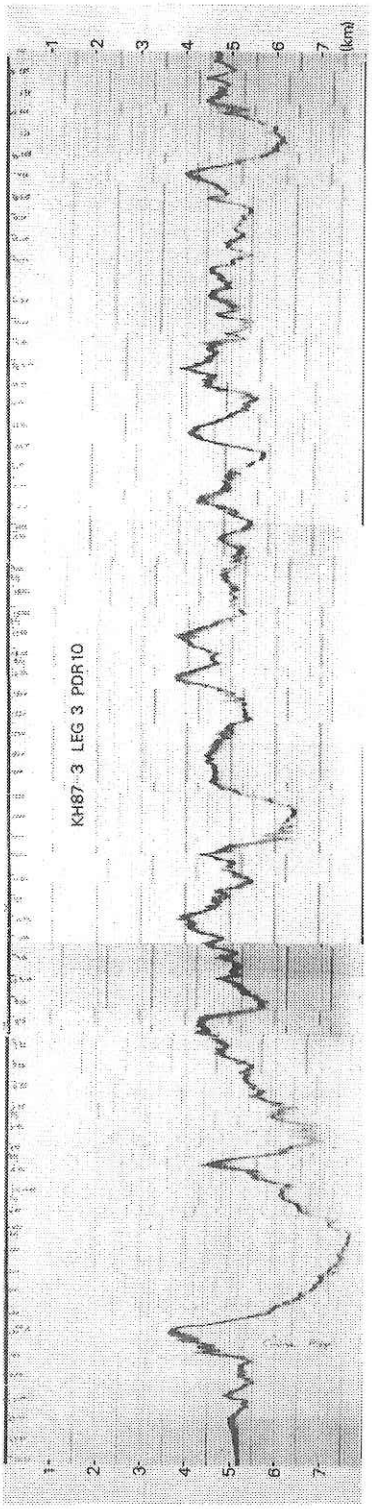

Fig. 20-4(j) Topographic cross-section revealed by echo sounder;line PDR-10

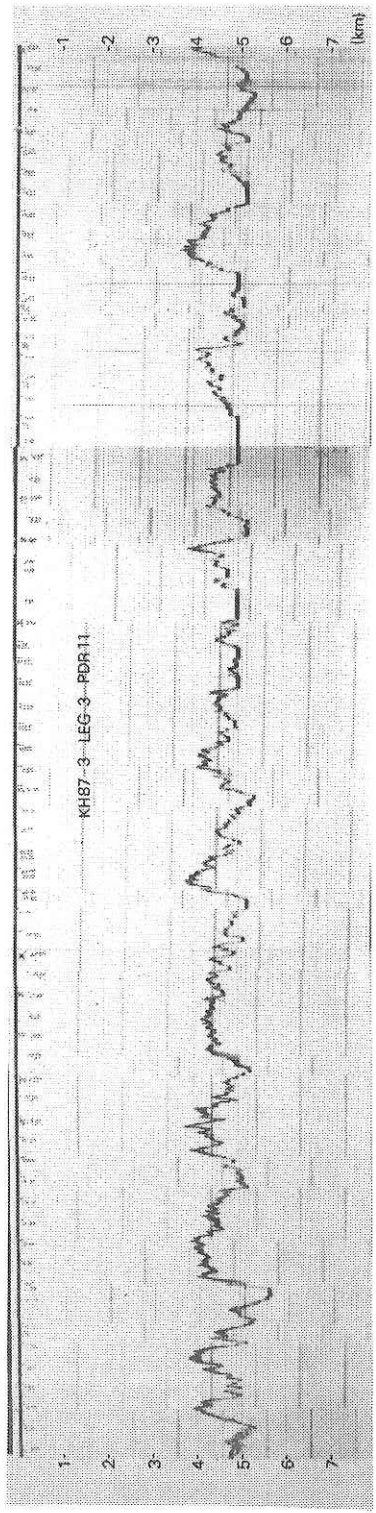

Fig. 20-4(k) Topographic cross-section revealed by echo sounder;line PDR-11

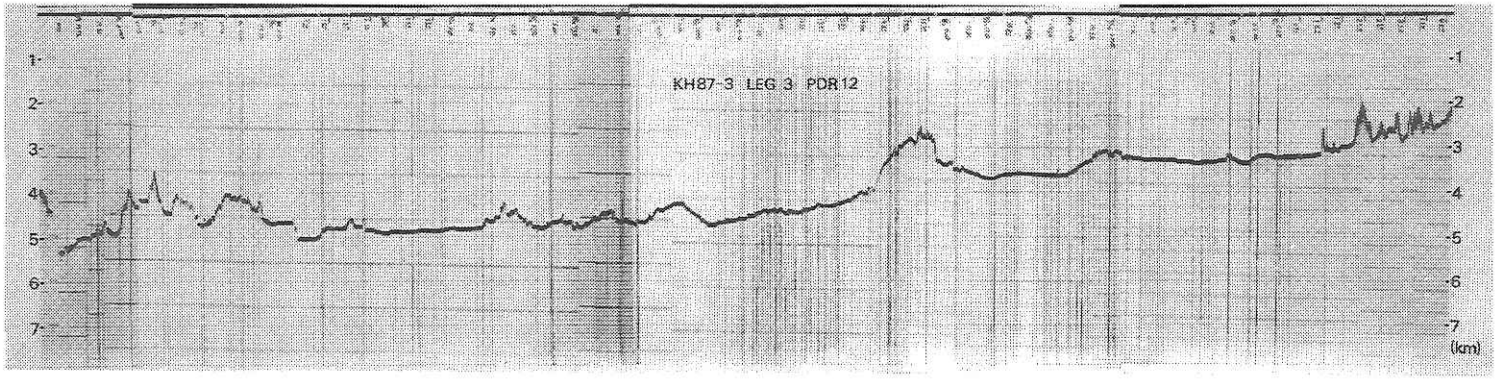

Fig. 20-4(1) Topographic cross-section revealed by echo sounder;line PDR-12

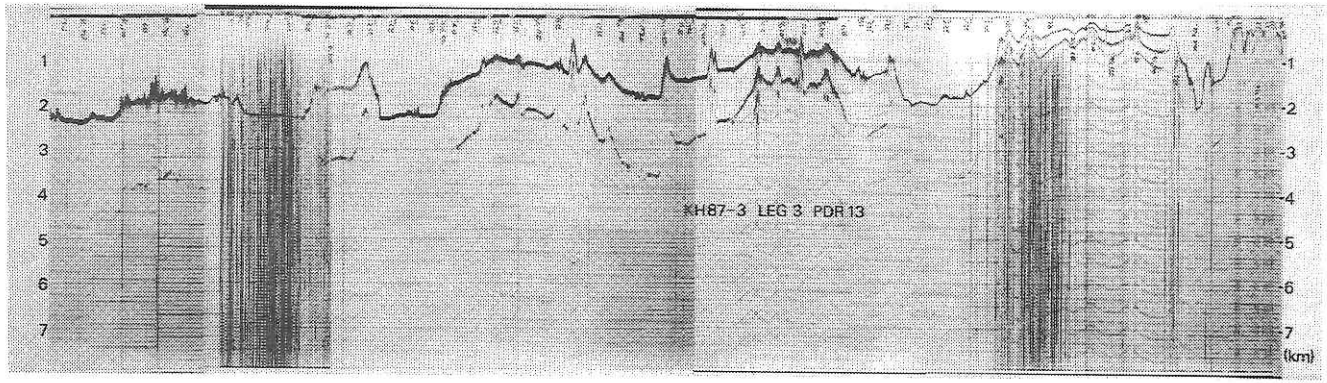

Fig. 20-4(m) Topographic cross-section revealed by echo sounder;line PDR-13

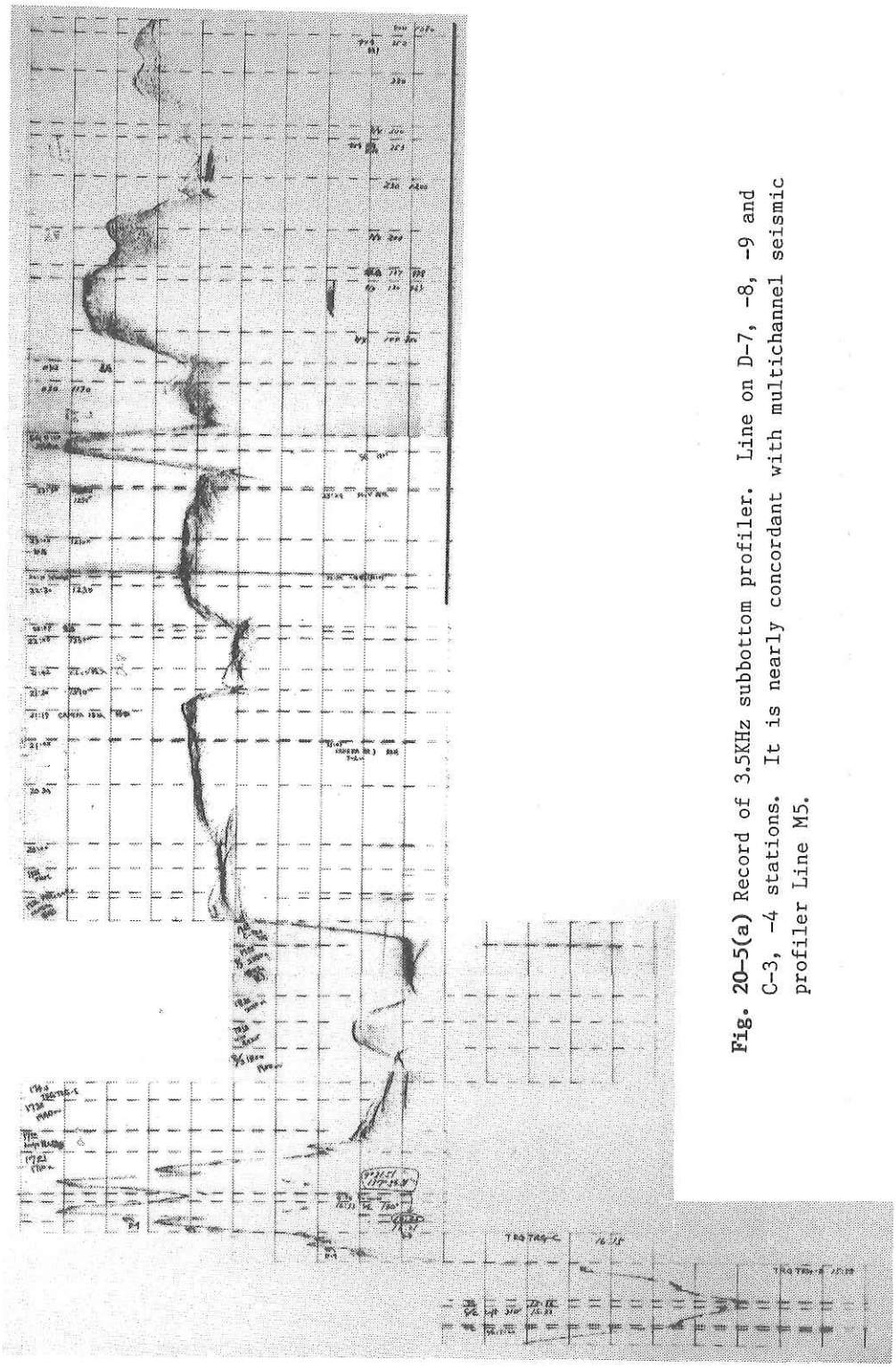

Fig. 20-5(a) Record of 3.5KHz subbottom profiler. Line on D-7, -8, -9 and C-3, -4 stations. It is nearly concordant with multichannel seismic profiler Line M5.

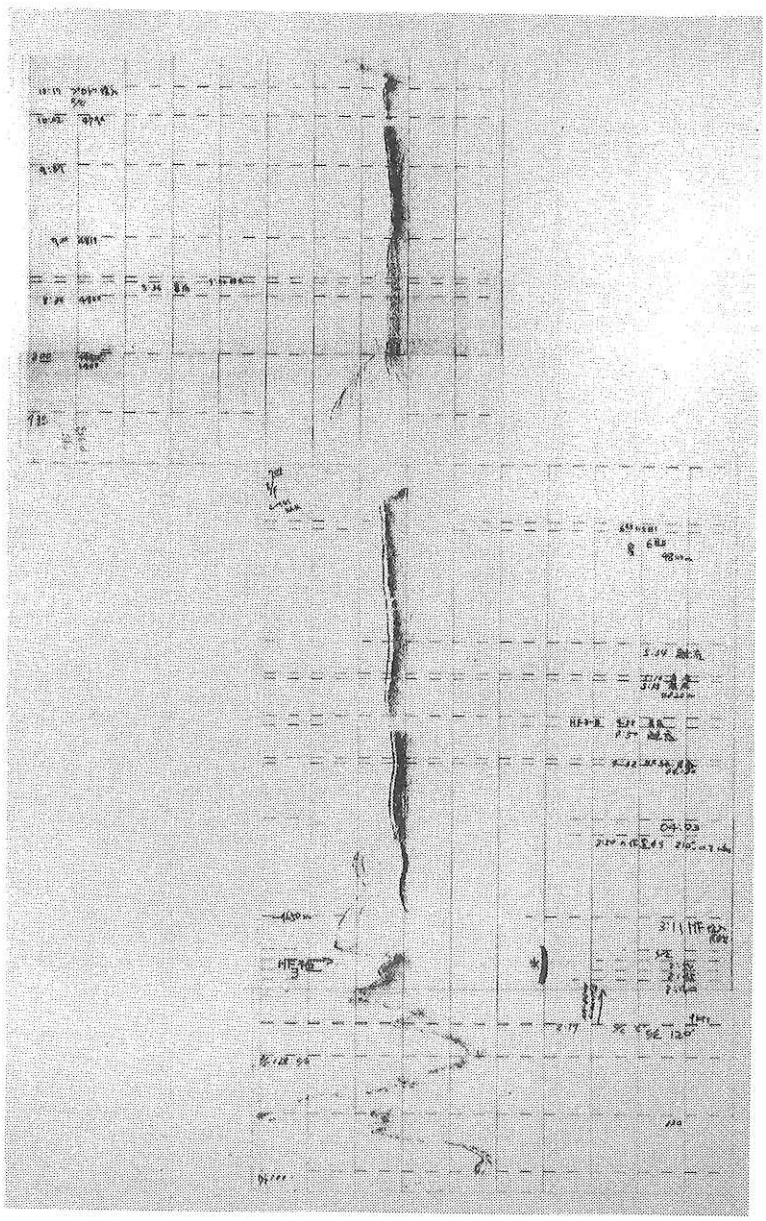

Fig. 20-5(b) Recordof3.5KHz subbottom profiler.Line onHF-3,P-3 stns.
It is nearly concordant with multichannel seismic profiler Line M3.

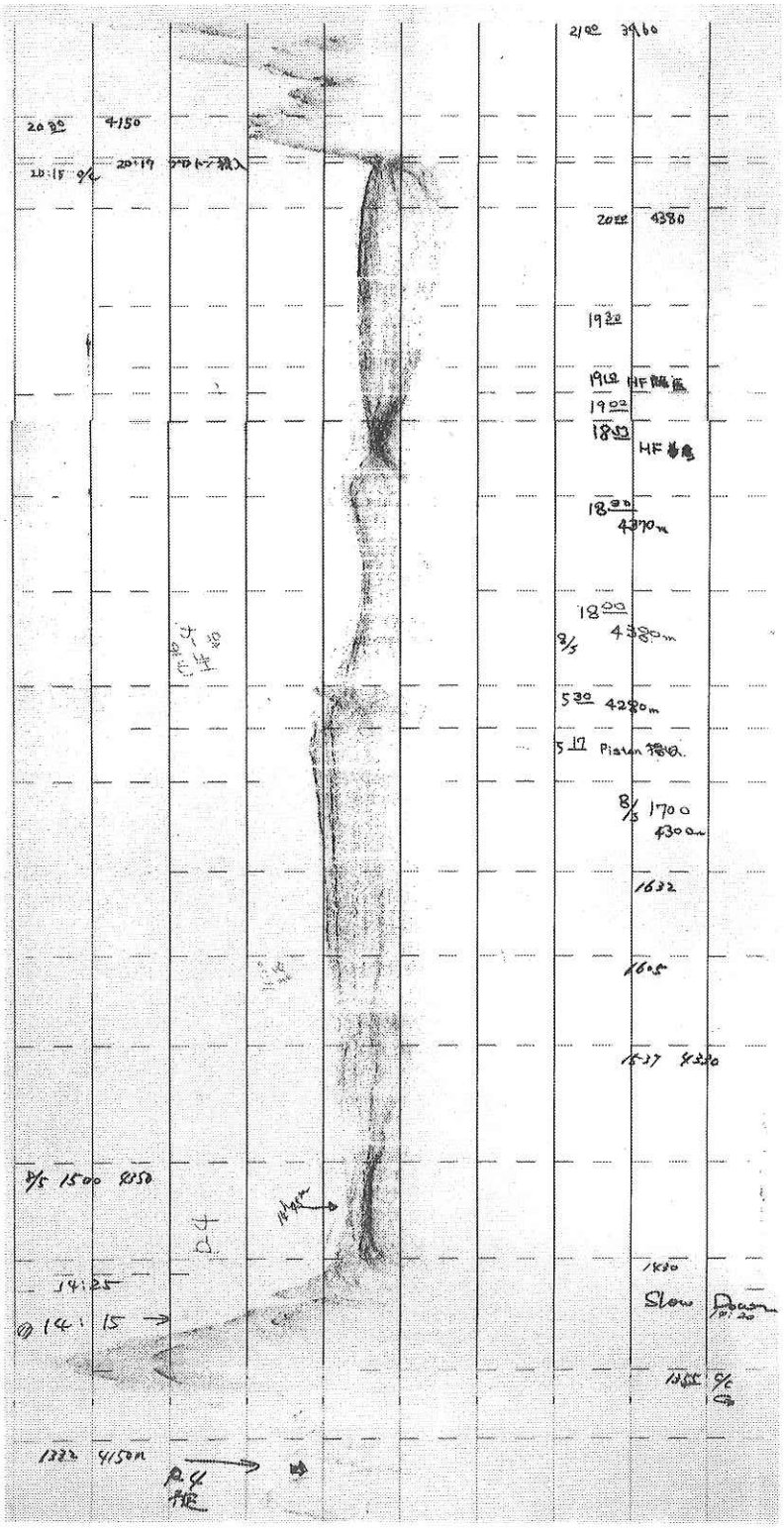

Fig. 20-5(c) Recordof3.5KHz subbottom profiler.
Line onP-4 and HF-4 stations.

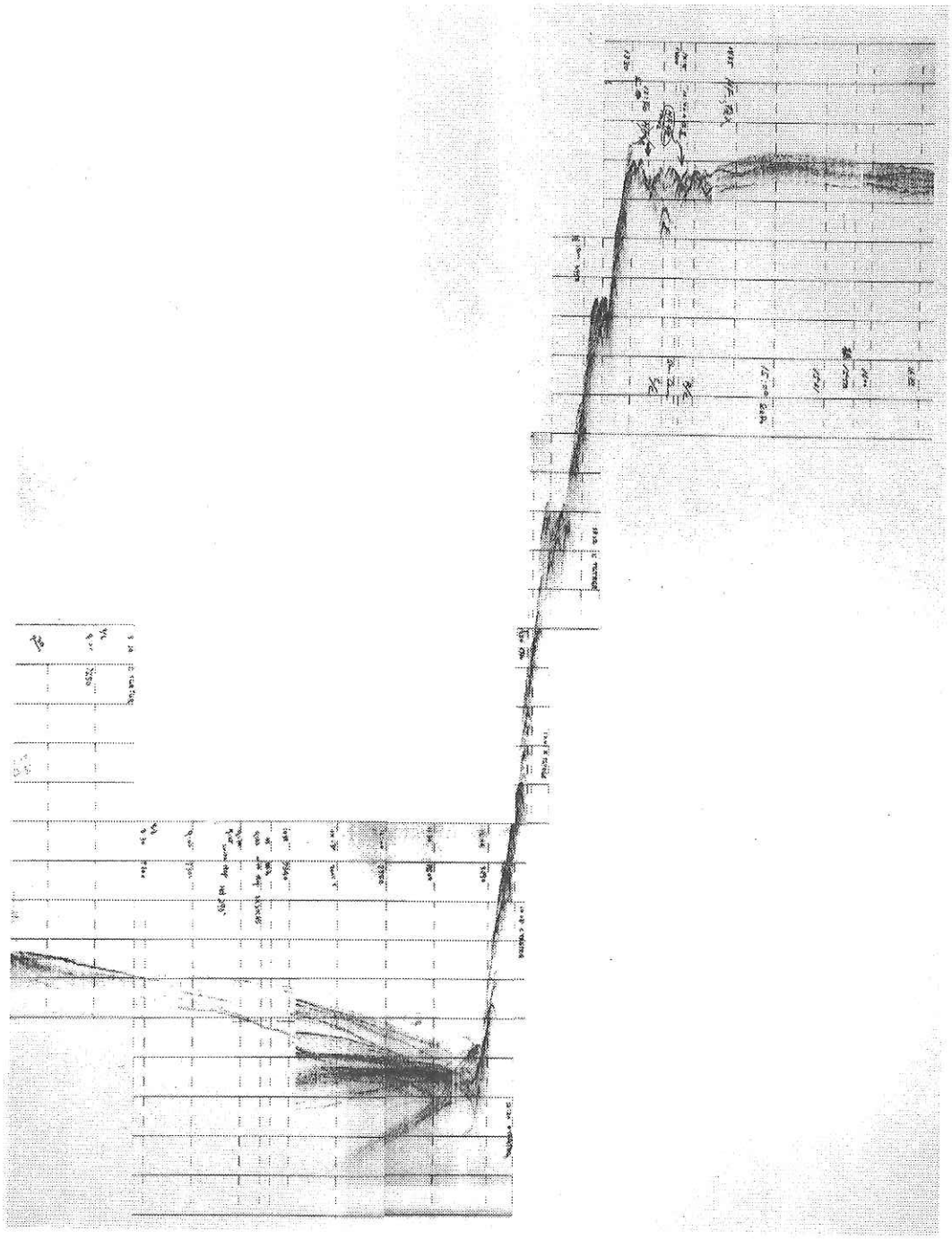

Fig. 20-5(d) Record of 3.5 kHz subbottom profiler. Line on P-5 and HF-5 stations. [1] Western half.

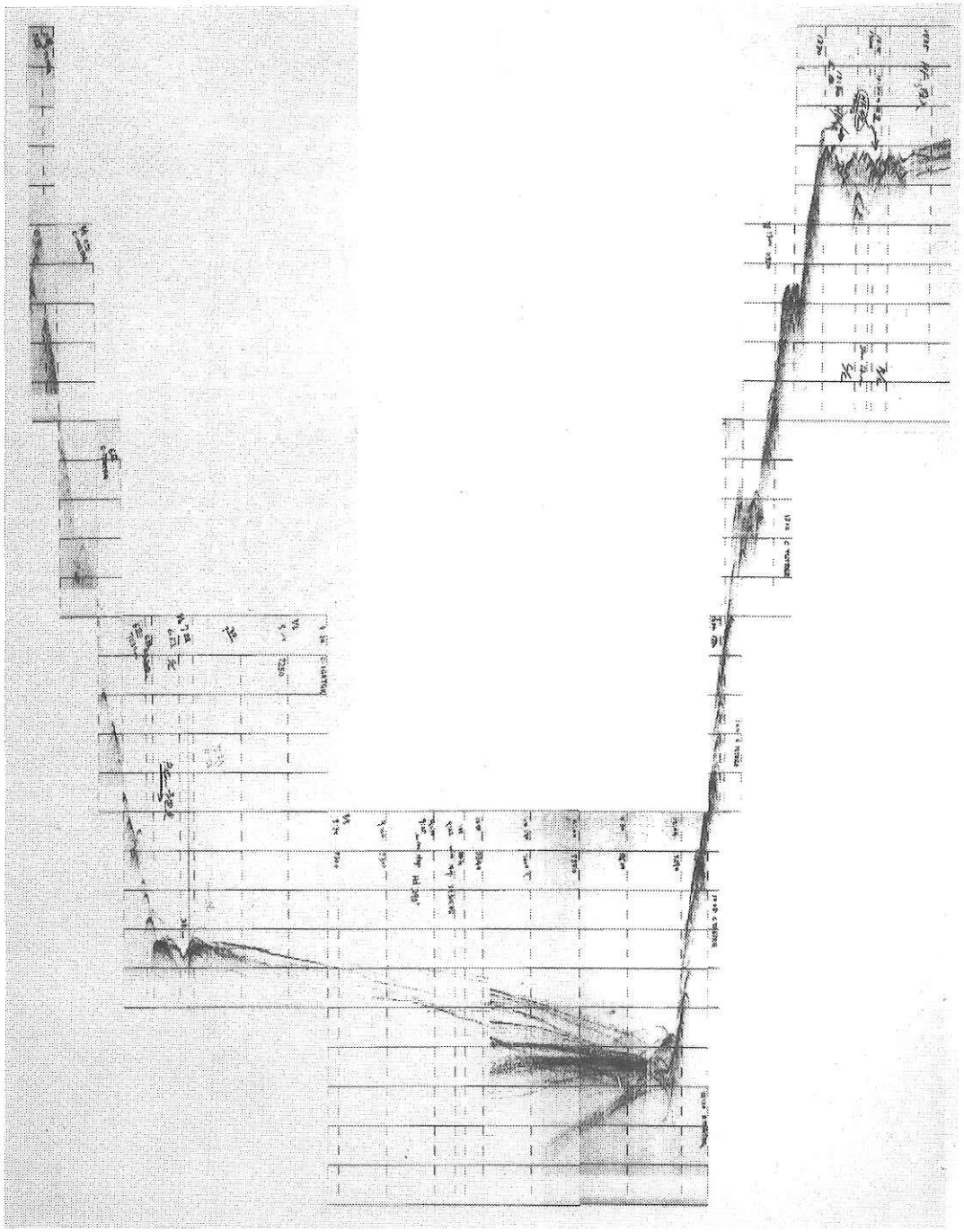

Fig. 20-5(e) Record of 3.5 kHz subbottom profiler.
Line on P-5 and HF-5 stations. [2] Eastern half

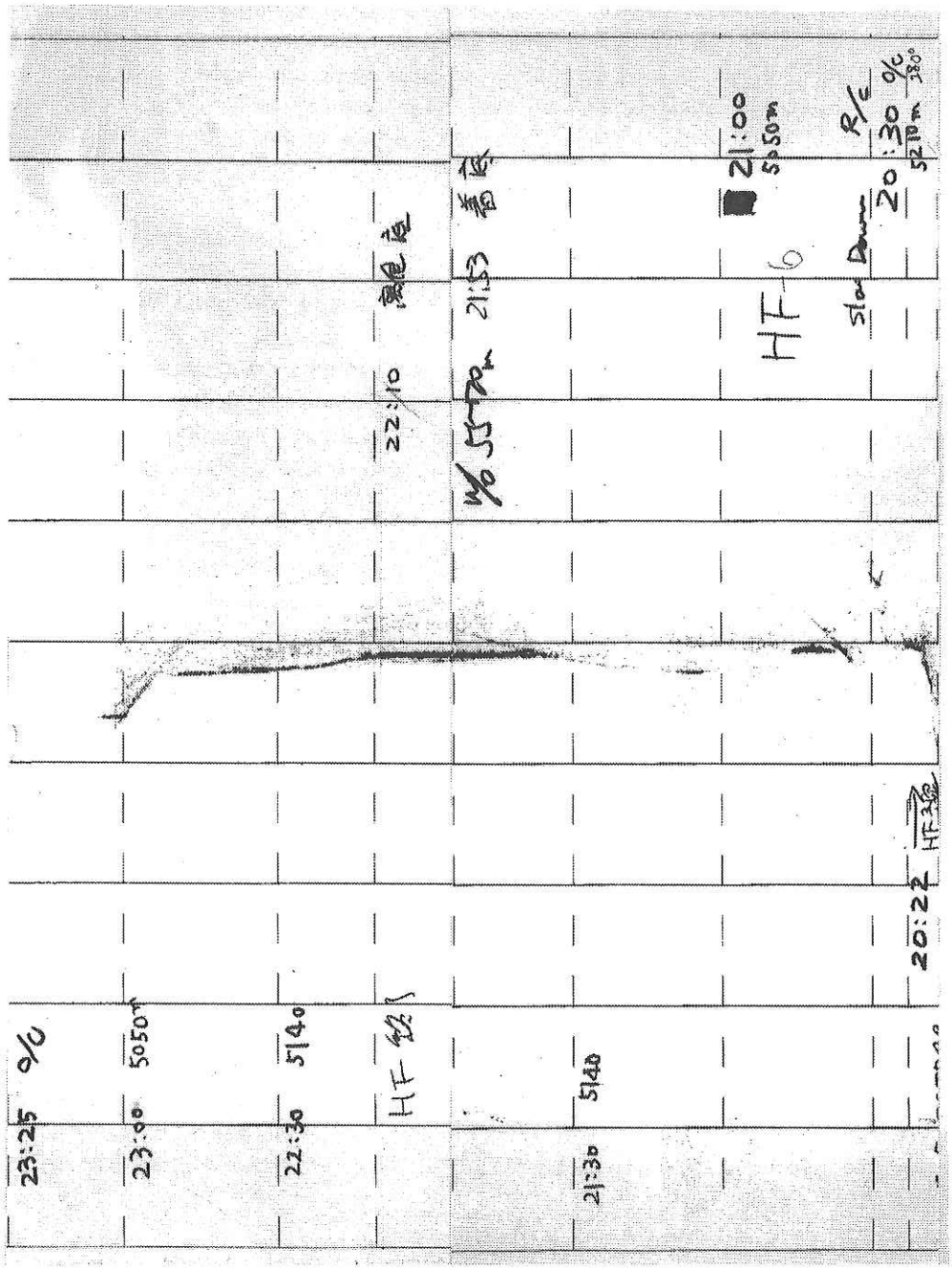

Fig. 20-5(f) Record of 3.5KHz subbottom profiler. Line on HF-6 station.

20-3. PISTON CORES

[1]. General remarks

Processes of sedimentation of the back-arc deposits mostly composed of volcanogenic and biogenic components have not been throughly understood. The Yap arc-trench system is one of the anomalous regions in the world, as it consists of metamorphic rocks such as greenschists and amphibolites insteadthat the ordinary arcs are composed of volcanic materials.

During the cruise of the KH 86-1 we obtained highly deformed surface sediments from the trench bottom near the junction area between Mariana and Yap trenches (Koga et al., in press). Tectonic style observed on the core sections is quite similar to that of the Middle America trench (Moore and Lundberg, 1986) and the Japan trench (Carson and Bruns, 1980). In such sense, the junction area seems to be quite important for the understanding the stress field governed by the movement of the subducting plates. The purpose of the present cruise was focused on the items stated above.

[2]. Operation

Two types of piston core systems were used for collection of bottom sediments in this cruise. A 12m-long aluminum corer was used at the backarc side of the Yap arc-trench system. An 8m-long stainless corer was used at one of the backarc sites and the trench bottom. Before lowering the piston corer to the bottom, precise topographic survey was done by using 12 kHz and 3.5 kHz echograms in order to confirm existence of enough sediments for the pipe to penetrate. Wind and current are also significant factors to be taken into account during coring operation.

[3]. Visual core description

Stations of piston cores taken during this cruise are shown in Fig. 20-1 and results of the smear slide observation is listed in Table 20-1.

KH 87-3-21 (P-3)

The core P-3 was taken from a back-arc basin; the Parece Vela Basin, in the Yap arc-trench system. This coring site P-3 is nearly on a multi-channel seismic reflection survey line M3 of KH86-1 cruise and its precise location is close to the shot no. 1600 on the line. Sediments thicker than 0.3 sec are observed only along the line M3. The reflectors show slightly eastward tilting.

Recovered sediments are dominated by bioturbated reddish brown soft clay with homogeneous lithology, possibly of pelagic origin. Very small amount of terrigenous materials, such as quartz and feldspars, are contained in its. Some fractions of micro-manganese nodules are commonly observed

in the sediments with spot or patch like forms. The recovered sediments have very poor sedimentary structures (Fig. 20-6).

Fig. 20-7 shows visual core descriptions of P-3. Highly bioturbated zones are observed in intervals of 75-85, 170-180, 290-295, 410, 660-670 and 870 cm core-depths. The zones are composed of reddish brown or brown clay with slightly bright colored clay, which seems to be burrow. Hardness of the cored sediments is weak through the top to bottom,although the sediments are more consolidated from the 441 cm toward the bottom. It was found by smear slide observations that some fractions of calcareous materials are contained in the sediments from 750 cm and downward. Dark reddish brown clay is faulted (?) with some offsets at 830 cm depth, and brown clay is folded around 836 cm depth section. There is brown colored clay between 880 cm depth and the bottom of the core that is presumably flow-in unit.

KH 87-3-22 (P-4)

On the slope break of the back-arc side of the Ya Ridge nearly at the shot no. 340 on the line M3 of KH86-1 cruise, the core P-4 was taken. This was chosen for the following reasons; (1) some sediments were acoustically found in a processed multichnnel seismic profile of the KH86-1 cruise. (2) terrigenous materials from the ridge suggesting the tectonic history of Yap Ridge are probably deposited there .

Length of the recovered sediment core is 298 cm. The sediment is dominantly dull reddish brown or brown clay. It characteristically contains some foraminifers and/or Mn nodules (Fig. 20-8). Between the top and 20 cm core-depth, there exists medium-sized foraminiferal sand containing many manganese nodules with maximum size of 5x4x3 cm. A section is not consolidated and composed of only foraminifers without manganese nodules. In 20-30 and 55-140 cm core-depths dull reddish brown clay is moderately bioturbated, causing burrows and moats, whereas in the 160-180 cm core-depth the same colored clay is well disturbed and looks like massive clay with no sedimentary structure.

Foraminifers are contained in the entire core, but particularly rich in 215 cm core-depth showing a lenticular section. In 270 cm core-depth dull yellow orange clay is probably ash bed about 2 cm thick. The contact at the bottom of ash bed is sharp and sediment below the sharp contact is composed of an about 3 cm thick layer of many manganese micro-nodules. The maximum size of nodule is 4 mm in diameters. Below the bed the core is brown clay dotted with some manganese micro-nodules. Visual core description of this core is shown in Fig. 20-9.

(written by S. Kuramoto, J. Ashi, H. Matsuoka and K. Fujioka).

TABLE 20-1 Smear slide descriptions of core samples P-3 and P-4.

KH87-3 St 21 P-3

Interval	D/M	Sand	Silt	Clay	Qz	F	Mica	Clay	V.G.	M.N.	Cab.	Foran	Nanno	Dia.	Ra.	Span.	
15	D		10	90	5	5		80		5							dark reddish brown clay
30	D		10	90	5	5		80		5						1	dull reddish brown clay
111	M		10	90	5	5	1	80		5							dull reddish brown clay
112	D		10	90	5	5	1	80		5							dull reddish brown clay
153	M		10	90	5	5		80		5							brown clay
190	D		10	90	5	5		80		5							dull reddish brown clay
239	M		10	90	5	5		80		5							brown clay
290	M		10	90	3	3	1	85		5							brown clay
344	M		10	90	3	3		80		5							
350	D		10	90	3	3		85		5							dark reddish brown clay
357	M		10	90	3	3		85		5							brown clay
387.5	M		10	90	5	5		80	1	5							dull reddish brown clay
439	M		10	90	5	3	1	80		5							yellowish brown clay
505	M																dull reddish brown clay
540	D		10	90	5	3		80		5							dull reddish brown clay
572	M		10	90	5	5		80		5							
594	M		10	90	3	3	1	85		5							dull reddish brown clay
650	D		10	90	5	5		80		5							
750	D		20	80	5	5		70		3	5	5	5				dark reddish brown clay
763	M		20	80	5	5	1	60		3	10	5	5				dull yellow orange clay
836	M		20	80	5	5		70		3	5	5	5				brown clay
870	D		30	70	5	5		60		5	10	5	3				dark reddish brown clay
950	D		30	70	5	5		55		5	10	5	10				brown clay

KH87-3 St 22 P-4

Interval	DM	Sand	Silt	Clay	Qz	F	Mica	Clay	V.G.	M.N.	Cab.	Foran	Nanno	Dia.	Ra.	Span.	
13	D	90	5	5	5	5		40		5	10	20	10			1	Foraminifera sand
22	M		30	70	3	3		10		5	10	20	40			1	dull reddish brown clay (burrow)
45	D		30	70	5	5		50		5	10	10	5			1	dull reddish brown clay
96.5	M		30	70	3	3		10		5	20	10	40			1	dull orange clay
107	M		30	70	5	5		10		5	20	10	40			1	dull reddish brown clay
187	D		30	70	5	5		40		5	20	10	10			1	dull reddish brown clay
236.5	M		40	60	5	5		30		5	20	20	10				dull orange clay
270	M		30	70	5	5		60	1	5	10						dull yellow orange ash?
275	M		30	70	5	5		50		20	10						Micro Mn-nodules
290	D		20	80	5	5		70		5	5					1	brown clay
296	D		20	80	5	5		70		5	10						brown clay
cc	D																

KH 87 3 P 3

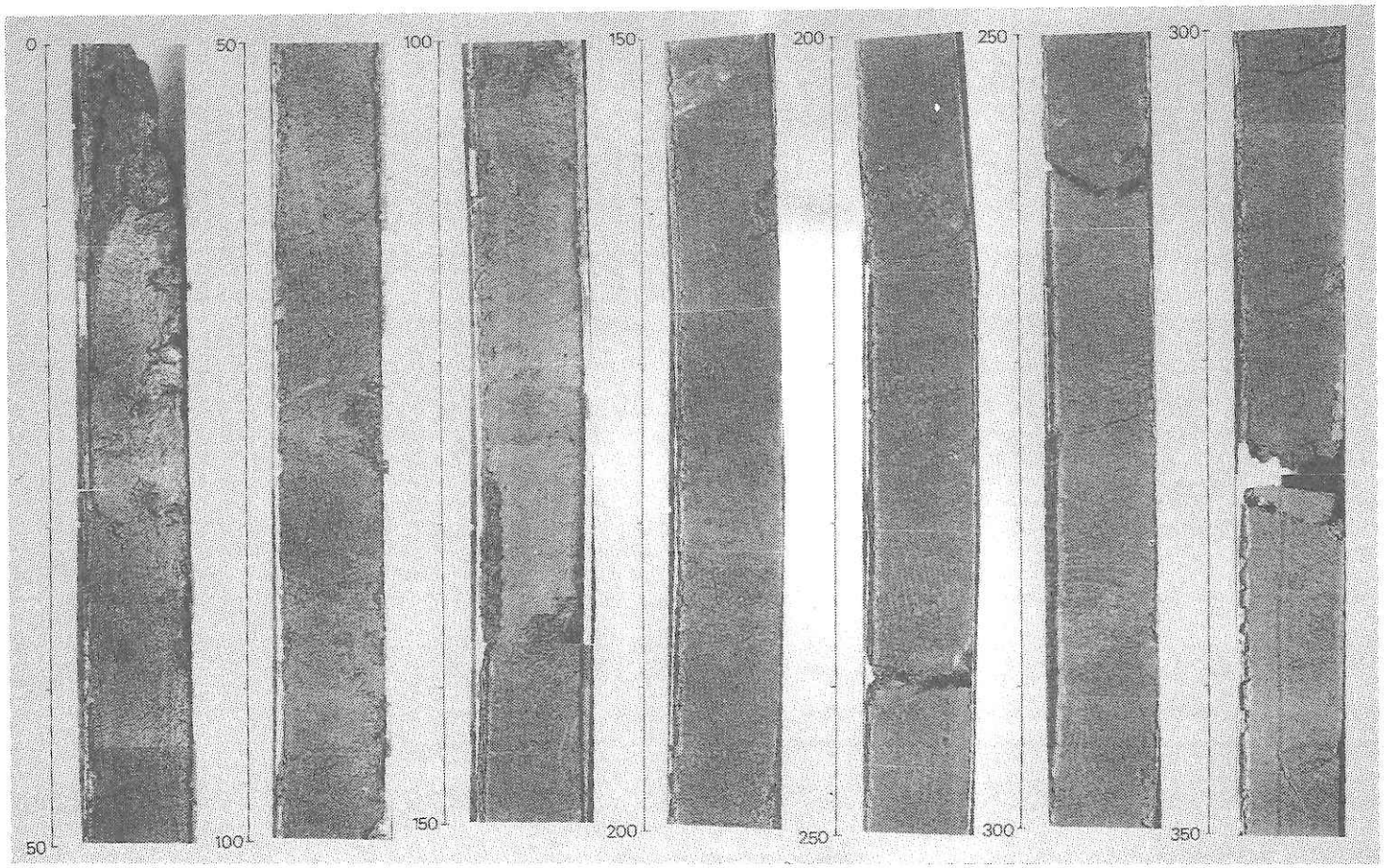

Fig. 20-6 Photographs of split half of piston core P-3.
(1). From the top to an interval 350cm.

KH 87 3 P 3

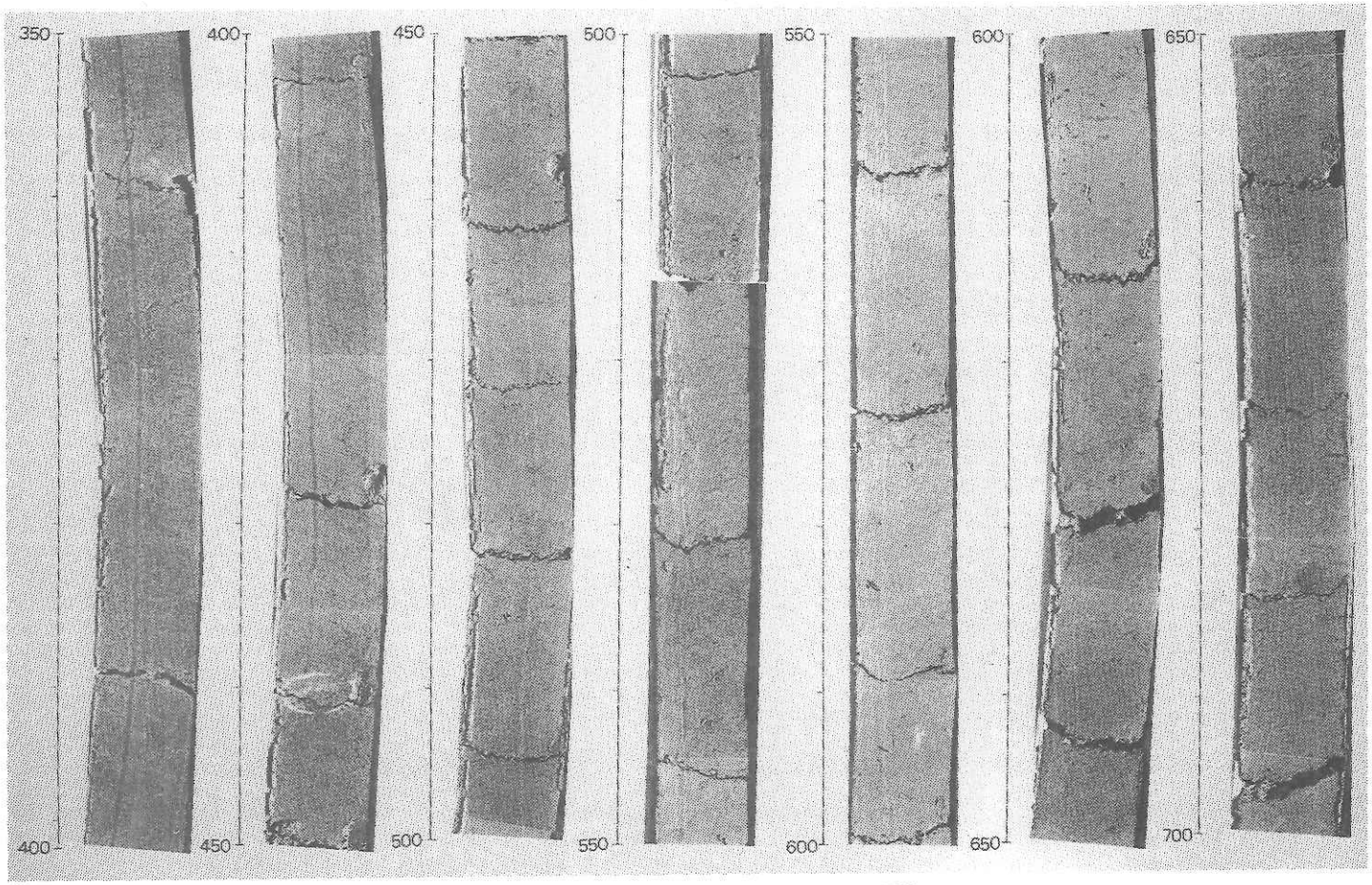

(2). From an interval 350cm to 700cm.

KH 87 3 P 3

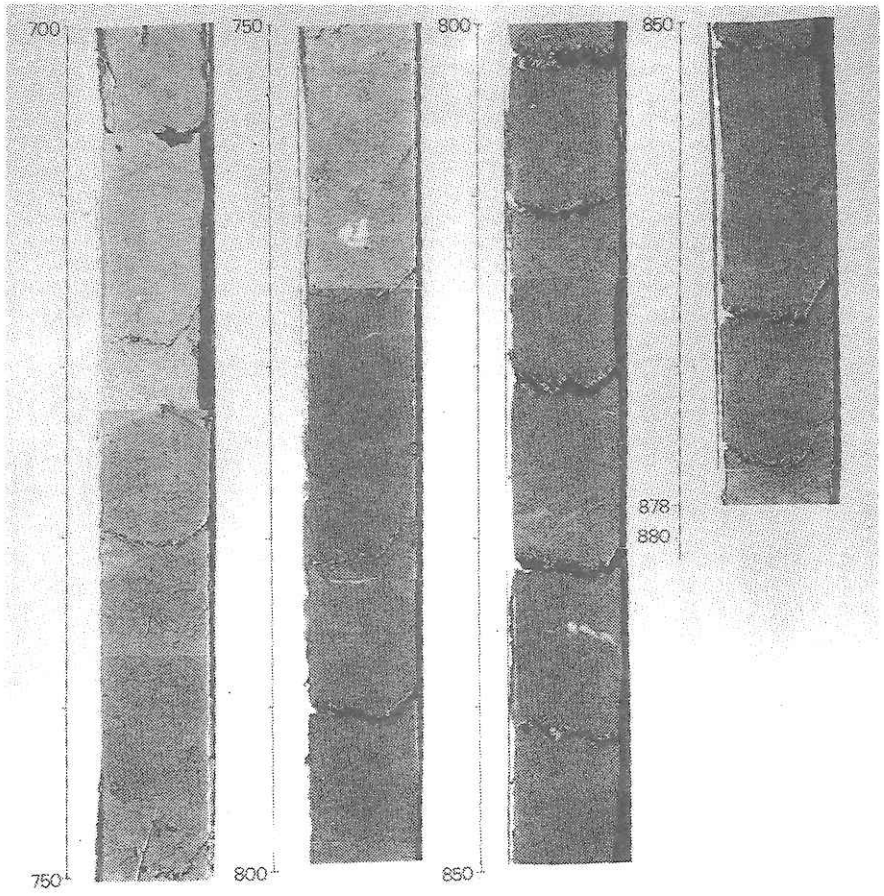

(3). From an interval 700cm to the bottom.

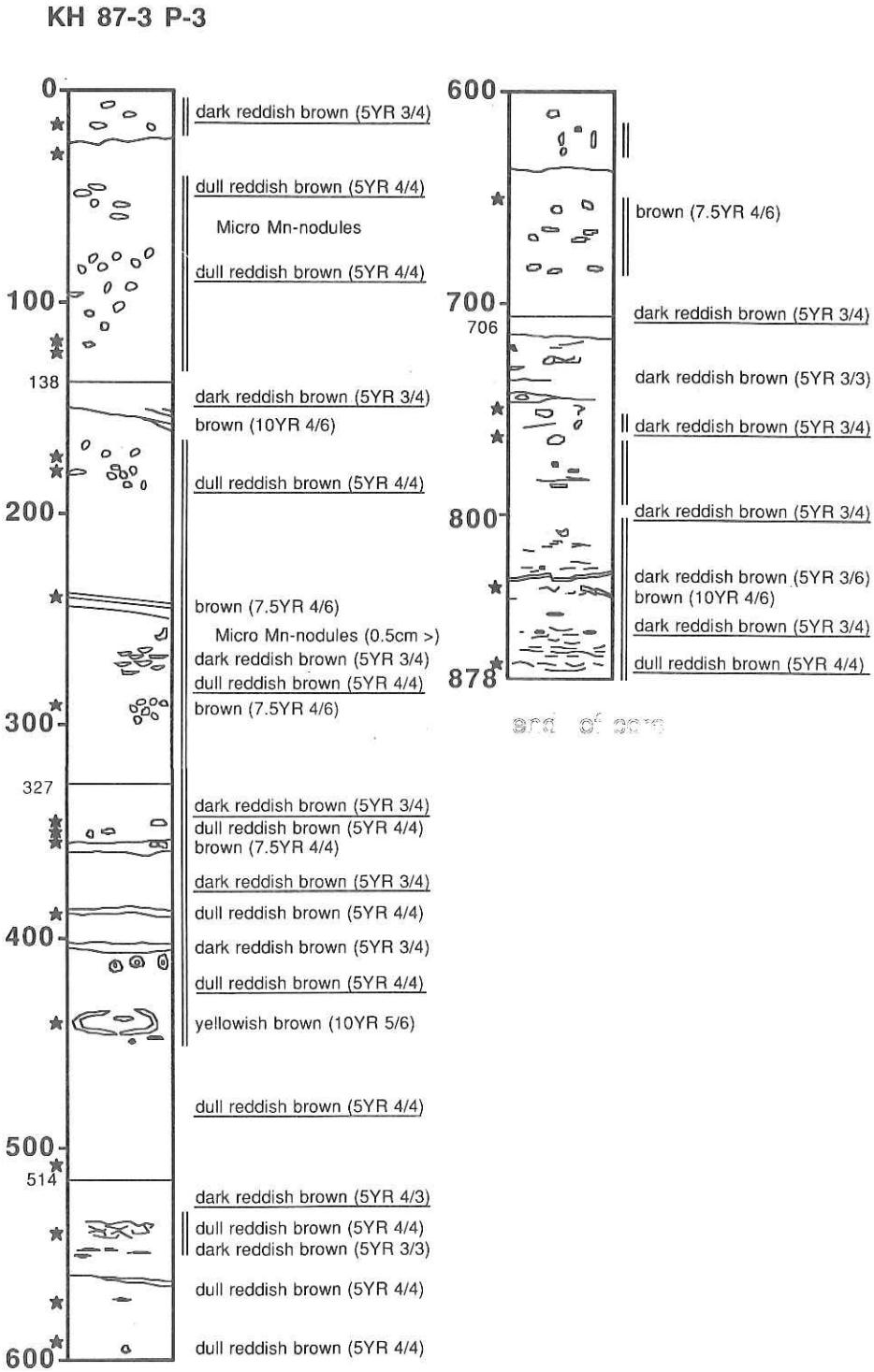

Fig. 20-7 Lithologic descriptions of piston core P-3.

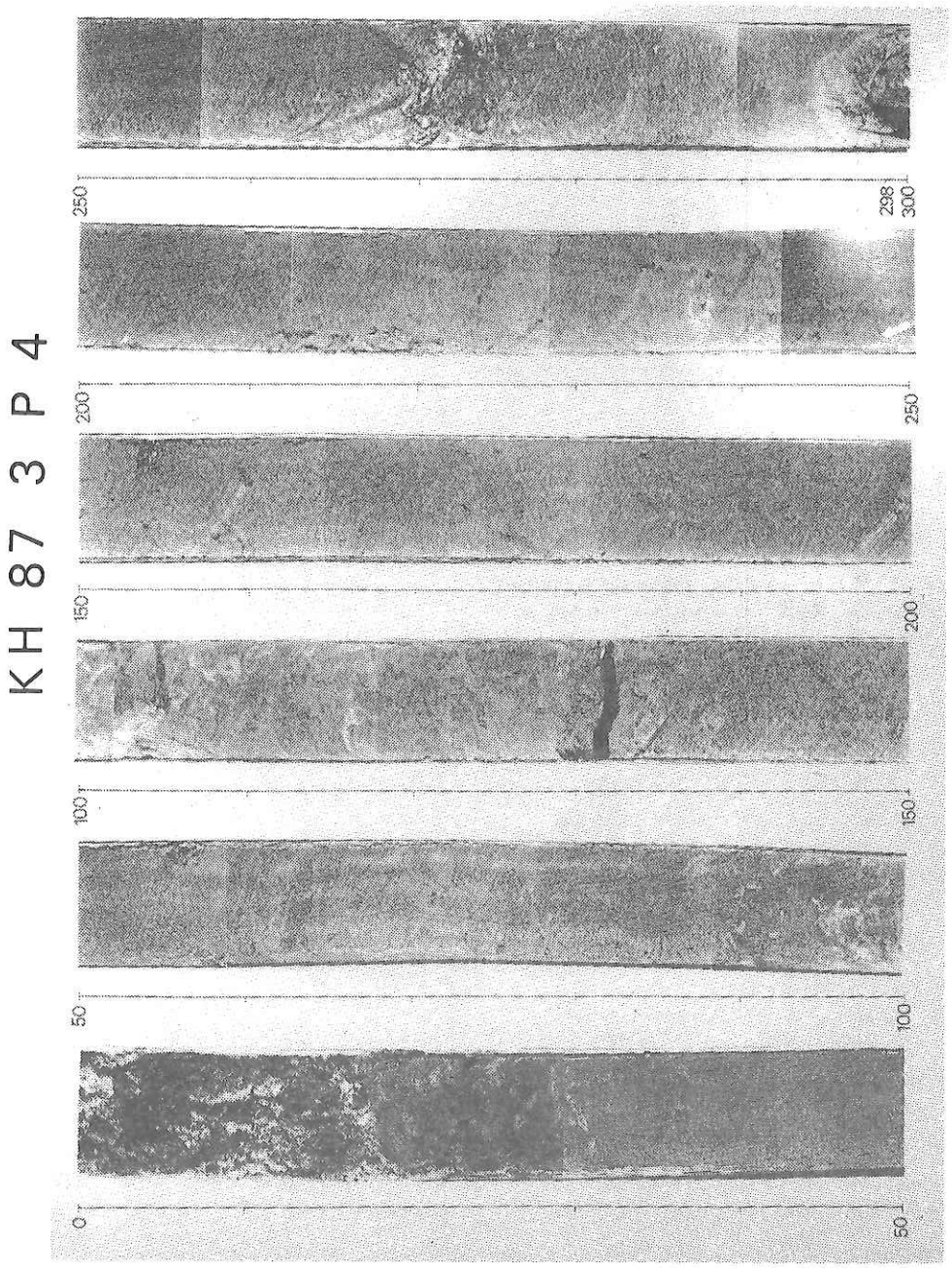

Fig. 20-8 Photograph of split half of piston core P-4.

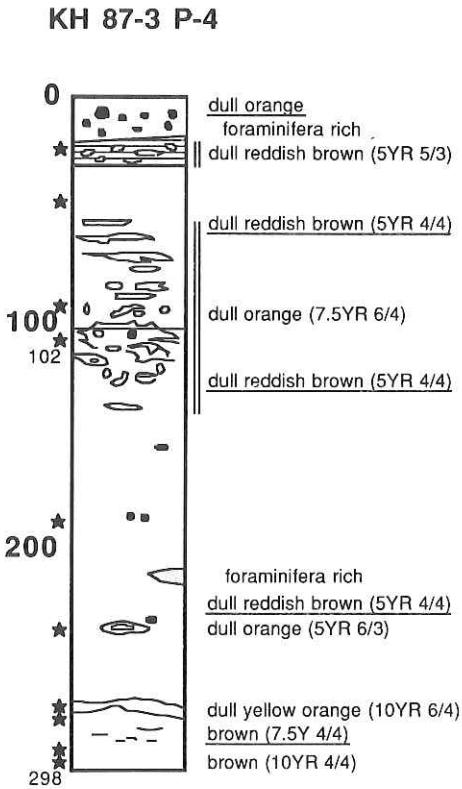

Fig. 20-9 Lithologic descriptions of piston core P-4.

20-4. DREDGE HAULS

[1]. General remarks

Occurrence of high-grade metamorphic rocks in the deep-sea floor similar to those exposed on the Yap Islands was confirmed during the cruise of the R/V Hakuho Maru, KH 86-1 (Fujioka et al., 1986). During the cruise, rocks not observed onland were also recovered by dredge hauls on two seismic profile lines, KH 86-1 M-5 and Yap-1, which are the reference lines across the Yap arc-trench system nearly perpendicular to the arc-trench system. As already stated, several significant morphological features are recognized in the seismic profiler as well as PDR lines. Two lines cut a topographic high including the Yap Islands on the lines. D-7, -8, -9 were carried out along the steep fault scarps and D-10, -11 were carried out on the seismic profile Yap-1 along the landward slope of the Yap Trench.

[2]. Operation

Dredge system used during this cruise was a cylindrical chain type dredge with two small cylinders connected with the chain bag. Outline of the system is almost the same as that used during KH 86-1 (Fujioka et al., 1986). Either No.1 or No. 5 winch was used depending on water depths of the dredge sites. Before the dredge operation, precise topographic survey by PDR and 3.5 KHz echograms were carefully done around the sites. The towing course of the dredge hauls was set up toward upslope taking into account effect of wind and current on the ship during the dredge operation. Tension meter was used for confirming the bottom hit of the dredge system. Duration of a haul on the bottom is about 40 minutes.

[3]. Description of dredge samples

Stations of dredge hauls during this cruise are shown in Fig. 20-1 and the collected samples are listed in Tables 20-2 (a)-(e) for D-7 to D-11.

(a). KH 87-3-13 (D-7)

This station was chosen to recover rocks exposed along a steep slope formed by fault movements. Multichannel seismic profiler line M-5 clearly represents existence of the fault scarps near the crestal part of the Yap Ridge (Tokuyama et al., 1985). The third steep slope was chosen for the sake of confirmation of the rocks extending southward from the Yap Islands.

Several pieces of thickly manganese coated meta-andesite were obtained by the dredge hauls (Fig.20-10(a)). Rocks are metamorphosed volcanic rocks such as andesite lavas, tuff breccias, lapilli tuffs and volcanic breccias. These types of rocks, especially andesitic in composition, are unknown in the onland geologic suites except for lateritized agglomerates in the Tomil Formation overlying the Yap Formation. The Tomil agglomerates is not affected by the metamorphism so that the dredged rocks are really unique in this area except on the Palau Islands.

(b). KH 87-3-15 (D-8)

A steep slope caused by normal faults on the seismic profile line M-5 was dredged at this station. Large amounts of foraminifara limestones and metabasites were obtained together with soft foraminifera sand includeing both planktonic and benthic ones (Fig. 20-10(a)). Limestones consist of coarse grained shell fragments, lithic fragments, corals and foraminifers mostly covered with thick manganese crust. Judging from hardness of the rocks as well as its low porosity, age of the limestones may be older than Quaternary. Another type of rock obtained is metabasite whose origin is lapilli tuff, basalt, tuff and tuff breccia. Mutual relationship between limestones and metabasites is unknown. Soft foraminifera sands were also obtained. They are possibly surface sediments covering the basement rocks.

(c). KH 87-3-16 (D-9)

This dredge haul was undertaken to get the rocks exposing along the first steep fault scarp on the seismic profile line M-5. However, actual site of the dredge haul was a steep slope of the backarc side. Because of appreciably large errors in the Loran C positioning at the sea adjacent to the Yap Islands it was difficult to find exactly desired position. If we recognize the steep slope is to be an extension of the faults observed onshore the Yap Island, the fault scarp may be equivalent to the great fault cutting the Yap Island.

A large amount of metabasites were obtained at the site. They are lavas, tuffs, lapilli tuffs tuff breccias of the greenschist facies and amphibolite facies and small amount of ultramafic rocks as well as acidic plutonic rocks (Fig. 20-10(b)). These rocks are quite similar to those metamorphic rocks exposing onland as the Yap Formation which consists mostly of volcanic rocks of the greenschist and amphibolite facies. Soft foraminifera sands were also obtained by two small cylinder type dredgers. This kind of sediments may be surface cover of the metabasites which are exposed on the bottom of the sea floor (see submarine photographs).

(d). KH 87-3-18 (D-10)

Seismic profile line Yap-1 perpendicularly crossing the Yap arc-trench system shows a typical morphologic feature of the ordinary arc-trench system. During KH 86-1 two dredge hauls were carried out along the line at water depths shallower than 4,500m, corresponding to the Upper unit of the morphologic unit. In the present cruise we intended to get rocks exposed in much deeper portions of the morphologic unit.

Dredge haul D-10 was attempted to get rocks along the Lower unit at about 6000 m water depth. Topography was complicated because of steepness of the slope and the sea condition was not so good during the operation so

that small amounts of small fragments were obtained (Fig. 20-10(c)). They are angular and tabular manganese crusts with angular granules of various kinds of rocks. Greenstone and amphibolite were also recovered. Soft sediments obtained by the small cylinder dredgers consist of green hornblende derived from greenschists and amphibolite of the Yap Islands.

(e). KH 87-3-19 (D-11).

This dredge site is on the seismic profile line Yap-1. Purpose of this site was the same as that of the site D-10. Dredge haul was carried out at water depths about 5,200m of the Middle unit. Greenstones, amphibolites as well as marbles were obtained (Fig. 20-10(c)). Some of the pieces are covered with thick manganese crust. The original rocks of greenstones are lavas, tuffs, and tuff breccias in basaltic composition. Soft sediments consist of green hornblende, biotite, magnetite and quartz which may be derived from the metamorphic rocks to the Yap Islands.

[4]. Discussion

Various types of rocks obtained during this cruise and the last cruise (KH86-1) are quite similar to those exposed onshore Yap Islands. Some of the dredge samples have not been found onland. Most of dredged rocks are thought to be in situ (not allochtonous) based on their freshness of the cut-section and angular shapes. This indicates that the high grade metamorphic rocks extend eastward as far as the axis of the Yap Trench. Rare occurrence of unknown rocks may suggest that gneisses and andesites are exposed under the deep-sea environment having the same geologic history and environment as the Yap Islands. Andesitic tuffs, lavas and tuff breccias obtained at site KH 87-3 D-7 are significant in their nature and age comparable to those in the Tomil agglomerate on land showing calc-alkalic affinity similar to the island arc volcanism. Dacitic rocks obtained in KH 86-1 at the back-arc region together with seismic data and heat flow values may indicate recent volcanic activity in this area. (written by K. Fujioka, A. Takeuchi, G. Kimura, J. Ashi, S. Kuramoto and H. Matsuoka).

20-5. DEEP-SEA CAMERAS

[1]. Deep-Sea Camera System

Constitution of deep sea camera system in this cruise was the same as that in KH 86-5 cruise, including two cameras, one storobescope, pinger and compass, as shown in Fig. 20-11. The timer circuit containing a storobescope was improved. As an electrical noise entered into the circuit, delay-time-counter was reset, resulting that the circuit was forced to come back to the initial mode in the old model. A new circuit was then made in which the interval timer IC beside photocoupler was isolated from power source. It endured heavy noise or abrupt large fluctuation in power due to DC switch circuit with thyristor.

[2]. Trouble

Three troubles happened in this cruise. First was in the operation KH 87-3-6, when flash valve socket came off in the storobe unit, so that flash shot stopped, then the film was unable to be rolled by about one third of the entire length. The second and third troubles happened with one camera and compass during KH 87-3-17. No photograph was successfully taken by the camera, because spool setting of a new film was so loose that parcoration of film broke down by turning of camera winder. In the compass, time previously set on deck was not memorized in the internal RAM area. All the cases mentioned above denote that such a hard shock as shaking the whole camera unit would make film loose, resulting in invasion of induced noises into the power supply circuit of compass.

[3]. Operation

Five operations of deep-sea camera were attempted during this cruise. Operation logs of each station are shown in Table 20-3. Data of direction and tilt of camera system, monitored by means of compass, are shown in the next section. Direction data indicate difference between the cardinal point locating at camera unit and geomagnetic north-pole. If the camera cases stood up-right within 5 degrees, a code "OK" is recorded in the memory of tilt data. Similarly another code "NG" is memorized if the case tipped up more than 5 degrees. Using these off-line data on attitude of the camera unit, spin motion and degree of collision with sea bottom are displayed on board as shown in Figs. 20-12(a) through 20-12(e).

[4]. Interpretation of deep-sea photographs

Fig. 20-13(a) shows submarine photographs of KH 87-3-4 (1)-(4).

(1) Meandering trails of some bottom dwelling organisms on clayey sediment.
(2) Manganese-coated sedimentary rock and angular pillow basalt debris.
(3) Talus deposit composed of manganese-coated conglomerates' boulders.
(4) Pillow basalt debris contained in manganese-coated sedimentary rocks covered with thin white clayey sediments.

Fig. 20-13(b) shows submarine photographs of KH 87-3-4 (5)-(8).

(5) Assembly of manganese-nodules. The surface structure is smooth.
(6) Pile of manganese-coated platy boulders.
(7) Outcrop of manganese-coated rock. Angular pebbles deposited in hollows.
(8) Conglomerate outcrop, well covered by manganese.

Fig. 20-13(c) shows submarine photographs of KH 87-3-6 (1)-(4).

(1) Outcrop of parallel sheared mudstone, partly covered by coarse sand.
(2) Fractured mudstone and transported boulders filled by pumice and scoria
(3) Scoria and pumice debris, and mudstone boulders.
(4) Boulders of manganese-coated mudstone.

Fig. 20-13(d) shows submarine photographs of KH 87-3-6 (5)-(8).
(5) Faulted mudstone outcrop and talus debris.
(6) Outcrop of manganese-coated mudstone. Faults are developed.
(7) Manganese-coated mudstone and boulder.
(8) Outcrop of pumice layer and its debris on the scoria sand.

Fig. 20-13(e) shows submarine photographs of KH 87-3-14 (1)-(4).
(1) Outcrop of amphibolites. Mostly angular pebbles, cobbles and granules. Matrix is white foraminifera sand. Pebbles are almost monolithologic.
(2) Ripple mark on white foraminifera sand. Large blocks of metabasite.
(3) Outcrop of metabasites and talus of their derivatives. Angular pebbles and cobbles mostly monolithologic materials are seen.
(4) Minor fault covered by thin coarse white foraminifera sand.

Fig. 20-13(f) shows submarine photographs of KH 87-3-14 (5)-(8).
(5) Outcrop of metabasite covered with thin white foraminifer sand. Surface of the basites is irregular owing to the erosion by tectonic activity.
(6) Outcrop of flute and groove casts on the base of sandstone.
(7) Outcrop of metabasite of pyroclastics origin cut by smalljoints forming a steep cliff.
(8) Angular pebbles of metabasites with white foraminifera sand.

Fig. 20-13(g) shows submarine photographs of KH 87-3-17 (1)-(4).
(1) Outcrop of metabasites forming irregular blocks at the western flank of the Yap Ridge.
(2) Steep slope consisting of angular metamorphic rocks at the Yap Ridge.
(3) Rather straight trail of some bottom dwelling organisms on the surface consisting of coarse sediments.
(4) Large metabasites outcrop with cobbles and pebbles of metamorphic rocks

Fig. 20-13(h) shows submarine photographs of KH 87-3-17 (5)-(8).
(5) A large fallen block of metamorphic rock at the Yap Ridge. Note small pieces of the same rocks around the large block.
(6) A small ridge covered with thick sediments forming a step at the Yap Ridge.
(7) Steep outcrop consisting of breccias covered with thin sediments at the Yap Ridge.
(8) Steep outcrop of metamorphic rocks at the Yap Ridge. Gentle surface is covered with thick sediments,whereas the steep slope is almost bared.

Fig. 20-13(i) shows submarine photographs of KH 87-3-24 (1)-(4).
(1) Steep outcrop consisting of pillow basalt and pillow lobe at the eastern slope of the extension of the Yap Ridge.
(2) tratified sediments forming a steep cliff at the extension of Yap Ridge

(3) Hard conglomerate outcrop at the extension of the Yap Ridge.
(4) Manganese coated basaltic rocks exposed at the eastern slope of the extension of the Yap Ridge.

Fig. 20-13(j) shows submarine photographs of KH 87-3-24 (5)-(8).
(5) Pebbly mudstone with ripple at the surface of the eastern slope of the extension of the Yap Ridge.
(6) Pebbly mud surface with ripples at the Yap Ridge. Pebbles are gathered in the hullow area near the basalt outcrop.
(7) Highly jointed steep slope of the metamorphic rock at the Yap Ridge.
(8) Manganese coated gentle steps consisting of the basaltic rocks at the Yap Ridge.

(Written by M. Watanabe, J. Ashi and K. Fujioka).

20-6. GEOLOGY OF THE YAP ISLANDS

[1]. General remarks

The Yap islands are well-known for occurrence of metamorphic rocks such as greenschists, amphibolites, metagabbros and others. Some workers considered that the original rocks of the metamorphics are ophiolites and suggested an obduction model for their emplacement (Hawkins and Batiza, 1977). Petrological data of the metamorphic rocks are reported (e.g. Shiraki, 1971), while no detailed study has been published on the geology of the islands after Tayama's work (1935). We had an opportunity to visit the Yap islands in 1986 and 1987 totally for seven days and observed more than eighty outcrops. In this paper, we preliminarily reports occurrences of the rocks in the field.

[2]. Localities and occurrences

Localities of outcrops are shown in Fig. 20-14. Occurrences and sample remarks are represented in Table 20-4. We describe general remarks of geology of the islands.

(a). Yap island

The Yap island is the biggest of the chain and composed mainly of greenschists and amphibolites. Along roads from Qaringeel to Colonia and from Qayireck to Gargey, there are many small outcrops. Strike of schistosity of the greenschists are mostly NE parallel to extension of the Yap island. Foliations of schistosity are changed partly, while stretching lineations showing a direction of ductile shear are NE everywhere. An NE trending fault is situated along the southeastern coast of the island. Outcrops on the fault show a cataclastic occurrence and geomorphology is changed along the fault. A sense of shear observed in the outcrops shows that the fault has sinistral strike slip component. Geomorphology suggests

that the southeastern part to the fault is relatively subsided. A seismic profile of Line Yap 1 of KH 86-1 (Tokuyama et al., 1986) indicates the southwestern continuation of the fault observed on the island. The profile represents step like normal faults consistent with observation on land.

(b). Rumung island

It consists of basic metamorphic rocks the same as those in Yap.

(c). Map island

Basement of this island is composed of amphibolites, gradually changed to breccias of amphibolite blocks. Matrix of breccia is originated from crashed amphibole grains and apparently suffered from retrograde metamorphism. The amphibolites and amphibolite breccias are uncomformably covered by debris flow deposits (Map Formation; Tayama, 1935) which include various kinds of rocks such as amphibolites, gabbros, greenschists, granites, rhyolites, andesites and others. The layers of sandstone and siltstone are found in some places, while they are not traced but truncated by faults or channel walls. The faults appear to have been formed contemporaneously with sedimentation of the debris flow deposits. At several points, we recognized that sandstone layer is a large block in debris flow deposits. Calcareous ooze layers are partly observed in the sandstone. Nannofossils indicating the Latest Oligocene are found from the layer (Matsugi and Okamura, personal comm.). Intensively weathered (latelalized) volcanic effusives (Tomir aggromerate; Tayama,1935) uncomformably overly the older rocks. The unconformity is observed along the Tagireeng Channel.

(d). Gagil island

This island is also composed of amphibolites and Tomir agglomerate. In the Map Formation, ultramafic rocks are frequently encountered at the eastern coast of the island.

(e). Garim island

The Garim island is a small island located to the southeastern corner of the Yap islands and consists of limestone. The older limestone is observed only at this island in the Yap islands. The age is unknown but Tayama (1935) reported similarity of the limestone with the Ryukyuu limestone.

(Written by G. Kimura, A. Takeuchi and K. Fujioka).

20-7. SUMMARY

During the second expedition for the Yap arc-trench system from 3 to 6 August, 1987, we successfully got sediments and rocks by piston corer, OKEAN type sampler and dredge haul. Topographic and subbottom profiles were taken by 12 kHz and 3.5 kHz echo sounders. Deep bottom photographs

were taken by a new deep-sea camera system. Results we obtained onboard the Hakuho Maru are summarized as follows;

1) The Yap arc-trench system is divided into six morphologic domains from geomorphologic viewpoint; a junction between Mariana and Yap systems (JM), North (N), north-central (NC), south-central (SC), southwest(SW) and junction between Yap and Palau system. Boundaries of domains are shown in Fig. 20-3.

2) The forearc region of the Yap Trench shows notable notches which may represent great tectonic boundaries. The notches exist around 4.0 sec and 8.0 sec of two way travel time of the 12 kHz echo sounder, respectively.

3) Sediments overlying the back-arc region of the Yap arc-trench system are reddish brown clay with highly bioturbated intervals including foraminifers and nannofossils. They were supplied from the land and sea.

4) Rocks obtained from various parts of the arc-trench system are similar to those exposed onshore the Yap Islands, while some of them are quite different from those onland.

5) Geologic history of the Yap Islands and adjacent area are summarized as follows;

Yap micro-plate was formed by subduction of the Pacific plate or North New Gunea plate. The Yap micro-plate formed basalts and their equivalents. The Yap micro-plate has suffered low-grade metamorphism and ocean floor metamorphism to cause greenschists and amphibolites. Transform fault between the Pacific and Yap micro plate made those metamorphics to cataclasites (Yap formation). Drastic change of direction of the Pacific plate took place around 42 Ma, when this transform fault was changed to trench and subduction began. Cataclastic rocks were transported downward trench slope as debris flow and formed debris of the metabasites overlying them.

EPILOGUE

During the cruise, we encountered hearty kindness of the native people of the Yap Islands for their helping our research both on land and sea. We would like to say "Karrimagar" and "Ala Kafel" to all those people. We encountered definitely sad event that Prof. Kazuaki Nakamura's fall down and his death on 7th and 13th August. We would like to express our hearty condolences to his family and at the same time we missed a great earth scientist in the world.

REFERENCES

Note: Papers older than 1934 are quoted in Tayama (1935).

Aoki,H., Ishikawa,M., Misawa,Y. and Egawa, R., The conglomerates of the plutonic and metamorphic rocks of the Yap Islands western Pacific. Mar. Sci., 8, 179-183, 1976.

Bagdanov, L., et al., Initial reports of the geological study of oceanic

crust of the Philippine sea floor. Ofioliti, **2**, 137-168, 1977.

Beccaluva, L., Macciotta, G., Savelli, C., Serri, G. and Zeda, O., Geochemistry and K/Ar ages of volcanics dredged in the Philippine sea (Mariana, Yap and Palau Trenches and Parace Vela Basin). in "the tectonic and geologic evolution of southeast asian seas and Islands." Ed. Hayes D. E., American Geophys. Union., Monograph 23, 268pp., 1980.

Cardwell, R.K., Isacks, B.L. and Karig, D. E., The spatial distribution of earthquakes, focal mechanism solutions, and subducted lithosphere in the Philippine and northern Indonesian islands. In "Tectonic and geologic evolution of southeast Asian seas and islands" ed. Hays, D.E. AGU, 1980.

Carson, B. and Bruns,T.R., Physical properties of sediments from the Japan Trench margin and outer trench slope. Init. Rept DSDP.**78A**,1187-1199,1980

Dewey, J. F., Ophiolite obduction. Tectonophys., **31**, 120, 1976.

Fujioka, K., Furuta, T., Kimura, G., Kodama, K., Koga, K., Kuramoto, S., Matsugi, H.,Seno, T.,Takeuchi, A.,Watanabe, M. and Yamamoto, S.,Sediments and Rocks in and around the Palau and Yap Trenches. In Tomoda, Y.(ed), Prel. Rept. Hakuho Maru Cruise KH 86-1, 38-148, 1986.

Fujioka, K., Geology of the Yap Islands and their adjacent areas. 1987.

Fujita, Y., The Yap orogen and Bonin crustal movement. Mar. Sci., **7**, 518-521, 1975.

Hamilton, W., Tectonics of the Indonesian region. Geol. Surv. Prof. Pap., **1078**, 270-288, 1979.

Hawkins, J. and Batiza, R., Metamorphic rocks of the Yap arc-trench system. Earth Planet. Sci. Lettr., **37**, 216-229, 1977.

Ito, M., Aoki, H., Uetake, H., Kim, Y., Linoshita, Y., Komatsuzaki, M. and Misawa, Y., The origin of the conglomerates of plutonic and metamorphic rocks of the Yap Islands, western Pacific. In "Izu Peninsula." Ed. Hayakawa, M. Tokai Univ. Press, 391-399, 1972.

Miyashiro, A., Evolution of metamorphic belts. J. Petrol.,**2**, 277-311,1961.

Moore, J.C., and Lundberg, N., Tectonic overview of Deep Sea Drilling Project transects of forearcs. Geol. Soc. Amer. Memoir 166, 1-12, 1986.

Shiraki, K., Metamorphic basement rocks of Yap Islands, western Pacific: possible oceanic crust beneath an island arc. Earth Planet. Sci. Lettr., **13**, 167-174, 1971.

Shiraki, K. and Maruyama, S.,Low pressure regional metamorphism in Yap Islands, western Pacific. Abs.Intern. Geodyn. Conf.,Tokyo,152-153, 1978.

Tayama, R., Morphology, geology and coral reef of the Yap Islands. Tohoku Univ., Sci. Rep., 2nd.(Geol.), **57**, 105-137, 1935.

Tokuyama, H., Asanuma, T., Nishiyama, E., Hatori, H., Chiba, H., Ueno, S. and Tomita, N., Multichannel seismic reflection survey. Prel. Rept. of the Hakuho-Maru, KH 84-1., 282-291, 1985.

Tsunakawa, H., Radiometric ages of the igneous activities in the Philippine sea area. Chikyu, **7**, 694-700, 1985.

TABLE 20-2(a) Materials recovered by dredge hauls at station D-7.

No.	X(cm)	Y(cm)	Z(cm)	Weight(g)	Roundness	Rock Name	Remarks
001	21	12	10	2420	SA	Meta-andesite	Mn coated
002	14	13	5	510	SA	Meta-andesite (tuff breccia)	Mn coated
003	12	7	4.5	470	SA	Meta lapilli tuff	Mn coated
004	9	6	4	220	SR	Meta lapilli tuff	Mn coated
005	11	6.5	4	270	SR	Meta lapilli tuff	Mn coated
006	8	5.5	4.5	270	SR	Meta-andesite	Mn coated
007	6	5.5	3	90	SR	Meta-lapilli tuff	Mn coated
008	6	4.5	3	90	SA	Meta-lapilli tuff	Mn coated
009	6.5	4.5	3	70	SA	Meta-lapilli tuff	Mn coated
010	6	4	2	50	SR	Meta-tuff breccia	Mn coated
011	7	4.5	3.5	110	SA	Volcanic breccia	Mn coated
012	6.5	4	2	50	SA	Volcanic breccia	Mn coated
013	6	4	2.5	40	SA	Volcanic breccia	Mn coated
014	6	3.5	2	30	SA	Volcanic breccia	Mn coated
015	5.5	2.5	2	30	SA	Volcanic breccia	Mn coated
016	4.5	3	2.3	40	SA	Meta-tuff breccia	Mn coated
017	5.5	2.5	3.3	40	A	Meta-andesite	Mn coated
018	3	2.5	2	30	SA	Meta-andesite	
019	3.7	2.2	1.5	20	SA	Volcanic breccia	Mn coated
020	3.5	2.4	1.8	10	SR	Tuff	Mn coated
021	3.8	3.8	1.4	10	A	Meta-andesite	Mn coated
022	3.0	2.6	2.2	20	SR	Tuff	
023	3.2	2.7	1.8	10	SA	Meta-tuff	Mn coated
024	4.2	2.1	1.8	10	A	Meta-tuff	Mn coated
025	2.8	2.5	2.2	10	SR	Tuff	Mn coated
026	3.0	2.5	2.0	10	SR	Tuff	Mn coated
027	4.0	3.2	1.0	10	SR	Meta-tuff	Mn coated

TABLE 20-2(b) Materials recovered by dredge hauls at station D-8.

No.	X(cm)	Y(cm)	Z(cm)	Weight(g)	Roundness	Rock Name	Remarks
001	29	15	13	6160	SR	Foram. Ls.	Layered, Photo
002	29	22	5	5130	SR	Foram. Ls.	Shell + rock fragments included, Mn coated
003	26	19	3.5	2110	SR	Foram. Ls.	Coarse grained, shell + rock fr., Mn coated, planar due to bedding
004	26	14	9	3460	SR	Foram. Ls.	Coarse grained, shell + rock fr., Mn coated, planar due to bedding
005	22	13	5	2300	SR	Foram. Ls.	Shell + lithic frts, max.2cmø rock fragment
006	21	10	6.5	1560	SR	Foram. Ls.	Shell + rock fragments
007	19	18	4	1430	SA	Coral Ls.	Coarse grained Closed-up photo
008	18	11	5	1500	SA	Foram. Ss.	Closed-up photo
009	17	14	8	1310	SA	Coral Ls.	Very coarse grained clastics, Closed-up photo
010	21	12	5	1460	SA	Coral Ls.	Mn coated
011	16	14	4.5	1190	SA	Coral Ls.	Coarse grained, Mn-coated
012	16	13	4	1060	SR	Coral Ls.	Coarse lithic, Mn-coated
013	16	11.5	3	620	SA	Foram-coral Ls.	Lithic, planer due to bedding
014	15	11	4	960	SR	Coral Ls.	Coarse, grained
015	15	11	6	1100	SR	Foram-coral Ls.	Very coarse grained
016	15	12	8	1350	SR	Foram-coral Ls.	Very coarse
017	17	11	6.5	1210	SR	Foram-coral Ls.	
018	13	11	3.5	400	SR	Foram-coral Ls.	Coarse grained, coral + shell fr.
019	15	11	5	560	SA	Foram Ss.	
020	13	9	6	440	SR	Foram Ss.	Medium grained, well-sorted
021	14	9	3	350	SR	Foram. Ls.	Mn coated
022	12	10	4	440	SA	Foram. sandstone	
023	15	8	5.5	610	SR	Foram-coral Ls.	Coarse grained
024	15	8	5	540	SA	Foram-coral Ls.	
025	12	10	3	380	SA	Foram. Ls.	Coarse shell
026	12	10	6	620	SR	Foram Ss.	
027	10	8	3.5	320	SR	Foram Ss.	Homogeneous
028	10.5	8	2	270	SR	Coral Ls.	Coarse, coral frag.
029	12	7	4.5	300	SA	Coral Ls.	Lithic, coral, coarse grained
030	13.5	7	4	390	SR	Coral Ls.	Same as 029
031	12	7	6	370	SR	Foram Ss.	Homogeneously medium grained
032	10	9	6	430	SR	Coral Ls.	5cmø coral, Mn coated, closed-up photo
033	11.5	6.5	3.5	230	SR	Foram Ss.	Mn coated
034	10.5	8	1.5	190	SA	Coral Ls.	Lithic, coarse
035	11.5	5	3	230	SA	Lithic Ls.	Coarse
036	11	7	2.5	190	SR	Lithic Ls.	Coarse, Mn coated
037	10	7	2.5	200	SA	Ls.	Lithic + coral fragments
038	11.5	8	2.5	270	SR	Lithic coral Ls.	Coarse
039	10	6	2	170	SA	Lithic coral Ls.	Coarse
040	11	7	3	190	SA	Lithic foram Ls.	Coral frag. included
041	11	7	3.5	210	SR	Ls.	Coarse
042	8	6	5	210	SR	Foram Ls.	
043	11	10	1	160	SA	Foram Ls.	Planar, Mn coated
044	10	7	2.5	210	SA	Coral Ls.	Coarse
045	9	6	4.5	210	SR	Foram Ls.	Mn coated
046	7.5	6	4	210	SR	Foram ls.	Mn coated
047	9	8	3.5	190	SA	Ls.	Coarse, Mn coated
048	9.5	6	4.5	210	SA	Lithic Ls.	Coarse grained

No.	X(cm)	Y(cm)	Z(cm)	Weight(g)	Roundness	Rock Name	Remarks
049	8	5.5	2	90	SA	Ls.	Mn coated
050	8.5	7.5	2.5	160	SR	Foram Ls.	Mn coated
051	8.5	6	3	180	SR	Foram Ls.	
052	8	6	3.5	140	SR	Foram Ls.	
053	8	7	1.5	100	SR	Foram Ls.	Planar
054	10	6	4.5	140	SR	Scoria	
055	9	7	2	110	SR	Foram Ls.	Coarse grained, Mn coated
056	8.5	8	2	100	SA	Foram Ls.	Mn coated
057	8.5	5	3	140	SA	Coral Ls.	Fragmental
058	8	6	2	130	SA	Coral Ls.	
059	8.5	6	3	120	SR	Foram Ls.	Mn coated
060	10	6	4	160	SA	Foram Ls.	Coarse, Mn coated
061	12	7	2.5	210	SA	Foram Ls.	ømas = 1.5cm lithic, Coral rich
062	9	6	5	210	SR	Foram Ls.	
063	8	8	3	210	SR	Foram Ls.	Coarse
064	7	5	5	150	SR	Lithic Ls.	Coarse
065	9.5	5	2	110	SR	Foram Ls.	Coarse
066	8.5	5	2.5	130	SR	Foram Ls.	Very coarse
067	9	8	2	110	SA	Coral Ls.	Mn coated
068	8	7	2	130	SA	Lithic Ls.	Mn coated
069	7	6	2	110	SR	Foram Ls.	Mn coated
070	7.5	5	4	110	SA	Foram Ss.	Fine grained
071	7	4.5	2.5	90	SA	Ls.	Coarse
072	10	5	3	120	SA	Ls.	Coarse, Mn coated
073	8.5	5	5	190	SR	Ls.	Coarse, Mn coated
074	7.5	5	2	70	SA	Ls.	Coarse, Mn coated
075	7	4.5	2.5	90	SR	Ls.	Coarse, Mn coated
076	7	5.5	1	50	SR	Ls.	Coarse, Mn coated
077	7	4	2.5	90	SR	Ls.	Coarse, Mn coated
078	7	5	2	50	SA	Ls.	Coarse, Mn coated
079	7	6	3.5	130	SR	Ls.	Coarse, Mn coated
080	8	5	3	90	SA	Coral Ls.	Coarse, Lithic
081	8	5	3	110	SA	Coral Ls.	Coarse, Lithic
082	7	3.5	2.5	110	SA	Foram Ss.	Fine grained
083	7.5	6	1.5	80	SR	Ls.	Coarse, Mn coated
084	6	5	2.5	120	SA	Ls.	Coarse, Mn coated
085	6	5	4	110	SA	Foram-Coral Ls.	Layered
086	6.5	4.5	1	50	SA	Ls.	Coarse, Mn coated
087	7.5	4.5	2	80	SR	Ls.	Coarse, Mn coated
088	6.5	5	2.5	70	SA	Ls.	Coarse, Mn coated
089	6	6	3	120	SA	Ls.	Coarse, Mn coated
090	7.5	5	2	90	SA	Lithic Ls.	Coarse
091	7	5	3	90	SA	Ls.	Coarse
092	7	5	3	110	SA	Ls.	Coarse, Mn coated
093	6	5	3	70	SA	Ls.	Coarse, Mn coated
094	12	7	2	110	SA	Ls.	Coarse, Mn coated
095	7	4	3	130	SA	Foram Ss.	
096	7	5	1	60	SA	Foram Ss.	
097	6	6	1.5	70	SA	Ls.	Coarse, Mn coated partly
098	7	5.5	3	110	SR	Foram Ls.	Coarse, Mn coated partly
099	6.5	4	3	100	SA	Foram Ss.	Sorted
100	6.5	5	1.5	50	SR	Ls.	Coarse, Mn coated
101	6	4.5	2	50	SR	Coral Ls.	
102	7	5	1.5	60	SR	Ls.	Rather coarse, Mn coated
103	6.5	4.5	3	90	SR	Ls.	Coarse, Mn coated

No.	X(cm)	Y(cm)	Z(cm)	Weight(g)	Roundness	Rock Name	Remarks
104	6	4	1.5	50	SR	Ls.	Coarse, Mn coated
105	5	5	1.5	40	SR	Foram Ss.	Coarse, Mn coated
106	5.5	5	4	90	SR	Ls.	Coarse
107	7	4	3	70	SA	Foram Ss.	Sorted
108	6.5	5	3	70	SA	Foram Ss.	Sorted
109	7	4.5	2	70	SR	Foram Ss.	Coarser
110	5.5	4	2.5	70	SR	Ls.	Coarse, Mn coated
111	7	4.5	3.5	90	SA	Ls.	Coarse
112	7.5	5	2.5	90	SR	Ls.	Coarse, Mn coated
113	6.5	5	4	120	SA	Ls.	Coarse, Mn coated
114	7	6	3	90	SR	Lithic	Coarse, 1.2ø pebble, closed photo
115	7.5	3.5	3	70	SR	Foram Ss.	
116	7	4.5	2.5	70	SA	Foram Ss.	
117	6.5	5	2	70	SA	Foram Ss.	Mn coated partly
118	5.5	4	3	50	SR	Foram Ss.	Coarser
119	5.5	4.5	2.5	60	SR	Foram Ss.	Mn coated
120	5	4.5	2	40	SR	Ls.	Very coarse
121	7.5	5	1.5	50	SA	Foram Ss.	
122	6	5	3.5	80	SA	Ls.	Coarse, Mn coated
123	6.5	5	2	70	SR	Ls.	Coarse, Mn coated
124	5	4.5	1.5	40	SR	Ls.	Coarse, Mn coated deeply
125	5.5	5	1.5	50	SR	Ls.	Coarse,
126	5.5	5	2.5	50	SR	Foram Ss.	Mn coated
127	6	4.5	1.5	50	SR	Ls.	Coarse
128	25	19	15	8340	SA		
129	17	16	12	2710	A		Pillow lava structure
130	16	13	6	1810	A		Close up
131	14	11	6	1070	A		
132	14	8.5	7	840	SA		
133	15	9	7	510	A	Ls.	Foraminifera sandstone
134	11	10	6	600	A	Lapilli tuff	
135	11.5	6.5	6.5	550	A		
136	10.5	6	6	510	A		
137	10.5	7	5	580	A		
138	11	7	4	390	SA	Siltstone	
139	10	8	4	440	SA		
140	10	4	4	290	SA	Meta-Lapilli tuff	
141	10	6	4	280	A	Meta-tuff	
142	9	7	4	310	SA		
143	8	7	4	240	A	Meta-tuff breccia	
144	7	4.5	3	160	SA		
145	8	5.5	5	300	A	Meta-basalt	
146	9	6	4	290	A	Meta-basalt	
147	6	5	2.5	140	SA	Meta-tuff	
148	8	4.5	4	160	SA		
149	6	5	4.5	180	A	Meta-tuff	
150	7.5	4.5	2.5	150	A	Meta-basalt	
151	6	4	3	130	A		
152	7	5	3	130	SA		Mn coated
153	6	5	4	160	SA		
154	5	4	3	120	A		
155	5	3.5	3	80	A		
156	4.5	4	2.5	100	A		
157	6	5	2.5	100	SA		
158	4.5	3	2.5	80	A		

No.	X(cm)	Y(cm)	Z(cm)	Weight(g)	Roundness	Rock Name	Remarks
159	6.5	3	3	70	SR		
160	10	6	3	260	A	Meta-tuff breccia	Close up
161	8	4	2	45	SA		
162	7	4	1.5	20	A		
163	7	3	1	20	SA		
164	5	4	2	35	SR		
165	5	4	3	60	R		
166	6	3	2	25	SA		
167	5	3	3	25	SA		
168	5	3	1	20	SR		
169	6	3	1	15	R		
170	5	3	2.5	20	SR		
171	5	3	2	30	R		
172	5.5	3	2.5	35	R		
173	5.5	4	2.5	70	SA		
174	6.5	2.5	2.5	40	R		
175	6	3	1.5	50	A		
176	5	4	2.5	50	R		
177	5	3	2	25	SR		
178	4.5	4	2	25	R		
179	4.5	4	2	30	SR		
180	6	4	2	40	R		
181	4.5	4	2	35	R		
182	6	3	1.5	25	R		
183	5	4	1.5	35	R		
184	6	3	1	20	SR		
185	4.5	3.5	2	35	R		
186	7	3	1	20	SA		
187	4	3	1.5	35	SA		
188	4.5	4	2.5	25	A		
189	4	3	2.5	35	R		
190	4	3	2	25	SR		
191	5	4	3	40	SA		
192	5	3.5	2	30	R		
193	5	4	1.5	20	R		
194	6	3	2	30	SA		
195	5	3	2	35	SA		
196	5	3	2	40	R		
197	4.5	3.5	2	30	R		
198	4	3.5	2.5	30	R		
199	4	3.5	2.5	45	R		
200	5.5	3	1	20	SR		
201	5	4	2	30	SR		
202	5	2.5	2	30	R		
203	3.5	3	2.5	30	SR		
204	3.5	3.5	2	40	SR		
205	5	3.5	1.5	20	R		
206	3	2.5	2.5	30	SR		
207	4	3	2.5	40	R		
208	5	2	1	20	SR		
209	4	3	1.5	20	SR		
210	5	4.5	1.5	30	SR		
211	4.5	3	2	25	R		
212	4	3	2.5	30	R		
213	4.5	2.5	1.5	15	SR		

No.	X(cm)	Y(cm)	Z(cm)	Weight(g)	Roundness	Rock Name	Remarks
214	4	3	2.5	20	SA		
215	4	3	2	20	R		
216	5.5	2.5	1	10	A		
217	4.5	3	1	20	SR		
218	4	3	2.5	20	SR		
219	5	3.5	1.5	20	R		
220	5	2.5	1	10	SR		
221	4	3	1	15	R		
222	3.5	3	2	25	SR		
223	4	3.5	1	10	SA		
224	3	2.5	2.5	30	A		
225	3	2.5	2	20	R		
226	5	3.5	2.5	25	SR		
227	4.5	3.5	2	20	R		
228	3.5	3	1	20	SA		
229	3.5	3	2	20	R		
230	4	2.5	1.5	20	SA		
231	4	3	2	20	R		
232	3	3	2	20	SR		
233	4	3.5	2	25	R		
234	4	3.5	1	15	SR		
235	3.5	3	1	20	R		
236	4	3	1	20	SA		
237	3.5	2.5	2	15	SR		
238	3.5	2.5	1.5	15	R		
239	4.5	2.5	1	15	A		
240	3	3	1.5	20	R		
241	4	2.5	1.5	15	A		
242	4	3	1.5	15	SR		
243	4.5	3	1.5	20	SR		
244	3	3	1.5	15	R		
245	3	2.5	2	20	R		
246	4	2.5	2	10	R		
247	3.5	3.5	1	15	R		
248	5	2.5	2	20	SR		
249	4	3	1.5	25	SR		
250	4	3	2	25	R		
251	4	3	2	15	A		
252	4	3.5	0.5	20	SA		
253	4	2.5	1	15	SR		
254	3	3	2	20	SR		
255	4.5	2.5	1	15	R		
256	3.5	3	1	10	SA		
257	3.5	2	1.5	15	R		
258	3.5	2.5	1.5	15	R		
259	3	2.5	2	15	R		
260	3	2.5	2	15	SR		
261	3	2	2	20	SA		
262	3	2.5	1.5	15	SA		
263	4	3	0.5	10	SA		
264	3.5	2.5	1.5	15	R		
265	3	2.5	2	20	R		
266	4	3	1	10	SR		
267	3.5	2.5	2	20	R		
268	3.5	2.5	2	15	R		

No.	X(cm)	Y(cm)	Z(cm)	Weight(g)	Roundness	Rock Name	Remarks
269	3	2.5	1	15	R		
270	4	2.5	1	10	SA		
271	3	2	1	10	SR		
272	3.5	2.5	1	10	SR		
273	4	3	1	10	A		
274	3	2.5	1.5	10	R		
275	4	2	1.5	15	SR		
276	3	2	1.5	10	SR		
277	3	2	1	10	SR		
278	4	2	1.5	15	A		
279	3.5	2.5	1	20	SR		
280	4	2	1.5	15	SA		
281	3	2	1	10	SA		
282	3	1.5	1	15	SR		
283	3	2	1.5	15	R		
284	3	3	1.5	15	R		
285	3.5	2	1.5	10	SR		
286	3	2	1.5	15	SR		
287	3	2.5	1.5	20	SR		
288	3	2	1	15	SR		
289	3	2	1	10	A		
290	3	2	1.5	15	SA		
291	3	1.5	1	15	SA		
292	3	1.5	1.5	15	SR		
293	3	2.5	1	10	R		
294	3	1.5	1.5	15	SR		
295	2.5	1.5	1.5	15	SA		
296	3.5	2.5	0.5	10	R		
297	3.5	2.5	1	10	SA		
298	2.5	2	1.5	10	R		
299	3	2	1.5	15	SR		
300	3.5	2	1.5	15	R		
301	3	2	1.5	15	SA		
302	3	2	1	20	R		
303	3	2.5	1.5	15	SR		
304	2.5	2	1.5	15	SR		
305	3	2	1.5	10	R		
306	2.5	2.5	1.5	15	SR		

TABLE 20-2(c) Materials recovered by dredge hauls at station D-9.

No.	X(cm)	Y(cm)	Z(cm)	Weight(g)	Roundness	Rock Name	Remarks
001	56	31	8	10000	SR	Andesite Meta-Pumice tuff	Very flatly
002	32	24	13	10000	SA	Greenschist	
003	24	19	11	4810	A	Meta-Lapilli tuff	
004	13	11	10	2100	A	Meta-tuff	Sharp plane
005	21	14	5	1400	A	Meta-tuff breccia	Mn coated
006	18	11	8	1720	SR	Meta-Lapilli tuff	
007	16	9	8	1530	R	Ultra-matic	Thin Mn coated
008	11	9	8	1210	A	Amphibolite	Crack
009	10	9	8	1010	SR	Tuff breccia (acidic)	Mn coated
010	11	9	6	1190	SA	Meta-Lapilli tuff	Parallel vein
011	12	10	7	780	SA	Meta-Volcanic breccia	Mn coated
012	10	8	6	550	SR	Dierite	Mn coated
013	10	6	5	620	SA	Meta-tuff	
014	10	8	5	400	SR	Meta-Lapilli tuff	Mn coated
015	9	7	6	370	SR	Tuff breccia (acidic)	Mn coated
016	9	6	5	300	SA	Diorite	Mn coated
017	6	6	5	330	SA	Meta-Lapilli tuff	Mn coated
018	8	6	5	230	SA	Meta-tuff breccia (acidic)	Mn coated, porous surface
019	10	6	4	290	A	Greenschist (Meta-Lapilli tuff)	
020	9	7	5	280	SR	Meta-Volcanic breccia	Weak Mn coated
021	10	5	4	280	SR	Micro diorite	Mn coated
022	10	7	4	310	A	Greenschist (Meta-tuff)	
023	7	5	3	190	A	Amphiborite	Weak Mn-coat
024	9	6	4	240	SA	Greenstone	
025	8	7	3	130	A	Meta-Volcanic breccia	Weak Mn coated
026	6	5	5	200	SA	Greenstone (Ultra?)	Weak Mn coated, sharp plane
027	7	5	4	110	SR	Meta-tuff breccia	Weak Mn coated
028	8	6	4	160	SR	Tuff breccia	Mn coated
029	7	5	5	190	SA	Greenstone (Meta-Lapilli tuff)	Weak Mn coated, sharp plane
030	7	6	4	140	SA	Greenstone tuff breccia	Weak Mn coated
031	8	5	4	130	SR	Meta-tuff breccia (acidic)	Mn coated, irregular surface
032	8	4	4	160	SR	Meta-Lapilli tuff	Schist, Mn coated
033	7	6	4	140	A	Meta-tuff	
034	6	4	3	120	SR	Amphibolite	Mn coated
035	8	4	4	70	R	Greenstone	Weak Mn coated
036	8	4	3	150	SR	Meta-tuff	Weak Mn caoted
037	8	5	3	130	SA	Meta-Lapilli tuff	Weak Mn coated, folded schist
038	6	5	4	120	R	Meta-tuff	Mn coated
039	6	5	3	110	A	Lapilli-tuff	Mn coated
040	7	5	4	100	SA	Meta-tuff breccia	Weak Mn caoted
041	6	4	4	90	SR	Meta-tuff breccia	Weak Mn caoted
042	6	4	5	110	SA	Greenstone	Mn caoted, sharp plane

No.	X(cm)	Y(cm)	Z(cm)	Weight(g)	Roundness	Rock Name	Remarks
						Meta-basalt	
043	5	4	2	70	SA	Greenschist	Mn coated
044	8	4	2	90	SA	Meta-Lapilli tuff	Weak Mn coated, schistosity
045	6	4	3	100	SR	Amphibolite	Mn coated
046	6	5	3	100	SA	Greenschist (Meta-tuff)	Weak Mn coated
047	5	3	3	50	A	Greenschist (Meta-tuff)	Weak Mn coated
048	6	4	4	100	SR	Greenstone tuff breccia	Mn caoted
049	6	5	3	90	SR	Greenschist Meta-Lapilli tuff	Mn coated
050	6	4	4	70	A	Greenschist	Weak Mn coated, sharp plane
051	5.5	2.5	3	60	SA	Ultramafic (?)	Mn coated
052	6	5.5	2.5	110	SA	Meta-basalt	Mn coated
053	5.5	4.5	3	130	SA	Meta-tuff	Mn coated
054	5	4.5	3	80	SR	Greenschist	Mn coated
055	4	3.5	2.5	50	SA	Metabasalt	Mn coated
056	6.5	4	2.5	90	SA	Meta-tuff	
057	6.5	4	3	80	SA	Greenstone	Mn coated
058	5.5	4	3.5	90	A	Metabasalt	Partly Mn coated
059	6	3.5	3	70	SA	Greenstone	Partly Mn coated
060	6	3.5	3	80	SA	Greenstone	Mn coated
061	5	4	3	60	SA	Greenstone	Mn coated
062	4.5	3	2.5	40	SA	Meta-basalt	Partly coated
063	4	4.5	3	50	SA	Greenstone	Partly coated
064	5	4	2.5	70	SA	Meta-basalt	Partly coated, week fissility
065	6	5	3	110	SA	Meta-tuff	Partly coated
066	5	3.5	3	60	SA	Meta basalt	Mn coated
067	4.5	4	3	50	SA	Ultramafic ?	Partly Mn coated
068	5.5	3.5	3	70	SA	Meta-Lapilli tuff	Weekly foliated
069	5.5	5	2	50	SA	Meta-basalt Tuff breccia(acidic)	Partly coated
070	5	5	2.5	70	SA	Greenschist (Lapilli tuff)	Mn coated
071	5	4	2	60	SR	Surpentinite	Mn coated completely
072	4	3.5	2.5	50	SA	Greenstone	Mn coated
073	5	5	3.5	80	SA	Greenstone	Mn coated
074	5	5	2	70	SA	Meta-tuff	Mn coated partly
075	5	3	1.5	50	SA	Meta-basalt	Mn coated partly
076	5	5	2	50	SA	Meta-tuff	Mn coated partly
077	4.5	3.5	3	60	SR	Meta-tuff	Mn coated completely
078	6	4.5	3	90	SA	Meta-basalt	Mn coated completely
079	5	4	3	70	SA	Meta-Lapilli tuff	Mn coated completely
080	5.5	5	3	140	SA	Meta-Lapilli tuff	Mn coated completely
081	5.5	5	2.5	100	SA	Meta-tuff	Mn coated completely
082	4.5	4.5	3	90	SA	Meta-Lapilli tuff	Mn coated completely foliation
083	5.5	4	2.5	60	SA	Meta-Lapilli tuff	Mn coated partly
084	4.5	4	2.5	50	SA	Meta-tuff	Mn coated partly
085	6	4	2.5	70	SR	Meta-tuff	Fissility
086	5	4	2.5	60	SA	Meta-Lapilli tuff	Week foliation
087	4.5	4.5	2.5	50	SA	Ultramafic	Mn coated completely
088	5.5	4.5	3	40	SA	Tuff breccia	Mn coated completely
089	5.5	4.5	2	70	SR	Meta-Lapilli tuff	Mn coated completely
090	4	4	2.5	40	SA	Meta-tuff	Mn coated completely

No.	X(cm)	Y(cm)	Z(cm)	Weight(g)	Roundness	Rock Name	Remarks
091	4	3.5	2.5	50	SA	Greenstone	Mn coated completely
092	6	4	2.5	70	A	Greenschist	Mn coated
093	5.5	3	3	70	SA	Meta-basalt	Mn coated completely
094	4.5	4	2	50	SA	Greenschist (Lapilli tuff)	
095	6.5	3	0.5	20	SA	Greenschist (Lapilli tuff)	Mn coated
096	5.5	4	3.5	70	SA	Meta-basalt	Mn coated completely
097	5	2.5	2	50	A	Meta-basalt	Mn coated partly
098	4.5	3.5	2	50	A	Greenschist	
099	5	3	2.5	50	SA	Greenschist	
100	5	4	2.5	50	SA	Meta-tuff	Mn coated completely
101	5	3	3	50	A	Meta-tuff	Mn coated
102	5	4.5	3	30	A	Foram Ss.	
103	4.5	4.5	3	60	A	Greenschist Meta-Lapilli tuff	
104	4.5	3.5	2.5	40	A	Meta-Lapilli tuff	Mn coated completely
105	3.5	3.5	2.5	30	A	Meta-basalt	Mn coated partly
106	4	2.5	2.5	30	A	Meta-basalt	
107	4	4	1.5	40	SA	Meta-Lapilli tuff	
108	4.5	3	2.5	40	SA	Meta-tuff	Mn coated partly
109	5	4	2	50	SA	Greenschist	Mn coated completely
110	4	3.5	2	30	SA	Greenschist	
111	5	3	1	10	SR	Foram Ss.	Mn coated partly
112	5	3.5	2.5	40	SA	Greenschist	
113	5	3	1.5	40	SA	Greenschist Meta-tuff	
114	4	3	2	30	SA	Meta-tuff	
115	5.5	4	3	60	SA	Meta-basalt	Mn coated completely
116	5	3	2.5	40	SA	Greenstone	
117	4.5	3.5	3	40	SA	Meta-Lapilli tuff	
118	4	3	2	30	SR	Meta-Lapilli tuff	Mn coated completely
119	4.5	3.5	2.5	40	SA	Greenstone	
120	4.5	3.5	2	40	SA	Meta-Lapilli tuff	Mn coated completely

TABLE 20-2(d) Materials recovered by dredge hauls at station D-10.

No.	X(cm)	Y(cm)	Z(cm)	Weight(g)	Roundness	Rock Name	Remarks
001	7.5	5.5	2.3	130	SA	Greenstone	
002	6.2	5.6	0.5	30	A		Mn-crust with angular granule
003	6	4.5	0.5	20	A		Mn-crust with angular granule
004	5	2.8	0.4	10	A		Mn-crust with angular granule
005	3.7	2	0.5	5	A		Mn-crust with angular granule
006	3	2	1	10	SA	Amphibolite	

TABLE 20-2(e) Materials recovered by dredge hauls at station D-11.

No.	X(cm)	Y(cm)	Z(cm)	Weight(g)	Roundness	Rock Name	Remarks
001	25	21	10	8760	SA	Metabasalt	Mn coated weakly
002	22	12	9	3450	SA	Metabasalt	
003	19	13	10	3030	SA	Metabasalt	
004	15.5	12	8.5	2660	A	Metabasalt	
005	18.5	9	7	2150	SA	Metabasalt	
006	17	12	7.5	2060	SA	Greenschist	
007	15	11	9	1790	SA	Meta lapili-tuff	
008	13	12	9	1630	SR	Schistose amphibolite	Closed up photo
009	19	7	7	1330	A	Metabasalt	
010	25.5	14	9	2260	A	Metabasalt	
011	19	12	9	2310	SA	Metabasalt	
012	15	12	9	2640	SA	Metabasalt	
013	15	10	9	1920	SA	Metabasalt	
014	15	11	9	1540	SA	Metabasalt	
015	15	11	7	1350	A	Metabasalt	
016	15	10	8	1010	A	Metabasalt	
017	10	10	9	1340	SA	Amphibolite	
018	12	8	8	1320	SA	Amphibolite	
019	13	10	7	1150	A	Metabasalt or Amphibolite	Mn coated completely
020	12	8	7	1210	A	Amphibolite	
021	14	8	7	1250	SA	Metabasalt	
022	13	8	8	1430	A	Amphibolite(?)	Mn coated
023	13	9	7	1130	SA	Greenschist	
024	17	8	3.5	600	SA	Greenschist	
025	11.5	11	5	750	SA	Greenschist	
026	15	9	6	1170	A	Greenschist	
027	12	8	4	710	SR	Greenschist	
028	12	7	4	490	SR	Greenschist	
029	9	7	5	610	A	Metabasalt	
030	10	7	5	540	SA	Greenschist	
031	12	7	5	710	SR	Greenschist	
032	13	6	5	730	A	Metabasalt	
033	12	7	6	670	A	Greenschist	
034	12	9	7	700	A	Greenschist	
035	11	7	4	660	SA	Amphibolite	
036	9	6	6	760	SA	Metabasalt	
037	8.5	7	4	520	SA	Greenschist	
038	12	8	6	630	A	Amphibolite	
039	11	8	4	670	SR	Greenschist	
040	11	8	5	490	A	Amphibolite	
041	12	9	5	540	SA	Greenschist	
042	10	7	7	660	SA	Amphibolite	
043	9	8	6	610	SR	Amphibolite	
044	9	7	5	400	A	Amphibolite	
045	10	7	6.5	590	SA	Amphibolite	
046	12	7	4.5	550	SA	Greenschist	
047	11	8	6	530	SA	Amphibolite	
048	12	5	5	450	A	Amphibolite	
049	9	6	5	390	SA	Metabasalt	
050	10	7	6	540	SA	Amphibolite	

No.	X(cm)	Y(cm)	Z(cm)	Weight(g)	Roundness	Rock Name	Remarks
051	9	7	6	420	A	Amphibolite	Closed up photo
052	10	7	5	430	SA	Greenschist	
053	9.5	5.5	4	390	A	Amphibolite	
054	12	7	3	450	SA	Greenschist	
055	10	7	5	650	SA	Amphibolite	
056	9	6	5	490	A	Amphibolite	Closed up photo
057	7	7	6	370	SA	Foram Ss.	
058	9	8	6	630	SA	Greenschist	
059	9	8	5	430	SA	Amphibolite	
060	11	6	4	410	A	Metabasalt	
061	11	7	5	450	SA	Amphibolite	
062	10	10	5	450	SA	Amphibolite	
063	11	7	2	230	SA	Greenschist	
064	8	6	5	270	SA	Amphibolite	
065	8	8	5	280	SA	Amphibolite	
066	8.5	8	4	350	SR	Greenschist	
067	10	8	4	330	SA	Serpentinite	Turk
068	9	6	6	390	SA	Amphibolite	
069	12	6	5	430	SR	Metabasalt	
070	10.5	6	3.5	330	SA	Amphibolite	
071	9	4	4.5	310	SA	Amphibolite	
072	14.5	5	4	290	A	Greenschist	
073	9	5.5	4.5	320	SA	Amphibolite	Slightly foliated
074	9	4.5	4.5	410	SA	Greenshcist	
075	10	6	4	390	SA	Greenschist	
076	10	7	4.5	390	SA	Greenschist	
077	9	8.5	4.5	380	SA	Greenschist	
078	10	6	5	380	A	Metabasalt	
079	9	8	3	300	SA	Greenschist	
080	11	6	5	270	A	Amphibolite	
081	10	7	4	350	SA	Greenschist	
082	7.5	6	4.5	310	SA	Greenschist	
083	9	7	2	290	SA	Greenschist	
084	7.5	5	4.5	290	SA	Amphibolite	
085	8	6	2.5	250	SA	Amphibolite	
086	7.5	7	5	310	SA	Amphibolite	
087	8.6	6	3	270	SA	Amphibolite	
088	11	5	3	310	SA	Amphibolite	
089	9	6	4.5	170	A	Amphibolite	
090	11	5	4	260	SA	Amphibolite	
091	7	6.5	4.5	260	SA	Amphibolite	
092	7	5.5	5	160	A	Amphibolite	A breccia in crystaline ls
093	6.5	4.5	4	160	SA	Amphibolite	
094	8	4.5	5	230	SA	Amphibolite	Well foliated
095	8	7	6	270	SA	Amphibolite	
096	11	4	4	310	A	Amphibolite	
097	8	6	4	210	SA	Amphibolite	
098	8	8	5	270	SA	Amphibolite	Attached by matrix of crystaline ls
099	8	7	4.5	330	A	Amphibolite	
100	7	5	3	200	A	Amphibolite	
101	9	6	5	290	SA	Amphibolite	
102	9	6	6	240	A	Amphibolite	Intercalated by plagio-rich band (wethered)
103	8	6	5	230	A	Amphibolite	
104	7	5.5	5	280	A	Greenschist	
105	8	5.5	5	310	SA	Amphibolite	

No.	X(cm)	Y(cm)	Z(cm)	Weight(g)	Roundness	Rock Name		Remarks
106	9	6	5	280	A	Metabasalt		
107	7	6	5	200	SA	Amphibolite		
108	8	4	3	210	A	Schistose Am.		
109	9.5	6	3.5	230	SA	Amphibolite	Schistosity	
110	8	6	3.5	210	SA	Amphibolite		
111	7	4.5	4	150	SA	Amphibolite		
112	8	5	3.5	160	A	Amphibolite		
113	6.5	5.5	3	140	SR	Amphibolite		
114	8.5	5.5	2.5	130	SA	Schistose Am.	Coarse	Closed up photo
115	6	5	3	160	A	Meta-Rhyolite		
116	7	5	4.5	220	SA	Metabasalt		
117	7	6.5	6	280	SA	Amphibolite		
118	8.5	5	5	290	SR	Amphibolite		
119	7.5	5	4	200	A	Greenschist		
120	9	6	4	280	SA	Schistose Am.		
121	8	6	3	250	SA	Amphibolite		
122	6.5	3.5	4	160	SA	Amphibolite		
123	7	5	4	190	SA	Amphibolite		
124	10	5.5	5	190	SA	Greenschist		
125	10	5	4	220	A	Amphibolite		
126	8.5	5	3	140	SA	Amphibolite		
127	8	6	5	220	SA	Amphibolite		
128	8	6	5	250	SA	Amphibolite		
129	12	5	3	170	SA	Schistose Am.		
130	7	5	5	210	A	Amphibolite		
131	9	6	3.5	200	SA	Amphibolite		
132	6	6	3.5	150	SA	Amphibolite		
133	5.5	4	3.5	100	SA	Amphibolite		
134	7.4	4	2.5	120	SA	Amphibolite		
135	7.5	5	5	230	A	Amphibolite		
136	10	4	4	260	SA	Amphibolite		
137	8	4	5	200	SA	Greenschist		
138	9	4	2	100	SA	Amphibolite		
139	7.5	4	3.5	150	SA	Amphibolite		
140	8.5	6.5	2	120	SA	Greenschist		
141	7	6	3.5	170	A	Amphibolite		
142	8	5.5	4	180	A	Amphibolite		
143	9	5	3.5	200	SA	Greenschist		
144	11	5	2.5	190	A	Metabasalt		
145	9	7	2.5	220	SA	Amphibolite		
146	8	6	5	200	SA	Amphibolite		
147	6	5	4	140	SA	Amphibolite		
148	7	5	3	140	SR	Amphibolite		
149	8	7	3	210	SA	Greenschist		
150	6	5	3	150	SA	Amphibolite		
151	8	6	4	190	SA	Amphibolite		
152	7	6	5	220	SA	Amphibolite		
153	10	5	3	170	SA	Amphibolite		
154	9	6	5	230	SA	Layered Am.		
155	8	5	3	170	SA	Amphibolite		
156	8	4	4	140	A	Amphibolite		
157	7	5	4	130	SA	Amphibolite		
158	6	4	3	110	SR	Greenschist		
159	8	5	4	150	A	Amphibolite		
160	7	5.5	3	140	SR	Greenschist		

No.	X(cm)	Y(cm)	Z(cm)	Weight(g)	Roundness	Rock Name	Remarks
161	6	5	3	100	SA	Amphibolite	
162	6	5.5	3	80	SR	Marble Ls.	Closed up photo
163	8	5	3	80	SA	Marble Ls.	Closed up photo
164	5	4.5	3	70	SR	Marble Ls.	
165	7	4	3.5	100	SR	Marble Ls.	
166	6	4.5	3	70	SR	Marble Ls.	Closed up photo
167	7	4	2	50	SR	Layered Am.	White part dominant
168	6	4.5	2.5	70	SA	Layered Am.	
169	7	4.5	3.5	110	SR	Layered Am.	White part dominant
170	7	5	4	140	SR	Marble Ls.	
171	7.5	7	4.5	160	SA	Layered Am.	White part dominant
172	5.5	5.5	4	110	SR	Sandstone	Parallel laminated
173	5.5	3.5	3	60	SR	Meta-tabbro	
174	5.5	3	2	30	SR	Layered Am.	White part
175	4.5	4	1	30	SR	Marble Ls.	Calcareous sandstone
176	5.5	5	1.5	30	SA	Marble Ls.	
177	6	4.5	3.5	70	SA	Layered Am.	White
178	4.5	4	2	30	SR	Marble Ls.	Granular, pure
179	4.5	4	2	30	SR	Marble Ls.	
180	4.5	2	1.5	10	SR	Marble Ls.	
181	3.5	3.5	1.5	20	SR	Meta-gabbro	
182	5.0	3.0	0.5	10	SR	Marble Ls.	Another half of #178
183	8	6	3	170	SA		
184	7	4.5	4.5	150	SR		
185	6	5.5	4	180	R		
186	7	4	4	85	SA		
187	7.5	4.5	2.5	145	SR		
188	7.5	4.5	3	105	SA		
189	6	4	3.5	140	SR		
190	7.5	5	3.5	140	SA		
191	7.5	4.5	3.5	125	SA		
192	8	5	3	110	A		
193	7	4.5	3	105	SA		
194	6	5	4	125	R		
195	7	4.5	3	125	SR		
196	5.5	5	3.5	125	R		
197	6	5.5	3	120	SR		
198	6.5	4	3.5	115	SA		
199	5.5	4.5	4.5	115	R		
200	8	4.5	2	85	A		
201	6	5	3	130	R		
202	7.5	4	2.5	95	SA		
203	6	4.5	3	115	R		
204	7	3.5	3	85	SA		
205	6	4.5	2	95	SA		
206	6.5	5	1.5	80	SA		
207	7.5	6	1	70	SA		
208	6	4	2.5	95	SA		
209	5.5	4	2.5	85	SR		
210	5.5	4	3.5	115	R		
211	6	4	3.5	95	SR		
212	5	4.5	3	75	SR		
213	5	4	3.5	80	SA		
214	7	4	1.5	90	SA		
215	5.5	4.5	2.5	110	SR		

No.	X(cm)	Y(cm)	Z(cm)	Weight(g)	Roundness	Rock Name	Remarks
216	6	3	2.5	70	SA		
217	4.5	4	3.5	70	A		
218	5.5	3	2.5	85	SR		
219	6	3	3	65	SR		
220	6.5	4	2.5	75	SR		
221	5	4	2	60	SA		
222	6	3.5	2.5	70	SA		
223	6	5	1.5	70	SA		
224	5	4	2.5	75	R		
225	5.5	3.5	2.5	70	R		
226	5.5	3	3	65	SR		
227	7	4	1	50	SA		
228	6	3.5	3	50	A		
229	5.5	4.5	1.5	50	SA		
230	5	3	3	65	SR		
231	5.5	4	3	65	R		
232	6	3	2	60	A		
233	5	4.5	3	75	SR		
234	4	3.5	3	60	SR		
235	6	3	3	75	R		
236	6	3.5	2.5	60	SA		
237	5	4	3	80	R		
238	5	3	3	60	SR		
239	5	2.5	2.5	50	SR		
240	4	3	2.5	60	R		
241	5	3	2	70	SR		
242	5.5	3.5	2	65	SR		
243	5	3.5	3	55	A		
244	5	3.5	3	65	SR		
245	4	4	2.5	50	SA		
246	4	3.5	3	65	R		
247	4.5	3	3	65	R		
248	4.5	3	2.5	65	R		
249	4.5	4	3	60	R		
250	4.5	3.5	3	60	SR		
251	5	3	3	65	SR		
252	6.5	4	2	60	SA		
253	4.5	4	2.5	55	SA		
254	5	4	2.5	55	SR		
255	6	3	1.5	50	SR		
256	4.5	4	2	55	SR		
257	6	3.5	2	50	SA		
258	6	3	2	60	R		
259	5	3	2	50	SR		
260	4	3.5	2	60	R		
261	6	3	1.5	50	R		
262	5	3	2	25	A		
263	4.5	3.5	2	50	R		
264	5	3	2	40	SR		
265	6	4.5	3	95	SR		
266	7	4	1.5	60	SA		
267	4	3.5	2	35	A		
268	5.5	3	2	40	A		
269	4	3	2.5	50	R		
270	5	3.5	2.5	55	R		

No.	X(cm)	Y(cm)	Z(cm)	Weight(g)	Roundness	Rock Name	Remarks
271	4.5	3	2	40	SA		
272	5.5	3	1	40	SR		
273	4.5	3.5	3	55	SR		
274	5	3	1.5	50	SR		
275	4	3	3	50	R		
276	6	3	2	50	SA		
277	3.5	3.5	1.5	45	SR		
278	4.5	4.5	3	60	SA		
279	4.5	4	2	50	SR		
280	4	3.5	2	40	SR		
281	4	3	2	35	SA		
282	4.5	3	2	50	SR		
283	4.5	3.5	3	55	SR		
284	4	3	2	30	SR		
285	3.5	3	2.5	45	SR		
286	4.5	3	2	30	SR		
287	4.5	3	1.5	35	SA		
288	5	3	0.5	25	SR		
289	5	2.5	1.5	30	R		
290	5.5	3.5	1.5	30	SA		
291	4.5	3	1.5	30	SR		
292	4.5	3	3	45	SR		
293	4.5	2.5	2	35	R		
294	4	3	2	40	SR		
295	3.5	3	2	35	R		
296	4	2.5	2	35	R		
297	5	3	2	35	SA		
298	4.5	3	2	30	R		
299	4	3	2	40	SR		
300	4.5	3	2.5	50	SR		
301	3.5	3.5	2.5	50	SR		
302	4.5	2.5	2	60	R		
303	3	3	2.5	40	R		
304	4.5	4	2	50	R		
305	5	2.5	2	30	SR		
306	4	3	2.5	40	SA		
307	4	3.5	3	40	R		
308	3.5	2.5	2	40	R		
309	4.5	3	1.5	30	R		
310	5	3	2	40	SR		
311	4	2.5	1.5	30	SR		
312	3	3	1.5	30	R		
313	4.5	2.5	2	25	SR		
314	5	2.5	1.5	35	R		
315	4	3	2	40	SA		
316	6	2	1	30	SR		
317	4.5	3.5	1.5	30	SR		
318	3.5	2.5	2	25	SA		
319	5	2	2	40	SR		
320	4.5	3	1.5	30	SR		
321	4	3	2	40	SR		
322	3	3	1.5	25	SR		
323	4	3	1.5	35	R		
324	3.5	3	1.5	25	R		
325	3	2.5	1.5	25	R		

No.	X(cm)	Y(cm)	Z(cm)	Weight(g)	Roundness	Rock Name	Remarks
326	4.5	2	1.5	20	R		
327	4	2.5	2	15	SA		
328	3	3	1	20	R		
329	4	2	2	25	SR		
330	4.5	1.5	1	25	SR		
331	4.5	2.5	1.5	35	SR		
332	4.5	2	1.5	30	SR		
333	4	3	2	30	SR		
334	3	2.5	1.5	20	SR		
335	3.5	3	2.5	40	R		
336	4	3	1.5	30	SR		
337	4	2	2	20	SA		
338	4	3	2	40	R		
339	3.5	2	1.5	20	SR		
340	3.5	2.5	1.5	30	R		
341	4.5	2.5	2	40	SR		
342	4	2.5	1.5	25	SR		
343	4	2	2	25	R		
344	2.5	2.5	2	20	SR		
345	3.5	2	2	20	SR		
346	4	2.5	1.5	15	SR		
347	3	2	1.5	20	R		
348	3.5	2	1.5	20	SR		
349	3	3	2	25	R		
350	2.5	2.5	2	20	R		
351	3	2	1.5	25	R		
352	4.5	2	1	15	R		
353	3	2.5	2.5	25	SR		
354	3.5	2.5	2	20	R		
355	7	4.5	3	150	R		
356	6	5	3.5	130	SR		
357	5.5	5	5	185	R		
358	8	4	2.5	100	R		
359	6	4.5	3	120	SR		
360	6	4.5	2.5	90	SA		
361	6	4	2.5	105	R		
362	6	5	4	170	R		
363	8	5	2.5	145	R		
364	8.5	5	2.5	130	SR		
365	7	3	3	135	R		
366	5.5	3.5	2.5	95	R		
367	6	5	2	85	SR		
368	5	4	3	110	R		
369	6	4	2.5	105	R		
370	4.5	4	3	110	R		
371	5	4	2	95	R		
372	5	4	2.5	100	R		
373	5	4	2	75	R		
374	5	3	2.5	50	R		
375	5.5	3.5	3	80	SA		
376	5	5	2.5	80	R		
377	5.5	4.5	1.5	55	SR		
378	5.5	4	2	70	R		
379	5	4	3	85	R		
380	5	3.5	2.5	65	R		

No.	X(cm)	Y(cm)	Z(cm)	Weight(g)	Roundness	Rock Name	Remarks
381	8	4	2	115	R		
382	7	5	2.5	100	SR		
383	9	4.5	2	105	A		
384	5	5	5	130	SA		
385	8	3.5	2	105	R		
386	5	4	3	100	R		
387	7.5	3.5	1.5	60	SR		
388	5.5	4	2.5	45	R		
389	6	4	2	70	R		
390	6	2	2	80	SR		
391	5	3.5	2	70	R		
392	5.5	3	2.5	55	SR		
393	5.5	3.5	3	80	SR		
394	5	4	2	60	R		
395	6	3	2.5	70	SR		
396	6	3.5	2.5	65	SA		
397	6	2.5	2	55	SR		
398	4	3.5	3	65	SR		
399	5.5	3.5	2.5	70	SR		
400	4	3.5	2.5	55	SR		
401	5	3.5	2	50	SR		
402	4.5	4	2.5	65	SA		
403	5	3.5	2.5	85	SR		
404	5	3	1.5	55	R		
405	5.5	3.5	2	50	SR		
406	6	3	2	55	R		
407	4.5	3	2	60	SR		
408	4	4	2.5	65	R		
409	4	3.5	2	55	R		
410	4	4	1.5	55	SR		
411	4	4	2	45	SA		
412	5	3	2	55	R		
413	4	3.5	2	60	R		
414	4.5	2.5	2	50	SR		
415	5	4	2	45	SR		
416	6	2.5	2.5	50	R		
417	4	2.5	2	50	SR		
418	5	3	1.5	45	SR		
419	5	3	2	50	R		
420	4.5	3	2.5	55	R		
421	4	2	2	55	SR		
422	5	4	1.5	40	SA		
423	4.5	3.5	2	55	SR		
424	5	3	2	50	R		
425	4	3.5	2	50	R		
426	4	3	2	45	SA		
427	4	3	2.5	50	R		
428	5	2	2	45	R		
429	5	3	1.5	40	SR		
430	4	3.5	1.5	40	SR		
431	5	3.5	1.5	35	A		
432	4.5	4	2	40	SR		
433	4	3	2.5	50	R		
434	4	4	1.5	35	SR		
435	5	2	2	40	SA		

No.	X(cm)	Y(cm)	Z(cm)	Weight(g)	Roundness	Rock Name	Remarks
436	5	3	1.5	40	R		
437	5.5	2.5	1.5	40	SA		
438	3	2.5	2.5	50	R		
439	4	3	2.5	40	R		
440	4	3	1.5	35	R		
441	4.5	4	1.5	50	SR		
442	4	3.5	2	40	SR		
443	4.5	3	2	45	R		
444	4.5	3	2	30	SR		
445	5	3	1	40	R		
446	4	3	2	40	R		
447	3	2.5	2.5	40	SR		
448	4	3	1.5	40	R		
449	4	2.5	2	40	A		
450	3.5	3.5	1.5	40	R		
451	5	3	1.5	40	R		
452	4	3	2	40	SR		
453	3.5	2.5	2	30	SA		
454	3.5	3.5	1.5	40	R		
455	4	3	2	35	R		
456	4	3	2.5	30	A		
457	4	2.5	2	30	SR		
458	4	4	1	30	SR		
459	3	3	2	30	A		
460	3.5	3	2	40	A		
461	3	2.5	2	40	R		
462	5.5	2.5	1	30	SR		
463	5	2	1.5	25	SR		
464	4	3.5	1.5	35	SR		
465	3	3	2	30	SA		
466	4	3	1	25	SA		
467	3	3	2.5	40	SA		
468	4	3	1	25	R		
469	4	2.5	1.5	25	A		
470	4	2.5	1.5	25	SR		
471	4	3	1.5	30	SR		
472	4	2.5	1.5	25	SR		
473	4	2.5	1	25	R		
474	4.5	3	1	35	R		
475	3	2	2	25	A		
476	4	3	0.5	25	SR		
477	5	2.5	1.5	20	A		
478	2.5	2.5	2	25	SR		
479	5	2	0.5	20	SA		
480	4	3.5	1	25	R		
481	3.5	2.5	1	20	R		
482	6	2	1.5	45	R		
483	4.5	2.5	2.5	30	SR		
484	4	2.5	2	35	R		
485	3.5	3	1.5	30	SR		
486	5.5	2	1.5	25	R		
487	4.5	3	1.5	30	R		
488	4	2	2	20	A		
489	4.5	2	2	20	A		
490	4	3	1.5	15	A		

No.	X(cm)	Y(cm)	Z(cm)	Weight(g)	Roundness	Rock Name	Remarks
491	3	2	2	20	SA		
492	3.5	3	2	20	SR		
493	3.5	2.5	2	20	SA		
494	3	2.5	1.5	20	SR		
495	4	3	0.5	20	R		
496	4	2	1.5	20	SA		
497	4	2	1.5	20	SR		
498	3	2.5	2	25	SR		
499	3.5	3	1	20	R		
500	3.5	2.5	2	25	SR		
501	3	2.5	1.5	20	SR		
502	3.5	2	2	25	SR		
503	3.5	2	2	15	SR		
504	3.5	2.5	1	15	SA		
505	3	3	1	20	SR		
506	4	2	2	20	SR		
507	3	2.5	1	20	SA		
508	3.5	1.5	1.5	20	R		
509	2.5	2.5	1.5	20	A		
510	3	2	1	20	R		
511	3	2.5	1.5	20	SR		
512	3.5	2.5	1	20	SA		
513	4.5	2	1.5	20	SA		
514	3	2.5	1.5	20	R		
515	5	2	1	15	A		
516	3	2	1.5	15	SR		
517	3.5	3.5	0.5	15	A		
518	4	1.5	1.5	15	SR		
519	4.5	3	0.5	15	SA		
520	3.5	2.5	1	15	SA		
521	3	2	1	15	SA		
522	3.5	2.5	0.5	15	R		
523	3	2	1	15	R		
524	3	1.5	1.5	15	R		
525	4	2.5	0.5	20	R		
526	4	2.5	1	20	SR		
527	3.5	2	0.5	10	R		
528	3	2.5	1.5	20	SA		
529	3	2	2	20	SR		
530	3.5	2	1.5	15	SR		
531	2.5	2	1.5	20	SR		
532	3	2	1.5	10	A		
533	3.5	2.5	1	15	A		
534	3	2	1.5	15	SR		
535	3.5	2.5	1	10	A		
536	2.5	2	2	20	R		
537	3	2	1	10	R		
538	3	2	2	10	R		
539	3.5	2	1	10	R		
540	3.5	2	1	15	SR		
541	4	1.5	1	10	SR		
542	3	2	1	20	SR		
543	4	2.5	1	20	R		
544	3	2.5	1.5	15	A		
545	4.5	1.5	0.5	10	SR		

No.	X(cm)	Y(cm)	Z(cm)	Weight(g)	Roundness	Rock Name	Remarks
546	3	1.5	1.5	15	SR		
547	3	2	1.5	10	R		
548	3	2	1.5	15	R		
549	3	2	1.5	20	SR		
550	3	2	1	15	SA		
551	3.5	3	0.5	15	A		
552	3	2	1	10	SR		
553	2	2	1.5	15	A		
554	2.5	2	1.5	10	SR		
555	3	1.5	1.5	10	SA		
556	3	2.5	1.5	15	A		
557	3.5	2	1.5	20	SR		
558	3	2	1	15	SR		
559	2.5	2	1.5	15	SA		
560	4	1.5	1.5	15	SR		
561	3	2.5	1	15	SA		
562	3	2	2	15	SA		
563	3	2	1	15	SR		
564	3.5	2	1.5	15	R		
565	3	2	1	10	A		
566	3	2	1.5	20	SA		
567	3	2	1.5	15	SR		
568	3	2	2	20	SA		
569	3.5	2.5	1.5	15	SA		
570	3.5	2	1	20	R		
571	3	1.5	1.5	15	SR		
572	3	2.5	1	20	SR		
573	3	1.5	1.5	10	SR		
574	2.5	2	1.5	15	SR		
575	3	2.5	1.5	15	SA		
576	2	1.5	1.5	10	R		
577	3.5	2	1	15	SA		
578	3	2.5	1	15	SA		
579	4	2.5	1	15	SA		
580	2.5	2.5	1	10	SR		
581	2.5	2.5	1	10	SR		
582	2.5	2	1	15	SR		
583	2.5	2	1	10	SA		
584	4	1.5	1	10	SR		
585	2.5	2	1.5	15	R		
586	3.5	2	1	15	SA		
587	2.5	2	1.5	15	SR		
588	3	2.5	1	10	SA		
589	2.5	2	1.5	10	SR		
590	3	2	1.5	15	R		
591	3	1.5	1	15	R		
592	2.5	2	1.5	15	SA		
593	3	2.5	1.5	15	A		

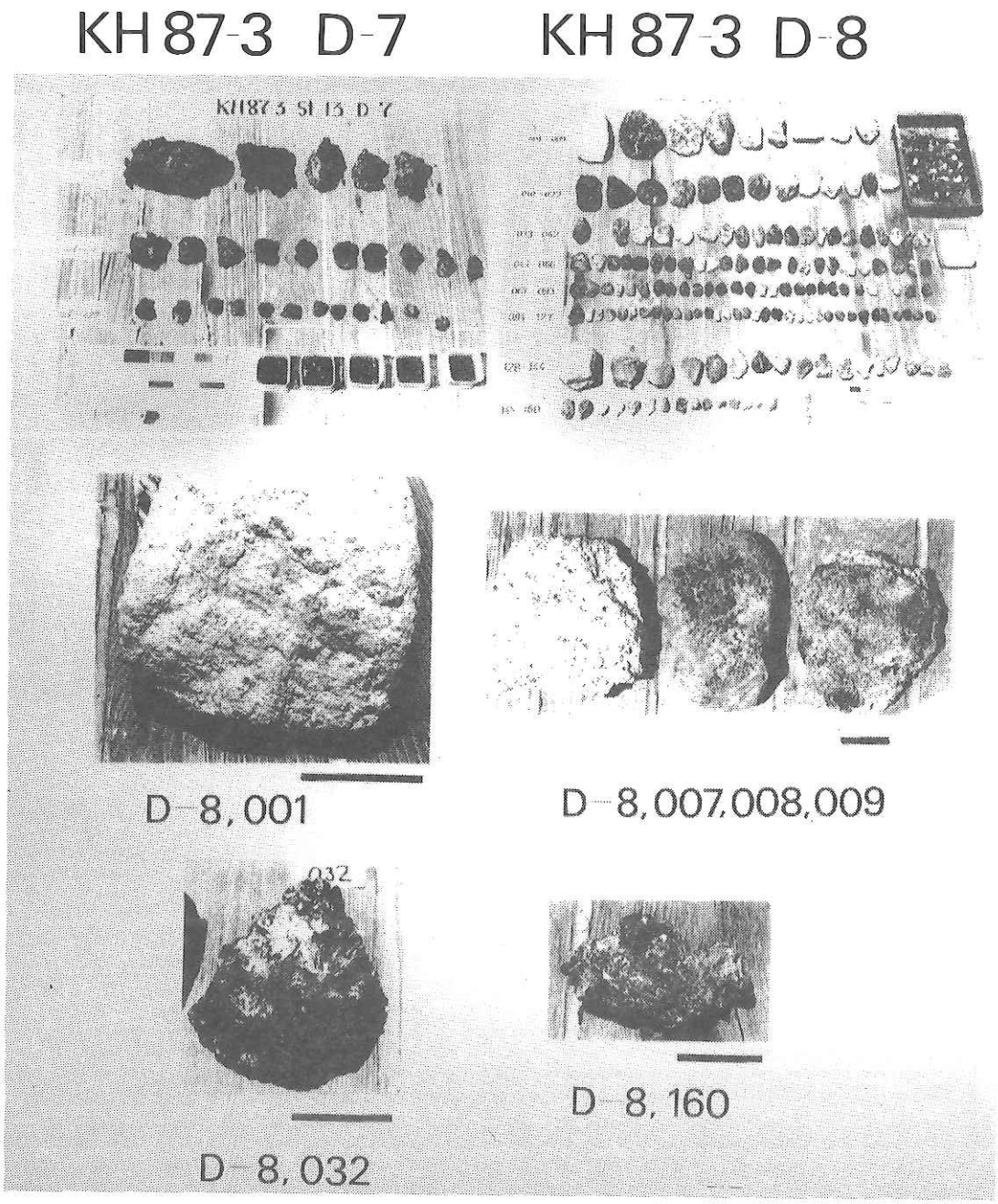

Fig. 20-10(a) Photographs of dredged samples from stations D-7 and D-8

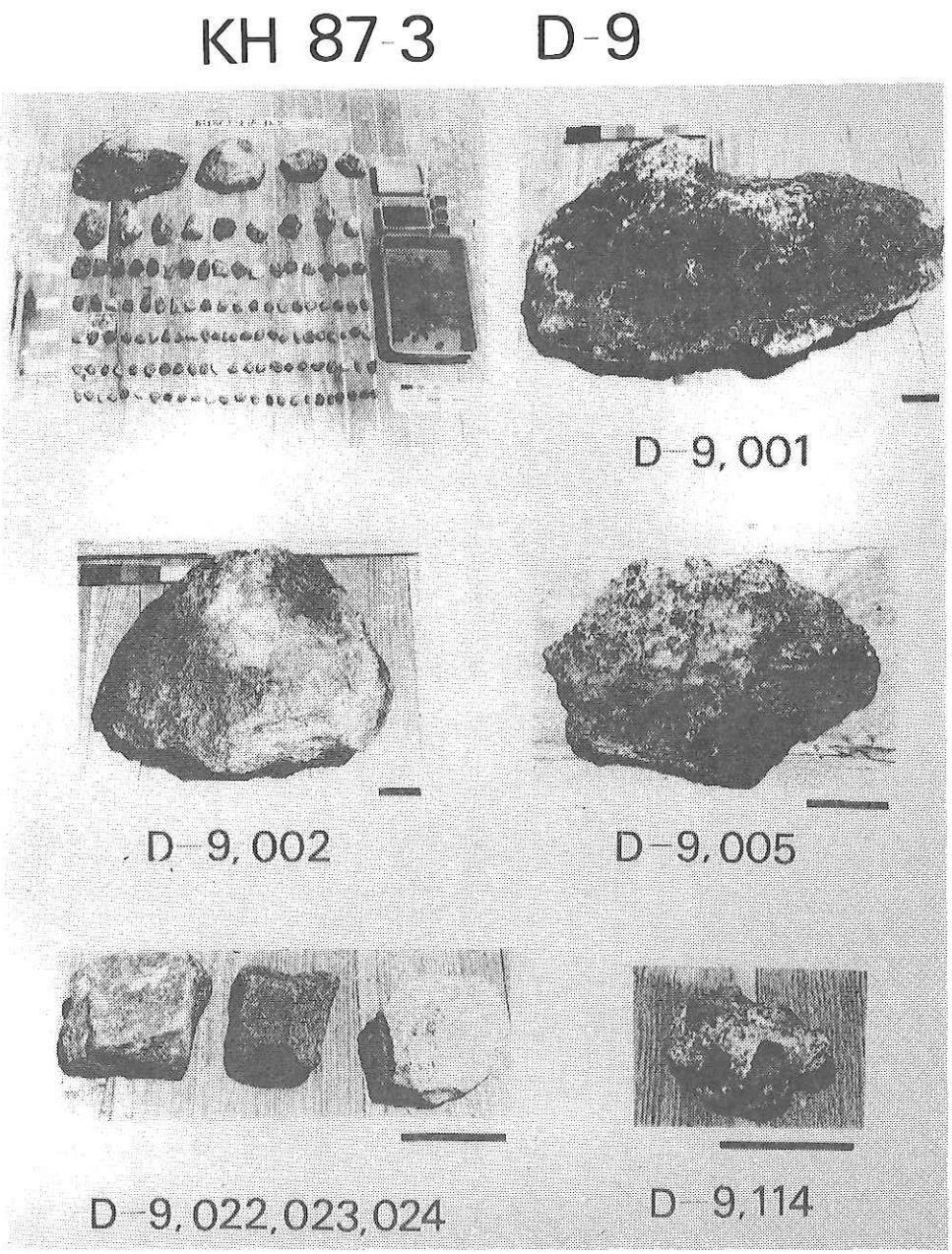

Fig. 20-10(b) Photographs of dredged samples from stations D-9

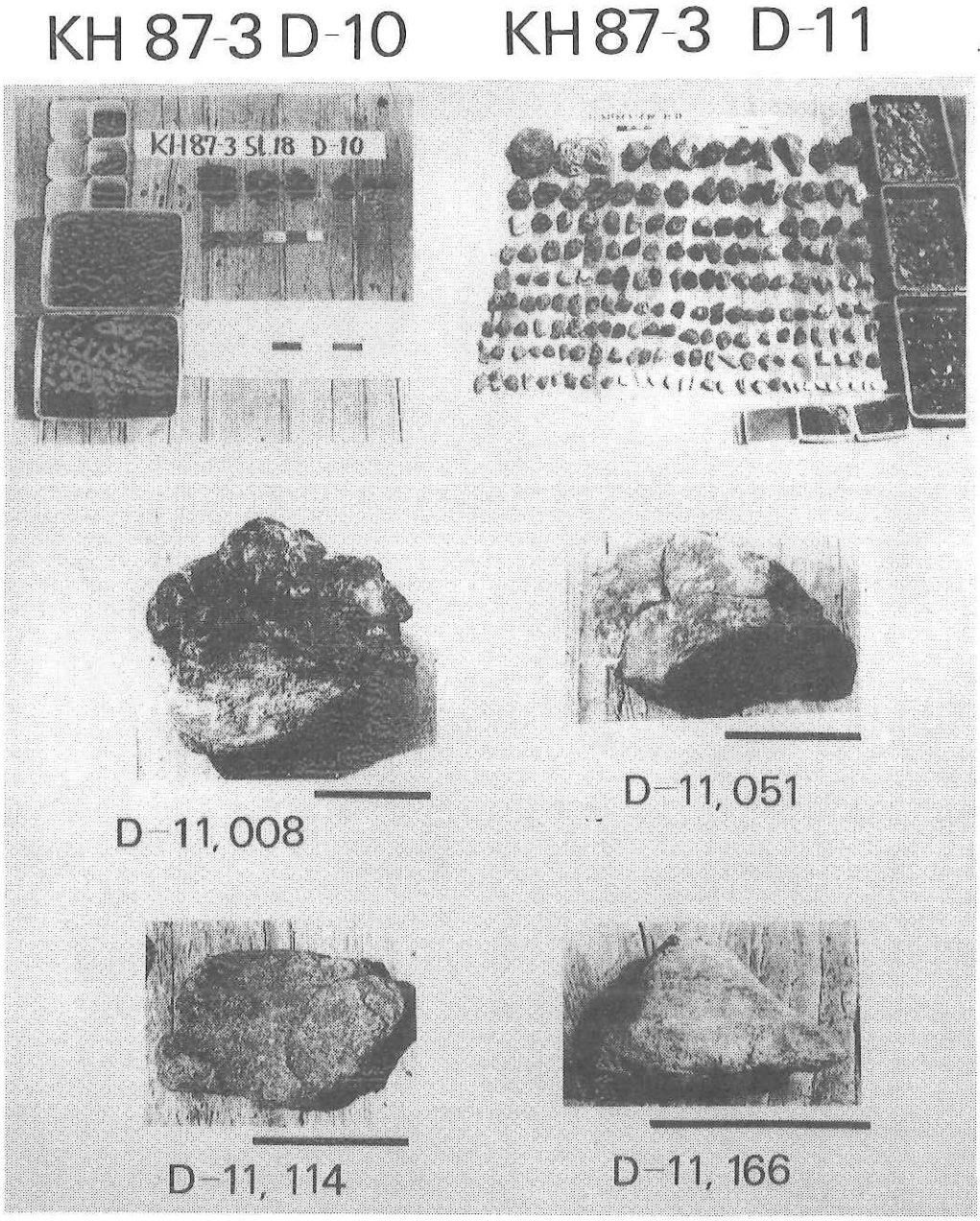

Fig. 20-10(c) Photographs of dredged samples from stations D-10 and D-11

TABLE 20-3 Operation logs of the deep-sea camera during cruise KH87-3.

Date	July 7, 1987	July 9,1987
Station No.	KH87-3-4	KH87-3-6
Location	Eastern Uyeda Ridge	Northern Ogasawara Platau
Weather	Fine	Fine
Wind	190° 2m/sec	130° 8m/sec
Sea	Good	Low swell
Bottom topography	Down slope	Flat
Water depth(start)	5500m	2400m
(finish)	5800m	2300m
Film & Film length	Sakura 400(100ft)	Sakura 400(100ft)
Battery No.	No.81-02	No.81-03
Lens focussed(camera A)	1.2m	1.2m
(camera B)	1.2m	1.2m
Iris(camera A)	8	8
(camera B)	8	8
Shot interval	6sec	6sec
Compass	Ext trigger(6sec)	Ext trigger(6sec)
Time lowed	19:10	10:27
& location	27°11.1N 143°32.1E	25°25.1N 143°30.0E
Shot start time	20:58	11:17
& location	27°11.1N 143°31.6E	25°25.4N 143°30.0E
Shot finish time	22:18	12:37
& location	27°11.5N 143°31.3E	25°25.6N 143°29.6E
Time surfaced	23:32	13:06
& location	27°12.0N 143°31.0E	25°25.9N 143°29.8E
Result	Photo.5-4-1,5-4-2	Photo.5-4-3,5-4-4
Remarks	Nothing	Combined with Dredge haul KH87-3-7

August 3,1987	August 4,1987	August 5,1987
KH87-3-14	KH87-3-17	KH87-3-24
Yap Trench	Yap Trench	Northern
Forearc	Forearc	Yap Ridge
Fine	Fine	Rine
40° 2m/sec	0° 0m/sec	70° 9m/sec
Good	Good	Good
Flat	Down slope	Flat
1350m	1200m	2200m
1350m	1050m	2100m
Sakura 400(100ft)	Sakura 400(100ft)	Sakura 400(100ft)
No.81-03	No.81-02	No.81-03
1.2m	1.2m	1.2m
1.2m	1.2m	1.2m
8	8	8
8	8	8
6sec	6sec	6sec
Ext trigger(6sec)	Ext trigger(6sec)	Ext trigger(6sec)
19:27	02:25	23:54
9°20.9N 137°57.7E	9°22.0N 137°56.7E	10°57.4N 138°37.3E
19:55	02:52	00:37
9°20.9N 137°57.5E	9°21.7N 137°56.4E	10°57.6N 138°36.5E
21:01	03:52	01:55
9°20.8N 137°56.7E	9°21.5N 137°56.1E	10°57.8N 138°36.0E
21:17	04:07	02:24
9°20.7N 137°56.7E	9°21.2N 137°56.2E	10°57.8N 138°36.0E
Photo.5-4-5,5-4-6	Photo.5-4-7,5-4-8	Photo.5-4-9,5-4-10
Combine with	Combine with	Nothing
Dredge haul KH87-3-15	Dredge haul KH87-3-19	

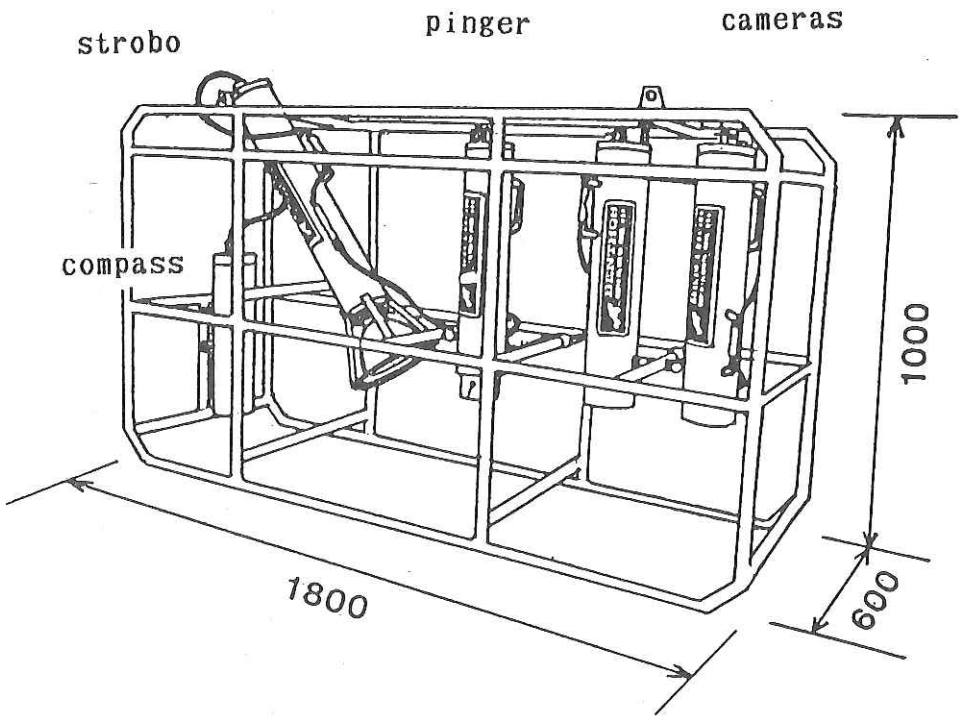

Fig. 20-11 The deep sea camera system of the Ocean Research Institute, Unversity of Tokyo. Designed by M. Watanabe.

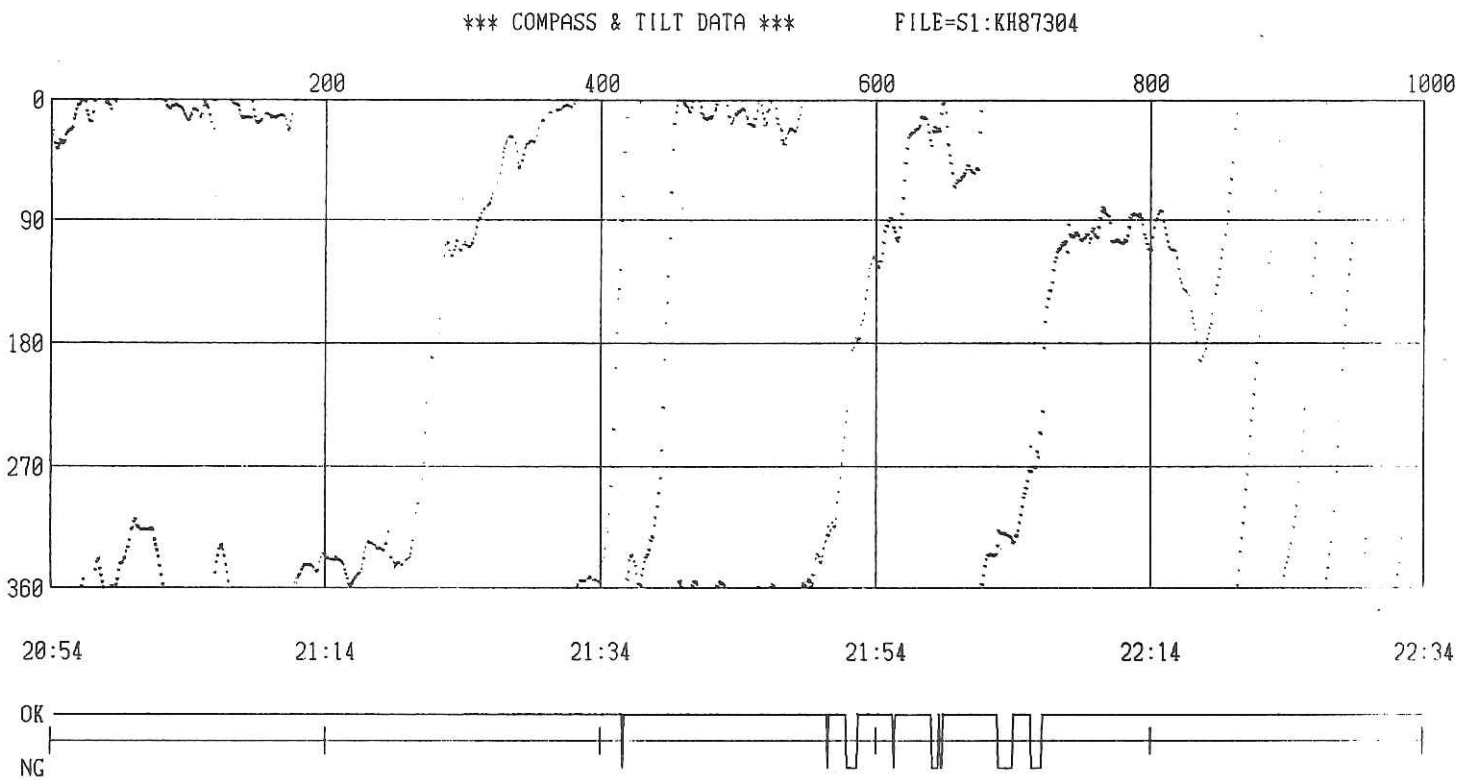

Fig. 20-12(a) Azimuths and tilts of the deep-sea camera system during the operation of the system. At KH 87-3-4.

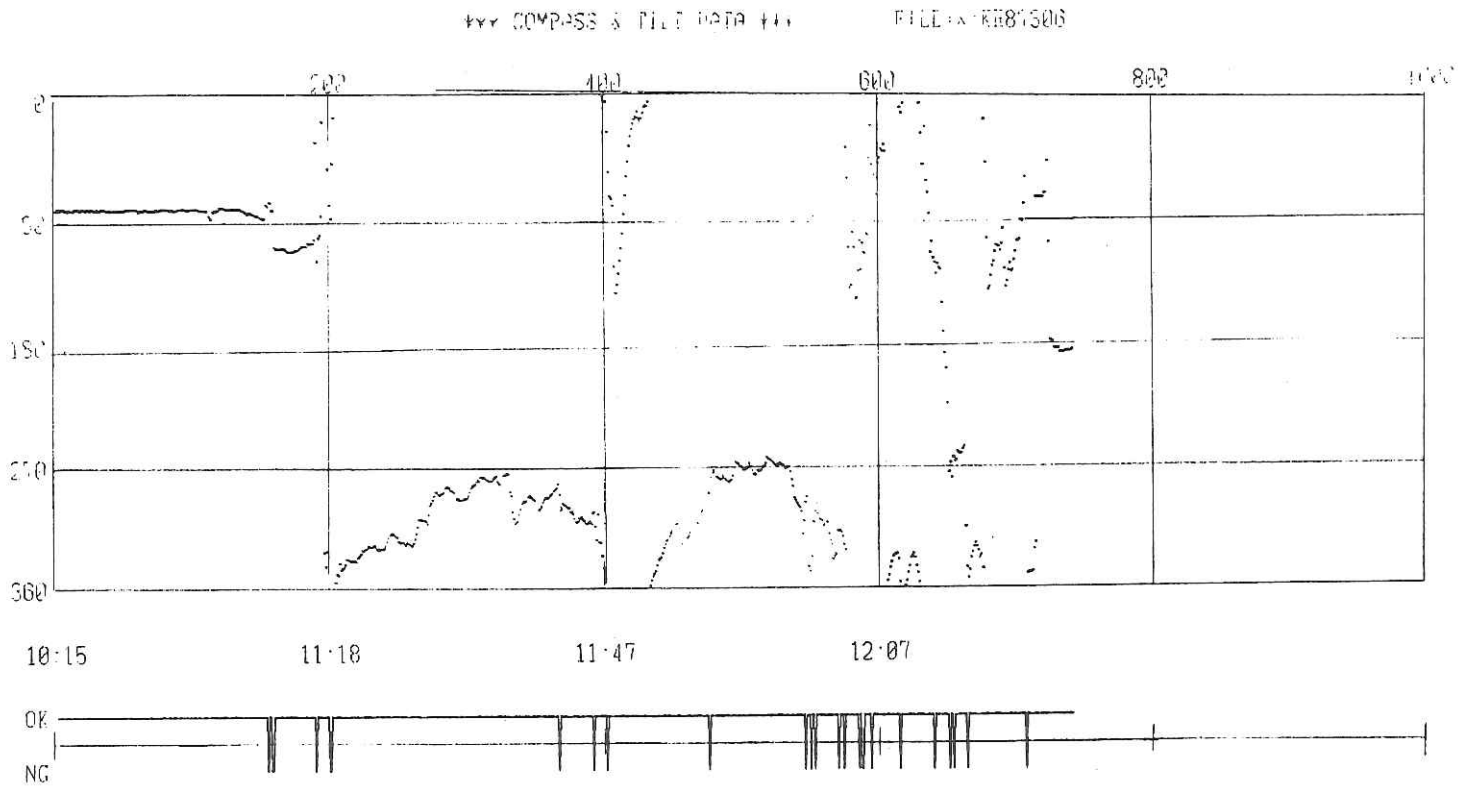

Fig. 20-12(b) Azimuths and tilts of the deep-sea camera system during the operation of the system. At KH 87-3-6.

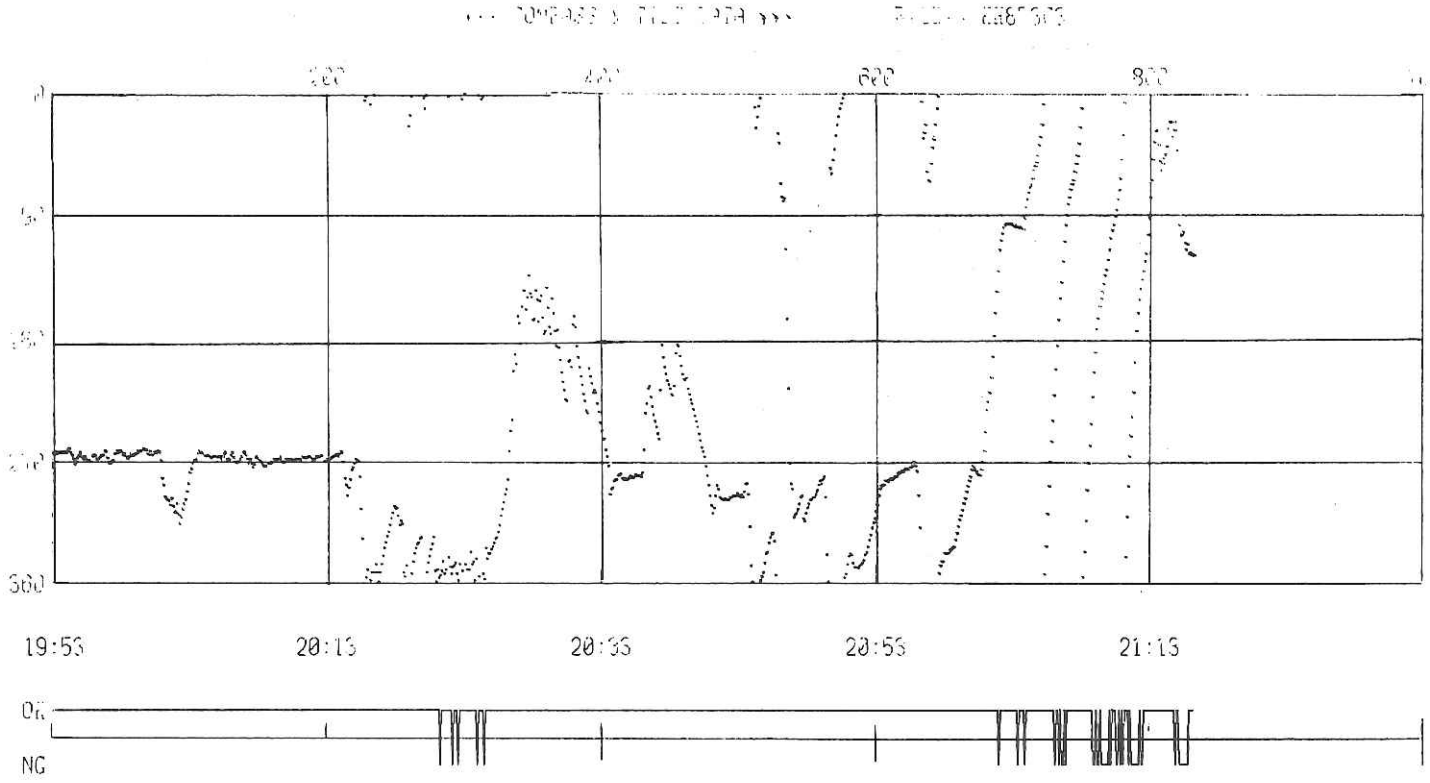

Fig. 20-12(c) Azimuths and tilts of the deep-sea camera system during the operation of the system. At KH 87-3-14.

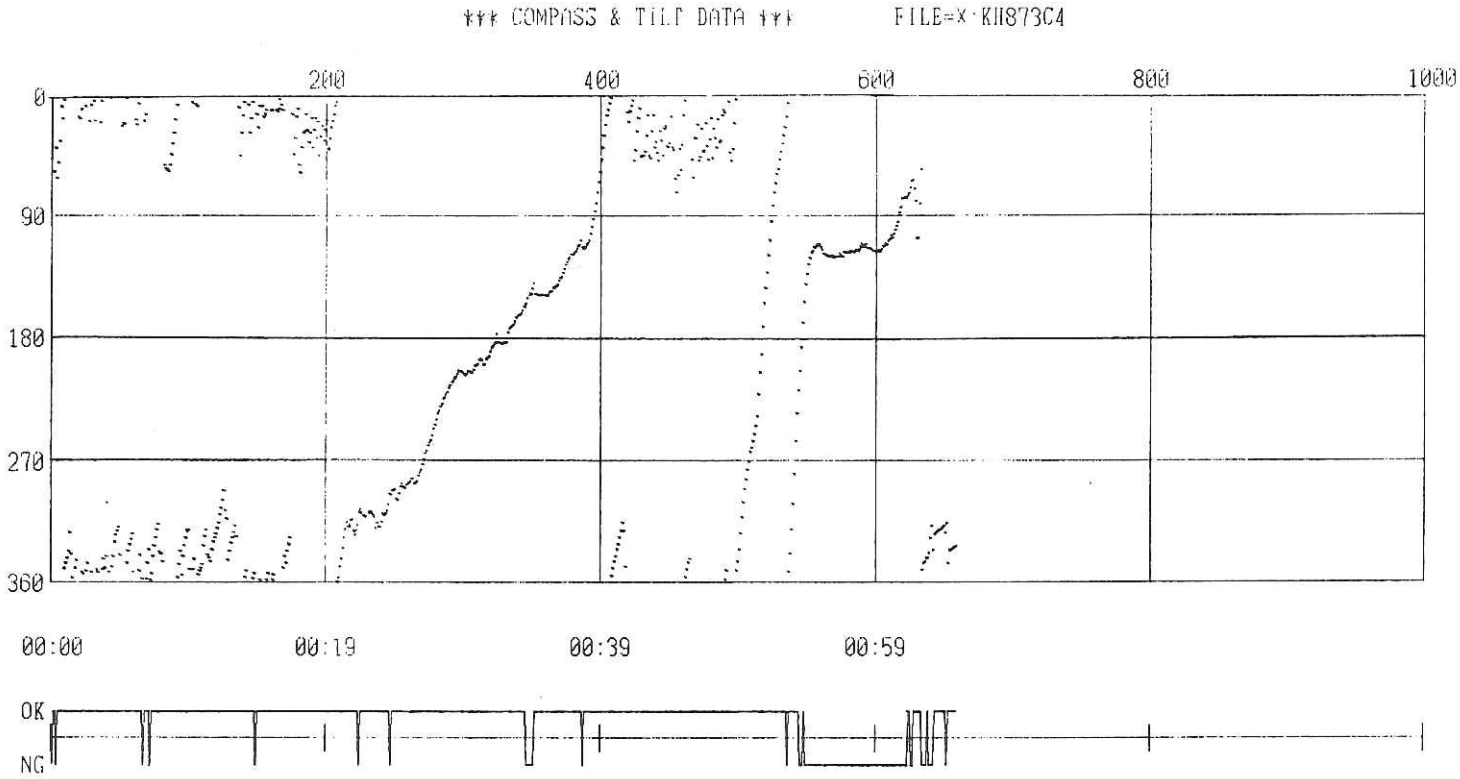

Fig. 20-12(d) Azimuths and tilts of the deep-sea camera system during the operation of the system. At KH 87-3-17.

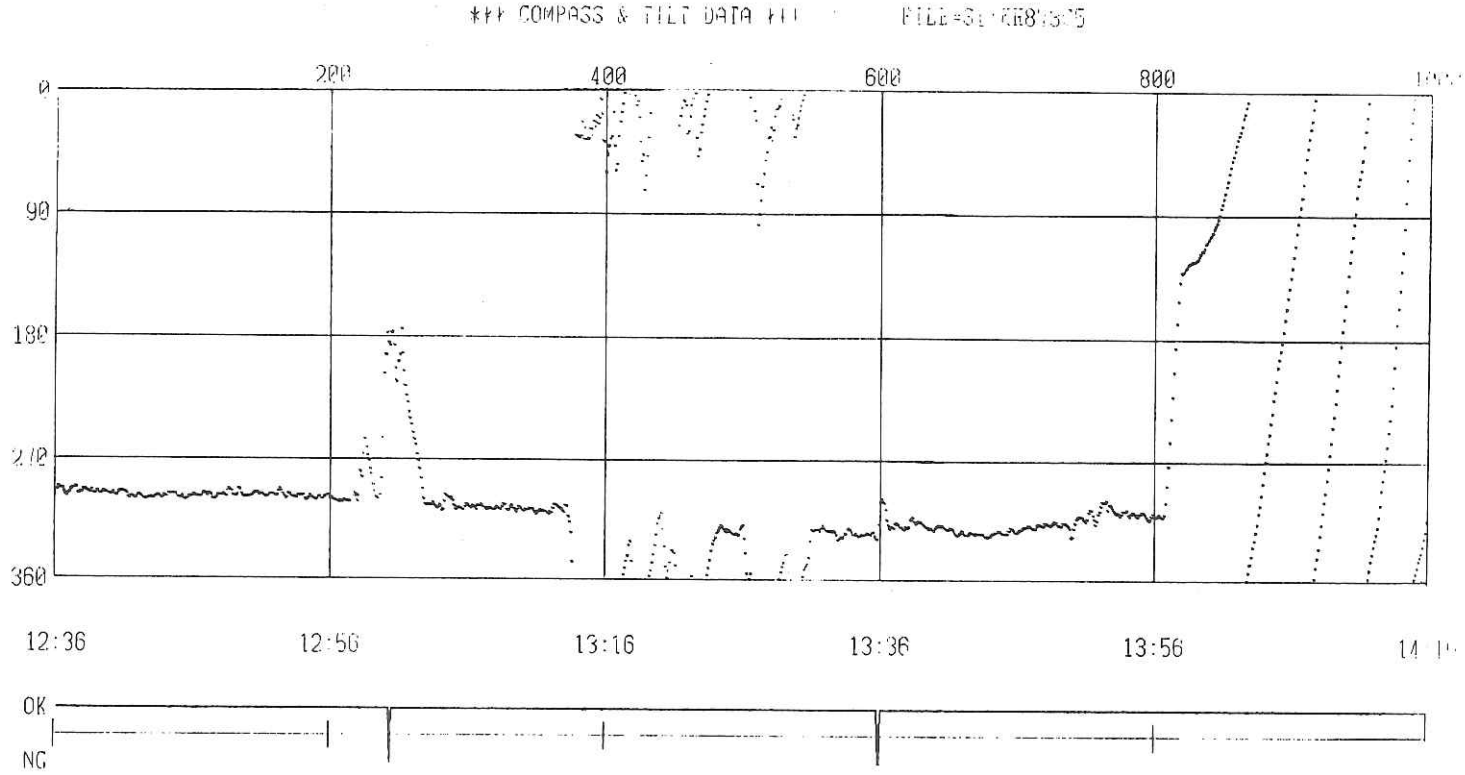

Fig. 20-12(e) Azimuths and tilts of the deep-sea camera system during the operation of the system. At KH 87-3-24.

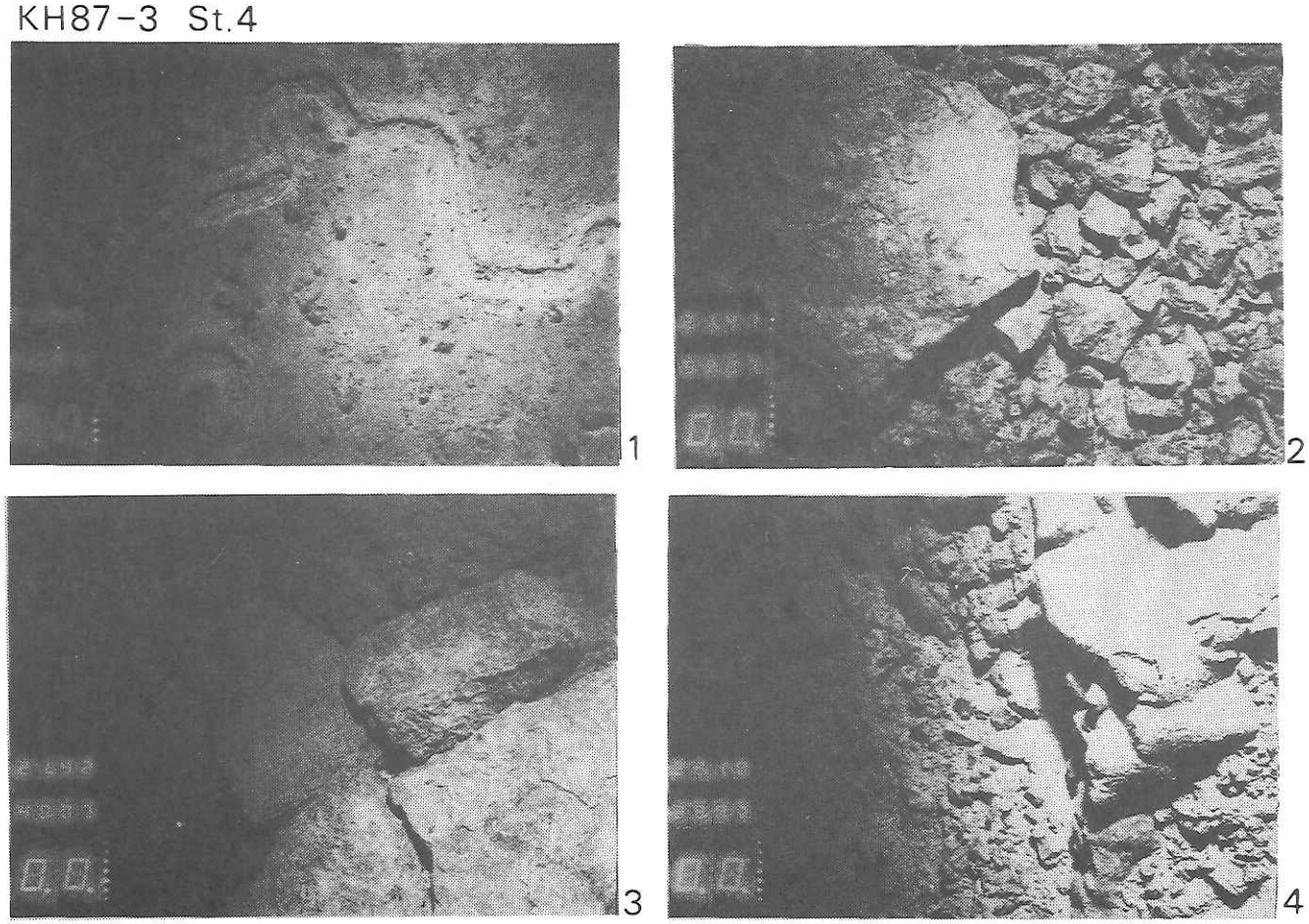

Fig. 20-13(a) Submarine photographs at station KH87-3-4 [1]-[4].

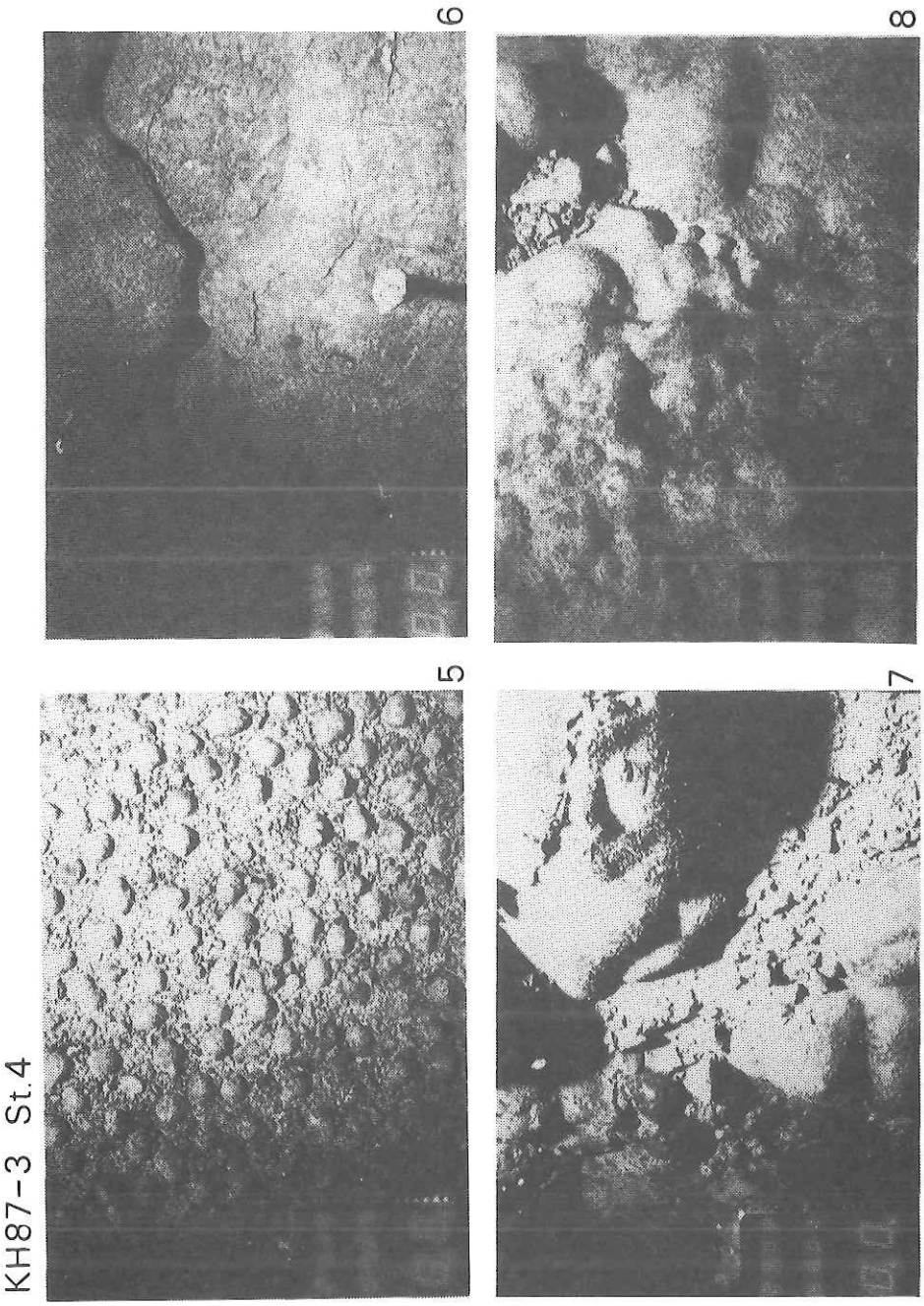

Fig. 20-13(b) Submarine photographs at station KH87-3-4 [5]-[8].

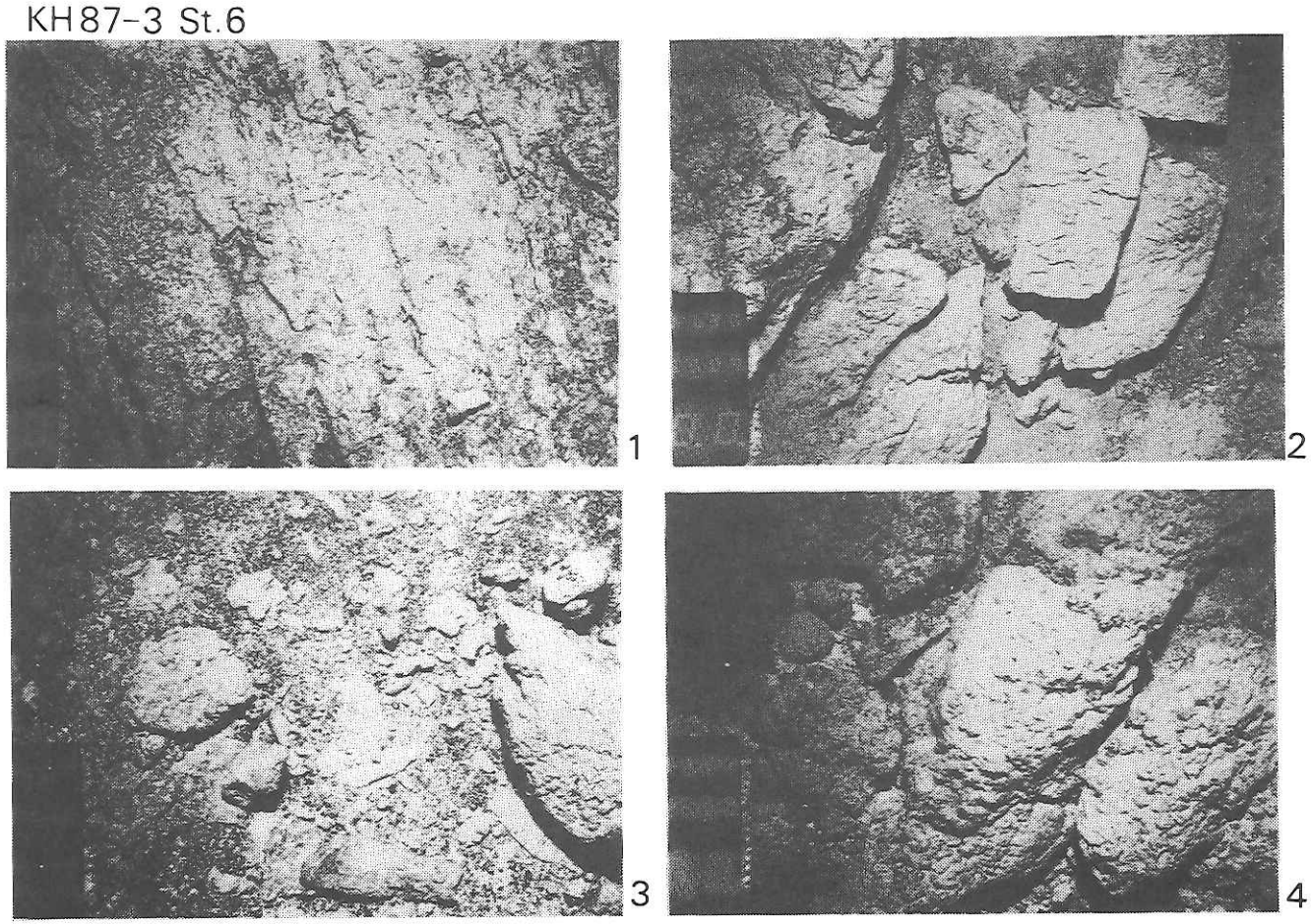

Fig. 20-13(c) Submarine photographs at station KH87-3-6 [1]-[4].

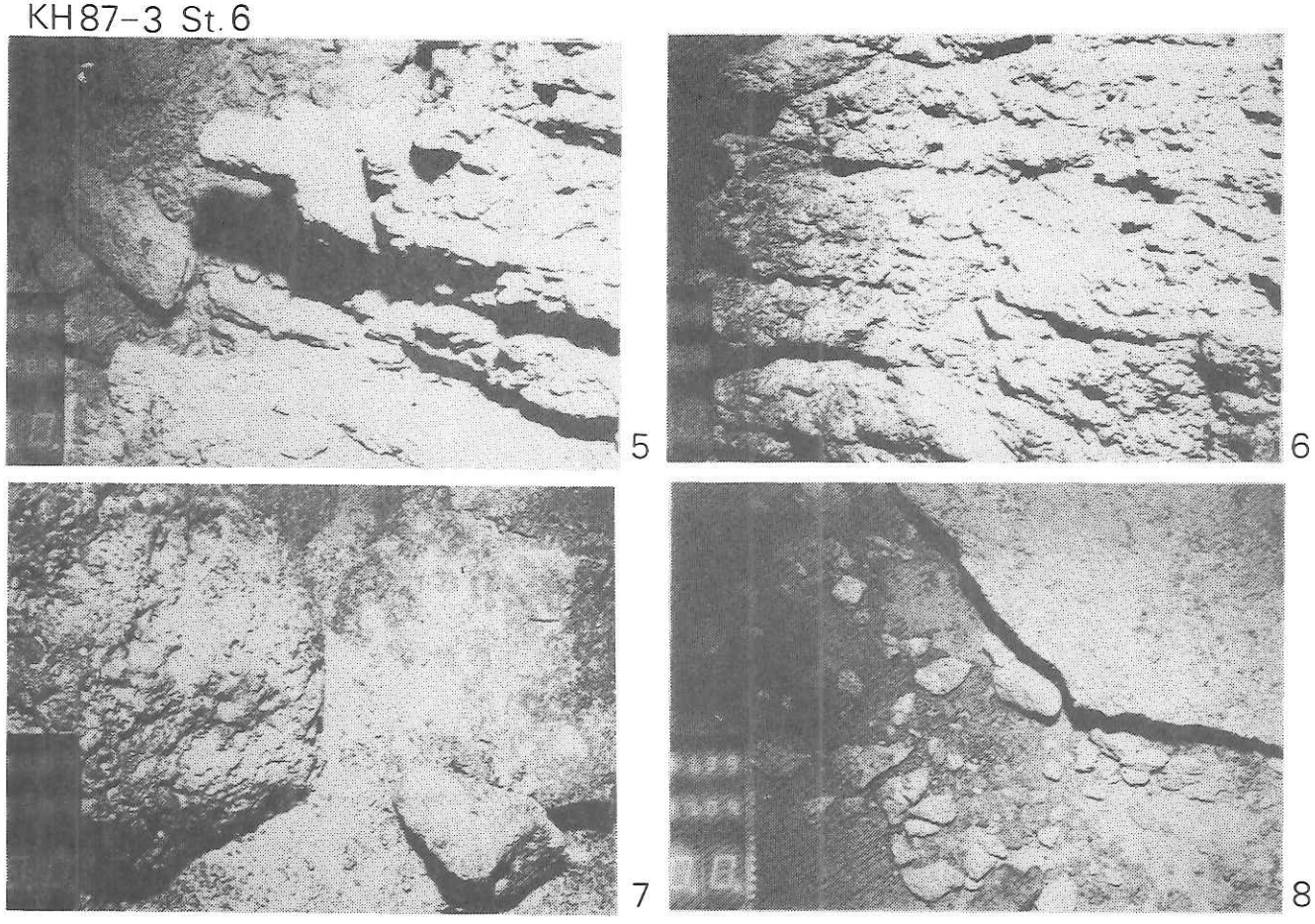

Fig. 20-13(d) Submarine photographs at station KH87-3-6 [5]-[8].

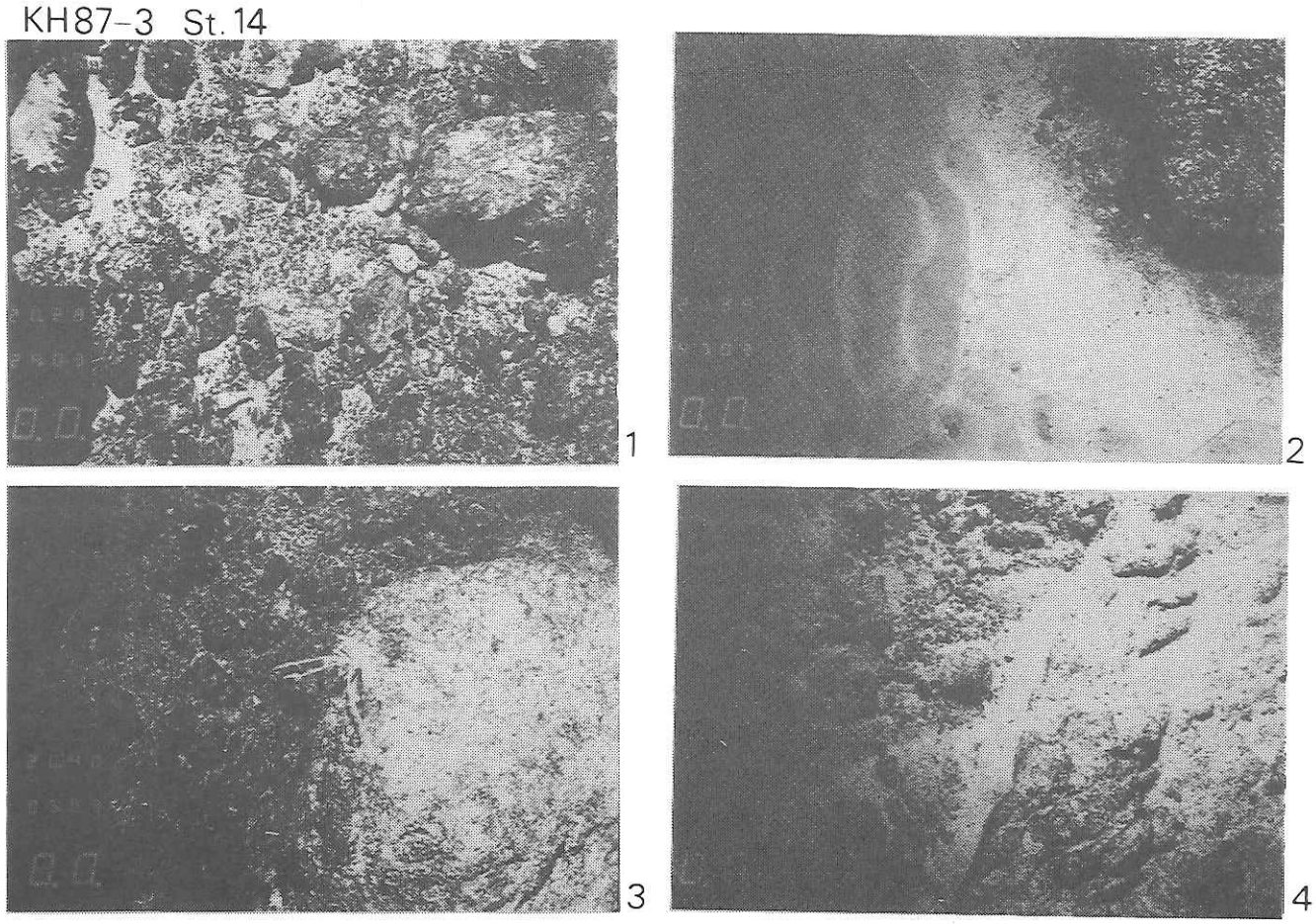

Fig. 20-13(e) Submarine photographs at station KH87-3-14 [1]-[4].

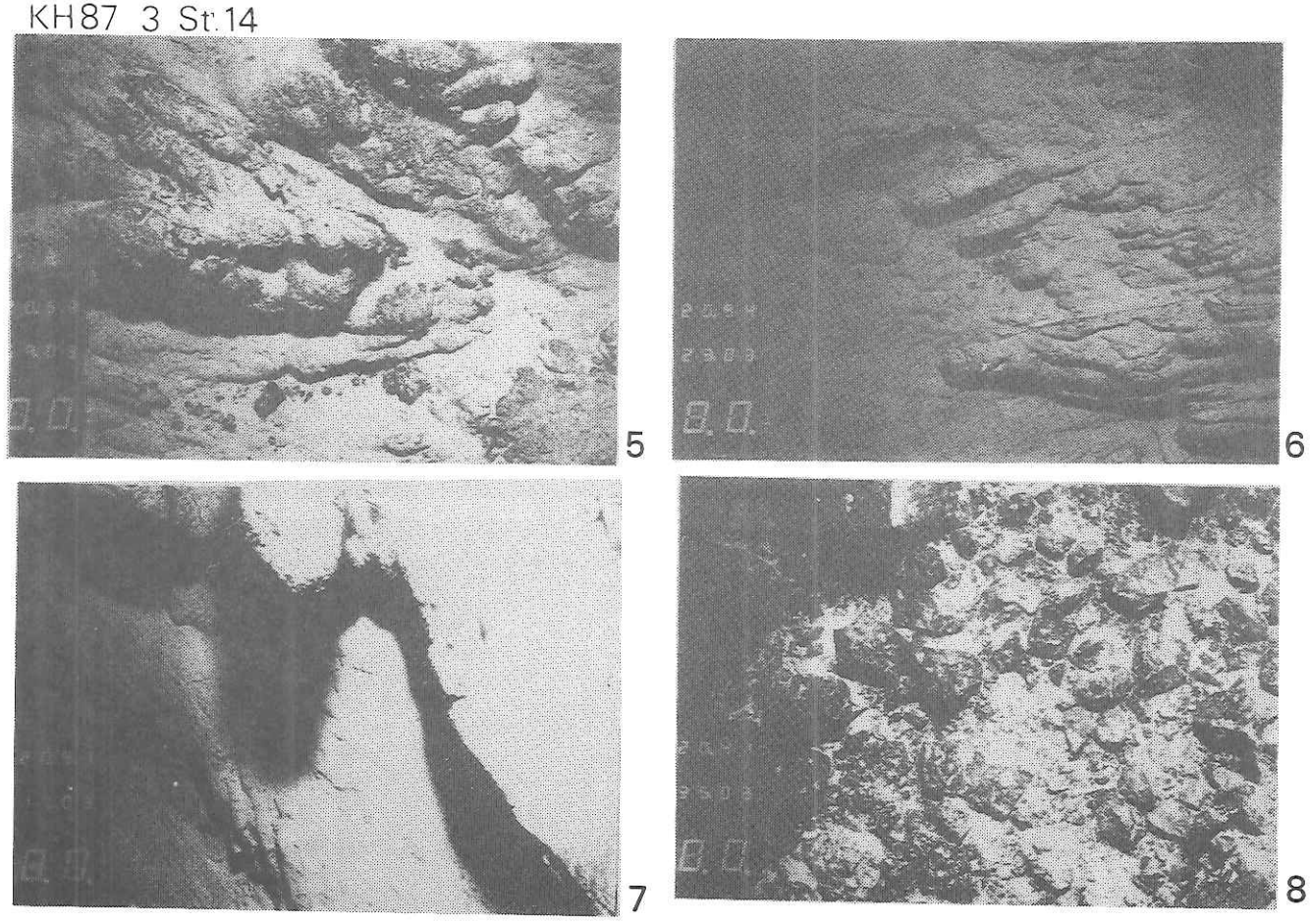

Fig. 20-13(f) Submarine photographs at station KH87-3-14 [5]-[8].

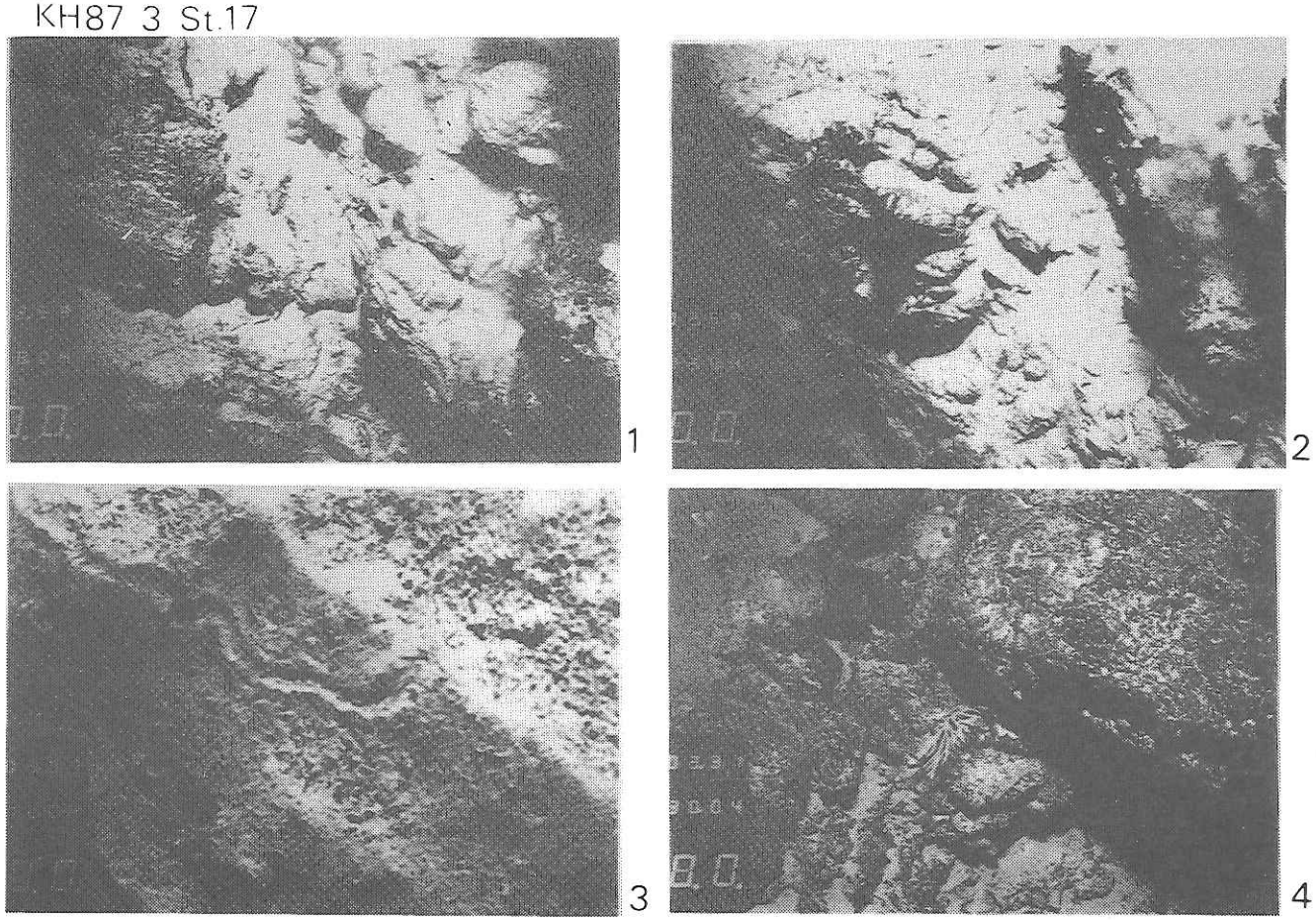

Fig. 20-13(g) Submarine photographs at station KH87-3-17 [1]-[4].

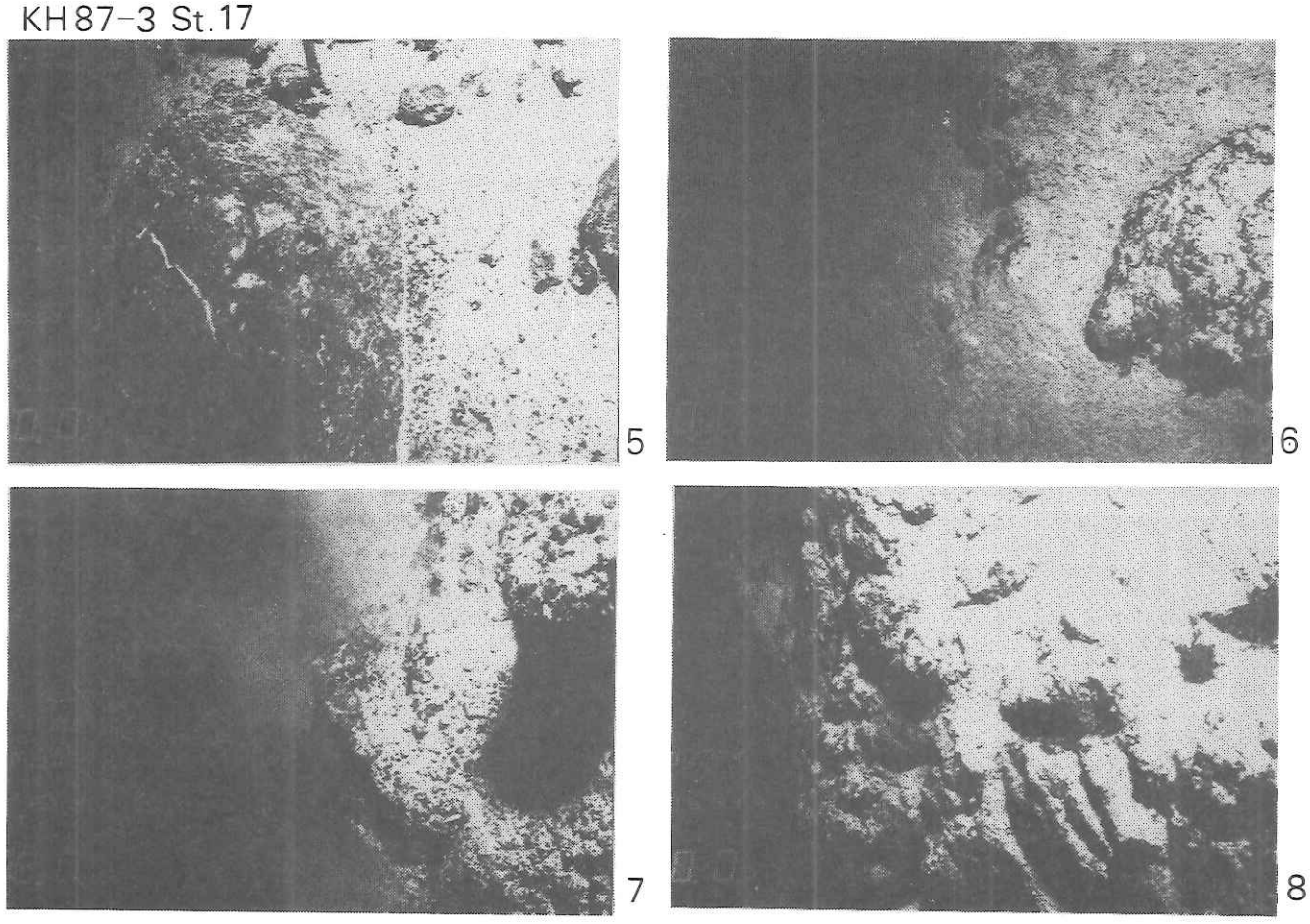

Fig. 20-13(h) Submarine photographs at station KH87-3-17 [5]-[8].

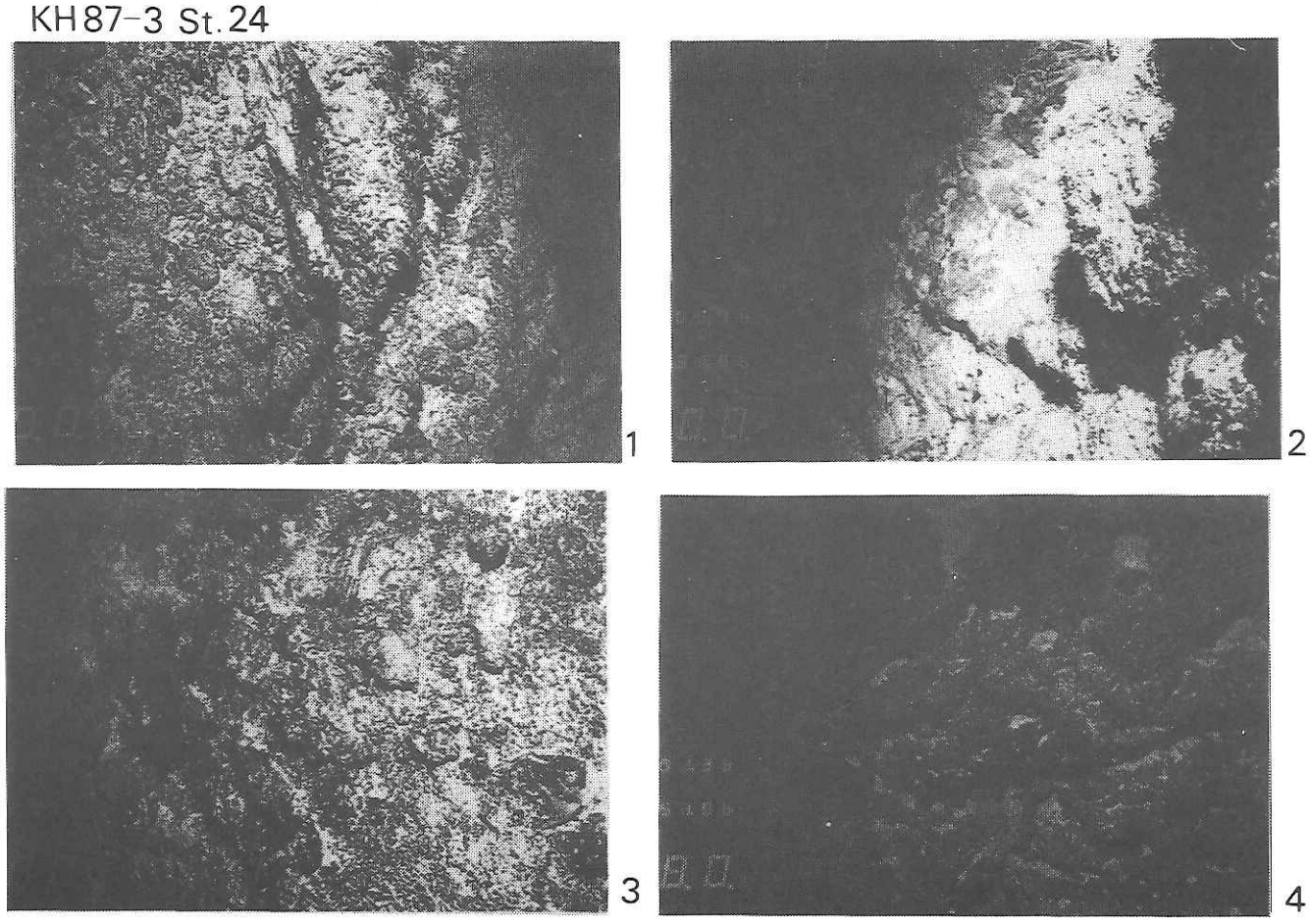

Fig. 20-13(i) Submarine photographs at station KH87-3-24 [1]-[4].

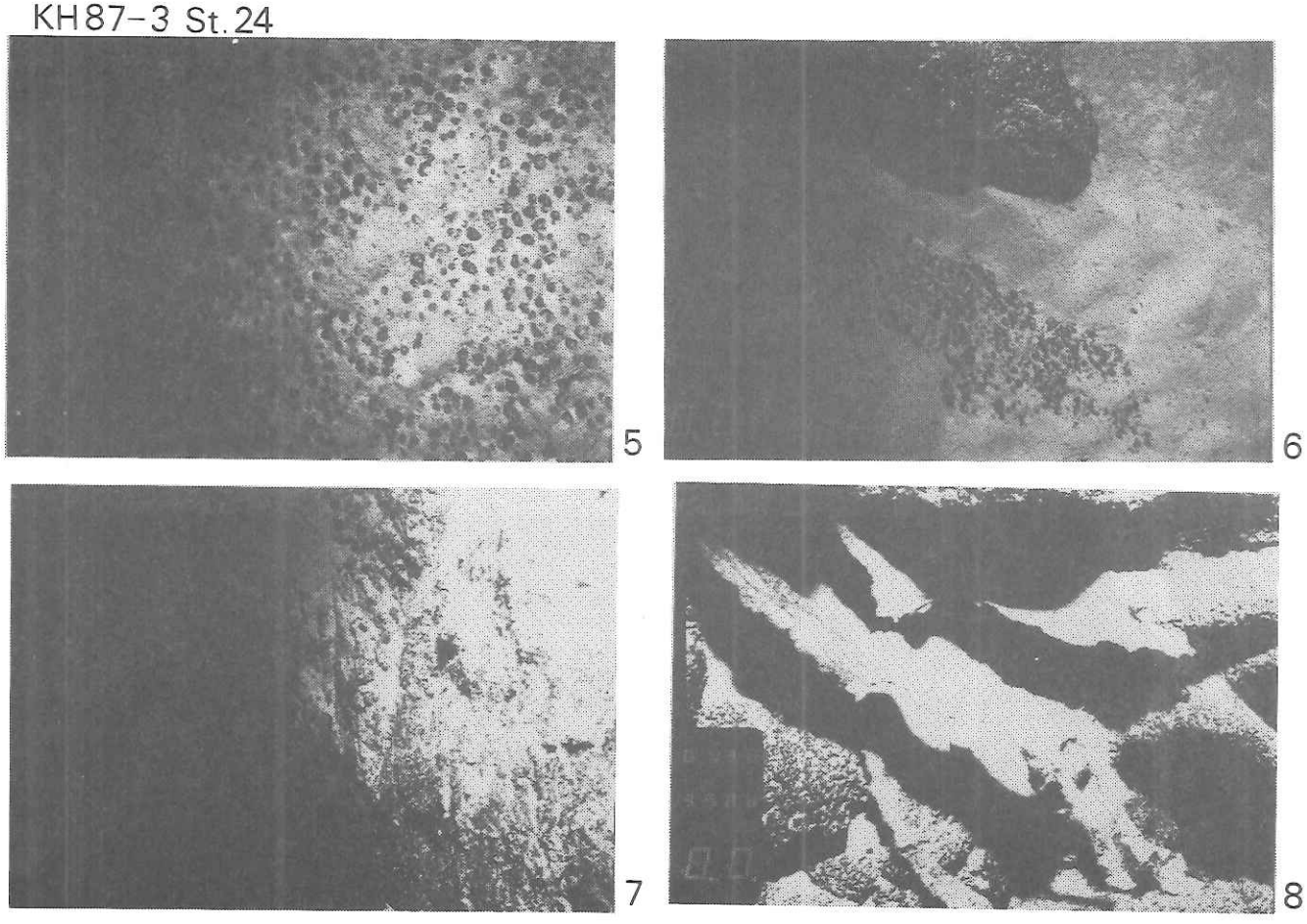

Fig. 20-13(j) Submarine photographs at station KH87-3-24 [5]-[8].

TABLE 20-4 Occurrences and remarks of rock samples obtained onshore the Yap Islands.

Sample No.	Fixed direction	Rock name	Other remarks (foliation etc.)
87-1	20W45W	Amphibolite	20W45W
87-2		Amphibolite	20E60W
87-3		Amphibolite	20E60W
87-4		Pebble	
87-5		Amphibolite	
87-6		Amphibolite	N40E30E
87-8		Calcareous lens	N30E60E(bedding) soft sediments
87-11	N80E40S	Amphibolite	N80E40S
87-12		Calcareous lens	
87-13		Pebble	
87-14	(For paleomagne)	Sand - Silt	TAKEUCHI
87-15		Calcareous layer	
87-16		Calcareous layer	
87-17		Calcareous layer	Fall block from the neighbor cliff
87-18		Phyllite	
87-22	N60W vert.	Amphibolite	(Same as YAP-14-5 - 8 1986)
87-21	N15W55E	Amphibolite	(Same as YAP-14-5 - 8 1986)
YAP			
87-23	N20E45W	Greenschist	N20E45W
87-24	N20E55E	Greenschist	N20E55E
87-25 1	EW30N	Greenschist	EW30N(50E)
2	70W20W	Greenschist	70W20N(55E)
87-26		Amphibolite	
87-27	60E70S	Greenschist	N40E60W(40E)
87-28		Greenschist	L48E
87-29	N60W25N	Greenschist	N10E60W
87-31		Greenschist	
87-32 (1)	N10E70E	Amphibolite	N10E70E
(2)		Amphibolite	
87-33		Amphibolite	N30E vert.
87-34	(1)	Amphibolite	N40E60W
87-34	(2)	Amphibolite	
87-35		Greenschist	N25W vert.
87-36		Greenschist	
87-37	NS80E	Greenschist	NS80E
87-39		Amphibolite	
87-40	NS30E	Greenschist	NS70E
87-41	NS vert.	Amphibolite	
87-43	S70E vert.	Amphibolite	NS vert.
87-44	NS vert.	Amphibolite	
87-45	N40W45N	Amphibolite	N30E vert.
87-46	N10E55E	Greenschist	N20E50E
87-47		Amphibolite	N10W vert.
87-48		Andesite	Volcanic breccia

Sample No.	Fixed direction	Rock name	Other remarks (foliation etc.)
87-49	N20E50W	Greenschist	
87-50		Massive greenstone	
87-51	N15E40E	Amphibolite	N15E40E
87-52	38E75N	Amphibolite	
87-53		Amphibolite	
87-54		Greenschist	
87-55		Greenschist	N30E30S
87-56		Amphibolite	
87-57		Rhyolite	
87-58			
87-59 (1)		Matrix sand	
(2)		Breccia	
(3)		Calcareous layer	
(4)		Sand	
87-60			
87-61			
87-62	N40E65N	Greenschist	N60E63N
87-63 (1)			N5W
(2)			
87-64			
87-65	N35W45E	Greenschist	N35W45E
87-66	N34E22S	Greenschist	N60E30S
87-67	N46W34E	Greenschist	N46W34E

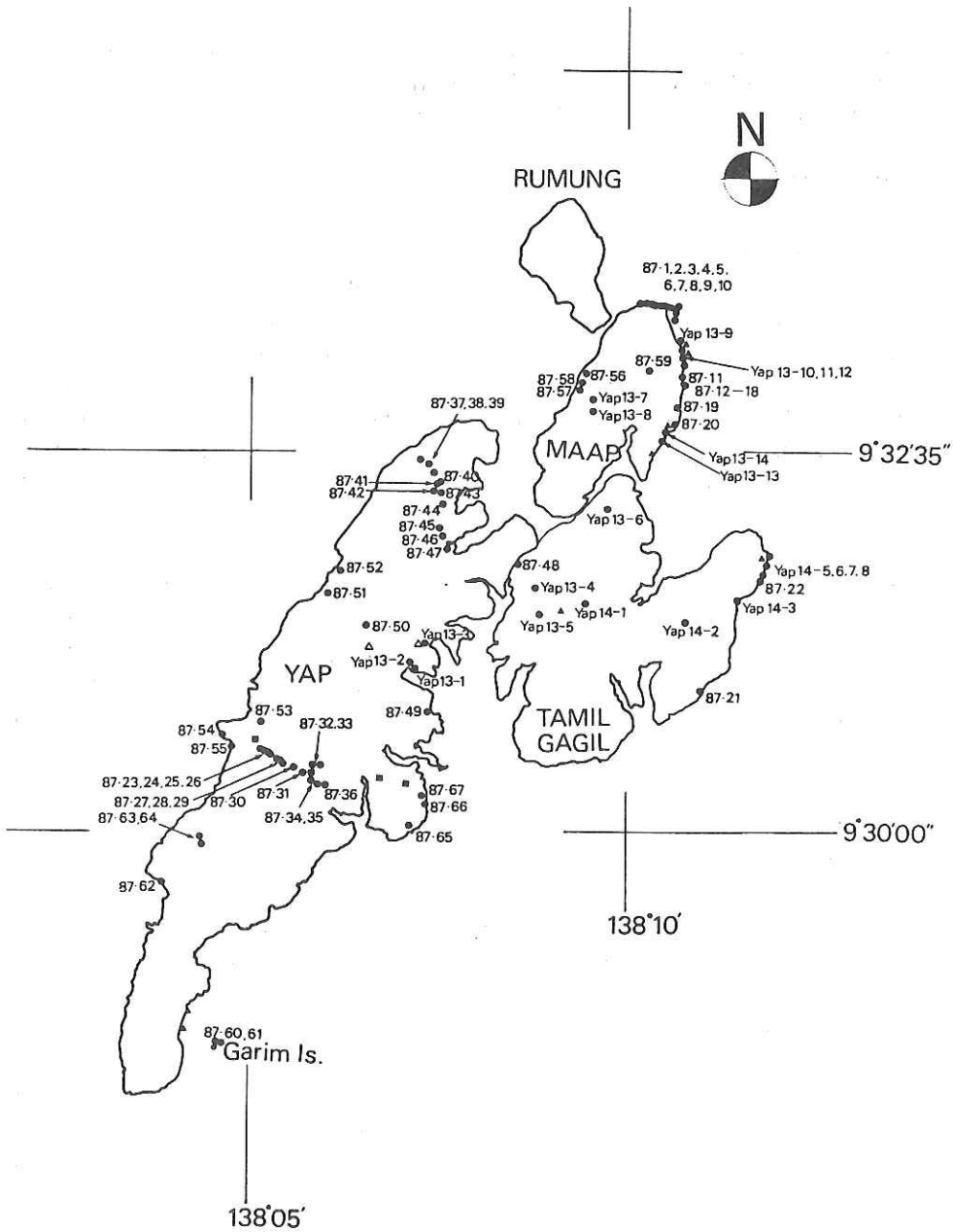

Fig. 20-14 Sampling localities on the Yap Islands during cruises KH 86-1 and KH 87-3.

21. MORPHOLOGY OF SUMISU RIFT

K. FUJIOKA, J. ASHI and H. MATSUOKA

The Sumisu Rift is one of the active volcano-tectonic depressions in the northern Izu-Ogasawara Arc. Topographic map and subbottom profiles were carefully examined during Leg 3 of the KH 87-3 cruise.

21-1. INTRODUCTION

The Sumisu Rift consists of two topographic depressions forming north-south trending elongated basins whose water depths are around 2,000m in the north and 2,200m in the south. The latter basin is much larger and deeper than the former. Geological and geophysical surveys have been carried out for the basins by R. V. Hakurei-Maru, Geological Survey of Japan as well as by R. V. Kana Keoki, the Hawaiian Institute Geophysics and the Sumisu Rift has been thought to be quite active volcano-tectonic depression, that is the youngest rift system in the Izu-Ogasawara Arc (Geol. Surv. Jap., 1985; 1986; 1987).

During the cruise of the KH 87-3, R. V. Hakuho-Maru of Ocean Research Institute, University of Tokyo visited the south Sumisu basin to settle the Ocean Bottom Magnetometer. Several subbottom profile lines were obtained during the pre-site survey of the OBM settlement in order to know the precise bottom condition of the basin. We will describe the topographic features of the Rift here by the interpretation of the topographic map and the subbottom profiles.

21-2. TOPOGRAPHY

Fig. 21-1 is a submarine topographic map of the Sumisu Rift "Bathymetric chart No. 6527" surveyed and compiled by the Hydrographic Department, Maritime Safety Agency (1987). The Sumisu Rift consists of two basins, namely, Kita-Sumisu Basin in the north and Minami-Sumisu Basin in the south, respectively. We call here Kita-Sumisu Basin north basin and Minami-Sumisu Basin south basin, respectively. The average water depth of the north basin is around 2,000m and that of the south basin is around 2,200m and the width of the former basin is 15 km and that of the latter is 35 km.

[1]. Volcanic front

Volcanic front of the northern Izu-Ogasawara Arc runs north to south on the Sumisujima Island, 31°25'N, 140°08'E. The volcanic front forms sporadic topographic highs which may consist of the Quaternary volcanics

such as basalt and andesite. They are volcanic island (Sumisu Island) and submarine volcanoes (Nos. 1-3 Sumisu Knolls).

[2]. Back-arc Depression

The north and south basins are the back-arc depressions according to Tamaki et al. (1981). The rifts have flat bottom which are covered with thich sediments mostly composed of the volcanogenic and biogenic materials (Geological Survey of Japan, 1985; 1986; 1987). The rifts are cut by the normal fault on both eastern and western sides forming the steep walls. In the central portion of the south rift, small topographic high consisting of round depth contours is seen. The shape of the basins are elipsoidal in the north and rectangular in the south and both basins are connected with a narrow gorge-like structure.

[3]. SUBBOTTOM PROFILES

(a). PDR

Topographic cross-sections of the Precise Depth Recorder (PDR) of the Sumisu Rift are show in Fig. 21-2. All the cross-sections are west-east section. The inclination of the eastern wall is always steeper than that of the western. Height of the wall from the floor is about 1,300-1,400m. On the eastern wall, several steps are recognized at water depths from 1,100m to 1,800m. These are the topographic expression of the faults bounding the Rift. On the western wall rough topography is seen at water depths 1,500-2,200m. They are also topographic expression of the faults but possibly a large slump or slide. The water depth of the basin is a little deeper in the eastern portion of the south basin. The central portion shows rugged topography reflecting that the central part consists of the youngest volcanics which may have erupted quite recently.

(b). 3.5 kHz echo sounder

Fig. 21-3 is east-west cross-sections of the 3.5 kHz echo sounder of the south basin. Two conspicuous normal faults are seen in the southern line. The faults cut the surface sediments so that the faults are thoght to be active ones. The sediments of the basin floor consists of three units; opaque 1, transparent and opaque 2 in the descending order. The surface opaque 1 may consist of volcanogenic sediment and the transparent unit consists of hemipelagic sediment and the opaque 2 consists of the acoustic basement. Thickness of each unit is several to tens meters.
In the central portion of the northern line, bared rugged topography which may consists of young volcanic rocks is seen. Sediment covers on it are rare or none. This means that the volcanic activity may have taken place quite recently and the hydrothermal activity together with the voclanic

activity would be expected in this region. The eastern wall of the Rift is steep and stepwise, which may be cut by the faults. The western wall is less steep but also has several fault knoches on the wall. Sediment covers of both walls are quite rare or none.

[4]. Discussion

The Sumisu Rift is the volcano-tectonic depression bounded by faults at both east and west sides and covered with thich sediments on the floor. The PDR and 3.5 kHz profiles suggest that the Rift was formed quite younger age in Quaternary. The history of the Sumisu Rift is summarized as follows;

(1) The south basin was formed by rifting of the back-arc of the Izu-Ogasawara arc.
(2) The north basin was formed after the formation of the south basin by the same mechanism.
(3) Both basins were covered with volcanogenic and biogenic materials following the rifting.

The seismic profile data (Fujioka et al., 1987) show remarkable normal fault system in the Hachijo and Mikura basins trending north and south direction. The faults are stepwisely deepnening toward the center of the basins suggesting that the basins were formed by the rifting. Surface sediments of the Sumisu Rift were collected by the R. V. Hakurei-Maru, Geological Survey of Japan and manganiferous sediments mask the surface of the floor (Geol. Survey of Japan, 1985; 1986; 1987). These facts strongly suggest that the rift is still active and the hydrothermal solutions are circulated in the basin forming manganiferous deposits.

[5]. SUMMARY

Topographic features of the Sumisu Rift are summarized as follows;

(1) The Sumisu Rift consists of two basins, north and south and the former is shallower and narrower than the latter.
(2) Two basins were fault bounded at both east and west sides forming the steep walls.
(3) The eastern wall is steeper than that of the west and may reflect the step fault scarp.
(4) The basins were formed by rifting of the back-arc area of the Izu-Ogasawara arc and age of the rift is expected to be quite young.
(5) Topographic high in the central portion of the south Sumisu basin is a young submarine volcano which has no sediment covers on the surface.
(6) The manganiferous sediments obtained by the Geological Survey of Japan suggests that the basin is still active and the hydrothermal deposits may be supplied from such kind of the volcanic activity.

REFERENCES

Fujioka, K. et al.: Preliminary report of the KT 86-10 cruise for the Mikura and Hachijyo basins. Bull. Earthq. Res. Inst., Univ. of Tokyo, **62**, 61-132, 1987.

Geological Survey of Japan: Investigation on the evaluation of heavy metal deposits accompanied by the hydrothermal activities. Geol. Surv. of Japan. 99pp, 1985.

Geological Survey of Japan: Investigation on the evaluation of heavy metal deposits accompanied by the hydrothermal activities. Geol. Surv. of Japan. 149pp, 1986.

Geological Survey of Japan: Investigation on the evaluation of heavy metal deposits accompanied by the hydrothermal activities. Geol. Surv. of Japan. 189pp, 1987.

Hydrographic Office Maritime Safety Agency: Bathymetric chart No. 6527 (1:200000), Sumisu Sima. 1987.

Tamaki, K. et al. : On the possibility of Quaternary back-arc spreading activity in the Ogasawara arc. The Earth, **3**, 421-431, 1981.

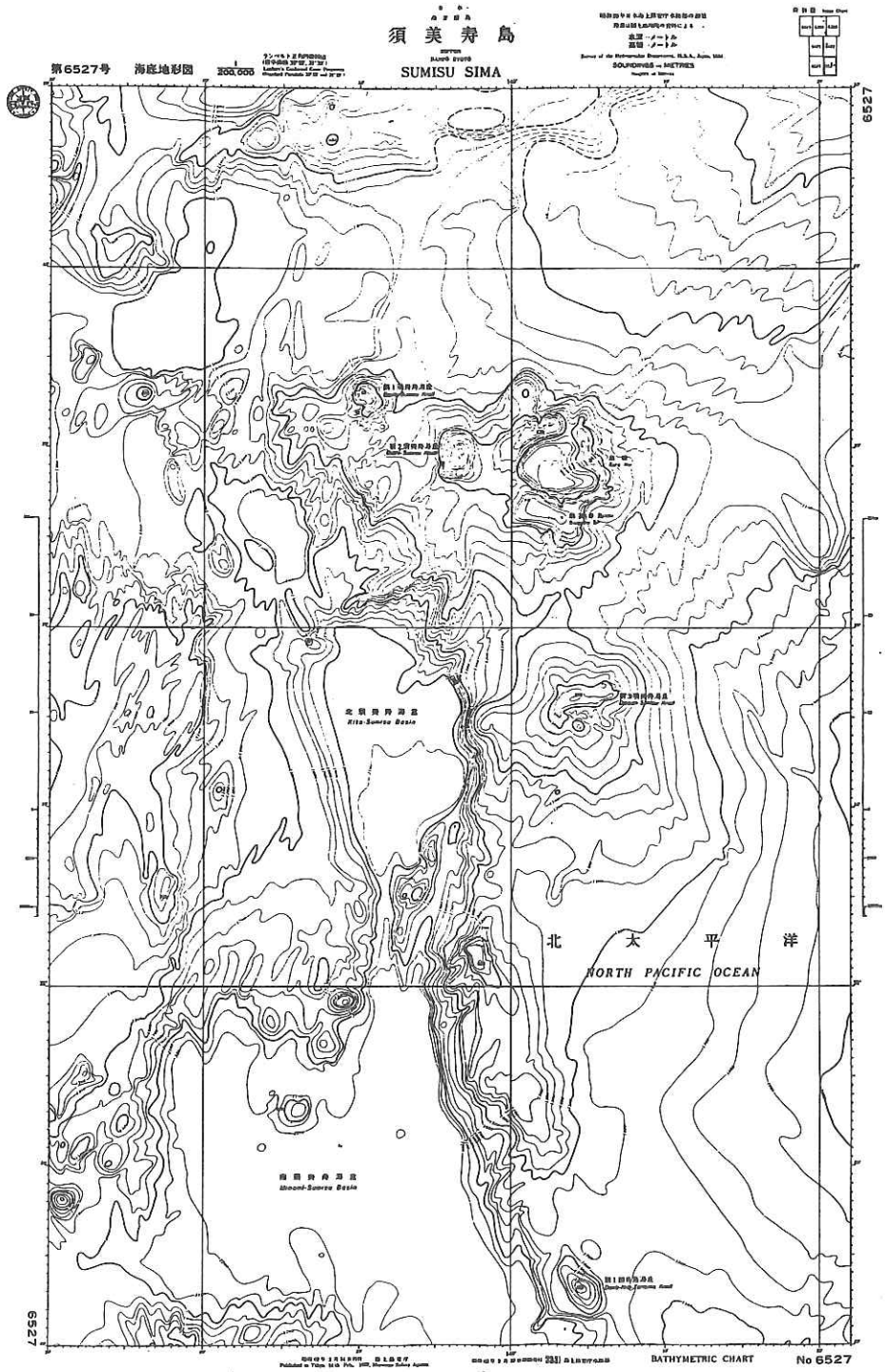

Fig. 21-1 Topographic map of the Sumisu Rift and adjacent area. Bathymetric chart of the Hydrographic Department, Maritime Safety Agency of Japan No. 6522 (1:200000).

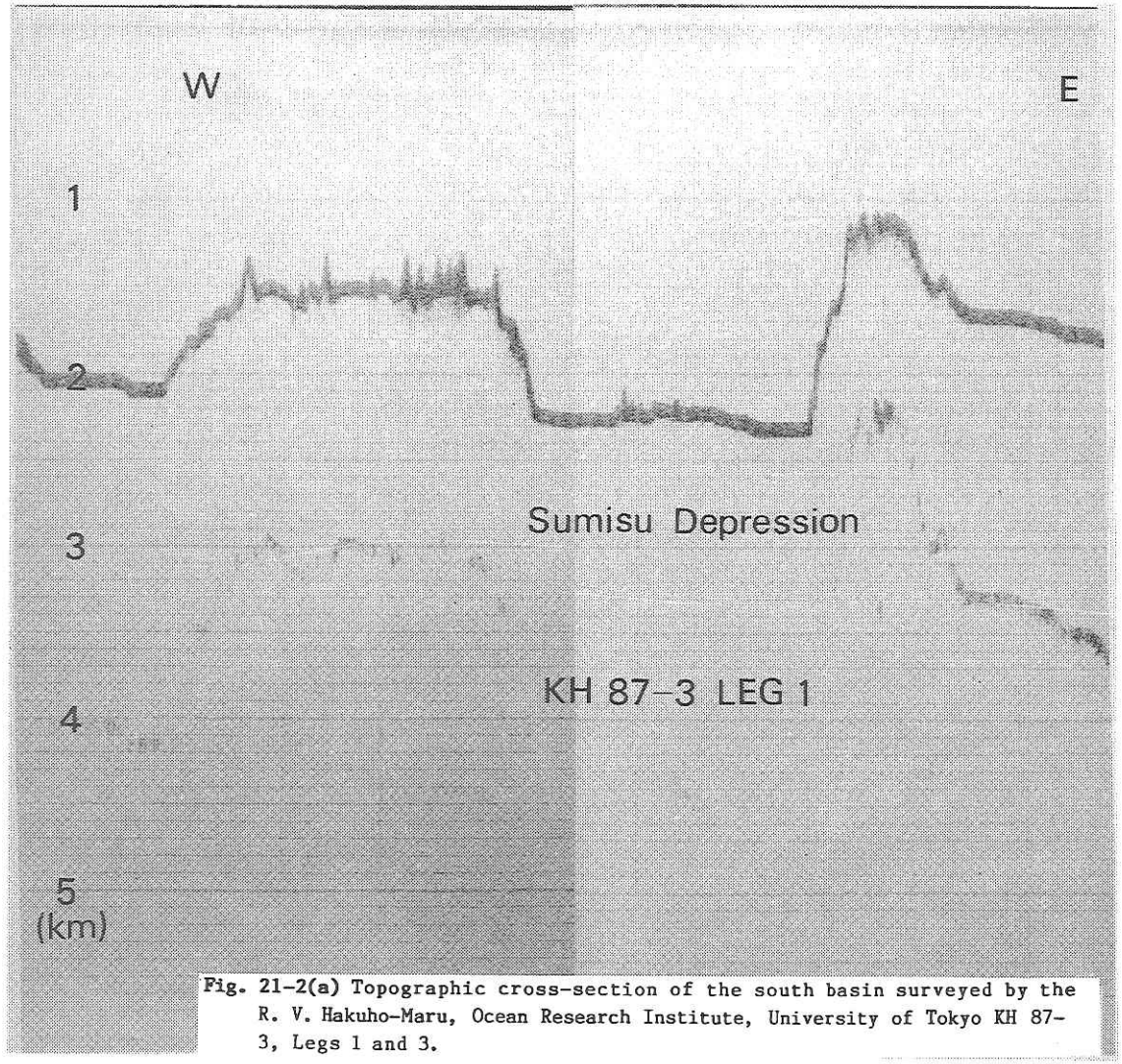

Fig. 21-2(a) Topographic cross-section of the south basin surveyed by the R. V. Hakuho-Maru, Ocean Research Institute, University of Tokyo KH 87-3, Legs 1 and 3.

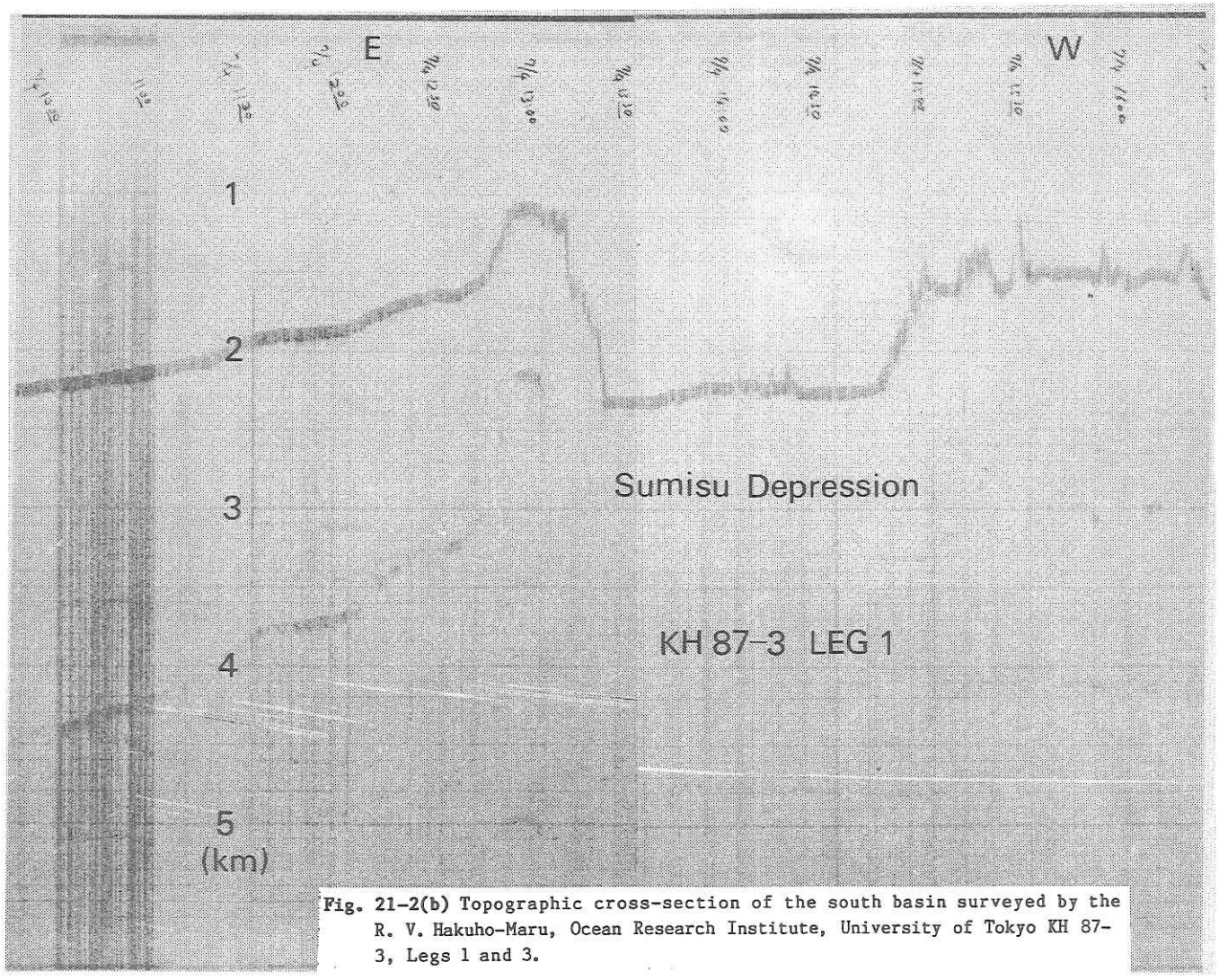

Fig. 21-2(b) Topographic cross-section of the south basin surveyed by the R. V. Hakuho-Maru, Ocean Research Institute, University of Tokyo KH 87-3, Legs 1 and 3.

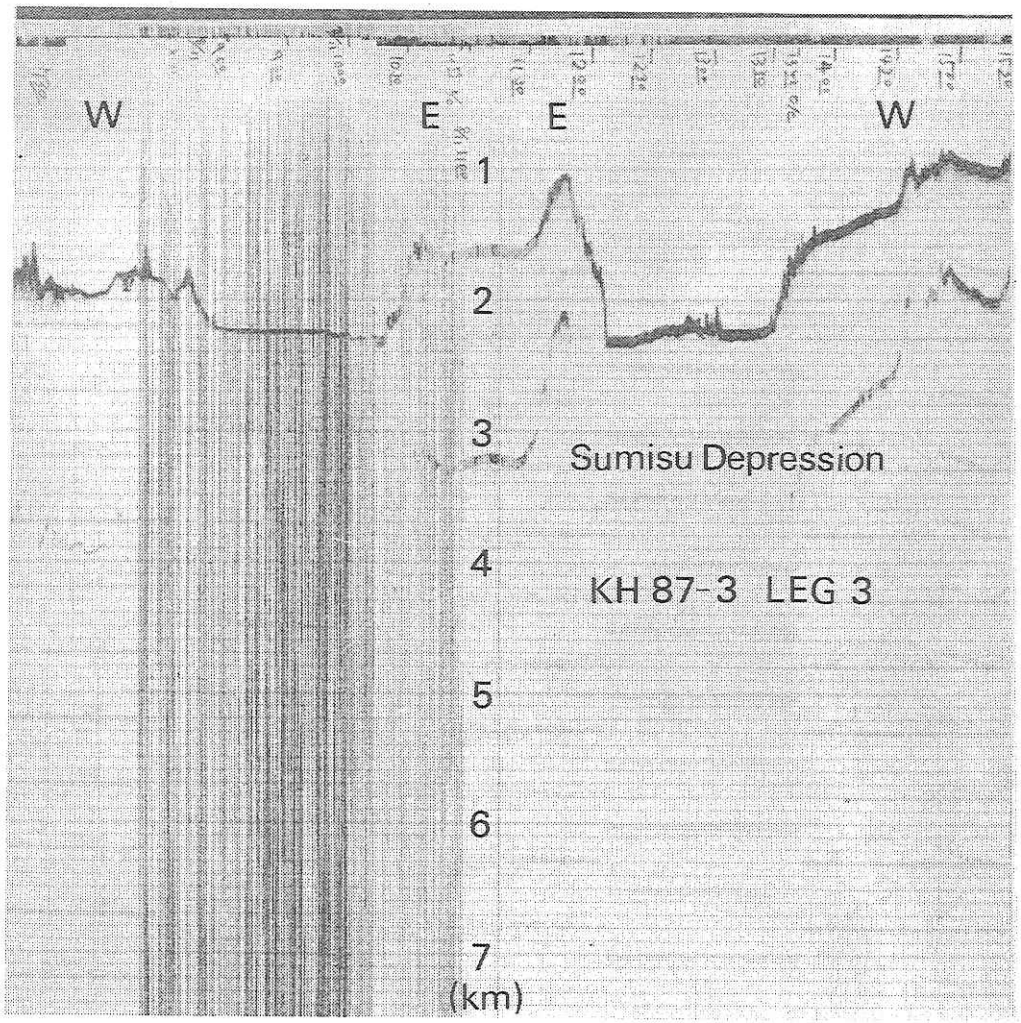

Fig. 21-2(c) Topographic cross-section of the south basin surveyed by the R. V. Hakuho-Maru, Ocean Research Institute, University of Tokyo KH 87-3, Legs 1 and 3.

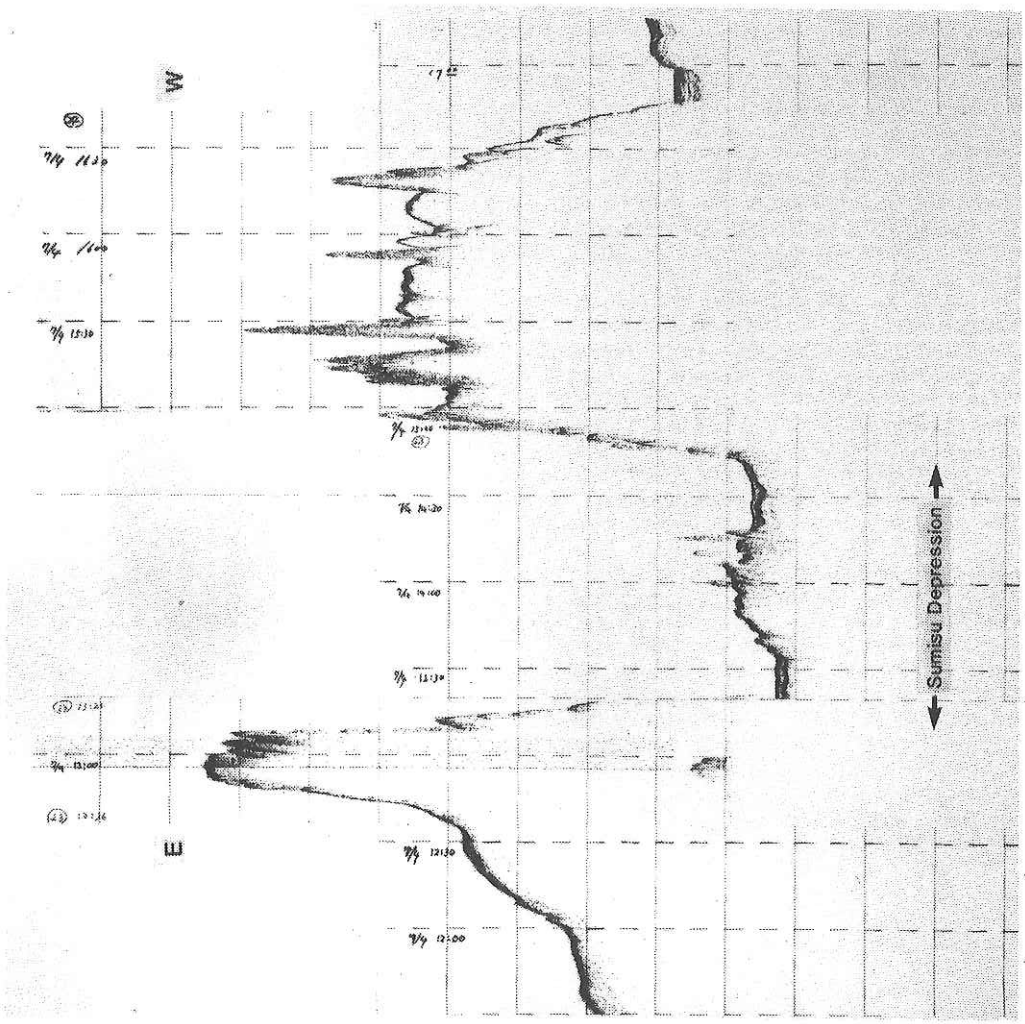

Fig. 21-3(a) 3.5 kHz echo sounder data crossing the south basin during the cruise of KH 87-3, Legs 1 and 3.

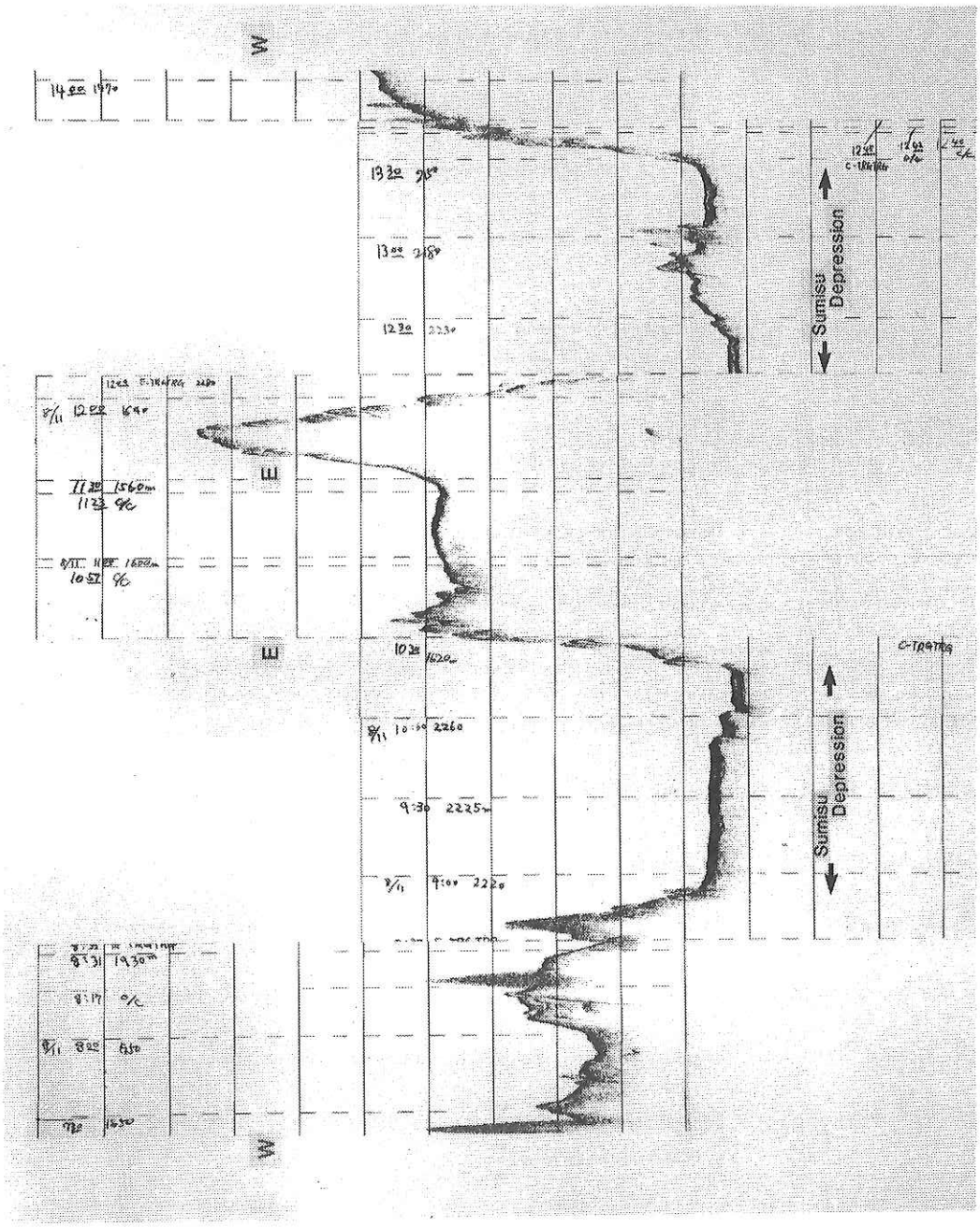

Fig. 21-3(b) 3.5 kHz echo sounder data crossing the south basin during the cruise of KH 87-3, Legs 1 and 3.

ANNEX

PRELIMINARY REPORT OF TANSEI MARU CRUISE KT 86-9

June 27 -July 9, 1986

Izu-Ogasawara (Bonin) Trench-Forearc Region and Ogasawara Plateau

A-1. SCIENTISTS ABOARD THE R.V. TANSEI MARU FOR THE CRUISE KT 86-9

KOBAYASHI, Kazuo	[Chief Scientist] Ocean Research Institute, University of Tokyo
ABE, Shintaro	Department of Earth Sciences, Chiba University
ISHII, Teruaki	Ocean Research Institute, University of Tokyo
KONISHI, Kenji	Department of Geology, Kanazawa University
MAEKAWA, Hirokazu	Department of Earth Sciences, Kobe University
NAKANISHI, Masao	Ocean Research Institute, University of Tokyo
OZAWA, Kazuhito	Faculty of Sciences, University of Tokyo
TANAKA, Akiko	Department of Earth Sciences, Kobe University
TOKUYAMA, Hidekazu	Ocean Research Institute, University of Tokyo
UNO, Ikuko	Department of Earth Sciences, Kobe University
YOSHIDA, Takeyoshi	Department of Petrology, Mineralogy & Mining Geology, Tohoku University

A-2. Index Map of the cruise KT 86-9

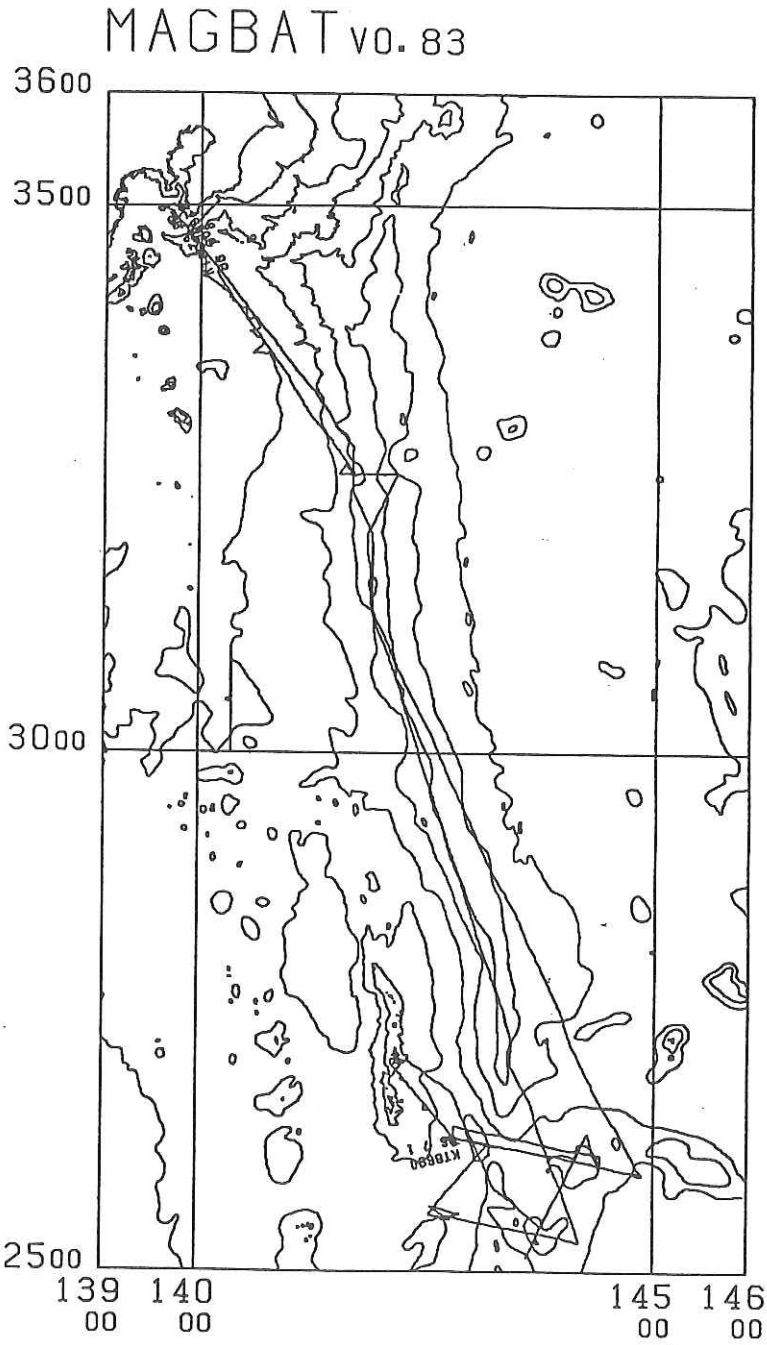

Fig. A-2-1 Ship's tracks of R. V. Tansei Maru in the cruise KT 86-9. Bathymetry is based upon the GEBCO Digital Data from JODC. Contour interval 2,000 m. Mercator projection.

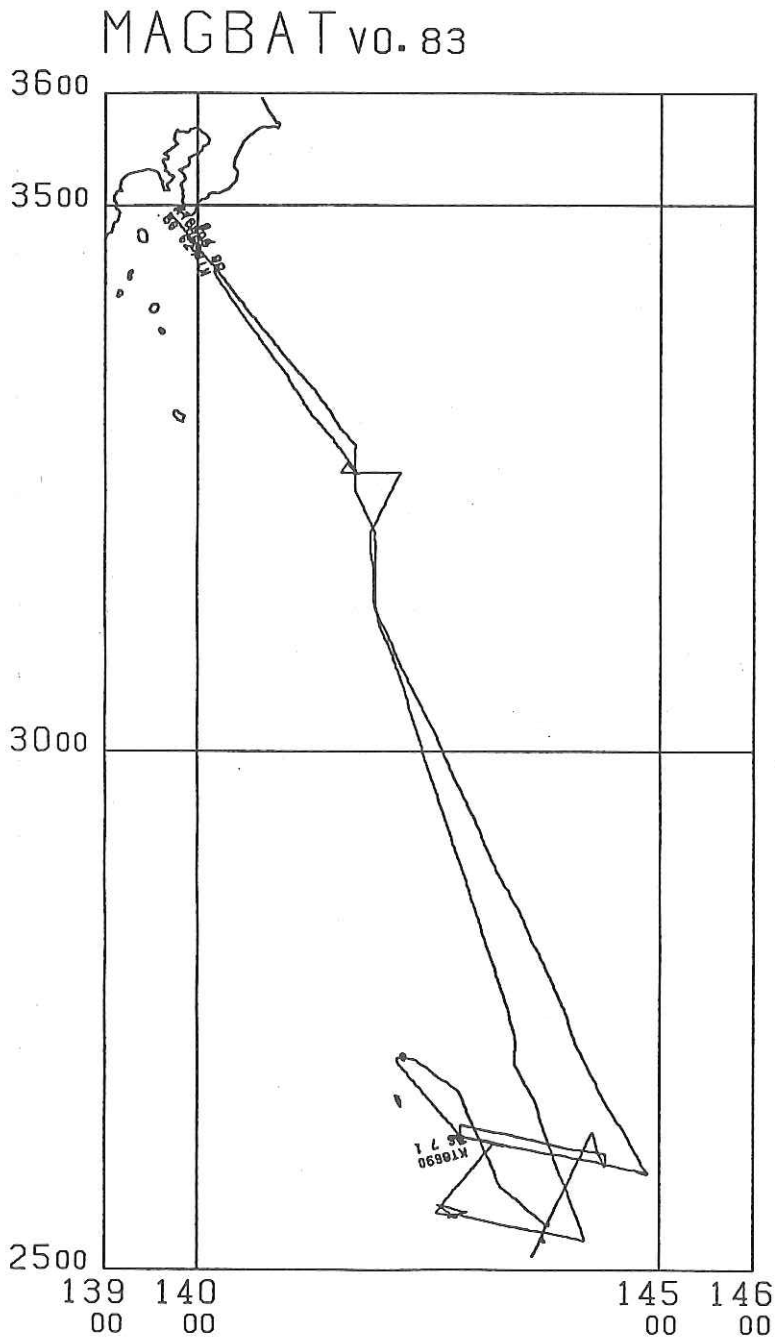

Fig. A-2-2 Ship's tracks of R. V. Tansei Maru in the cruise KT 86-9.

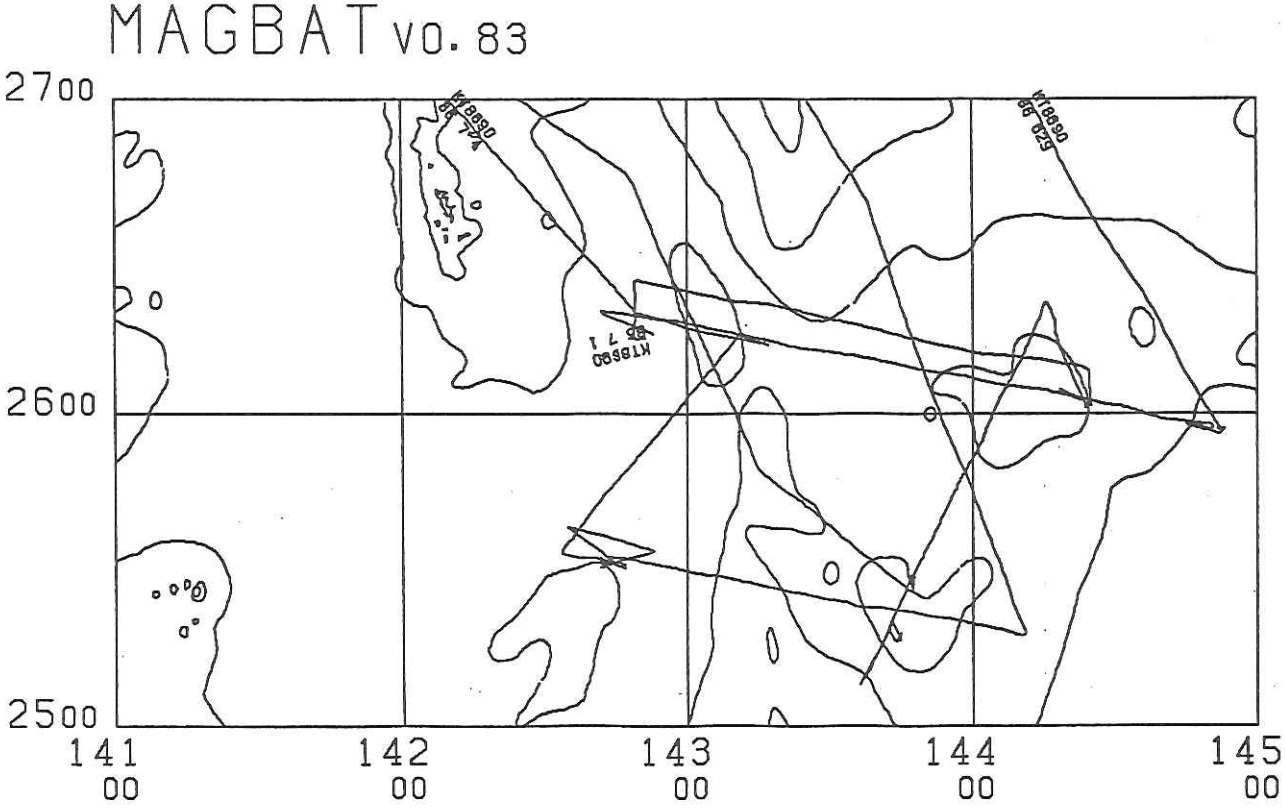

Fig. A-2-3 Ship's tracks of KT 86-9 in the Ogasawara Plateau region.

A-3. LIST OF RESEARCH STATIONS IN THE CRUISE KT 86-9

Site No.	Position Lat.(N)	Long.(E)	Investigation	Water Depth(M)	Date & Time		Remarks
					June		
0			Leave Tokyo		27	13:00	Odaiba Pier
					July		
1	26°02.3'	144°23.2'	Dredge Haul	1390	1	10:23	on Bottom
	26°02.2'	144°23.1'		1460	1	11:31	final on Bottom
2	26°03.6'	144°18.9'	Dredge Haul	1227	1	12:56	on Bottom
	26°03.8'	144°18.8'		1155	1	14:20	final on Bottom
3	26°01.9'	144°25.0'	Dredge Haul	2420	1	16:16	on Bottom
	26°00.9'	144°24.4'		2668	1	18:00	final on Bottom
4	25°19.1'	143°43.1'	Dredge Haul	1548	2	14:02	on Bottom
	25°18.6'	143°42.7'		1511	2	15:10	final on Bottom
5	25°16.7'	143°44.8'	Dredge Haul	1445	2	16:41	on Bottom
	25°16.4'	143°45.1'		1457	2	17:39	final on Bottom
6	25°27.7'	143°47.8'	Dredge Haul	2488	2	20:32	on Bottom
	25°26.9'	143°47.6'		2137	2	21:58	final on Bottom
P	27°05.5'	142°11.6'	Port of Call		3	13:00	Ogasawara
				until	4	09:00	Futami pier
7	26°13.9'	143°13.9'	Dredge Haul	2905	4	17:50	on Bottom
	26°14.1'	143°13.7'		2885	4	18:33	final on Bottom
8	26°13.9'	143°12.6'	Dredge Haul	2852	4	20:14	on Bottom
	26°14.7'	143°12.1'		2672	4	21:40	final on Bottom
9	25°31.2'	142°43.2'	Dredge Haul	1734	5	08:33	on Bottom
	25°31.5'	142°42.6'		1734	5	09:36	final on Bottom
10	25°30.6'	142°47.8'	Dredge Haul	2335	5	11:32	on Bottom
	25°30.6'	142°46.4'		2003	5	12:53	final on Bottom
11	25°31.5'	142°43.4	Dredge Haul	1751	5	14:18	on Bottom
	25°32.1'	142°44.2		1791	5	15:23	final on Bottom
12	32°34.8'	141°42.3'	Dredge Haul	4255	8	07:39	on Bottom
	32°35.2'	141°41.9'		4206	8	09:20	final on Bottom
A			Arrive at Yokohama		9	13:00	

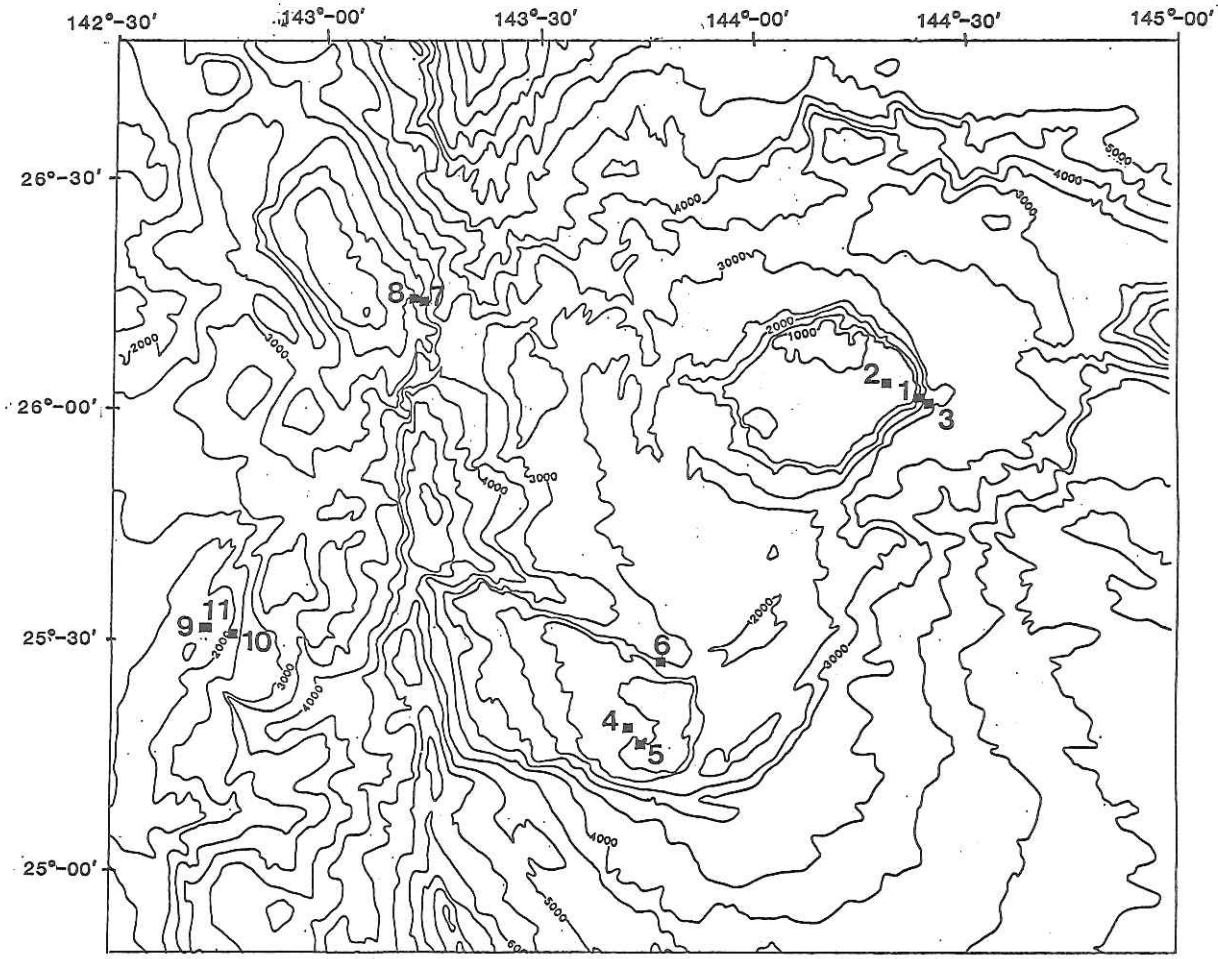

Fig. A-4-1 Positions of dredge hauls (D-1 to -11) in the cruise KT 86-9. Bathymetry is based upon unpublished Seabeam data of Hydrographic Department, MSA Japan. Contour interval 500 m.

A-4. DREDGE HAULS

A-4-1. OPERATION LOGS

Date July 01, 1986 Ship Tansei Maru KT 86-9 Station No. KT86-9 D-1
Location Steap slope of Broken-Top Guyot
Weather Fine Wind Southerly 7 m/s Sea Calm, fair swell
Bottom Topography Steap rugh topography
Type of Dredge Nalwalk chain bag Add.Wt. 0 kg
Time lowered 09 h 43 m Uncorr. Water Depth 1583 m
Initial Time on Bottom 10 h 23 m Uncorr. Water Depth 1390 m
Wire Length 1672-1661 m Wire Angle 0°
Ship Position Lat. 26°02.345'N Long. 144°23.175'E
Direction of Haul 279.8° Ship Speed 2-0.3 kt. (till h m)
Speed Wire-in 0.5 m/min (from h m) Winch No.
Final Time on Bottom 11 h 31 m Uncorr. Water Depth 1460 m
Wire Length 1470 m Wire Angle
Ship Position Lat. 26°02.165' Long. 144°23.139'
Time Surfaced 11 h 53 m
Condition of Haul Installed pinger 300 m above dredge
Dredged Materials About more than 10 gravels, scoria 3, abyssal basalts, carbonate rocks 2 (pieces).

Date July 01, 1986 Ship Tansei Maru KT 86-9 Station No. KT86-9 D-2
Location Eastern edge of the summit of the Broken-Top seamount
Weather Very fine Wind Southerly 7 m/s Sea Calm, occasional swells
Bottom Topography
Type of Dredge Nalwalk chain bag Add.Wt. 0 kg
Time lowered 12 h 32 m Uncorr. Water Depth 1218 m
Initial Time on Bottom 12 h 56 m Uncorr. Water Depth 1227 m
Wire Length 1247 m Wire Angle
Ship Position Lat. 26°03.598' Long. 144°18.942'
Direction of Haul 250° Ship Speed 0.3 kt. (till h m)
Speed Wire-in m/min (from h m) Winch No.
Final Time on Bottom 14 h 20 m Uncorr. Water Depth 1155 m
(fused wire: cut)
Wire Length 1467 m Wire Angle
Ship Position Lat. 26°03.826' Long. 144°18.782'
Time Surfaced h m
Dredged Materials 3 small pebbles of sandstone with filmy coating of Fe-Mn oxide and carbonate mudstone.

Date July 01, 1986 Ship Tansei Maru KT 86-9 Station No. KT86-9 D-3
Location Bottom of western slope of Broken-Top Guyot
Weather Very fine Wind Easterly 7 m/s Sea Calm, occasional swell
Bottom Topography
Type of Dredge Nalwalk chain bag Add.Wt.
Time lowered 15 h 32 m Uncorr. Water Depth 2525 m
Initial Time on Bottom 16 h 16 m Uncorr. Water Depth 2420 m
Wire Length 2552 m Wire Angle
Ship Position Lat. 26°01.866' Long. 144°24.975'
Direction of Haul 210° Ship Speed kt. (till h m)
Speed Wire-in 0.5 m/min (from 16 h 05 m) Winch No. 1
Final Time on Bottom 18 h 00 m Uncorr. Water Depth 2668 m
Wire Length 2650 m Wire Angle
Ship Position Lat. 26°00.898' Long. 144°24.444'
Time Surfaced 18 h 33 m
Dredged Materials 1 pumice & Mn-coated carbonate, 41 Mn-coated phosphorite.

Date July 02, 1986 Ship Tansei Maru KT 86-9 Station No. KT86-9 D-4
Location Top of "Ogasawara Plateau"
Weather Very fine Wind Southerly 9-11 m/s Sea Calm, occasional
Bottom Topography Bumpy relief close to cliff fair swells
Type of Dredge Nalwalk chain bag Add.Wt. 0 kg
Time lowered 13 h 33 m Uncorr. Water Depth 1579 m
Initial Time on Bottom 14 h 02 m Uncorr. Water Depth 1548 m
Wire Length 1594 m Wire Angle
Ship Position Lat. 25°19.103' Long. 143°43.094'
Direction of Haul 245° Ship Speed 0.3 kt. (till h m)
Speed Wire-in m/min (from h m) Winch No.
Final Time on Bottom 15 h 09 m Uncorr. Water Depth 1511 m
Wire Length 1508 m Wire Angle
Ship Position Lat. 25°18.623' Long. 143°42.662'
Time Surfaced 15 h 25 m
Dredged Materials Gravels of Neogene hemipelagic volcaniclastics & some phosphorite, 1 star fish (alive), 1 sponge.

Date July 02, 1986 Ship Tansei Maru KT 86-9 Station No. KT86-9 D-5
Location Ogasawara Plateau
Weather Very fine, windy Wind Southerly 9 m/s Sea Calm, occasional swells
Bottom Topography Supposedly steep scarp
Type of Dredge Nalwalk chain bag Add.Wt.
Time lowered 16 h 06 m Uncorr. Water Depth 1518 m
Initial Time on Bottom 16 h 41 m Uncorr. Water Depth 1445 m
Wire Length 1616 m Wire Angle
Ship Position Lat. 25°16.744' Long. 143°44.829'
Direction of Haul 206° Ship Speed 1.1 kt. (till h m)
Speed Wire-in 10 m/min (from 17 h 30 m) Winch No.
Final Time on Bottom 17 h 39 m Uncorr. Water Depth 1457 m
Wire Length 1450 m Wire Angle
Ship Position Lat. 25°16.415' Long. 143°45.080'
Time Surfaced 17 h 58 m
Dredged Materials Mn-nodules

Date July 02, 1986 Ship Tansei Maru KT 86-9 Station No. KT86-9 D-6
Location Northern cliff of Ogasawara Plateau
Weather Very fine, shower Wind Southerly 9 m/s Sea Calm
Bottom Topography
Type of Dredge Nalwalk chain bag Add.Wt. 0 kg
Time lowered 19 h 44 m Uncorr. Water Depth 2523 m
Initial Time on Bottom 20 h 32 m Uncorr. Water Depth 2488 m
Wire Length 2673 m Wire Angle 15° (21 h 33 m)
Ship Position Lat. 25°27.726' Long. 143°47.785'
Direction of Haul 200° Ship Speed 0.4 kt. (till h m)
Speed Wire-in 30 m/min (from 21 h 31 m) Winch No. 1
Final Time on Bottom 21 h 58 m Uncorr. Water Depth 2137 m
Wire Length 2100 m Wire Angle
Ship Position Lat. 25°26.932' Long. 143°47.595'
Time Surfaced 22 h 35 m
Dredged Material

Date July 04, 1986 Ship Tansei Maru KT 86-9 Station No. KT86-9 D-7
Location Western (Landward) slope of the trench wall, Bonin Trench
Weather Very fine Wind Westerly 3 m/sec Sea Extremely calm,
Bottom Topography Bumpy salient on the landward trench wall. occasional swells
Type of Dredge Nalwalk chain bag Add.Wt. 0 kg
Time lowered 17 h 00 m Uncorr. Water Depth 3020 m
Initial Time on Bottom 17 h 50 m Uncorr. Water Depth 2905 m
Wire Length 3165 m Wire Angle 10°+
Ship Position Lat. 26°13.888' Long. 143°13.876'
Direction of Haul 275 (300) ° Ship Speed 0.7 kt. (till h m)
Speed Wire-in 15 m/min (from 18 h 20 m) Winch No. 1
Final Time on Bottom 18 h 33 m Uncorr. Water Depth 2885 m
Wire Length 2883 m Wire Angle
Ship Position Lat. 26°14.144' Long. 143°13.687'
Time Surfaced 19 h 05 m
Dredged Materials Shallow-water carbonate

Date July 04, 1986 Ship Tansei Maru KT 86-9 Station No. KT86-9 D-8
Location Flat bottom in arc-trench gap : close to trench wall
Weather Very fine Wind Westerly 3 m/sec Sea Calm, occasional swells
Bottom Topography Flat
Type of Dredge Nalwalk chain bag Add.Wt. 0 kg
Time lowered 19 h 29 m Uncorr. Water Depth 2823 m
Initial Time on Bottom 20 h 14 m Uncorr. Water Depth 2852 m
Wire Length 2921 m Wire Angle
Ship Position Lat. 26°13.944' Long. 143°12.605'
Direction of Haul 280° Ship Speed 0.8 kt. (till h m)
Speed Wire-in 25 m/min (from 21 h 24 m) Winch No. 1
Final Time on Bottom 21 h 40 m Uncorr. Water Depth 2672 m
Wire Length 2650 m Wire Angle
Ship Position Lat. 26°14.703' Long. 143°12.068'
Time Surfaced 22 h 10 m
Dredged Material Sand (unconsolidated) and scoria

Date July 05, 1986 Ship Tansei Maru KT 86-9 Station No. KT86-9 D-9
Location Eastern slope of a fore-arc seamount
Weather Fine Wind Southeasterly 3.3 m/s Sea Calm, westerly swell
Bottom Topography Ruggish, "rocky"
Type of Dredge Nalwalk chain bag Add.Wt. 0 kg
Time lowered 08 h 02 m Uncorr. Water Depth 1657 m
Initial Time on Bottom 08 h 33 m Uncorr. WaterDepth 1734 m
Wire Length 1865 m Wire Angle
Ship Position Lat. 25°31.173' Long. 142°43.235'
Direction of Haul 300° Ship Speed 0.5 kt. (till h m)
Speed Wire-in 20 m/min (from 09 h 28 m) Winch No. 1
Final Time on Bottom 09 h 36 m Uncorr. Water Depth 1734 m
Wire Length 1734 m Wire Angle
Ship Position Lat. 25°31.517' Long. 142°42.617'
Time Surfaced 09 h 56 m
Dredged Materials Abundance of volcanic silty sandstones with sand and silicisponge.

Date July 05, 1986 Ship Tansei Maru KT 86-9 Station No. KT86-9 D-10
Location Eastern slope of a fore-arc seamount, Bonin
Weather Occasionally cloudy, w./sprinkle Wind SE 3 m/sec Sea Calm,
Bottom Topography Steep slope with swells
Type of Dredge Nalwalk chain bag Add.Wt. 0 kg
Time lowered 10 h 53 m Uncorr. Water Depth 2229 m
Initial Time on Bottom 11 h 32 m Uncorr. Water Depth 2335 m
Wire Length 2376 m Wire Angle
Ship Position Lat. 25°30.556' Long. 142°47.761'
Direction of Haul 257° Ship Speed kt. (till h m)
Speed Wire-in 20 m/min (from 12 h 29 m) Winch No. 1
Final Time on Bottom 12 h 53 m Uncorr. Water Depth 2003 m
Wire Length 2020 m Wire Angle
Ship Position Lat. 25°30.593' Long. 142°46.435'
Time Surfaced 13 h 10 m
Dredged Material

Date July 05, 1986 Ship Tansei Maru KT 86-9 Station No. KT86-9 D-11
Location Close to the summit of a fore-arc seamount, Bonin
Weather Fine Wind 1 m/sec N (almost none) Sea Calm
Bottom Topography
Type of Dredge Nalwalk chain bag Add.Wt. 0 kg
Time lowered 13 h 47 m Uncorr. Water Depth 1800 m
Initial Time on Bottom 14 h 18 m Uncorr. Water Depth 1751 m
Wire Length 1877 m Wire Angle
Ship Position Lat. 25°31.448' Long. 142°43.386'
Direction of Haul 53° Ship Speed 0.8 kt. (till h m)
Speed Wire-in m/min (from h m) Winch No.
Final Time on Bottom 15 h 23 m Uncorr. Water Depth 1791 m
Wire Length 1795 m Wire Angle
Ship Position Lat. 25°32.102' Long. 142°44.217'
Time Surfaced 15 h 41 m
Dredged Materials Brownish silty sandstone and sponge (alive).

Date July 08, 1986 Ship Tansei Maru KT 86-9 Station No. KT86-9 D-12
Location Summit of a fore-arc seamount
Weather Rain Wind 230° 9 m/sec Sea Fair, but considerable swells
Bottom Topography
Type of Dredge Nalwalk chain bag Add.Wt. 0 kg
Time lowered 06 h 30 m Uncorr. Water Depth 4350 m
Initial Time on Bottom 07 h 39 m Uncorr. Water Depth 4255 m
Wire Length 4667 m Wire Angle about 5°
Ship Position Lat. 32°34.776' Long. 141°42.286'
Direction of Haul ° Ship Speed 0.2 kt. (till h m)
Speed Wire-in m/min (from h m) Winch No.
Final Time on Bottom 09 h 20 m Uncorr. Water Depth 4206 m
Wire Length 4418 m Wire Angle
Ship Position Lat. 32°35.212' Long. 141°41.921'
Time Surfaced 10 h 15 m
Dredged Material Abundant gravelsof tuffaceous siltstone and sandstone

A-4-2. LIST OF DREDGED MATERIALS DURING KT 86-9

Sample No.	Diameter(mm) L	M	S	Round-ness	Wt(g)	Mn-coating(mm)	Lithology & Remarks
KT 86-9-1							
1-001	175	110	65	0.37	990	0-10	manganese / nodule (core: mudstone)
002	80	69	45	0.25	175	0-6	〃 (〃)
003	55	42	18	0.2	35	1-3	〃 (core: sediment v. ?)
1-011	88	78	60	0.35	270	0	scoria
012	54	40	33	0.4	40	0	〃
1-021	75	68	60	0.3	175	film	mudstone(fossil bearing)
022	46	40	29	0.3	28	0-2	〃
023	19	12	5	0.3	1	1-3	tuffaceous mudstone
1-031	47	39	30	0.3	67	film	phosphorite & limestone
032	81	40	25	0.2	48	0.5-1	phosphorite
033	54	30	25	0.3	47	f-2	phosphorite & tuff. ss.
034	46	25	17	0.27	22	f	phosphorite
1-041	40	25	21	0.3	25	0-f	limestone
042	13	10	7	0.35	0.5	0	〃
KT 86-9-2							
2-001	47	27	23	0.5	25	f	sandstone
002	48	28	20	0.4	20	0	〃
003	19	14	11	0.35	2	0	〃
2-011	powder		<4,3,1	<0.5		0	mudstone, white color
KT 86-9-3							
3-001	52	30	29	0.3	25	0	pumice
002	40	22	18	0.4	16	2	Mn nodule(core: sediments)
003	23	21	18	0.4	9.5	2	phosphorite & mudstone
KT 86-9-4							
4-001	120	108	80	0.3	650	f	scoria
002	45	30	19	0.3	20	f	〃
003	32	28	25	0.3	14	0	〃
004	77	45	43	0.3	80	0	〃
005	38	24	22	0.4	11	0	〃
006	49	38	35	0.4	44	0	pumice
007	76	40	36	0.3	63	0	scoria
4-011	53	33	30	0.4	61	4-5	phosphorite
012	40	27	20	0.3	20.5	2-3	〃
013	38	30	18	0.27	14.5	0.5-1	〃
4-021	197	120	80	0.29	825	0-2	sandstone(tuffaceous)
022	120	100	65	0.3	785	f	〃 (〃)
023	140	95	44	0.2	482	2-4	sandstone(tuffaceous)
024	98	72	55	0.4	352.5	f	〃 (〃)
025	130	70	60	0.2	275	f	sandy siltstone
026	95	69	55	0.2	282	f	tuffaceous silty sandstone

Sample No.	Diameter(mm) L	M	S	Round-ness	Wt(g)	Mn-coating(mm)	Lithology & Remarks
4-027	95	70	56	0.3	244	f	laminated tuffaceous silty sandstone
028	120	70	48	0.2	259	f	silty sandstone
029	120	98	50	0.2	219	f-5	" "
030	98	85	68	0.3	367	f	sandstone
031	68	57	31	0.25	98.5	f	silty sandstone
032	60	50	27	0.3	74.2	f	" "
033	60	50	29	0.27	85.6	f	sandstone
034	64	53	38	0.3	102	f	silty sandstone
035	52	46	32	0.4	62.9	f	silt(tuffaceous)
036	50	48	30	0.4	79.5	f	silty sandstone
037	57	42	34	0.3	61.9	f	(bedded)silt/silty sandstone
038	55	40	37	0.3	75.0	f	silty sandstone (vague bedding)
039	62	40	18	0.2	37.5	f	silty sandstone
040	61	30	28	0.2	50.1	f	" "
041	43	38	26	0.3	48.7	f	" "
042	54	42	38	0.3	62.6	f	" "
043	53	35	20	0.3	38.2	f	" " (laminated)
044	60	38	24	0.3	40.8	f	" "
045	50	42	22	0.25	39.5	f-1	" "
046	52	35	32	0.3	58.2	f	" "
047	50	30	21	0.2	22.5	0-3	" "
048	36	33	23	0.3	24.1	f	silt
049	40	30	25	0.3	26.1	f	silty sandstone
4-051	120	100	58	-	232	-2	sponge
052	62	16	7	-	9.2	1	"
4-061					70		sand & granule with fossil
062					25		" "
4-071	15 x 5				30		starfish
KT 86-9-5							
5-001	310	200	150	0.3	5004	0	scoria
002	67	60	28	0.3	65	0	"
003	72	12	38	0.3	81	0	"
004	50	38	34	0.2	33	0	"
005	50	35	26	0.2	35	f	"
006	40	30	21	0.2	16	0	"
007	45	35	31	0.3	18	0	"
008	50	35	20	0.25	14	f	"
009	40	40	15	0.3	14	f	"
010	50	22	18	0.2	5	f	"
011	25	25	17	0.2	6	0	pumice (2)
	24	19	14	0.2	3	0	
5-021	350	190	105	0.25	6760	0.5-2	phosphorite
5-031	290	180	80	0.25	2870	f-6	tuffaceous silty sandstone
032	210	170	70	0.3	2030	f-3	silty sandstone(phosphorite)
033	230	120	85	0.35	2110	f-2	silty sandstone
034	175	158	60	0.3	1780	1-3	" "

Sample No.	Diameter(mm) L	M	S	Round-ness	Wt(g)	Mn-coating(mm)	Lithology & Remarks
035	230	150	20	0.25	875	1-2	silty sandstone
036	235	80	35	0.25	695	1-2	" "
037	125	90	50	0.3	445	2-3	" "
038	145	65	45	o.25	450	f-1	" "
039	90	75	35	0.3	295	1-2	" "
040	90	67	48	0.25	278	1-1.5	" "
041	100	65	40	0.25	195	0.5-2	" "
042	135	65	20	0.25	205	1-2	tuffaceous silty sandstone
043	110	75	30	0.2	176	f-4	silty sandstone
044	105	65	50	0.25	275	1-3	" "
045	95	55	55	0.35	172	f-1	laminated silty sandstone
046	75	55	42	0.3	162	f-1	silty sandstone
047	95	55	25	0.25	109	f-2	" "
048	89	67	15	0.35	115	1-2	" "
049	103	56	42	0.25	150	f-10	" "
050	120	55	40	0.25	221	2-4	" "(phosphorite)
051	90	50	39	0.25	139	0.5-4	sandstone
052	159	45	16	0.3	116	0.5-2	silt
053	74	60	30	0.35	81	1-3	silty sandstone
054	80	52	35	0.35	114	f-0.5	silt
055	64	50	20	0.25	71	1-2	silty sandstone
056	85	35	32	0.3	91	-4	" "
057	70	36	20	0.3	60	f-1	" "
058	55	50	35	0.35	109	1-4	silt(phosphorite)
059	77	40	20	0.2	65	f-1	silty sandstone
060	60	47	27	0.2	54	f	" "
061	55	52	20	0.25	58	-1	" "
062	62	43	22	0.25	43	-1	" "
063	54	40	31	0.3	54	1-1.5	" "
064	54	49	18	0.25	39	0.5-2	" "
065	47	30	27	0.3	35	0.5-1.5	mudstone(phosphorite)
066	70	35	23	0.2	36	f	silty sandstone
067	75	34	23	0.25	44	f-1	" "
068	45	42	30	0.2	36	0.5-3	" "
069	50	35	18	0.3	26	0	" "
070	39	35	24	0.3	26	f	" "
071	57	53	20	0.25	30	f-2	silt
072	30	20	15	0.2	7	f	silty sandstone
073	50	25	16	0.25	26	f-3	" "
5-081	95	55	50	0.4	355	2-3	Mn-nodule
082	65	55	55	0.4	200	-32	"
083	50	47	45	0.45	116	20-23	" (core: siltstone)
084	47	46	43	0.5	108	9-30	" (")
085	56	48	40	0.4	112	-10	" (core: silt
086	44	40	40	0.4	93	12-24	" (core: siltstone)
087	45	40	40	0.5	88	7-25	" (")
088	40	40	32	0.45	74	18-20	Mn-nodule
089	46	38	22	0.3	32	5-9	" (core: siltstone)
5-091	309	80	39		660	f	sponge
5-111					110		pebbles
5-121					67		pebbles

Sample No.	Diameter(mm) L	M	S	Round-ness	Wt(g)	Mn-coating(mm)	Lithology & Remarks
KT 86-9-6							
6-001	130	120	90	0.35	1390	f	calcareous sandstone with trace fossil
002	170	100	60	0.35	775	f	calcareous sandstone
003	90	80	40	0.3	255	f	calcareous silty sandstone
004	92	65	48	0.4	330	f	" " "
005	90	75	35	0.3	210	f	" " "
006	73	62	49	0.35	165	f	" " "
007	70	54	41	0.35	164	f	" " "
008	80	77	43	0.35	223	f	" " "
009	80	77	43	0.35	225	f	" " "
010	82	60	60	0.35	170	f	" " "
011	77	60	55	0.3	175	f-0.2	" " "
012	52	50	47	0.3	73	f	" " "
013	90	50	27	0.4	102	f	" " "
014	82	50	32	0.45	110	f	" " "
015	50	50	33	0.3	66	f	" " "
016	60	40	34	0.45	79	f	" " "
017	64	49	30	0.4	73	f	" " "
018	49	46	44	0.35	69.5	f	" " "
019	62	43	34	0.35	78.6	f	" " "
020	48	43	43	0.4	59	f	" " "
021	53	44	32	0.35	69	f	" " "
022	71	40	25	0.3	61.3	f	" " "
023	58	43	37	0.4	67	f	" " "
024	45	40	30	0.4	53	f	" " "
025	58	35	30	0.4	43.5	f	" " "
026	60	45	32	0.25	61	f	" " "
027	50	49	48	0.3	85	f	" " "
028	50	32	26	0.4	34.6	f	" " "
029	60	40	31	0.45	54	f	" " "
030	49	34	29	0.45	36	f	" " "
031	71	35	32	0.2	36	f	" " "
6-041	82	62	60	0.3	220	f-3	silty sandstone
042	70	65	44	0.25	118	f-2	" "
043	100	54	25	0.3	94	f	" "
044	80	62	30	0.25	118	f-2	" " (phosphorite)
045	82	57	25	0.25	71	f-1	" "
046	90	56	19	0.3	85	f	" "
047	67	55	30	0.4	84	f	" "
048	58	55	40	0.2	116	f	" " (phosphorite)
049	75	45	25	0.4	77	f	silty sandstone
050	78	50	25	0.3	62	f	" "
051	72	46	24	0.3	81	f	" "
052	72	45	22	0.25	64.5	f	" "
053	55	45	20	0.4	39.5	f	" "
6-061	82	65	19	0.3	110	f	scoria
062	92	56	46	0.4	150	f	"
063	65	65	43	0.15	85	f	"
064	82	48	40	0.15	74	f	"
065	72	40	32	0.15	45	f	"
066	66	40	30	0.35	53	f	"

Sample No.	Diameter(mm) L	M	S	Round-ness	Wt(g)	Mn-coat-ing(mm)	Lithology & Remarks
067	67	40	32	0.35	47	f	〃
068	47	35	27	0.25	22	f	〃
069	32	25	17	0.25	6	f	〃
6-071	90	77	47	0.5	240	f	pumice
072	72	60	42	0.05	37	f	〃
073	55	52	47	0.5	67	f	〃
074	64	60	36	0.4	64	f	〃
075	54	42	22	0.2	33	f	〃
076	54	45	35	0.35	56	f	〃
077	59	27	25	0.35	24	f	〃
078	18	18	12		5		coelenterata
KT 86-9-7							
7-001	230	180	175	0.1	7500	f	fossiliferous limestone
002	178	145	100	0.15	1930	f	〃 〃
003	142	112	103	0.1	1390	f	〃 〃
004	130	100	80	0.15	1190	f	〃 〃
005	120	92	80	0.1	1040	f	〃 〃
006	110	95	68	0.1	565	f	〃 〃
007	120	100	84	0.15	740	f	〃 〃
008	110	100	80	0.1	750	f	〃 〃
009	132	90	70	0.15	760	0-0.2	〃 〃
010	92	70	65	0.1	555	f	〃 〃
011	105	95	55	0.1	424	f	〃 〃
012	94	75	70	0.1	450	f-0.2	〃 〃
013	105	85	60	0.1	530	f	〃 〃
014	100	70	70	0.1	220	f	〃 〃
015	103	85	80	0.1	590	f	〃 〃
016	105	80	55	0.15	260	f	〃 〃
017	95	74	60	0.1	440	f	〃 〃
018	82	75	63	0.1	310	f	〃 〃
019	72	70	66	0.1	230	f	〃 〃
020	90	64	45	0.15	260	f	〃 〃
021	77	60	53	0.15	260	f	〃 〃
022	70	70	60	0.1	255	f	bivalvia
023	77	40	33	0.1	190	0-f	fossiliferous limestone
024	89	59	40	0.1	195	f	〃 〃
025	65	53	30	0.1	150	f	〃 〃
7-026	67	40	30	0.1	130	f	fossiliferous limestone
027	60	53	27	0.1	105	f	〃 〃
028	62	52	28	0.1	86	f	〃 〃
029	46	42	40	0.15	68	f	〃 〃
030	56	48	22	0.2	57	f	〃 〃
031	50	42	25	0.2	63	f	〃 〃
032	55	42	40	0.15	95	f	〃 〃
033	50	50	40	0.1	118	f	〃 〃
034	62	40	35	0.1	71	f	〃 〃
035	44	40	32	0.15	67.5	f	〃 〃
036	55	39	27	0.1	40.5	f	〃 〃
037	32	25	23		21	f	Nerinea
038	14	11	4		1	f	fossil
039					65		fossiliferous limestone
040					71		〃 〃

Sample No.	Diameter(mm) L	M	S	Round-ness	Wt(g)	Mn-coating(mm)	Lithology & Remarks
041					74		〃
042					43		〃
043					47		〃
044					42		〃
045					24		〃
046					49		〃
047					17		〃
048					26		〃
049					45		〃
050					27		〃
051					74		〃
052					23		〃
053					72		〃
054					24.5		〃
055					23		〃
056					22		〃
057					39		〃
058					21		〃
059					28		〃
060					24		〃
061					20		〃
062					39		〃
063					33		〃
064					32		〃
065					34		〃
066					12		〃
067					13		〃
068					24		〃
069					12		〃
070					16		〃
071					23		〃
072					21		〃
073					4		〃
074					18		〃
075					11		〃
076					12		〃
077					51		〃
078					22		fossiliferous limestone
079					28		〃
080					57		〃
081					3		〃
082					20		〃
083					27		〃
084					24		〃
085					17		〃
086					19		〃
087					21		〃
088					50		〃
089					23		〃
090					14		〃
091					7		〃
092					10		〃
093					29		〃

Sample No.	Diameter(mm) L	M	S	Round-ness	Wt(g)	Mn-coating(mm)	Lithology & Remarks
094					6		" "
095					11		" "
096					17		" "
097					6		" "
098					20		" "
099					43		" "
100					6		" "
101					11		" "
102					6		" "
103					2		" "
104					11		" "
105					17		" "
106					9		" "
107					17		" "
108					5		" "
109					7		" "
110					14		" "
111					11		" "
112					22		" "
113					26		" "
114					18		" "
115					2		" "
116					3		" "
117					5		" "
118					14		" "
119					9		" "
120					7		" "
121					1		" "
122					14		" "
123					7		" "
124					9		" "
125					17		" "
126					4		" "
127					37		" "
128					8		" "
129					11		" "
130					9		fossiliferous limestone
131					6		" "
132					9		" "
133					9		" "
134					5		" "
135					4		" "
136					3		" "
137					12		" "
138					10		" "
139					7		" "
140					12		" "
141					2		" "
142					72		" " (fragments)
143					23		fossiliferous limestone (fragments)
144					216		"

Sample No.	Diameter(mm) L	M	S	Round-ness	Wt(g)	Mn-coating(mm)	Lithology & Remarks
7-151	25	20	8	0.2	3	f?	scoria
7-161	32	27	18	0.4	11	f?	pumice
162	19	18	13	0.4	4	0	"
7-171	190	160	160	0.3	5600	f	mudstone & sandstone
172	180	125	110	0.25	2900	f	sandstone
173	170	98	90	0.2	1150	f	"
174	60	40	35	0.25	125	f	"
175	85	75	25	0.25	127	f	"
176	60	50	35	0.25	93	0	"
177	57	54	28	0.3	62	f	"
178	53	32	28	0.25	48	f	"
179	32	28	27	0.25	20	f	"
180	27	22	15	0.25	15	f	"
181	34	32	30	0.25	30	f	"
182	35	27	25	0.25	24	f	"
183	27	23	14	0.3	11	f	"
184	25	20	15	0.2	10	f	"
185	28	23	16	0.2	13	f	"
186	20	10	10	0.3	8	f	"
187	20	10	10	0.25	8	0	"
188	20	20	10	0.25	7	f	"
189	24	21	9	0.2	6	0	"
190	21	20	10	0.2	6	f	"
191	25	15	15	0.3	6	f	"
192	20	20	10	0.3	6	0	"
193	20	20	10	0.25	5	f	"
194	20	10	10	0.2	4	f	"
195	20	10	10	0.15	6	f	"
196	15	15	10	0.3	5	f	"
197					150		"
7-201					20		limestone & sandstone
7-211					2300		sand & mud & water
212					1750		" " "
213					1360		" " "
214					2000		" " "
KT 86-9-8							
8-001	60	45	25	0.4	44	f?	scoria
002					7	-	scorias
003					2	-	"
8-011					910		sand & mud & water
KT 86-9-9							
9-001	90	75	35	0.35	160	f?	scoria
002	80	70	40	0.15	110	?	"
003	35	30	25	0.35	17	?	"
004	60	45	40	0.25	80	f?	"
005	80	60	55	0.35	165	f?	"
006	50	40	35	0.5	33	?	"

Sample No.	Diameter(mm) L	M	S	Round-ness	Wt(g)	Mn-coating(mm)	Lithology & Remarks
9-011	80	50	50	0.1	97	f	pumice
012	60	45	25	0.1	36	f	"
013	70	65	40	0.1	73	f	"
9-021	210	150	140	0.3	5024	f	laminated sandstone & mudstone
022	220	170	150	0.35	4650	f	sandstone
023	230	170	130	0.35	4350	f	"
024	150	130	110	0.3	2020	f	"
025	150	120	60	0.3	1240	f	"
026	165	110	90	0.35	1140	f	"
027	160	90	90	0.25	1080	f	"
028	140	130	110	0.35	1530	f	"
029	170	90	90	0.35	1360	f	"
030	160	130	60	0.4	1700	f	"
031	150	130	80	0.4	1550	f	"
032	130	110	70	0.3	790	f	"
033	230	110	70	0.35	1160	f	"
034	140	100	90	0.35	1450	f	"
035	135	80	70	0.35	770	f	"
036	120	110	50	0.35	690	f	"
037	110	110	60	0.35	700	f	"
038	100	100	60	0.35	720	f	"
039	105	90	30	0.4	520	f	"
040	110	100	60	0.4	700	f	"
041	105	80	60	0.4	830	f	"
042	110	70	60	0.4	420	f	"
043	110	75	50	0.35	360	f	"
044	100	80	50	0.4	390	f	"
045	100	90	70	0.35	420	f	"
046	120	75	70	0.3	540	f	"
047	120	80	60	0.25	450	f	sandstone
048	90	80	70	0.3	690	f	"
049	130	110	70	0.4	710	f	silty sandstone
050	100	70	60	0.3	500	f	sandtone
051	100	70	60	0.3	330	f	"
052	95	70	70	0.4	440	f	"
053	110	70	65	0.25	520	f	siltstone
054	120	70	60	0.35	630	f	sandstone
055	130	90	60	0.3	630	f	"
056	100	70	55	0.3	310	f	"
057	95	70	45	0.25	340	f	"
058	90	75	60	0.35	430	f	"
059	80	55	50	0.25	260	f	"
060	110	70	60	0.25	410	f	"
061	130	110	50	0.3	740	f	"
062	100	80	55	0.3	330	f	"
063	80	75	70	0.3	410	f	"
064	100	80	40	0.35	340	f	"
065	110	60	50	0.35	280	f	"
066	80	60	30	0.35	160	f	"
067	80	60	40	0.3	190	f	"
068	80	60	45	0.25	200	f	"
069	110	90	40	0.3	410	f	"

Sample No.	Diameter(mm) L	M	S	Round-ness	Wt(g)	Mn-coating(mm)	Lithology & Remarks
9-070	80	70	70	0.4	330	f	"
071	110	40	10	0.1	65	f-0.5	coarse grained sandstone
072	110	100	75	0.35	550	f	sandstone
073	55	50	30	0.25	95	0	silt with sandstone
074	100	50	20	0.2	103	0	sandstone
075	80	65	30	0.2	180	f	"
076	90	80	50	0.3	260	f	"
077	90	80	45	0.35	250	f	"
078	110	90	80	0.3	650	f	"
079	85	70	35	0.4	250	f	"
080	80	70	55	0.4	290	f	"
081	140	80	60	0.35	550	f	sandy siltstone
082	120	100	35	0.3	340	f	" "
083	130	80	50	0.3	360	f	sandstone
084	100	80	40	0.4	390	f	"
085	105	65	60	0.4	470	f	"
086	110	100	60	0.25	530	f	"
087	90	70	60	0.25	360	f	"
088	140	100	55	0.3	740	f	"
089	120	80	70	0.3	670	f	"
090	100	80	60	0.35	540	f	"
091	80	65	55	0.35	280	f	"
092	80	80	50	0.4	320	f	"
093	100	65	45	0.4	220	f	"
094	110	70	50	0.35	480	f	"
095	105	65	60	0.3	390	f	"
096	80	70	70	0.3	430	f	"
097	90	65	70	0.35	550	f	"
098	100	70	30	0.35	210	f	"
9-099	80	60	50	0.3	330		no cut from this
100	120	90	50	0.4	360		
101	100	150	40	0.3	220		
102	70	50	40	0.25	180		
103	110	100	50	0.3	620		
104	90	60	40	0.35	340		
105	80	60	50	0.35	260		
106	100	80	60	0.3	330		
107	90	60	50	0.3	190		
108	80	70	30	0.3	220		
109	80	60	40	0.35	190		
110	90	80	60	0.35	370		
111	90	70	50	0.3	320		
112	70	70	50	0.3	220		
113	80	70	40	0.35	190		
114	90	60	55	0.35	260		
115	90	80	40	0.4	210		
116	70	60	30	0.4	110		
117	80	60	40	0.35	120		
118	70	60	40	0.3	210		
119	90	60	50	0.4	295		
120	70	60	50	0.3	330		
121	90	80	60	0.3	350		

Sample No.	Diameter(mm) L	M	S	Round-ness	Wt(g)	Mn-coating(mm)	Lithology & Remarks
122	80	70	40	0.3	180		
123	90	70	20	0.25	60		
124	80	70	50	0.3	190		
125	70	60	20	0.3	85		
126	80	70	50	0.35	230		
127	80	50	50	0.35	180		
128	130	70	40	0.35	320		
129	80	60	50	0.3	280		
130	90	60	50	0.3	240		
131	90	70	50	0.35	240		
132	70	60	50	0.3	230		
133	70	55	40	0.4	115		
134	60	60	40	0.4	125		
135	80	60	40	0.4	175		
136	80	60	60	0.35	230		
137	60	55	30	0.25	125		
138	60	50	40	0.35	115		
139	70	60	40	0.3	190		
140	30	30	25	0.45	30		
141	90	70	40	0.25	195		
142	50	40	30	0.45	64		
143	60	50	30	0.3	110		
144	70	55	40	0.4	155		
145	50	50	40	0.4	120		
146	70	40	35	0.15	67		
147	55	40	10	0.2	290		
148	65	55	40	0.3	235		
149	60	50	50	0.3	125		
150	85	50	40	0.3	135		
9-151	50	40	30	0.35	67		
152	90	70	30	0.3	195		
153	60	50	40	0.4	93		
154	70	60	40	0.3	120		
155	60	45	40	0.3	71		
156	40	35	30	0.25	49		
157	90	90	50	0.25	280		
158	85	60	50	0.35	210		
159	40	40	30	0.35	54		
160	30	30	25	0.3	360		
161	40	35	30	0.3	53		
162	50	50	30	0.35	65		
163	60	50	40	0.5	125		
164	70	50	30	0.4	135		
165	10	60	40	0.3	220		
166	60	50	40	0.5	125		
167	60	50	20	0.3	72		
168	80	50	40	0.35	275		
169	50	40	30	0.45	57		
170	70	60	40	0.4	120		
171	90	60	50	0.45	230		
172	70	50	40	0.45	230		
173	40	40	30	0.3	42		
174	70	40	40	0.25	125		

Sample No.	Diameter(mm) L	M	S	Round-ness	Wt(g)	Mn-coating(mm)	Lithology & Remarks
9-175	60	40	25	0.4	52		
176	65	45	40	0.4	101		
177	40	30	30	0.3	42		
178	55	50	30	0.35	84		
179	50	45	30	0.4	68		
180	70	60	40	0.35	125		
181	50	40	20	0.45	76		
182	70	50	25	0.4	82		
183	50	40	30	0.35	180		
184	50	30	20	0.3	43		
185	50	40	30	0.4	71		
186	50	35	20	0.25	30		
187	55	30	20	0.3	41		
188	50	30	20	0.3	32		
189	80	70	50	0.4	155		
190	50	50	30	0.35	53		
191	40	30	30	0.35	41		
192	30	20	20	0.4	25		
193	40	30	20	0.35	38		
194	50	40	25	0.35	44		
195	60	40	30	0.3	84		
196	90	80	45	0.35	170		
197	65	60	40	0.4	130		
198	40	30	20	0.5	30		
199	60	50	35	0.35	87		
200	70	50	40	0.4	140		
201					42		
202					150		
203					120		
204					43		
205					120		
206					130		
207					130		
208					265		
209					360		
210					320		
211					440		
212					190		
213					310		
214					240		
215					200		
216					190		
217					340		
218					260		
219					175		
220					120		
221					82		
222					54		
223					34		
224					215		
225					83		
226					115		
227					165		

Sample No.	Diameter(mm) L	M	S	Round-ness	Wt(g)	Mn-coating(mm)	Lithology & Remarks
228					360		
229					35		
230					250		
231					330		
232					410		
233					79		
234					220		
235					71		
236					160		
237					49		
238					51		
239					37		
240					47		
241					115		
242					56		
243					23		
244					52		
245					42		
246					115		
247					21		
248					37		
249					115		
250				0.3	115	F	
251					56		
252					160		
253					140		
254					37		
9-255					165		
256					120		
257					55		
258					125		
259					115		
260					170		
261					130		
262					180		
263					225		
264					265		
265					110		
266					56		
267					45		
268					140		
269					94		
270					37		
271					150		
272					170		
273					180		
274					33		
275					195		
276					56		
277					75		
278					41		
279					35		
280					160		

Sample No.	Diameter(mm) L	M	S	Round-ness	Wt(g)	Mn-coating(mm)	Lithology & Remarks
281					20		
282					85		
283					110		
284					105		
285					175		
286					125		
287					60		
288					100		
289					170		
290					145		
291					56		
292					93		
293					165		
294					170		
295					93		
296					235		
297					86		
298					130		
299					110		
300					21		
301					92		
302					52		
303					71		
304					150		
305					70		
306					125		
9-307					230		
308					120		
309					77		
310					86		
311					180		
312					120		
313					79		
314					235		
315					305		
316					105		
317					63		
318					160		
319					145		
320					160		
321					88		
322					86		
323					135		
324					180		
325					77		
326					195		
327					88		
328					120		
329					72		
330					99		
331					105		
332					73		
333					81		

Sample No.	Diameter(mm) L	M	S	Round-ness	Wt(g)	Mn-coat-ing(mm)	Lithology & Remarks
334					210		
335					97		
336					180		
337					85		
338				0.3	82	F	
339				0.25	110	F	
340					85		
341					82		
342					125		
343				0.3	120	F	
344					110		
345				0.3	72	F	
346					140		
347				0.25	87	F	
348				0.3	64	F	
349					71		
350				0.25	98	F	
351					165		
352				0.3	160	F	
353					115		
354					120		
355					105		
356				0.3	73	F	
357					110		
358				0.35	135	F	
359				0.3	65	F	
360				0.35	145	F	
361				0.3	175	F	
362				0.35	140	F	
363					270		
364				0.35	350	F	
365				0.3	88	F	
366				0.25	90	F	
367				0.3	77	F	
368					125		
369					130		
370				0.3	125	F	
371					84		
372					175		
373					92		
374					130		
375					73		
376					145		
377					140		
378					76		
379					85		
380					110		
381					81		
382					115		
383					185		
384					225		
385					110		
386					145		

Sample No.	Diameter(mm) L	M	S	Round-ness	Wt(g)	Mn-coat-ing(mm)	Lithology & Remarks
387					71		
388					97		
389					132		
390					100		
391					125		
392					150		
393					180		
394					135		
395					55		
396					195		
397					73		
398					105		
399					220		
400					215		
401					100		
402					140		
403					93		
404					78		
405					76		
406					135		
407					41		
408					83		
409					105		
410					62		
9-411					85		
412					185		
413					65		
414					93		
415					90		
416					180		
417					86		
418					185		
419					110		
420					155		
421					145		
422					140		
423					155		
424					150		
425					135		
426					62		
427					205		
428					176		
429					240		
430					230		
431					155		
432					225		
433					105		
434					120		
435					77		
436					150		
437					87		
438					105		
439					55		

Sample No.	Diameter(mm) L	M	S	Round-ness	Wt(g)	Mn-coat-ing(mm)	Lithology & Remarks
9-440					115		
441					125		
442					125		
443					127		
444					135		
445					245		
446					123		
447					100		
448					145		
449					230		
450					74		
451					130		
452					140		
453					240		
454					210		
455					78		
456					69		
457					125		
458					76		
459					160		
460					165		
461					95		
9-501					730		pebbles
502					980		"
503					1120		"
504					670		"
505					780		"
506					1280		"
507					950		"
508					990		"
509					1130		"
510					1220		"
511					810		"
512					840		"
513					740		"
514					580		"
515					860		"
516					660		"
517					790		"
518					800		"
519					670		"
520					1100		"
521					640		"
522					660		"
523					680		"
524					920		"
525					570		sand
526					640		"
527					820		"
9-531					5650		sand & mud
532					4600		" "
533					2100		" "

Sample No.	Diameter(mm) L	M	S	Roune-ness	wt(g)	Mn-coating(mm)	Lithology & Remarks
9-534					110		sand
9-601	190	90	1		7	0	sponge
KT 86-9-10							
10-001	75	60	40	0.35	134		scoria
002	45	40	40	0.4	64		"
10-011	100	50	20	0.5	105	f	pumice
012	60	45	35	0.15	45	0?	"
013	55	45	40	0.1	54	f?	"
014	50	40	35	0.15	33	f	"
015	50	40	20	0.1	27	f	"
10-012	70	45	20	0.15	52	f	sandstone
10-031					640		sand, mud, water
KT 86-9-11							
11-001	230	140	50	0.15	1230	f-2	silty sandstone
002	100	70	50	0.3	230	1-2	sandstone
003	100	60	50	0.3	135	1-2	"
004	90	60	20	0.25	66	1-2	"
005	60	45	35	0.2	47	3	"
006	80	35	25	0.2	31	3-4	"
007	65	35	20	0.2	20	1-4	"
008	45	25	20	0.2	11	f-2	"
009	25	20	10	0.35	7	f	"
010	30	20	10	0.25	5	8	Mn nodule (sandstone core)
011	20	15	10	0.25	2	0	sandstone
11-025	110	100			21	0	sponge
KT 86-9-12							
12-001	70	60	40	0.45	140	0	pumice
002	70	70	40	0.2	110	0	"
003	60	50	40	0.4	130	0	"
004	80	50	30	0.6	89	0	"
005	45	45	35	0.35	59	0	"
12-011	450	330	130	0.35	16300	F	sandy mudstone
012	600	240	110	0.35	12900	F	" "
013	240	200	150	0.35	6650	F	mudstone
014	210	210	90	0.35	3000	F	laminated mudstone
015	160	140	70	0.4	2150	F	silty sandstone
016	150	140	100	0.4	1620	F	brown mudstone
017	150	120	80	0.45	1320	F	silty sandstone
018	270	100	70	0.35	2050	F	" "
019	210	150	90	0.35	2250	F	mudstone
020	160	150	60	0.25	1420	F	"
021	120	80	70	0.2	660	0	"
022	110	100	50	0.45	550	0	"
023	130	90	70	0.4	690	0	"
024	120	60	60	0.25	310	F	sandstone & mudstone
025	130	90	60	0.4	580	F	sandy mudstone
026	100	40	25	0.35	110	F	" "

Sample No.	Diameter(mm) L	M	S	Round-ness	wt(g)	Mn-coating(mm)	Lithology & Remarks
12-027	100	80	40	0.3	295	F	silty sandstone
028	100	70	40	0.3	280	F	laminated sandy mudstone
029	95	85	50	0.3	195	F	sandy mudstone
030	150	70	60	0.25	270	F	" "
031	110	70	50	0.25	290	F	black mudstone
032	130	90	50	0.35	405	F	silty sandstone
033	80	70	50	0.3	270	F	" "
034	120	80	25	0.3	210	F	sandy mudstone
035	90	70	25	0.25	205	F	laminated muddy sandstone
036	90	60	30	0.3	260	F	sandy mudstone
037	80	70	30	0.35	280	0	laminated mudstone
038	80	50	25	0.3	105	0	sandy mudstone
039	80	60	20	0.3	96	F	"
12-040	40	10	6	0.4	4	F	sandstone
041	15	10	10	0.3	2	F	laminated mudstone
042	100	35	30	0.3	125	F	black laminated mudstone
043	50	30	20	0.35	39	F	black mudstone
044	70	50	40	0.35	145	0	laminated mudstone
045	40	25	25	0.35	21	F	laminated sandy mudstone
046	30	20	10	0.3	8	0	laminated mudstone
047	15	15	10	0.25	4	F	" "
048	25	25	20	0.25	8	F	" "
049	10	10	10	0.25	2	?	" "
050	80	50	40	0.2	115	F	mudstone
051	70	60	60	0.25	250	F	"
052	130	90	60	0.35	390	F	sandy mudstone
053	110	70	60	0.25	440	0	laminated sandy mudstone
054	60	60	30	0.4	98	0	mudstone
055	110	90	70	0.25	660	0	"
056	100	90	50	0.35	430	0	"
057	70	50	30	0.45	92	F	"
058	70	60	40	0.25	160	F	sandy mudstone
059	80	60	20	0.4	115	F	mudstone
060	70	60	30	0.35	110	F	sandy mudstone
061	70	50	30	0.25	95	F	mudstone
062	80	80	40	0.25	230	F	" (pumice fragments)
063	120	80	50	0.3	280	F	sandy mudstone
064	70	60	20	0.3	120	F	mudstone
065	80	60	20	0.35	115	0	"
066	80	40	25	0.35	105	0	"
067	90	70	30	0.3	155	F	"
068	90	70	40	0.35	240	F	"
069	70	50	25	0.35	84	0	"
070	80	60	30	0.35	130	F	"
071	100	80	30	0.35	200	F	"
072	90	70	30	0.3	185	F	"
073	80	60	40	0.4	225	F	sandy mudstone
074	70	50	40	0.4	135	F	" "
075	120	100	50	0.35	385	F	" "
076	100	80	60	0.35	270	0	" "
077	80	70	60	0.4	250	F	sandstone
078	110	70	50	0.35	180	F	sandy mudstone

Sample No.	Diameter(mm) L	M	S	Round-ness	wt(g)	Mn-coating(mm)	Lithology & Remarks
12-079	110	70	60	0.3	235	0	sandy mudstone
080	100	80	50	0.35	260	F	" "
081	110	70	40	0.35	255	F	mudstone
082	70	60	30	0.3	140	F	"
083	100	60	50	0.3	180	0	"
084	100	80	60	0.25	270	0	"
085	100	50	40	0.25	175	F	"
086	60	50	40	0.3	115	F	"
087	90	70	40	0.25	160	F	sandy mudstone
088	110	70	60	0.4	360	F	mudstone
089	100	70	60	0.35	250	F	"
090	90	70	25	0.35	180	F	black sandy mudstone
091	110	70	40	0.45	150	F	mudstone
12-092	80	70	20	0.3	115	0	mudstone
093	60	50	40	0.4	105	0	sandy mudstone
094	100	90	30	0.25	255	F	" "
095	110	100	30	0.3	270	0	mudstone
096	70	50	30	0.35	105	0	"
097	100	80	60	0.4	305	0	"
098	110	110	70	0.4	390	F	"
099	150	130	40	0.35	620	F	"
12-100	70	60	20	0.3	120	F	sandy mudstone
101	90	50	20	0.35	84	F	" "
102	110	80	40	0.3	300	F	sandy mudstone
103	70	70	30	0.3	160	0	mudstone
104	80	60	20	0.4	120	0	"
105	120	70	40	0.35	240	F	"
106	70	60	40	0.4	110	F	"
107	50	50	40	0.2	115	0	"
108	160	80	40	0.3	330	F	sandy mudstone
109	100	70	50	0.25	160	F	" "
110	70	60	30	0.35	130	F	" "
111	90	60	40	0.25	180	F	" "
112	100	70	50	0.2	230	F	mudstone
113	80	60	50	0.25	140	F	sandy mudstone
12-121					1390		mudstones & sandstones
122					1530		" "
123					1060		" "
124					1120		" "
125					990		" "
126					1570		" "
127					1750		" "
128					1620		" "
129					1410		" "
130					540		" "
131					2500		sand
132					3020		"
133					4050		"
134					3340		"
135					2600		"

A-4-3. LIMESTONES COLLECTED AT THE LANDWARD MARGIN OF THE SOUTHERN IZU-OGASAWARA TRENCH

A dredge haul KT 86-9-7 was undertaken at the lowest landward slope of the Izu-Ogasawara Trench. The site is located at the front of a collision of north-western flank of the Ogasawara Plateau with a fore-arc seamount (Hahajima Seamount) at which the trench axis shoals to as shallow as 3,500 m (Fig. A-4-1). Fig. A-4-3-1 represents a record of a deep-sea echogram across this site in nearly EW direction. A small topographic high is clearly recognized at the lowest margin of the landward slope. One hundred and forty four (144) fragments [exceeding 50 kgs in total] of fossiliferous limestones were recovered by the dredge haul there. Some samples contain megafossils such as Nerinea with the maximum length of nearly 4 cm and a diameter of roughly 1.5 cm (Fig. A-4-3-2).

Occurrence of this type with other kinds of shallow water fossils in the limestones indicates that they were possibly formed at reefal environment in Cretaceous period. Considering the Eocene age of the Ogasawara islands it can be concluded that the limestones collected by the present dredge haul originated from a seamount in the oceanward plate but not at the arc. Mechanism of accretion of the limestones to the fore-arc toe will be a problem to be solved. Since no oceanic island basalts have been found in the landward slope of this region, main body of the seamount capping the reef limestone may have been subducted under the trench, with only fragments of its cap left behind accreted to the accreted toe.

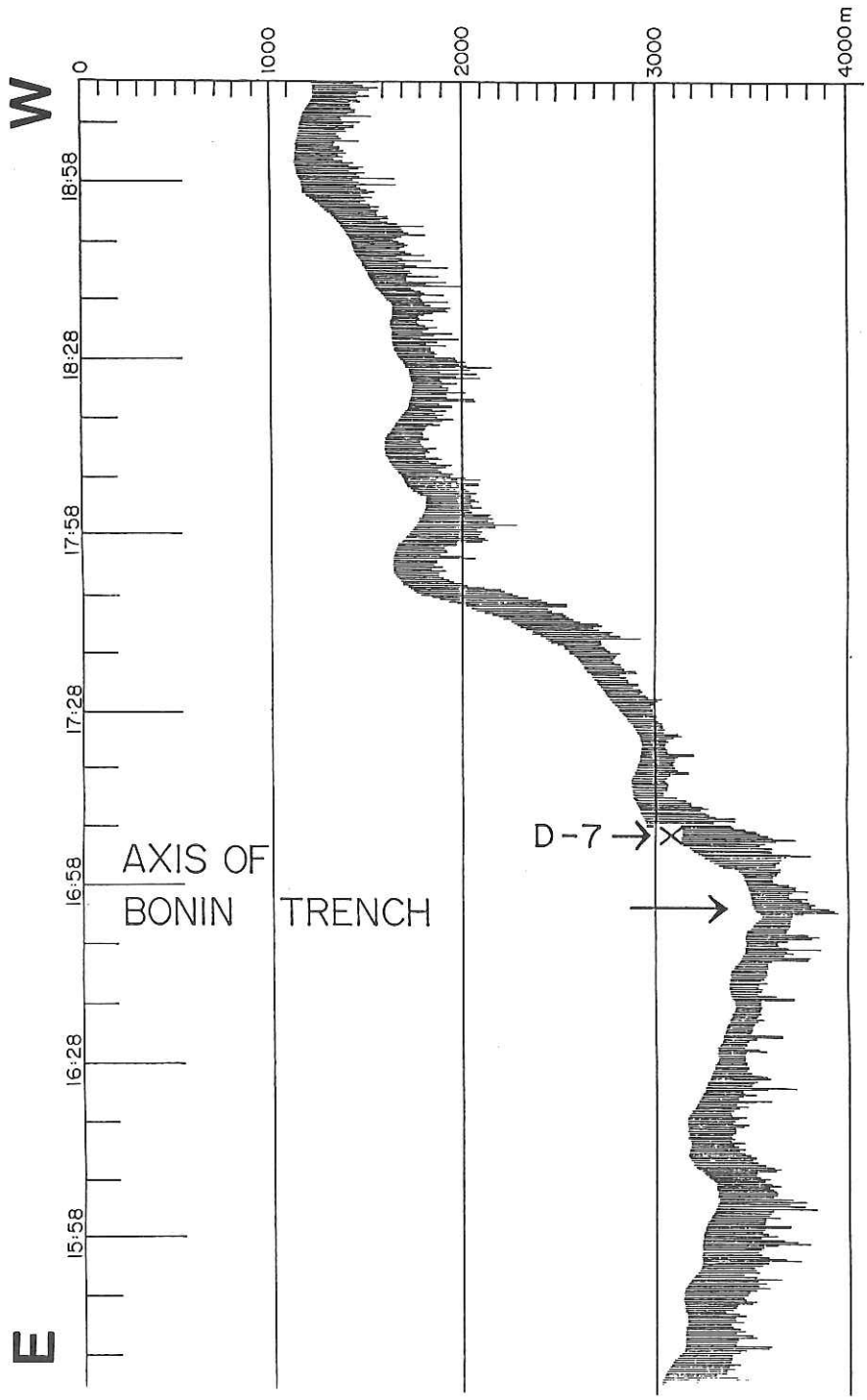

Fig. A-4-3-1 An E-W profile of topography across the dredge station KT 86-9-7 roughly normal to the collision front of the northwestern flank of Ogasawara Plateau with the Ogasawara (Bonin) Arc-trench system.

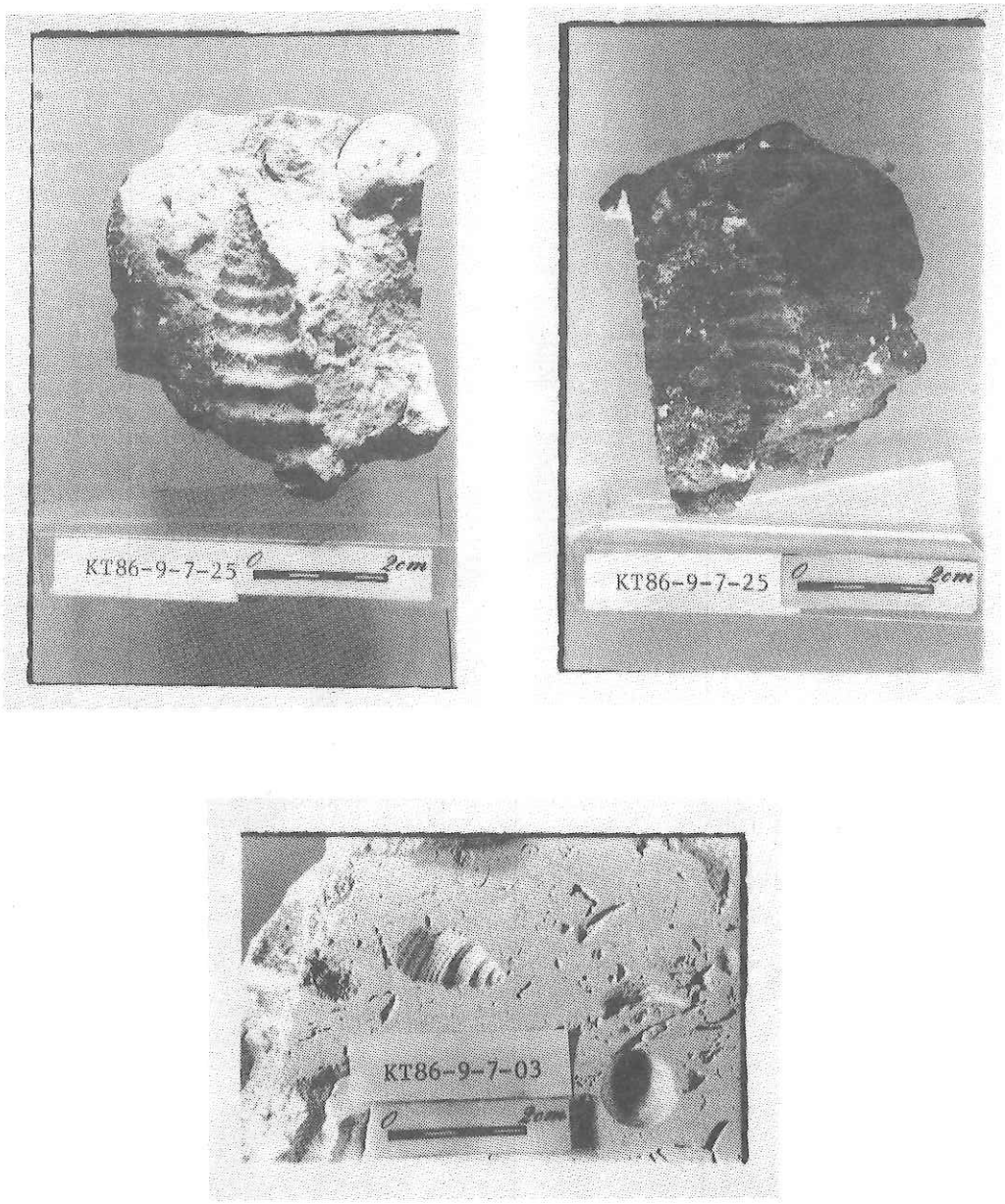

Fig. A-4-3-2 Photographs of limestones containing megafossils Nerinea collected by a dredge haul KT 86-9-7 at fore-arc toe of the southern Izu-Ogasawara (Bonin) Trench.

A-5. MULTICHANNEL SEISMIC REFLECTION SURVEY

H. Tokuyama, S. Abe, M. Nakanishi, I. Uno and K. Konishi

Seismic reflection survey in the cruise KT 86-9 was done using six-channel receivers installed in a streamer cable of 50 m length. One airgun with 550 cubic inches capacity of 90 atmosphere of firing pressure. The ship sailed by a constant speed of 5 knots. Shots of the airgun was controlled by electric signals at 50 meters' intervals of shot points.

Locations of the survey tracks are shown in Fig. A-5-1. Positions of the ship were fixed by Loran C controlled by NNSS. Accuracy of positions is approximately 200 m, since one of the Loran C stations, Iwo-jima is too close to the survey area.

Table A-5-1 represents longitudes and latitudes of shot points with water depths. Reflected signals were recorded in magnetic tapes and processed in a shore-based computer laboratory at Ocean Research Institute. Seven sheets of records after CDP stack, deconvolution and digital filtering for Line 1 (E-F), Line 2 (K-L) and Line 3 (W-X) are reproduced in Fig. A-5-2. Two migrated records for Line 2 (K-L) are also shown in Fig. A-5-3. Sediment structures with normal fault blocks of the Ogasawara Plateau are clearly seen in these records.

TABLE A-5-1 Table of Shot Point Positions of the Multichannel Reflection Survey in the Cruise KT 86-9

LINE 1

Shot No.	Time	Latitude	Longitude	Water Depth (uncorrected)
0300	June 29 23:47	25°57.6'N	144°50.8'E	4952 m
0400	June 30 00:20	58.1	47.6	4746
0474	00:46	-	-	-
0500	00:54	58.4	44.5	3654
0514	01:18	-	-	-
0600	01:27	58.7	41.2	3455
0700	02:00	59.0	38.5	3123
0800	02:34	59.6	34.9	3245
0900	03:07	26°00.4	33.8	3214
1000	03:40	01.1	30.7	3163
1018	03:48	-	-	-
1100	04:15	01.684	27.5	2866
1102	04:16	-	-	-
1200	04:47	02.281	24.2	2180
1202	04:48	-	-	-
1231	04:57	-	-	-
1300	05:20	02.975	21.0	1147
1400	05:52	03.555	18.0	1281

LINE 1 (continued)

Shot No.	Time June 30	Latitude	Longitude	Water Depth (uncorrected)
1500	06:25	26°04.162	144°15.0	1285
1532	06:34	–	–	–
1600	06:57	04.611	12.0	1266
1700	07:30	04.937	09.1	1259
1800	08:02	05.297	05.9	1205
1900	08:34	05.817	02.8	1207
2000	09:05	06.609	143°59.59	1124
2036	09:16	06.851	58.583	1650
2037	09:17	06.851	58.583	1700
2100	09:37	07.251	56.829	2165
2170	09:58	07.443	54.657	2455
2200	10:07	07.544	53.770	2455
2300	10:38	08.025	50.724	2412
2400	11:19	08.533	47.733	2555
2500	11:40	09.139	44.594	3144
2548	11:56	–	–	–
2600	12:11	09.611	41.566	2819
2700	12:41	10.114	38.456	2771
2800	13:12	10.591	35.436	2815
2900	13:44	11.023	33.023	2878
3000	14:14	11.452	30.747	
3052	14:	–	–	3093
3100	14:41	11.794	28.472	3159
3200	15:15	12.080	25.649	2889
3300	15:41	12.480	22.487	3141
3400	16:19	13.128	19.386	3167
3500	16:50	13.770	16.332	3485
3565	17:10	–	–	–
3580	17:14	–	–	2893
3600	17:20	14.359	13.323	2900
3700	17:51	14.950	10.425	1693
3710	17:54	–	–	–
3800	18:22	26°15.447	143°07.627	1709
3900	18:53	16.327	02.667	1329
4000	19:24	16.824	01.315	1258
4069	19:45	–	–	–
4100	19:55	17.383	142°58.283	1373
4200	20:24	17.806	55.322	1733
4300	20:55	18.143	52.398	3085
4400	21:26	18.516	49.582	3313
4500	21:57	18.874	46.737	3149
4558	22:15	19.089	45.057	3044

LINE 2

Shot No.	Time July 01	Latitude	Longitude	Water Depth
0001	21:13	26°16.836'N	144°13.826'E	2878 m
0016	21:18	16.419	13.645	2805
0100	21:43	14.211	12.633	2430
0128	21:53	11.656	11.357	–
0200	22:14	09.211	10.028	951
0300	22:46	06.809	08.620	693
0400	23:15	04.492	07.058	850
0500	23:46			1228
0515	23:51	–	–	–
0516	23:52	–	–	–
	July 02			
0600	00:17	01.996	05.652	1069
0700	00:48	25°59.600	04.399	1117
0800	01:19	57.296	03.247	1044
0900	01:50	54.806	02.299	1463
1000	02:21	52.394	00.912	2226
1020	02:28	–	–	–
1100	02:51	50.040	143°59.384	2646
1200	03:22	47.724	58.038	2308
1300	03:53	45.407	56.724	2162
1313	03:58	–	–	–
1396	04:25	–	–	–
1400	04:25	43.039	55.505	2175
1500	04:56	40.576	54.204	2286
1600	05:27	38.044	52.824	2294
1700	05:58	35.293	51.367	2370
1800	06:29	32.715	49.886	2389
1900	06:59	30.276	48.440	2475
2000	07:30	27.806	47.032	2405
2022	07:37	–	–	–
2100	08:01	25.222	45.750	1615
2200	08:31	22.737	44.602	1448
2300	09:02	20.136	43.351	1547
2338	09:14	–	–	–
2400	09:34	17.657	42.145	1512
2500	10:04	15.122	40.885	1704
2600	10:34	12.794	39.685	2558
2700	11:05	10.480	38.457	3526
2721	11:12	09.941	38.132	3742

LINE 3

Shot No.	Time	Latitude	Longitude	Water Depth (uncorrected)
	July 05			
0001	16:36	25°31.799'N	142°48.161'E	2475 m
0034	16:46	31.673	49.093	2768
0100	17:08	31.317	50.905	2890
0200	17:39	30.827	53.785	3106
0300	18:09	30.337	56.804	3215
0400	18:40	29.672	59.944	3015
0500	19:11	29.008	143°03.142	3525
0515	19:16	-	-	-
0600	19:42	28.90	05.59	3926
0700	20:11	28.069	08.929	4975
0800	20:43	27.483	11.117	6019
0900	21:14	26.999	14.782	4691
1000	21:44	26.480	17.772	4080
1019	21:50	-	-	3980
1020	21:50	-	-	-
1031	21:53	-	-	3791
1100	22:14	25.880	20.819	3151
1200	22:45	25.327	23.856	2777
1300	23:15	24.624	26.889	2634
1400	23:47	24.051	29.991	2398
1425	23:56	-	-	-
	July 06			
1500	00:18	23.598	33.047	2023
1535	00:30	-	-	-
1600	00:49	22.715	35.706	1887
1700	01:20	22.485	38.434	1753
1800	01:50	22.407	41.100	1571
1900	02:21	21.902	43.766	1469
2000	02:52	21.701	46.566	1360
2040	03:06	-	-	-
2100	03:23	21.131	49.503	1294
2123	03:32	-	-	-
2200	03:55	20.575	52.632	1900
2300	04:26	20.174	55.816	2175
2400	04:57	19.636	58.876	2236
2500	05:28	18.942	144°01.806	1939
2554	05:44	-	-	-
2600	05:59	18.398	04.887	2208
2700	06:29	17.825	07.902	3158
2717	06:35	-	-	-

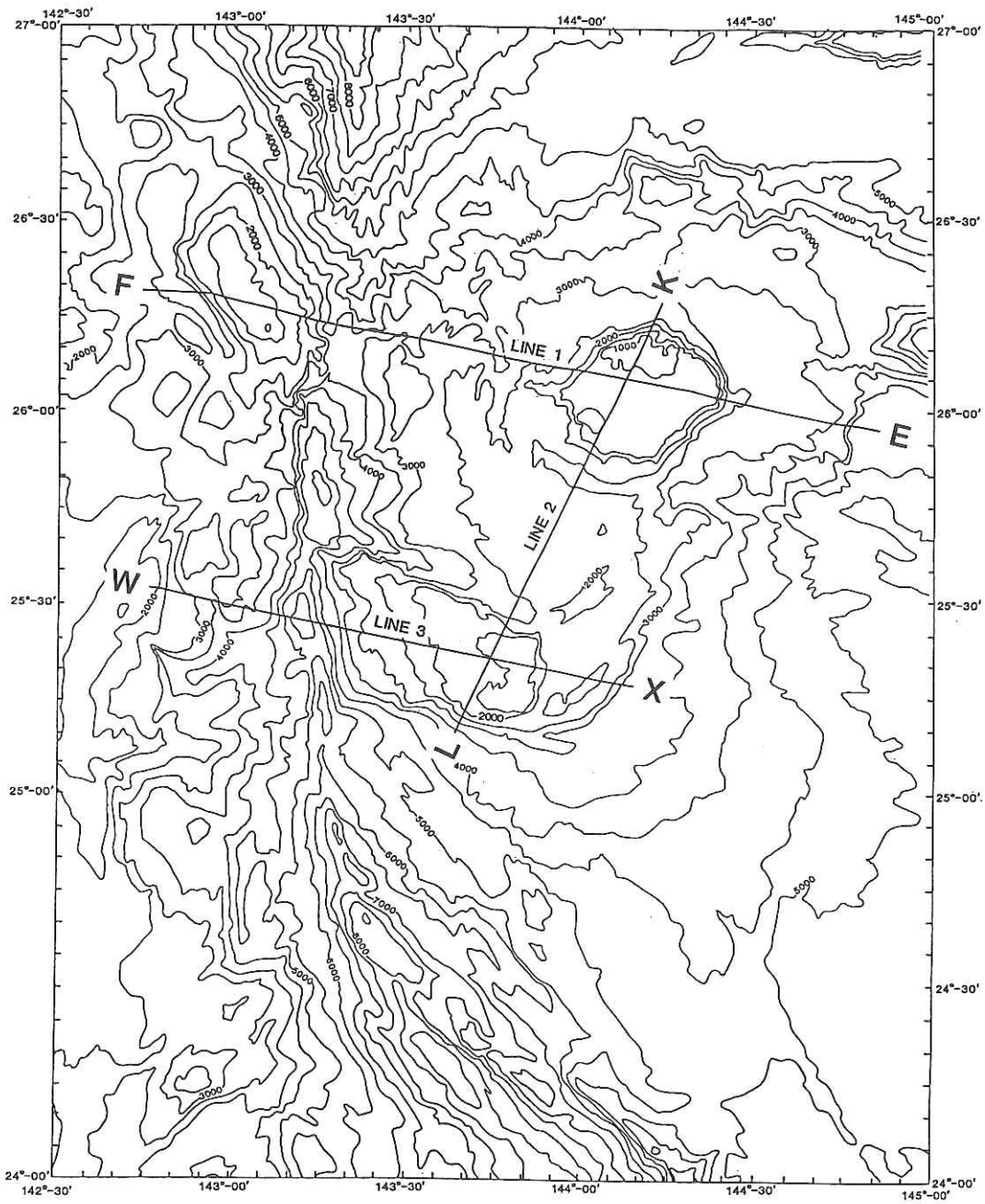

Fig. A-5-1 Locations of multichannel seismic reflection profiler lines. Line 1: E-F, Line 2: K-L, Line 3: W-X. Precise positions of shot points are shown in Table A-5-1. Bathymetry is based upon unpublished Seabeam data of Hydrographic Department, MSA. Contour interval; 500 m.

Fig. A-5-2-1 Seismic profiler record on the eastern part of Line F-E in the Ogasawara Plateau region (after CDP stack, deconvolution and digital filtering).

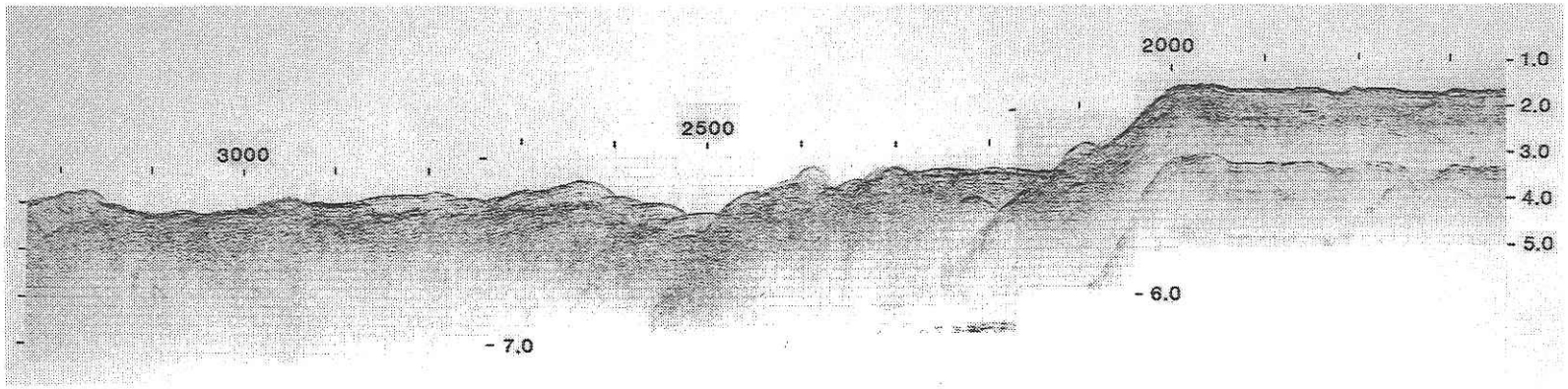

Fig. A-5-2-2 Seismic profiler record on the central part of Line F-E in the Ogasawara Plateau region (after CDP stack, deconvolution and digital filtering).

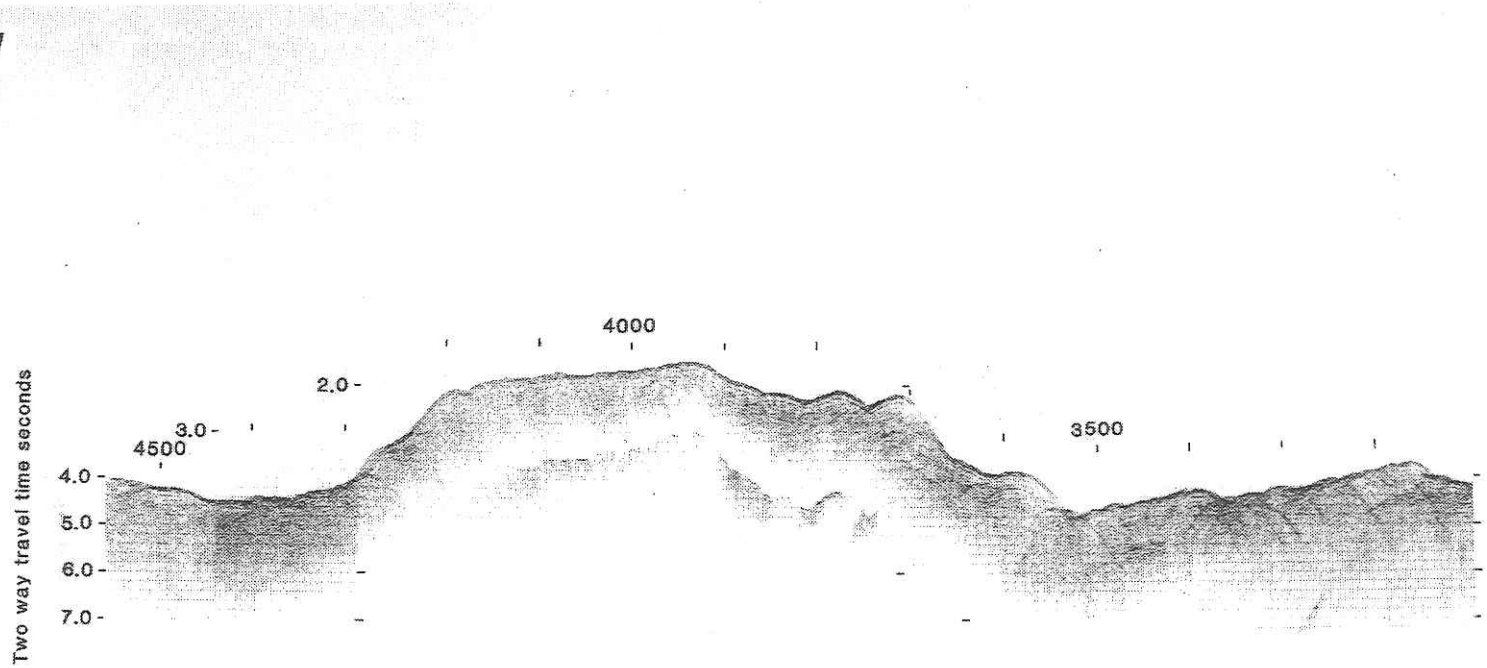

Fig. A-5-2-3 Seismic profiler record on the western part of Line F-E in the Ogasawara Plateau region (after CDP stack, deconvolution and digital filtering).

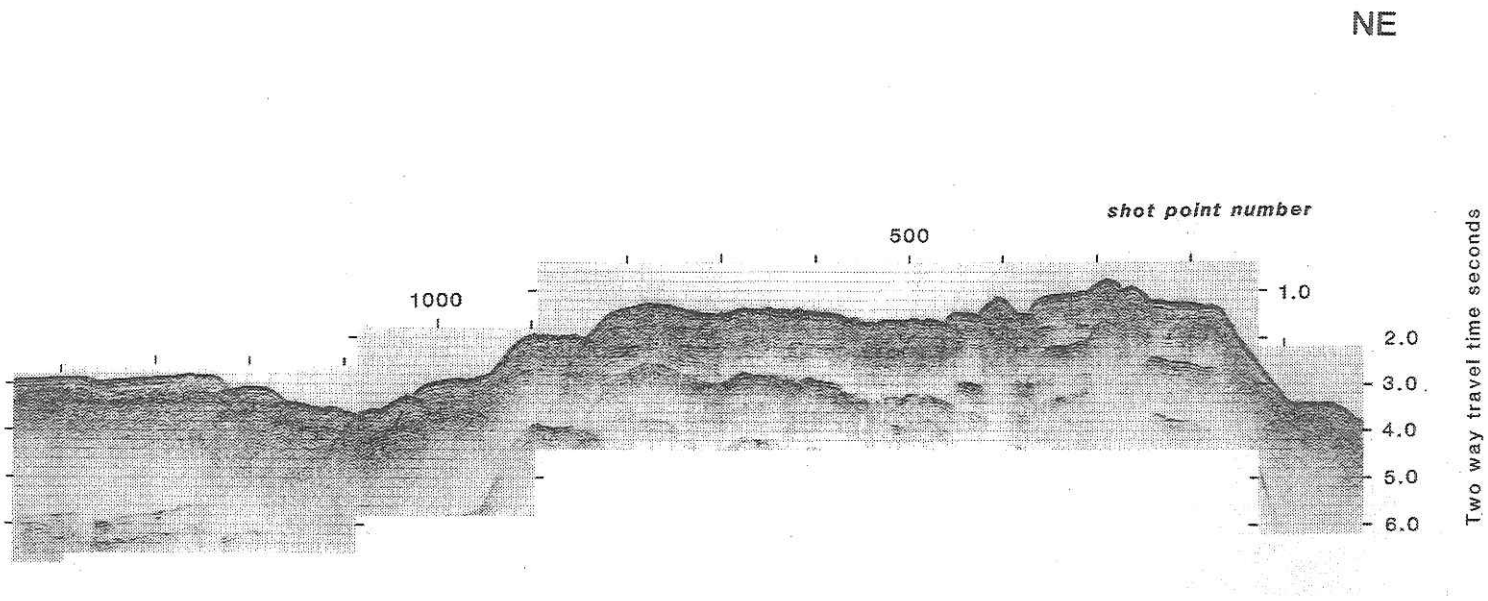

Fig. A-5-2-4 Seismic profiler record on the northeastern half of Line K-L in the Ogasawara Plateau region (after CDP stack, deconvolution and digital filtering).

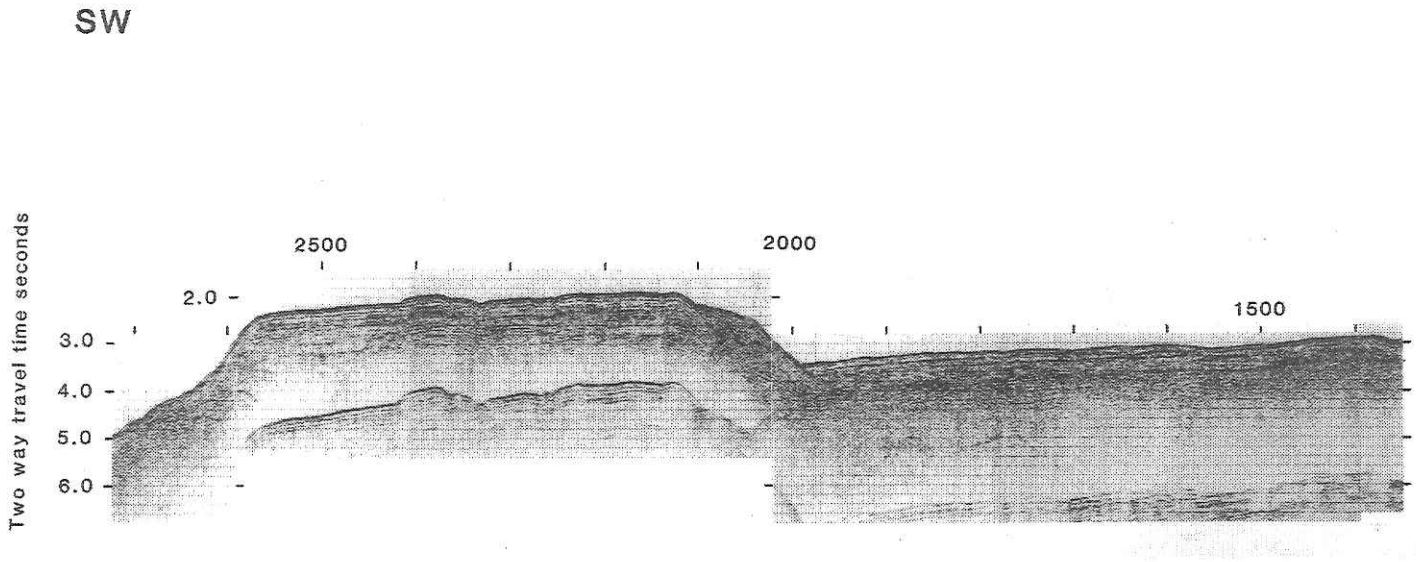

Fig. A-5-2-5 Seismic profiler record on the southwestern half of Line K-L in the Ogasawara Plateau region (after CDP stack, deconvolution and digital filtering).

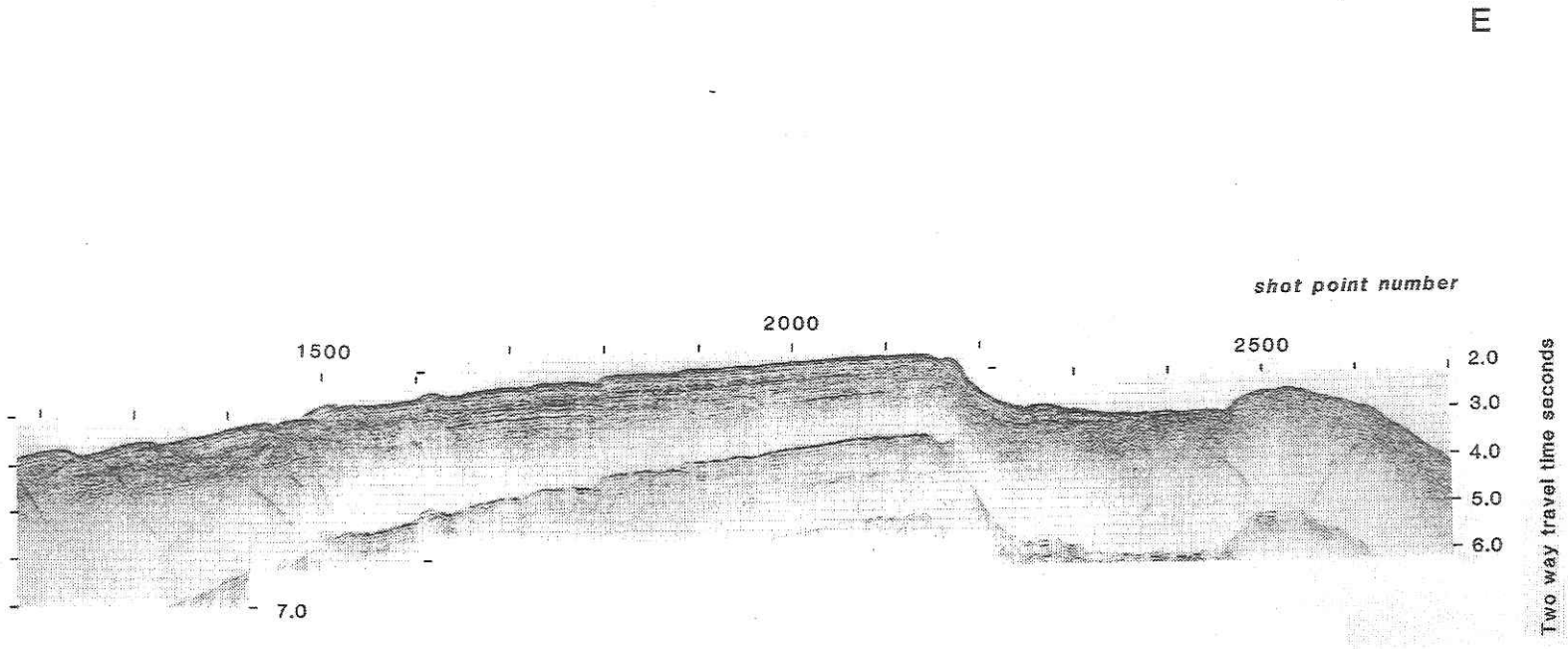

Fig. A-5-2-6 Seismic profiler record on the eastern half of Line W-X in the Ogasawara Plateau region (after CDP stack, deconvolution and digital filtering).

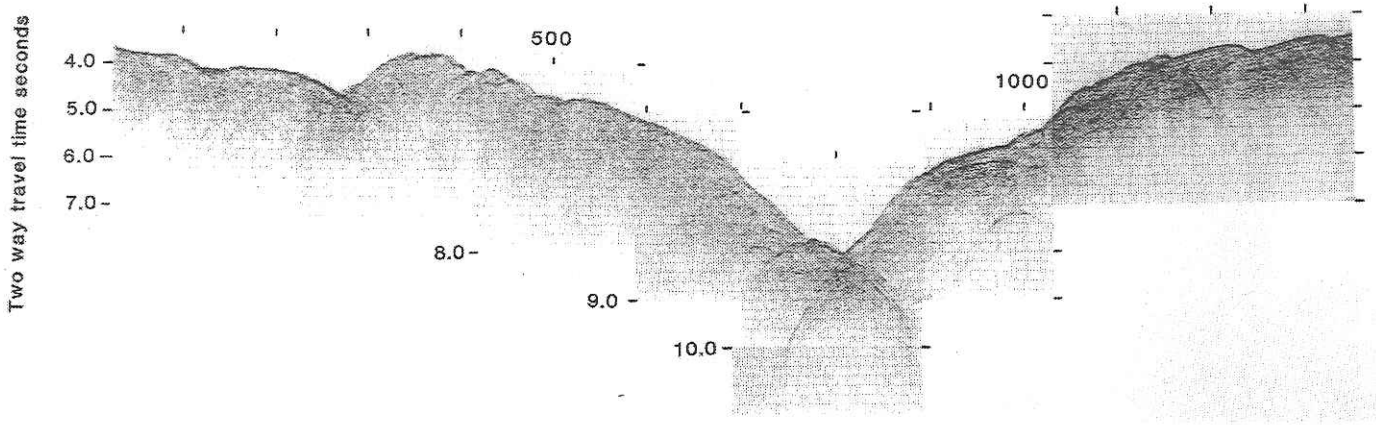

Fig. A-5-2-7 Seismic profiler record on the eastern half of Line W-X in the Ogasawara Plateau region (after CDP stack, deconvolution and digital filtering).

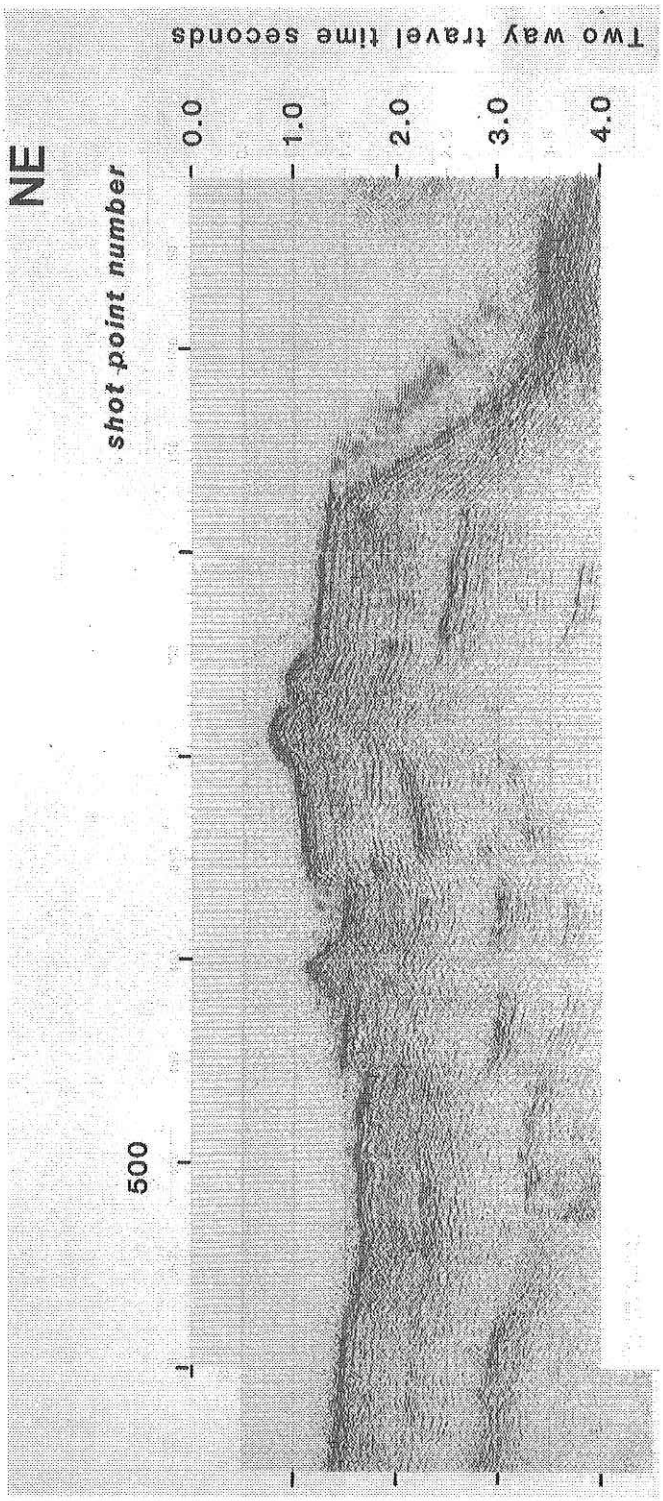

Fig. A-5-3-1 Eaxample of migrated seismic profiler record on the northeastern half of Line K-L in the Ogasawara Plateau region.

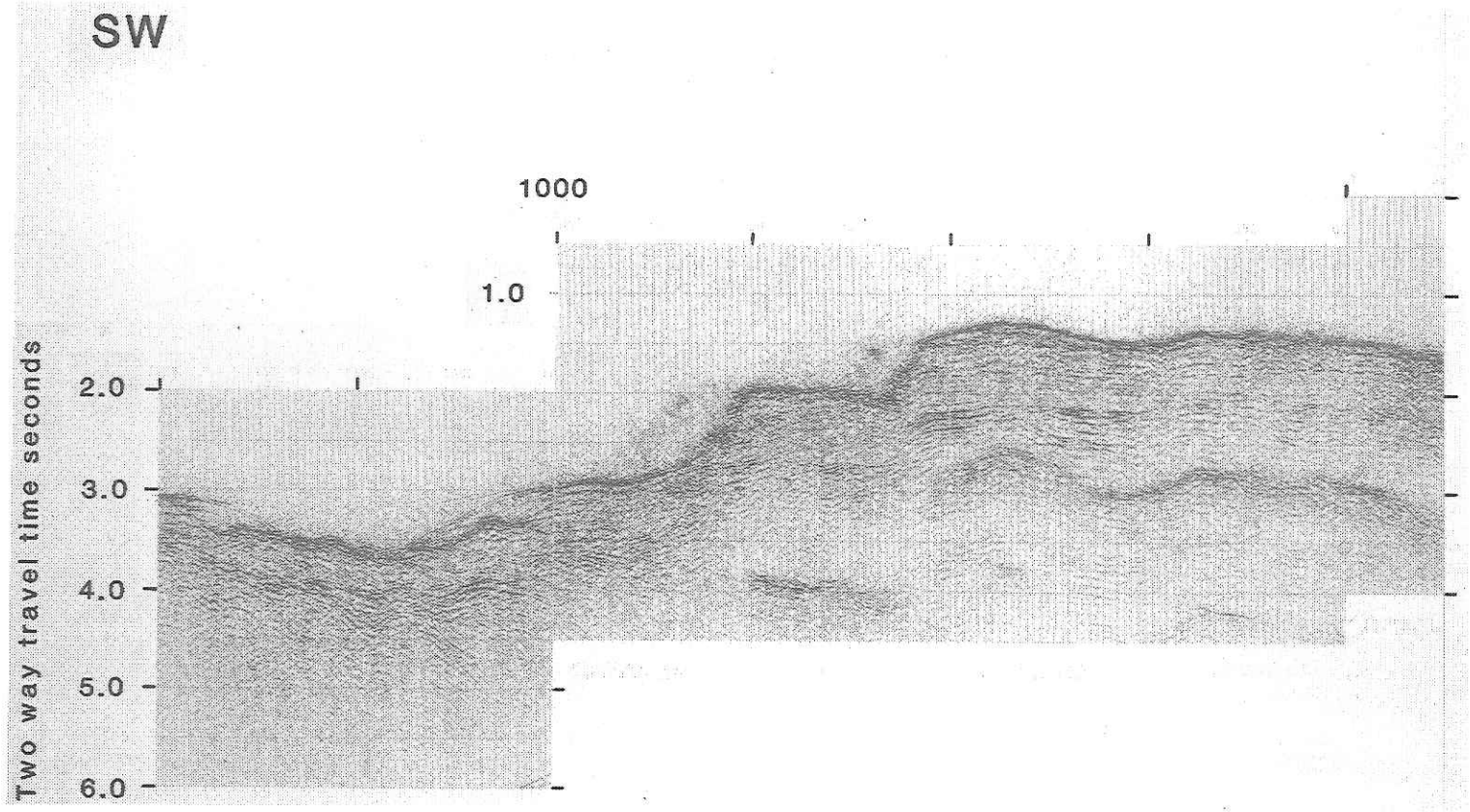

Fig. A-5-3-2 Eaxample of migrated seismic profiler record on the southwestern half of Line K-L in the Ogasawara Plateau region.

A-6. RECENT BENTHIC FORAMINIFERAL ASSEMBLAGES OFF THE BONIN ISLANDS OBTAINED IN CRUISE KT 86-9

K. Akimoto and T. Yoshida

[1]. INTRODUCTION

There are many recent benthic foraminiferal assemblages in the shallow shelf areas to the middle bathyal zones around Japan. However, very little hasbeen treated with recent benthic foraminiferal assemblages in the Izu-Bonin area. It is intended in this cruise to investigate distribution of recentbenthic foraminiferal assemblage in the area off the Bonin Islands. Samplesexamined in this study are collected by dredge hauls at fivestations on the Ogasawara Plateau (KT 86-9 D-4), the Bonin trench (KT 86-9 D-7, D-8) and the eastern slope of the Bonin Islands (KT 86-9 D-9, D-10).

[2]. METHOD

The samples were washed over a screen with 0.063 mm (250 mesh) and dried at about 80°C in an oven. The dried samples were then divided by the splitter to an aliquot of workable size from which approximately 200 specimens of benthic foraminifera were counted.

[3]. RESULT

Benthic foraminiferas occur abundantly in each sample but agglutinated forms are rare. Preservation of benthic foraminiferal tests is good except in one sample (D-4). The benthic foraminiferal assemblage is as follows;

D-4

Cassidulina? perumbonata	VA
Globocassidulina subglobosa	VA
G. elegans	C
Burseolina marshallana	C
Cibicidoides wuellerstorfi	F
G. parva	F

D-7

Cibicidoides wuellerstorfi	VA
Bulimina alazanensis	C
Favocassidulina favus	C
Pseudoparrella exigua	C

D-8

Cibicidoides wuellerstorfi	A
Pseudoparrella exigua	A
Bulimina alazanensis	C
Pullenia bulloides	C
Siphouvigerina proboscidea	C

D-9

Pseudoparrella exigua	A
Bulimina alazanensis	C
G. elegans	C
Osangulina culter	C

D-10

Pseudoparrella exigua	A
Pullenia bulloides	A
Brizalina vescistriata	C
Gyroidina orbicularis	C
Melonis pacificus	C
Tosaia hanzawai	C

CORRECTION AND ADDITION TO KH86-2 CRUISE REPORT

[Editor's Remark]:

In the previous cruise report KH86-2 produced by the same editor, Mr. S. Nagihara's name and address (Department of Earth Sciences, Chiba University) were deleted by mistake from the list of Scientists. Paper by S. Nagihara and T. Asanuma in page 110 was erroneously replaced by its draft version. The editor expresses his apology to the authors and publishes their final version here.

14. HEAT FLOW MEASUREMENTS [KH86-2,1988]

S. Nagihara and T. Asanuma

Heat flow measurements were made at three stations (KH 86-2-7, -8 and -12) during the cruise KH 86-2. At KH 86-2-7 and -8, thermal conductivities as well as temperature gradients were measured. At KH 86-2-5, -6 and -10, only thermal conductivities were measured.

14-1. METHOD AND INSTRUMENT

The heat flow measuring system is developed recently at Chiba University (Nagihara et al., 1986). It has a probe of Ewing type (4 m length) and permits multiple penetrations. Six thermistors are equipped on the probe for temperature gradient measurements. One of the thermistors is equipped with a heating wire for in-situ thermal conductivity measurements. By the system, the conductivity data are obtained from the observation of the thermal decay after transient heatine (pulse-probe method) (Hyndman et al., 1979; Lister, 1979). In this cruise, however, the conductivity system did not function well. Thus, thermal conductivities were measured on the samples recovered by a piston corer, using the needle probe technique (Von Herzen and Maxwell, 1959).

14-2. RESULTS OF OBSERVATION

The obtained heat flow data are listed in Table 14-1. Temperature profilesin the sediment and thermal conductivities are shown in Figs. 14-1 and 14-2, respectively.

KH 86-2-7 (HF1-A, B)

Station KH86-2-7 is located in the central part of the eastern Japan Basin. We made two POGO penetrations (HF1-A, B), both of which are successful. Thermal conductivity was also measured.

KH 86-2-8 (HF2-A, B)

Station KH 86-2-8 is located at the southern edge of the eastern Japan Basin. There is a NE oriented fault just north of the station. We made two POGO penetrations (HF2-A, B). Two of the sensors were broken or unstable during the lowering.

KH 86-2-12 (HF3-A, B)

Station KH 86-2-12 is located about 10 km south of KH 86-2-8 and on the slope formed by the fault just south of the station. It is parallel to the one near KH 86-2-8. We attempted two penetrations (HF3-A, B). The probe seems to have fallen down and bent a little in the first lowering. In the second trial, three thermistors were in the mud, but one of them was broken. Temperature gradient was obtained from the two sensors and the value is extremely low. It is possible that the part of probe in the mud was not vertical because of the bending. And there might be some anomalies in the thermal regime relating the nearby fault.

THERMAL CONDUCTIVITY MEASUREMENTS

At KH 86-2-5, -6 and -10, only thermal conductivities were measured. Their average values are 0.84, 0.81 and 0.81, respectively. Increase of the conductivity with depth can be seen at KH 86-2-6.

ACKNOWLEDGEMENTS

Scientists and crews on board supported the measurements. Mr. Y. Kasumi at Chiba University did much of the preparation for this cruise and his devotion is greatly thanked.

REFERENCES

Hyndman, R.D., Davis, E.E. and Wright, J.A.: The measurement of marine geothermal heat flow by a multipenetration probe with digital acoustic telemetry and insitu thermal conductivity. Marine Geophys. Res., **4**, 181-205, 1979.

Lister, C.R.B.: The pulse probe method of conductivity measurement. Geophys. J. R. Astr. Soc., **57**, 451-461, 1979.

Nagihara, S., Suzuki, S., Boh, R. and Kinoshita, H.: Development of a 16-channel heat flow measuring system and its test application on the deep sea floor. Zisin J. Seism. Soc. Japan, in press (in Japanese with English abstract), 1986.

Von Herzen, R.P. and Maxwell, A.E. : The measurement of thermal conductivity of deep-sea sediments by needle-peobe method, J. Geophys. Res., **64**, 1557-1563, 1959.

TABLE 14-1

Station	Location		Depth (m)	dT/dZ (K/m)	K (W/mK)	Q (mW/m^2)
KH 86-2-7						
HF1-A	$42^{o}13.6$ N	$137^{o}40.2$ E	3690	0.124	0.77	**95**
F1-B	$42^{o}13.6$	$137^{o}40.1$	3690	0.125	0.77	**96**
KH 86-2-8						
HF2-A	$41^{o}19.9$ N	$138^{o}29.4$ E	3690	0.105	0.77	**81**
HF2-B	$41^{o}19.8$	$138^{o}29.4$	3690	0.112	0.77	**86**
KH 86-2-12						
HF3-A	$41^{o}12.4$ N	$138^{o}27.2$ E	3670			
HF3-B	$41^{o}12.4$	$138^{o}27.3$	3670	0.023	(0.77)	**18**

[Notes]:
dT/dZ is the temperature gradient determined by the least squares fit, K is the average thermal conductivity; Q is the heat flow.

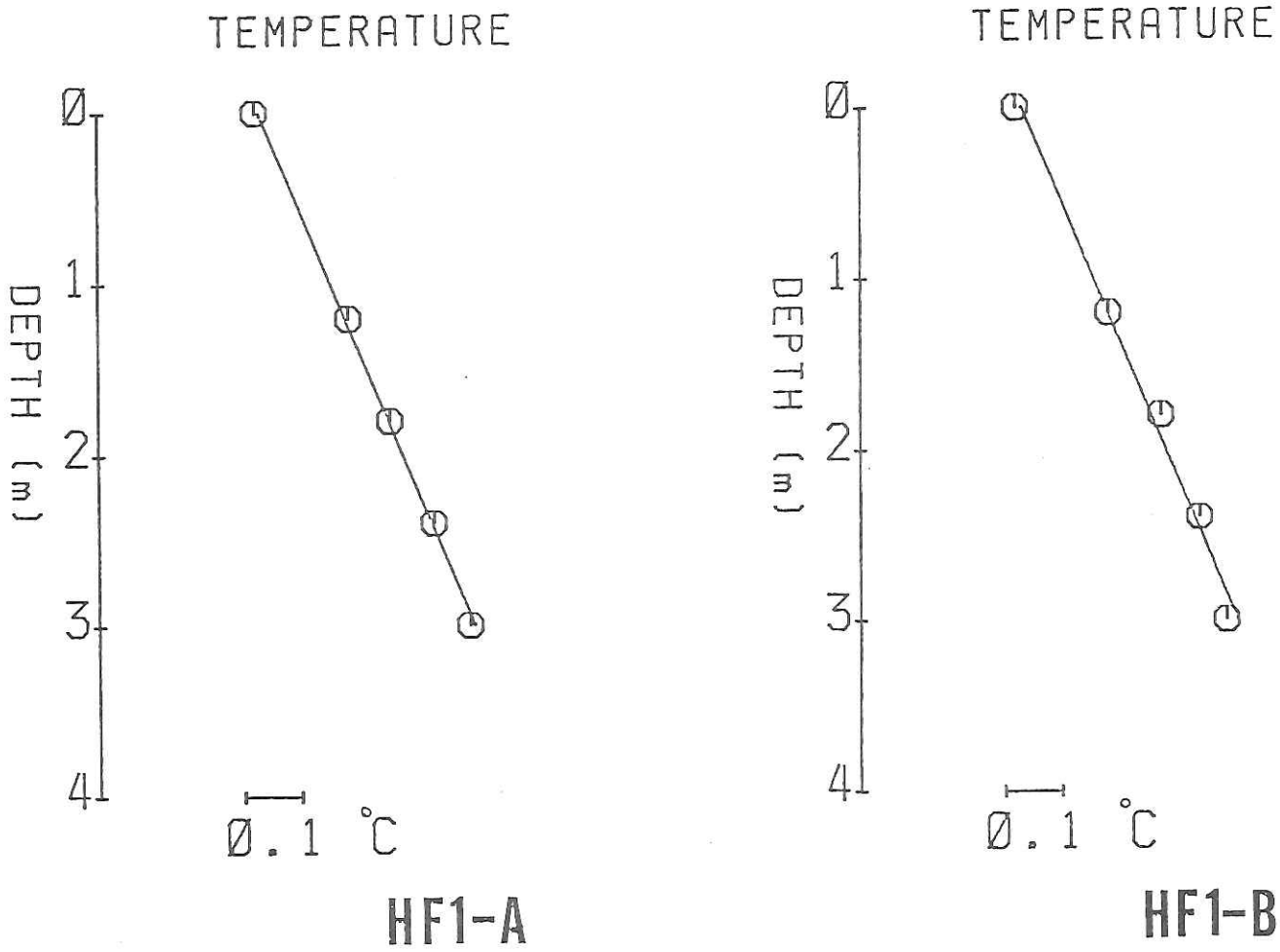

Fig. 14-1(a) Temperature profiles in sediment at HF1-A and HF1-B in the Japan Basin.

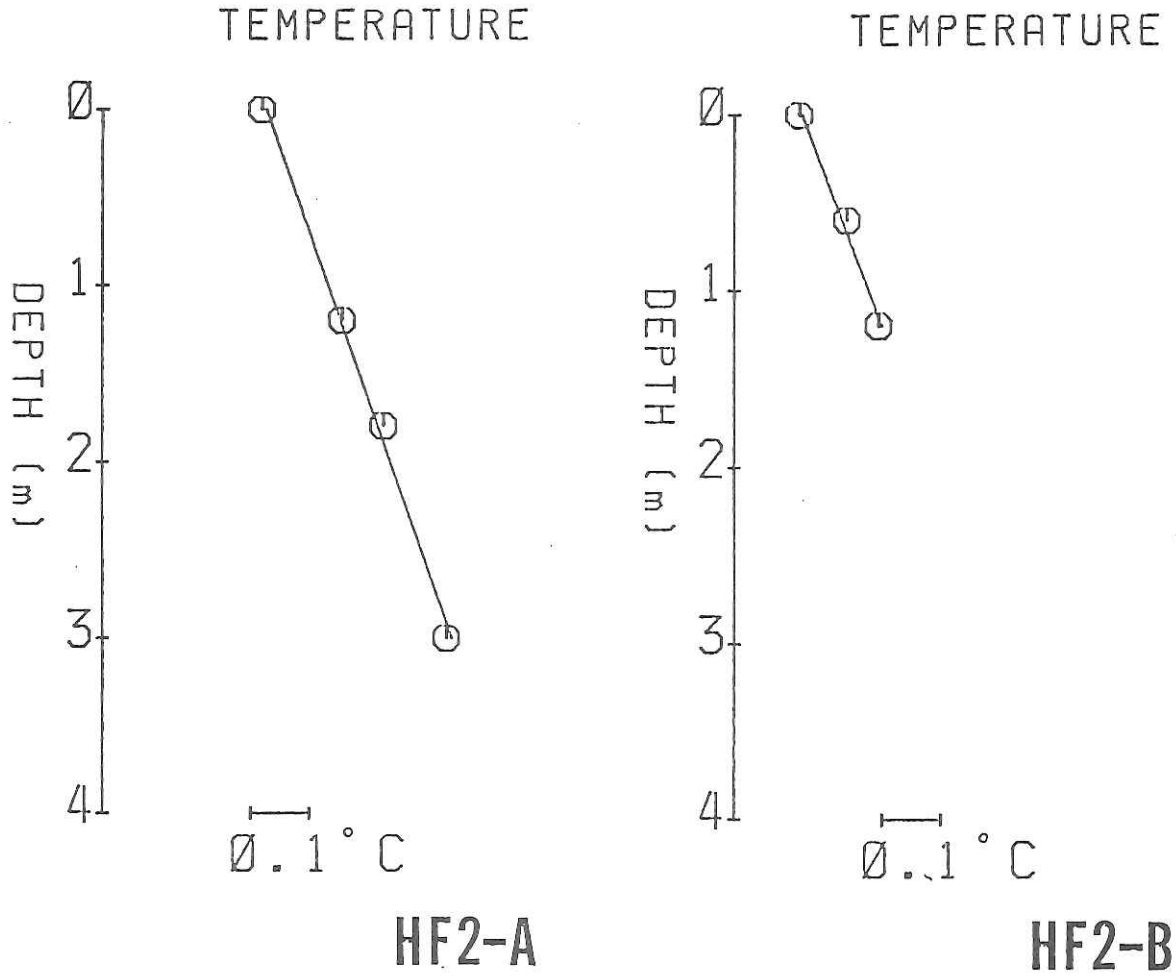

Fig. 14-1(b) Temperature profiles in sediment at HF2-A and HF2-B in the Japan Basin.

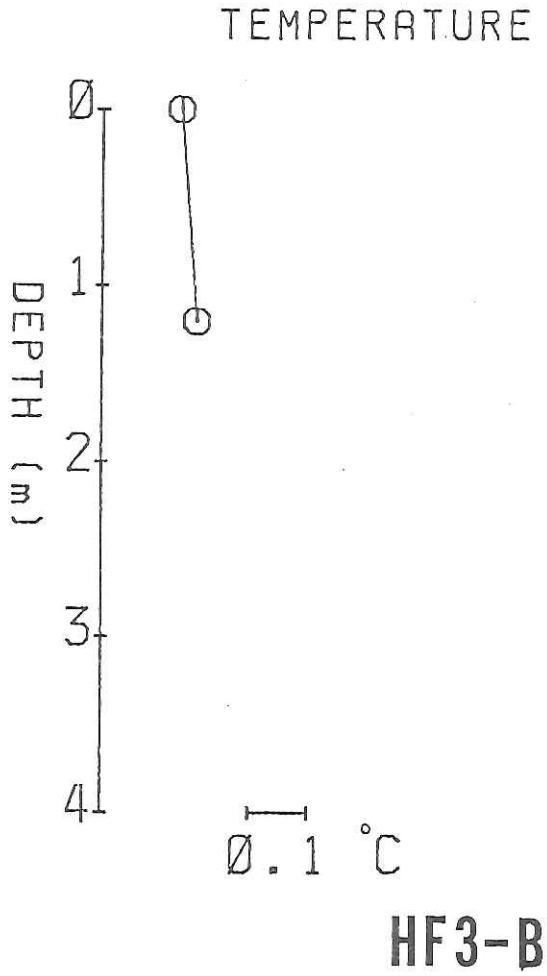

Fig. 14-1(c) Temperature profiles in sediment at HF3-B in the Japan Basin.

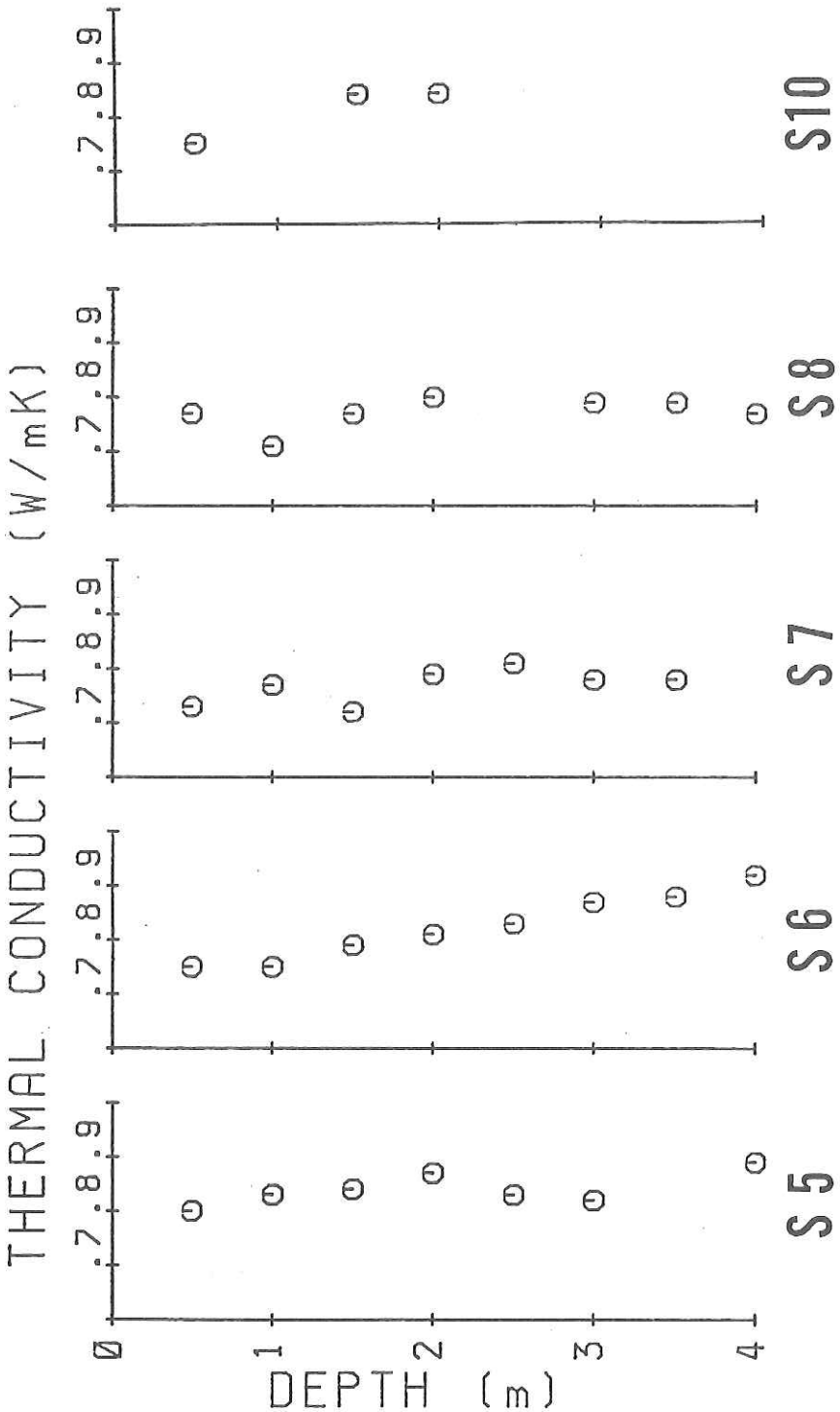

Fig. 14-2 Thermal conductivity measured with piston cores S-5, -6, -7, -8, S-10.